INTERACTIVE DESIGN OF POWER ELECTRONIC CONVERTERS WITH GUARANTEED PARAMETERS

MSc. Zoran Zlatev

A thesis submitted to the PhD students School of French Faculty for Electrical Engineering at the Technical University of Sofia in fulfillment of the requirements for the degree of Doctor of Philosophy in the Technical University of Sofia.

Scientific specialty: "Industrial Electronics"

Professional direction: 5.2 "Electrical engineering, electronics and automatics

ABSTRACT

In order to better understand the mother nature, people far backward are making investigations on certain phenomena. Different type of measurements had been performed centuries ago. With many ways and methods, from big amount of measurements, the first scientists had started to understand how our planet behave. In past two centuries, electronic components are going smaller and smaller, and thousand times faster. This causes so called "digitalization" of the earth. Later comes the conclusion that, as fast as the information, that fast are the benefit from it. Electronic industry is the main engine that drives this growth of the information technology, and the planet is digitalizing. A lot of different instruments are produced that perform measuring different types of parameters.

At the very beginning of digitalizing the planet, computers are generally used for calculations and transfer of information. After that are the 90's when is discovered the "friendly graphic user interface" on Windows. With Microsoft Windows 95, the internet become more used for multiple tasks and needs. Parallel exponential devices that are also speeding to this are the mobile phones with their first Java software platforms and browsers, games, etc. Every second new website, new electronic device and new game.

Making summary, nowadays, people and scientists are forcing whole our knowledge in combining multiple technologies for making and leaving a better earth for the future generations.

This dissertation aims to show the benefit of using software engineering in electronic industry and to point the results in investigation of big mass data from output voltage in dc – dc pulse converters. There are a lot of researchers who had already made a huge progress in some fields of investigation that is obtained in this dissertation. It will be connected set of different technologies and systems, with one aim, making an integrated project that can be used in future as a test model for the benefits of researchers, students and companies. As one of the most common and important technique explained in the first part is the "Fast Fourier Transformation" that provides frequency and spectral measurements, in different working environments. Second chapter represents a set of results that are obtained from an analysis of three types of dc – dc converters in different modes of operation, ideal conditions and real time working conditions of the output voltage, and the frequency analysis and difference between the different operational

modes. The third chapter is introducing an interactive web design for previewing and analysis of FFT and Power Spectrum with the ability of the program languages like PHP, Phyton, HTML and gives explanation of importing data to complete results with graphs. Chapter 4 represents an analysis via LabView of the same results that are imported from LTSpice in string format of the output voltage. Already mentioned data files are processed through LabVIEW block diagrams such as the frequency and spectral measurements. The result of the investigation is considering the difference between different working conditions of the dc – dc converters and the usability of the Fast Fourier Transformation implemented in different techniques and software packages.

- **Motivation**

  The object of investigation are power electronic converters. The dissertation proposed is motivated by teaching and research activities in electrical engineering and electronics, particular in power electronics. Mathematics, control theory, study of semiconductor elements, analog, digital and microprocessor circuits are used in this approach. Students are difficult in studying in this specific matter; the last one is widely applied in industry and everyday life, and often the lack of fundamental knowledge is an obstacle to integration into the labor market. The use of modern information and communication technologies is a tool through which the study of power electronics becomes attractive; it allows gradual acquisition and developing of competences in young people.

- **The aim**

  This dissertation is to be presented and used, in particular designed and realized using a new approach, various technologies for interactive design of power electronic converters with guaranteed parameters.

ACKNOWLEDGEMENTS

TABLE OF CONTENTS

LIST OF FIGURES

LIST OF ABREVIATIONS

FFT	Fast Fourier Transformation
PHP	Hypertext Preprocessor
HTML	Hyper Text Markup Language
VD Diode	Voltage Down Diode
UI	User Interface
UX	User Experience
CSS	Cascading Sheets Styles
XHR	XML HTTP Request
VI	Virtual Instrument
DSP	Digital Signal Processor
DLL	Dynamic Link Library
DAQ	Data Acquisition

1. INTRODUCTION

1.1. PREWORD

In order to achieve the desired result and exceed conclusion from a scientific paper, researchers have to work in several environments at the same time, in order to authenticate the results developed from the analysis in different software solutions, that are one of the most complete in that field of investigation in present time.

According to nowadays technologies, there are multiple ways for investigating some problem, that can be combined for better results and faster solutions in area of researching.

It is not always simple and easy to work with technology that is unknown and needs to be learned in a very short period of time, and here takes a big role the computer science technologies in the world of web-based applications that enable data-driven work without the knowledge of a researcher's special techniques and software packages of engineering type, which is actually a short description of the very term 'abstraction'. But the idea is not to get only results without understanding better the functionality of the system, the aim is to make a different angle of view to some complex system and a different approach of unknown technologies in order to make the investigation and researching as teaching more flexible and user – friendly. From this the conclusion is obtained in using more information technologies in scientific and researching fields rather than in common everyday application forms.

1.2. SPECTRAL ANALYSIS METHODS IN DATA SETS

Fourier analysis had been applied in engineering, seismology, big data analysis, and other areas of investigation, and further had become very important tool for providing a fast and reliable way of gathering results and conclusions from processed data (T.A. de Perez ; M. Juanatey ; M.C. Stefanelli ; M. Abondano, 1998). With much more information obtained from certain analysis, the scientists had explained a lot of phenomena which have make easier for whole population to understand some behavior of mother nature.

This type of "problem" investigation was an inspiration for two mathematicians J.W. Cooley and J.W. Turkey who presented a paper in 1965 in which they described a solution algorithm that will radically reduce the computational effort required for Fourier Transform. This algorithm turned out to be very efficient and very soon came known as the Fast Fourier Transform Algorithm.

1.3. FAST FOURIER TRANSFORMATION

Fast Fourier Transform is considered like faster than Fourier Transformation because it starts with 2 points Fourier transformations instead of one, and then the two are divided in four, the four are divided in eight-point arrays, then sixteen-point arrays and so on until it is developed a single array (A. Ortega-Monux ; J.G. Wanguemert-Perez ; I. Molina-Fernandez ; E. Silvestre ; P. Andres, 2006). This is very similar to the "divide and conquer" algorithm and helped increase the speed for more than 1000 times.

When expressing the k Fourier coefficient, the result will be the famous, well known, Fourier transformation.

Writing the equation like function of variable $\frac{k}{L}$ like this:

$$F\left(\frac{k}{L}\right) = \int_{-\frac{L}{2}}^{\frac{L}{2}} f(x) e^{-\frac{2\pi k x i}{L}} dx. \tag{1}$$

From this the new formula for Fourier's queue will be:

$$f(x) = \sum_{k=-\infty}^{\infty} \frac{1}{L} F\left(\frac{k}{L}\right) e^{\frac{2\pi i k x}{L}}. \tag{2}$$

Further, $L \to \infty$, and realizing that the variable $\frac{k}{L}$ will turn out from discrete to continuous. Even if it's thought that for fixed value of **k** this expression will approach 0, the idea is that $-\infty < k < \infty$ and with increasing the number **L** it is decreased the difference between the values of the variable. The variable $\frac{k}{L}$ is now continuous variable **s** and it is approved that:

$$F(s) = \int_{-\infty}^{\infty} f(x)e^{-2\pi sxi}dx. \tag{3}$$

The result function $F: C \to C$ is called Fourier's transformation function knowing that expressions with F have complex numbers and give complex numbers. Considering that $L \to \infty$ now can be seen that sum becomes integral and $\frac{1}{L}$ is infinite small value **ds**.

$$f(x) = \int_{-\infty}^{\infty} F(s)e^{2\pi isx}ds \tag{4}$$

In this expression *f(x)* is inverse Fourier transform based on coefficient *F(s)* for every $s \in R$. It is very important to notice that it is invoked Fourier transformation from the same equation of Fourier's queue, and the inverse transformation.

Example 1: If it is considered the function given with this expression:

$$f(x) = \begin{cases} 1, x \in \left(-\frac{1}{2}, \frac{1}{2}\right); \\ 0, otherwise. \end{cases} \tag{5}$$

This function is very often called rectangle function because of its graphic look, but it's very important for signal processing.
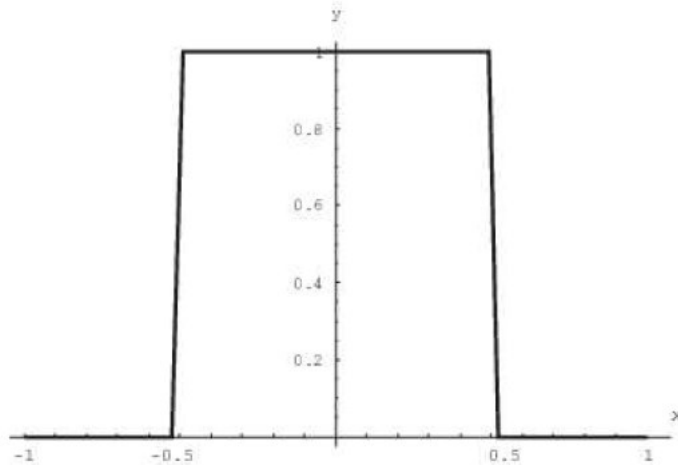
Figure 1.1 Rectangle function

Fourier transformation:

$$F(s) = \int_{-\infty}^{\infty} f(x)e^{-2\pi sxi}dx. \tag{6}$$

To be able to get the integral of the given function $f(x)$, the integral must be divided into three parts:

$$F(s) = \int_{-\infty}^{-\frac{1}{2}} 0 \cdot e^{-2\pi sxi}dx + \int_{-\frac{1}{2}}^{\frac{1}{2}} 1 \cdot e^{-2\pi sxi}dx + \int_{\frac{1}{2}}^{\infty} 0 \cdot e^{-2\pi sxi}dx. \tag{7}$$

From this expression all integrals can be deleted except the one in the middle which is:

$$F(s) = \int_{-\frac{1}{2}}^{\frac{1}{2}} e^{-2\pi sxi}dx. \tag{8}$$

Then using Euler's formula:

4

$$F(s) = \int_{-\frac{1}{2}}^{\frac{1}{2}}\left(\cos(-2\pi sx) + i\sin(-2\pi sx)\right)dx = \int_{-\frac{1}{2}}^{\frac{1}{2}}\cos(-2\pi sx)\,dx +$$

$$i\int_{-\frac{1}{2}}^{\frac{1}{2}}\sin(-2\pi sx)\,dx = -\frac{1}{2\pi s}\left(\sin\left(-2\pi s\cdot\frac{1}{2}\right) - \sin\left(-2\pi s\cdot\left(-\frac{1}{2}\right)\right)\right) - \frac{i}{2\pi s}\left(\cos\left(-2\pi s\cdot\right.\right.$$

$$\left.\left.\frac{1}{2}\right) - \cos\left(-2\pi s\cdot\left(-\frac{1}{2}\right)\right)\right). \tag{9}$$

Using the property of even function cosine and odd function sine:

$$F(s) = -\frac{1}{2\pi s}\left(-\sin(\pi s) - \sin(\pi s)\right) - \frac{i}{2\pi s}\left(\cos(\pi s) - \cos(\pi s)\right) =$$

$$-\frac{1}{2\pi s}\left(-2\sin(\pi s)\right) = \frac{\sin(\pi s)}{\pi s}. \tag{10}$$

With this expression it is defined the Fourier transformation of the given function. This process of transforming rectangle function with Fourier transformation in signal analysis is often called *sinc* function and it's defined with this equation:

$$sinc(x) = \frac{\sin(\pi x)}{\pi x} \tag{11}$$
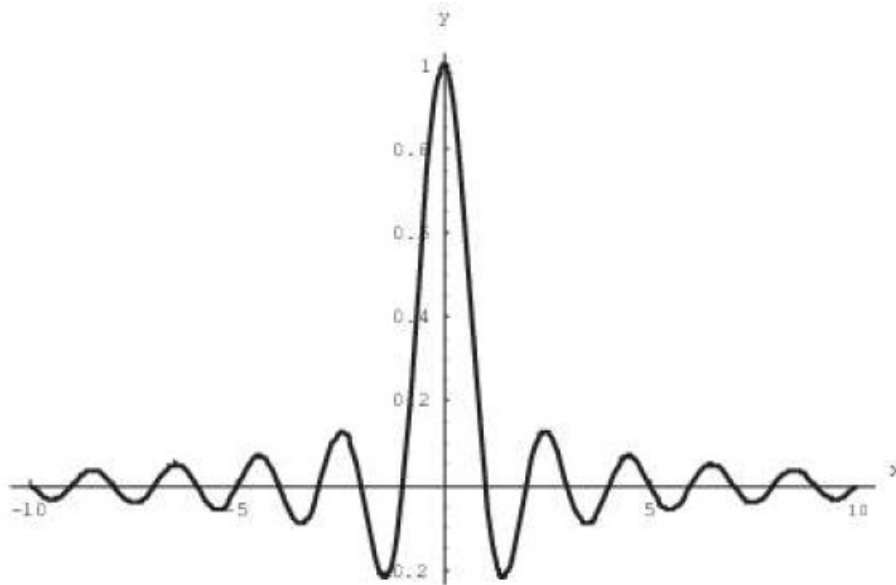
Figure 1.2 Graph of sinc function

When Fourier transform is discussed, its meaning invokes thinking of it like a function that transforms one function into different sets of basic functions. Fourier transform aims to decompose a cycle of arbitrary waveform into multiple sine components making sure that the inverse transformation will convert the series of sine components into the first waveform (Shumin Zhou; Bin Tang; Rui Chen, 2009).

When a researcher in mathematics and physics have a desire to describe his surrounding, virtually everything in the around can be described as a form of waveform. That means, that everything is a function represented by time, space or another variable. The main purpose of Fourier definition is explaining one fundamental fact that all waveforms are just a sum of simple sinusoids of different frequencies.

Processing and analyzing big data sets is an old method like mentioned above. Maybe like term is relatively new, from this century, but as a technique is very old. From first accounting in Mesopotamia before 7000 years with aim recording the growth of herds and crops, to 1663 when the person John Graunt takes accounting about mortality in London and was trying to develop an alarm system for the bubonic plague. After his gathering results from lot of books, he makes a statistic and that is why later he is the innovator of the term "statistics".

A little much further, in 2005 Roger Mougalas set the definition of the term "big data" for the first time, which meanings aims to large set of data that are very difficult for processing and analyzing with old methods.

The large sets of data that are recorded for a long time on mass scale, often hiding some important information after precise and complex processing. In the present, for example, companies use these sets of data for business goals, and, with long analysis they can make enough accurate predictions how the market trends will continue, which is of great importance (Zhang, P., Yang, H., & Xu. Y., 2014).

Making big data analysis have never been a simple and fast process. Most of the time, this is complex and slow process, where are included and processed large data sets, to see the hidden messages in every natural phenomenon.

This type of problem becomes very popular in some companies, because, sometimes the most balanced solution must be developed from some analytics. Examination on large data sets, with the right technologies and techniques often drive the business to the right path and keep the people well informed (X. Y Wu, J. R Ming., 2015). After some advanced analytics, it can be derived some predictive models and what – if analysis that will be done on high performance analytic systems.

The benefits of using such high - powered systems that that are capable of processing of large sets of data are very often crucial for some business (David T., 2012). More effective predictions bring better efficiency, keeping the step with the rivals, much better customer service etc.

The whole process of investigating some problem, or making deep analysis of some data, must include computer science and information technology for better results and saving a lot of time. Top area of investigating for researchers in the field of electronics and computer science is the alternative sources of energy and energy flow in everyday systems (Zilong Yang; Zhuo Chen; Lidong Guo; Yuanyuan Chen; Xinke Huang; Yibo Wang, 2017). In the last 30 years the software engineering is a mega – trend and today it can find a lot of applications that will provide the wanted results for the user. However, it must not be forgotten that growing of the electrical engineering is crucial for whole computer science technology.

One of the aims in dissertation is to develop a more faster and user – friendly solution for processing data exported from output voltage of the DC – DC converters, available for all users and without installing particularly on one machine. It can be available on cloud and flexible enough for converting on different data sets, in a much easier way. But, considering few important things when talking about big data analysis. First, there are the raw data that are collected every day from every single process in mother nature and every electrical impulse, from every device. That type of data represents only lot of numbers if it is not processed and analyzed (Yan Li; Junming Ma; Bo An; Donggang Cao, 2018). With processing large amount of data, sometimes can be seen certain dependencies in the sets, which leads to gathering information that sometimes has bigger value than usual. With a collection of a lot of conclusions about investigated problem, the scientist starts to better understand the given data and to gain certain knowledge. With gathering certain amount of knowledge, a prediction can be done of

every connected process. With making prediction, a wisdom in that area has been produces, which is the main aim that is supposed for the researchers.

The whole process must be accurate and obtained with the correct mathematical methods and formulas. Another important idea of this dissertation is, to be re-used in future in other projects or commercial benefits, which can be of certain value. Computer science has provided so far, such a nice collection of professional software platforms that allow researchers making different types of calculations according to the field and the needs of the investigation. Very often are used MATLAB, LTSpice, LabView and a lot of similar software solutions (Harvey, A. F., & Cerna, M., 1993).

1.5. DC – DC CONVERTERS

Although, there are a lot of types of data for investigating, the main data that is investigated will be the data gathered from the output voltage from the dc – dc converters that are presented in next section. It is considered that in the future, if one has need to make research in different type of data, will be of much help to use this thesis with small changes in the dependencies of the filters.

In the figure 1.3., there is a model shown for the selected dc – dc pulse converters (David C. W. Ng, William Y. T. Wong, Ngai Wong, Karen W. H. Wan, David K. K. Kwong, 2007).
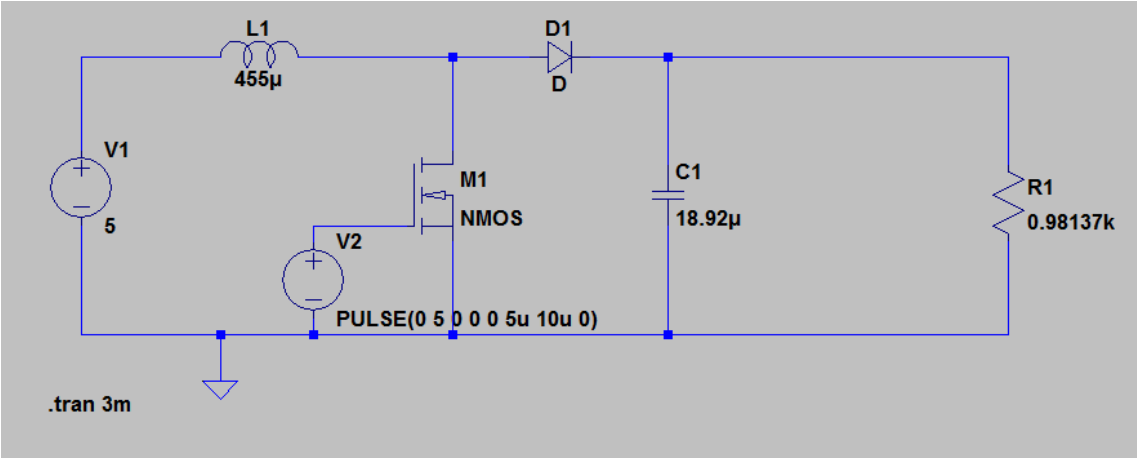
Figure 1.3. Model of DC - DC converter in LTSpice

1.6. CONCLUSION AND DISCUSSION

Fourier transformation stands like one of the most common used mathematic tools in engineering. The presence of FFT in engineering world is also very bih and the function have wide spectra of usability (Adisorn Kamlungpetch; Prajuab Inrawong; Wutthichai Sa-nga-ngam, 2017).

Engineers very often use Fourier's transformation when they have one function (signal) and they want to translate it to function which for a given frequency k will give $F(s)$, result from which we can get information about amplitude, phase and frequency s. Fourier transformation has properties that make analysing functions easy and more understandable.

> The aim of the dissertation is to be presented and used, designed and realized using a new approach, various technologies for interactive design of power electronic converters with guaranteed parameters.
>
> To accomplish this, the following tasks are formulated:

- Investigating the possibilities of applying spectral analysis to automate the design of power electronic converters.
- Checking the possibilities for estimating the dynamics of power electronic devices based on FFT analysis of DC-DC converters.
- Analysis of results of FFT analysis in terms of achievement of guaranteed performance.
- Developing of up-to-date web-technologies of special algorithms and user interface for power electronic converters handling.
- Implementation of databases with building blocks, topologies and numerical experiments.

2. DC – DC PWM CONVERTERS

DC – DC PWM converters (DC-DC converters) have become widely used in modern industrial electronics. Both the thyristor and DC regulators for the regulation and stabilization of the output voltage use the methods of pulse-width and frequency-pulse regulation (Dariusz Czarkowski, L. Rai Pujara and Marian K. Kazimierczuk, 1993). Transistor converters can be, with or without galvanic separation, between input and output and have very good power and mass dimensions, and almost all power sources are based on them.

2.1.   BUCK DC – DC CONVERTER

The Buck converter (step-down,) is used in cases where the output voltage is required to be lower than the input pressure. Its diagram is shown in Figure 2.1, consisting of a semiconductor key with one-way conductivity S (transistor), smoothing LC filter and diode VD (labeled with "a" on the diagram). The analysis of this and other schemes will be conducted in an established mode, assuming that all circuit elements are ideal. The principle of action of the lowering converter is illustrated by the diagrams from Figure 2.1 (labeled with "b", right site of the diagram) showing the voltage and current of the inductance. At the moment 0, the control of the transistor is passed, the key closes and through the inductance L flows into a linear increasing current that loads the C capacitor. At the moment T1 is clogged transistor (the key opens), but the inductance is a reserve energy that is The current constant and creates a voltage unclogging for the diodes VD. Therefore, for the time of the open key, the current over the inductance decreases again by linear law, depending on the size of L and the time of shutdown current T2, when the key is closed again it may not get to zero, as shown in the form Figure 1b or become equal to zero, i.e. to break. The principle of operation of the scheme shows that, for the duration of transistor ton on inductance L, the difference between the input and output voltage is applied, and when the switch is off (time toff) – Output voltage (Figure 2.1 - b). It is known from the laws of electrical engineering that the average of the voltage on one inductance per period is zero:
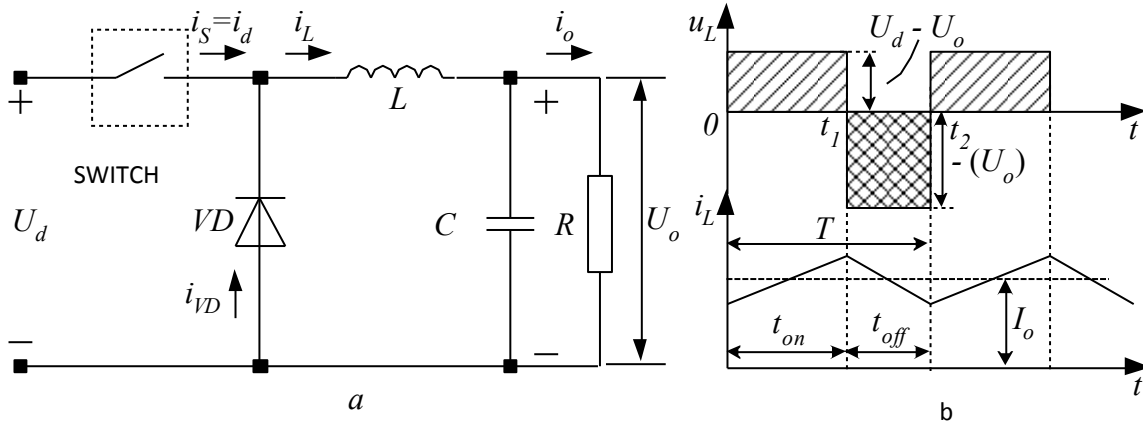
Figure. 2.1 Buck DC – DC transistor voltage converter

$$U_L = \frac{1}{T}\int_0^T u_L dt = \frac{1}{T}\int_0^{t_{on}} (U_d - U_o)dt - \frac{1}{T}\int_{t_{on}}^T U_o dt = 0 \tag{12}$$

After solving the integral is obtained equality:

$$(U_d - U_o)t_{on} = U_o(T - t_{on}), \tag{13}$$

of which the connection between the output and the input voltage for the lowering converter is determined:

$$\frac{U_o}{U_d} = \frac{t_{on}}{T} = D \tag{14}$$

In the assumptions made for the ideality of the minimize elements, the input power $P_d = U_d I_d$ is equal to the power given to the load $P_o = U_o I_o$ and the relationship between the output and the input current is obtained:

$$\frac{I_o}{I_d} = \frac{T}{t_{on}} = \frac{1}{D} \tag{15}$$

Thus, the lowering converter is equivalent to a DC transformer, and its prewater ratio can be changed electronically, with the help of the change of the coefficient D.

11

If it is necessary to obtain output voltage greater than the input supply, a replacement (step-up, boost) converter is used. Its scheme is shown in Figure 2.2(a) and in Figure 2.2(b) are presented the voltage and current of inductance diagrams when operating in continuous current mode. The increasing converter consists of the same elements as the lowering only, that they are connected in different ways. When the transistor is switched on 0, the current over the inductance L is increased by a linear act (figure 2.2(b)), the diode VD is obstructed, and the previous operating period of The circuit capacitor C, provides the tension in the load. Currently t_1, The transistor is clogged and the L-energy supply creates an unclogging voltage for the diode, it plugs in and starts to flow along the chain $+U_d$, L, VD, R and $-U_d$. The C capacitor is charged by restoring energy providing cargo voltages in the previous half-period of operation of the circuit. As the power source attaches power to the load at the time the transistor (switch) is turned off, so the converter is called a reverse. The determination of the main dependencies in the pattern of the inverse transducer in the load is carried out as in the scheme of the straight converter. In the transistor conductivity range t_{on}, on the inductance, the input voltage is applied and at the time when the transistor is obstructed t_{off} – The difference between the output and the input voltage (figure 2.2(b)). Because in an established mode, the mean value of the inductance voltage within a period is zero, the following equation is obtained:
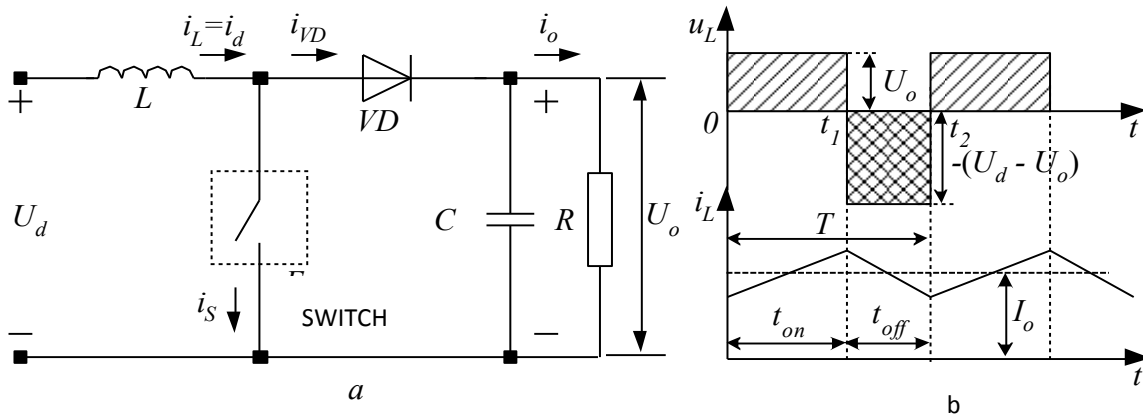
Figure. 2.2 Boost DC – DC transistor voltage converter

$$U_d t_{on} = \left(U_o - U_d\right)\left(T - t_{on}\right) = \left(U_o - U_d\right)t_{off}, \qquad (16)$$

from which the connection between the output and the input voltage is obtained after conversion:

$$\frac{U_o}{U_d} = \frac{T}{t_{off}} = \frac{T}{T - t_{on}} = \frac{1}{1 - D} \tag{17}$$

From this dependence it is established that the output voltage is always higher than the input, since the fill coefficient D is always less than 1. In the assumption that there are no losses of active power in the scheme elements, the output and the input capacity are equal: $U_d I_d = U_o I_o$ and therefore the ratio of the loading and input current is obtained:

$$\frac{I_o}{I_d} = 1 - D \tag{18}$$

2.3. INVERT BUCK-BOOST CONVERTER

The invert Buck-Boost converter is presented in Figure 2.3(a). When the switch is on, a linear, increasing current is accumulated and the energy supplied by the DC power source is cumulated, as shown in the diagrams in Figure 2.3(b). The diode VD is clogged and the capacitor C provides tension in the load. When the switch is turned off, the diode is drained to provide a path for dissipation in the capacitor and the load of the energy accumulated in the inductance. For the time when the key is closed on L the input voltage is applied, and when it is open – the output. A feature of the contested scheme is that the output voltage is reversed polarity to the input and therefore the converter is called inversion. Similarly to the analysis of the other transistor voltage converters, the expression of the mean value of the inductance voltage, which for a period of operation of the scheme has a value of zero, thus resulting in equality:

$$U_d t_{on} = U_o t_{off} = U_o \left(T - t_{on} \right) \tag{19}$$

After conversion, the relationship between the output and the input voltage for the transducer concerned is obtained:

$$\frac{U_o}{U_d} = \frac{t_{on}}{t_{off}} = \frac{t_{on}}{T - t_{on}} = \frac{D}{1 - D}, \tag{20}$$

as values of the coefficient $D=0,5$ $U_o=U_d$; at $D<0,5$ $U_o<U_d$, i.e. converter is lowering; and for values of $D>0,5$ $U_o>U_d$, we have a changing converter mode. In practice, it is preferred to

13

operate the circuit in continuous current mode and to avoid D values close to 1, because then the voltages and currents in the scheme are strongly increased and there is a risk of damage to the elements. With the ideal scheme for the voltage flows, the dependence is in effect:

$$\frac{I_o}{I_d} = \frac{1-D}{D} \qquad (21)$$
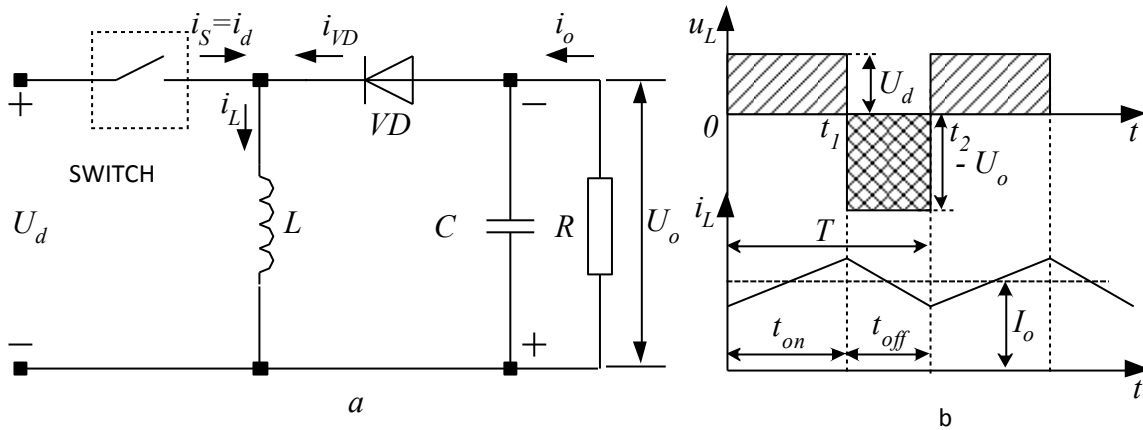
Figure. 2.3 Buck – Boost DC-DC converter

2.4. CHUCK CONVERTER

In the converter of the hammer between the input and output circuit, the power is connected to a sequential capacitor as shown in Figure 2.4(a). When the power supply voltage is switched on, the capacitor C_1 to the value of the input voltage U_d, with the specified polarity, and then no current is consumed from the power source. When the switch is on, the inductance L_1 and energy is accumulated in the stream and the diode VD is obstructed by the voltage of the C_1. At the same time, the tension of C_1 Generates a current in the chain C_1, key, C_2, L_2, thus charging the capacitor C_2, which provides cargo voltage at the moment t_1, the key opens and starts to flow along the chain $+U_d$, L_1, C_1, VD, $-U_d$, as current over the inductance L_1 reduces, and C_1 is recharging. In the moment t_2, The key is closed and the processes in the scheme are repeated. The currents and voltages of the two inductors of the converter are shown on Figure 2.4(b), with the voltages applied to them for the open t_{off} and closed t_{on} key. In accordance with the analysis of the previous transducer schemes, the equations are obtained:

14

$$U_d t_{on} = \left(U_{C1} - U_d\right) t_{off} \text{ и } \left(U_{C1} - U_o\right) t_{on} = U_o t_{off} , \tag{22}$$

After their resolution, the relationship between the:

$$\frac{U_{C1}}{U_d} = \frac{1}{1-D} \text{ и } \frac{U_{C1}}{U_o} = \frac{1}{D} , \tag{23}$$

that determine the relationship between the output and the input voltages in the scheme:

$$\frac{U_o}{U_d} = \frac{D}{1-D} \tag{24}$$

Therefore, the converter of the chuck has the same voltage transmission characteristic as the seamlessly already circuit of the invert lowering-changing converter.
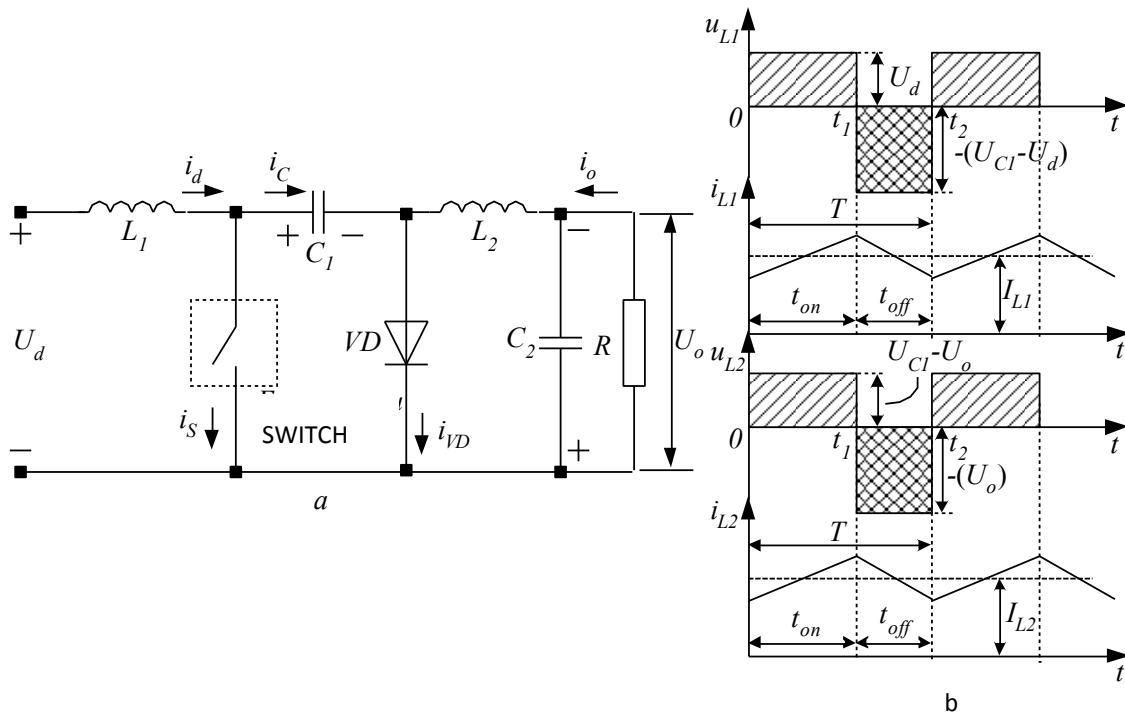
Figure. 2.4 Chuck DC-DC converter

15

For the purpose of the study was made a model of a lowering DC-DC converter in the working environment LTspice. A standard methodology was used to determine the initial values of minimize elements. The purpose of the study is to find a link between the actual form of output voltage and that obtained by using FFT's analysis in order to achieve an iterative transition process and a minimum possible duration of the transition process. Studies have been conducted for the case of a continuous current regime which is more commonly used in practice. The future work provides for a summary of the results and for the interrupted current regime. In Figure 2.5 is shown a model of a lowering converter. Cases of a converter with ideal (the scheme above) and real elements (the scheme below) are considered. The aim is to ascertain whether there is a significant difference in the nature and duration of the transition processes.
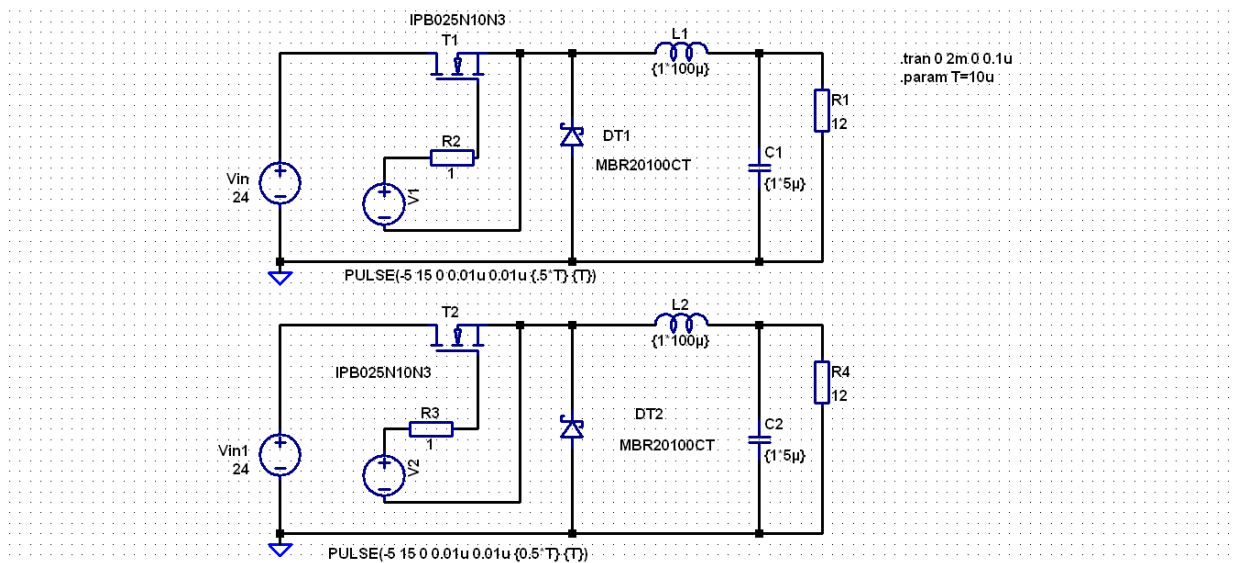
Figure 2.5 Simulation model of a Buck DC-DC converter

The following values of scheme parameters are used: Input voltage Uin=24V; Operating frequency f=100kHz; capacitor filter 5uF, loading resistance 12 Ω. The purpose of the study is to change the value of the fill coefficient D (initial value 0.5) and the filter inductance (initial value L=100uH).

The results for the output voltage format (V (n003 in a diagram with ideal elements, and V (n008 in a real-element scheme) are shown in Figure 2.6.
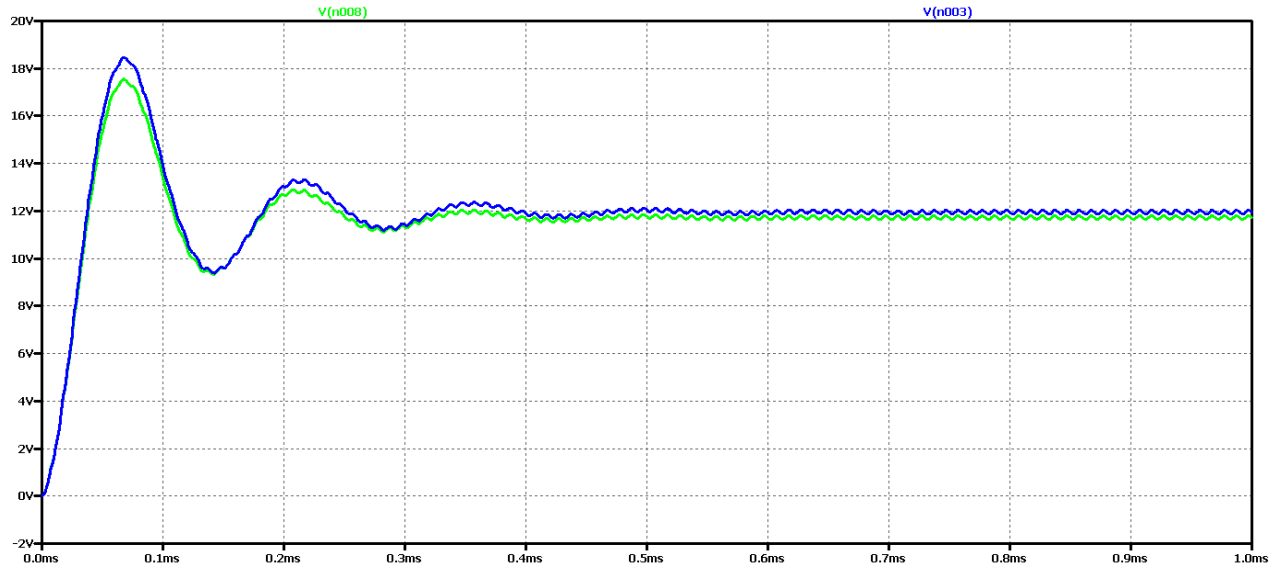
Figure. 2.6 Simulation results of a Buck DC-DC converter

It is evident that the difference between the results with real and ideal elements is that the scheme with the ideal output voltage in the established mode is higher and the amplitude of the fluctuations is greater with less attenuation. In both cases, it is a disputable type of transient process that is not desired in practice due to the long transient process and poor dynamic properties of the scheme. This is removed with the presence of a soft start at launch, however this type of transient process creates difficulties in the synthesis and adjustment of the controller. On the other hand, the parasite elements in the real scheme reduce fluctuations, but worsen the effectiveness of the converters.

Figure 2.7 shows the results of Fourier transform (FFT analysis) of output voltage.
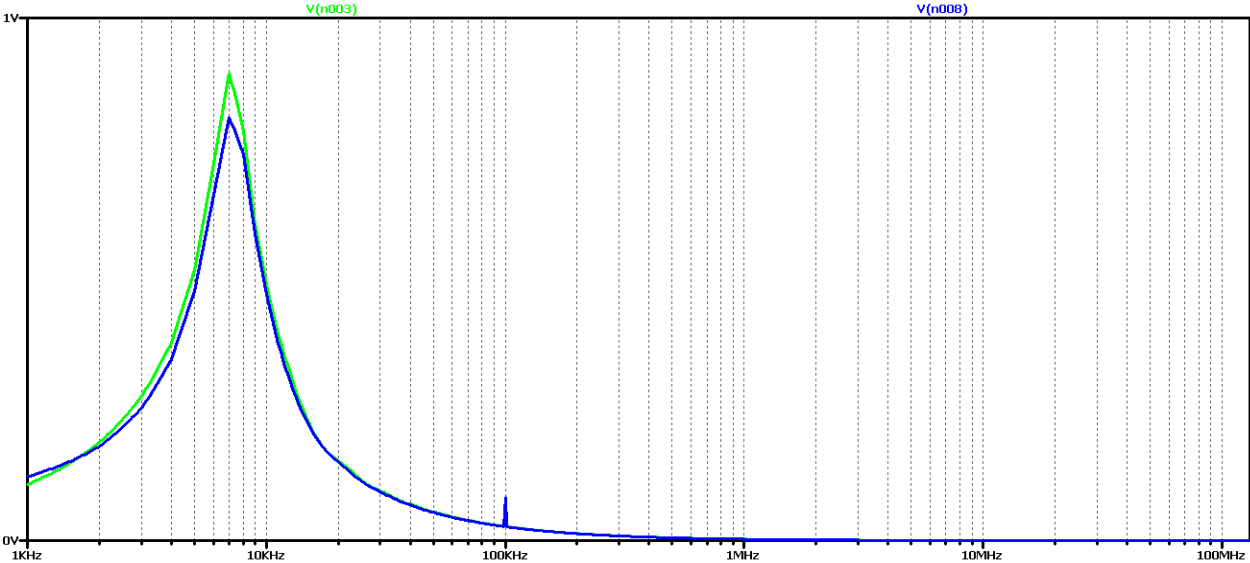
Figure. 2.7 FFT output voltage analysis of a Buck DC-DC converter

It is evident that the diagram has a pronounced maximum of about 10kHz and a harmonics at 100kHz (operating frequency). Obviously, this chart corresponds to the disputable type of the transition process.

Now let's try to achieve an interim transition process by increasing the value of filter inductance 5 times. The value of the filter capacitor will not change in order not to increase the pulse output voltage.
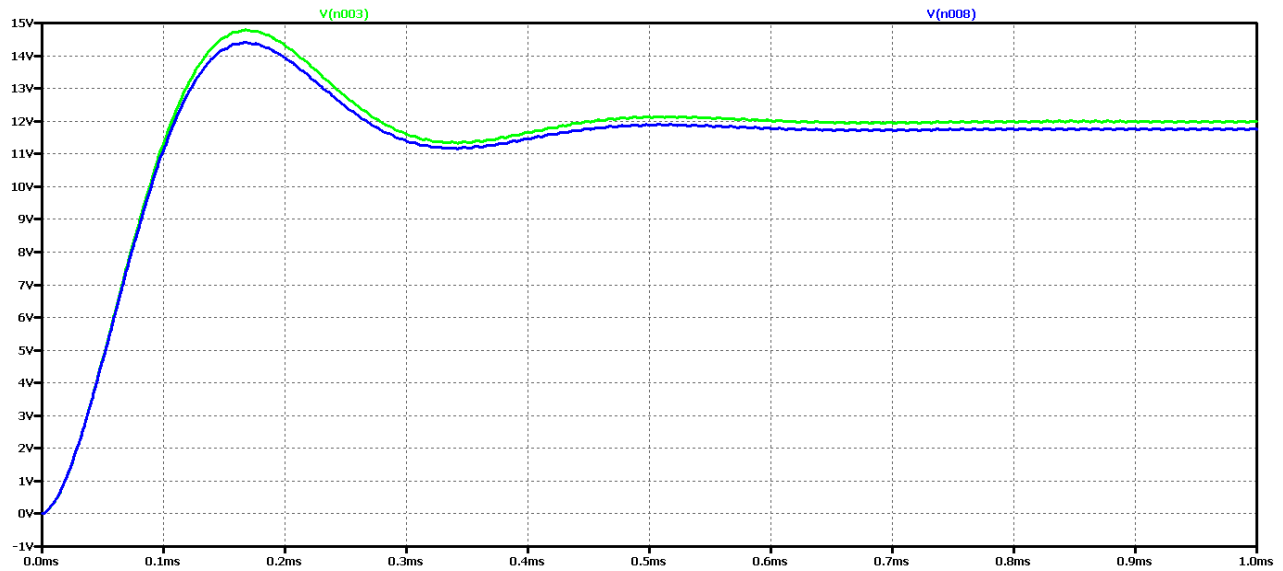
Figure. 2.8 Simulation results of a Buck DC-DC converter, at 5 times greater value of the filter inductance
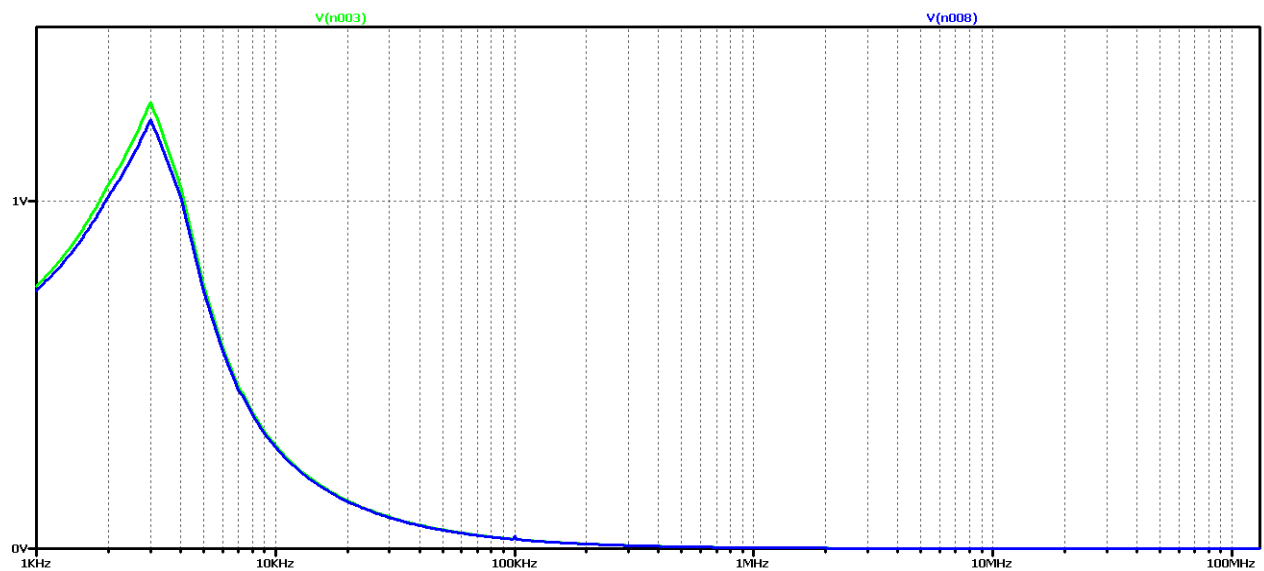
Figure. 2.9 FFT analysis of output voltage of a Buck DC-DC converter, at 5 times the value of the filter inductance

It can be seen that with the increase in filter inductance the fluctuations in the output voltage are reduced. From FFT, the analysis shows that the value of the harmonic with the frequency of management decreases significantly compared to the previous case. On the other hand, the maximum value has a harmonica with a frequency of about 3 kHz.

Now, let's increase the value of the filter inductance 10 times again. In this way, we should achieve an interim transition process or a closer approach to it than the previous version.
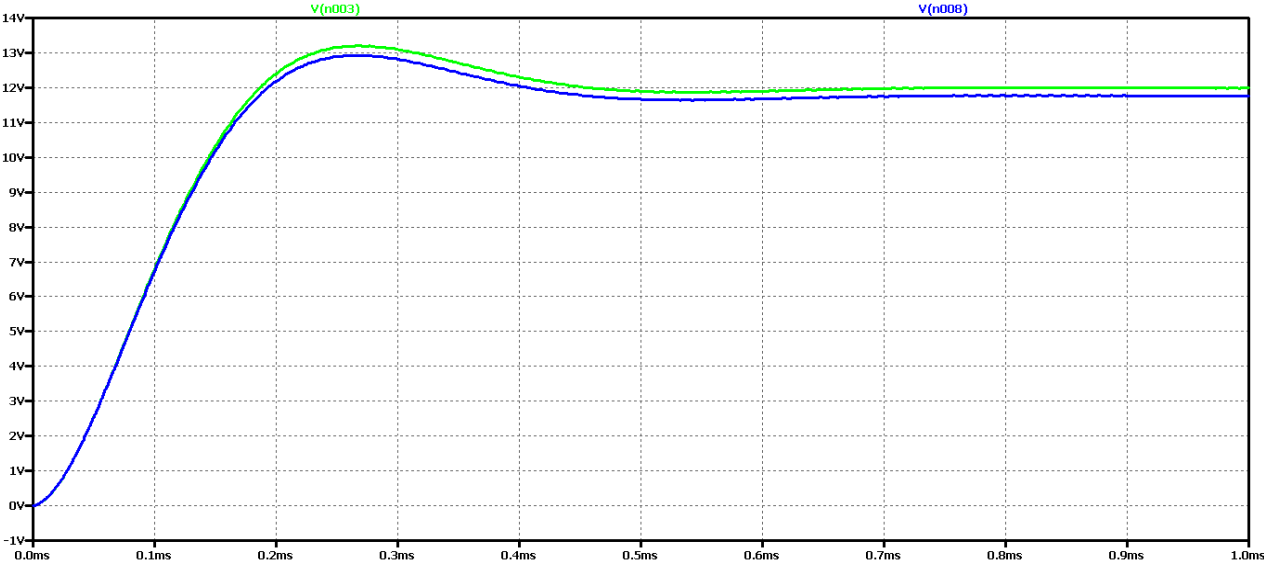
Figure. 2.10 simulation results of a Buck DC-DC converter, at 10 times the value of the filter inductance

It can be seen that the increase in filter inductance significantly reduces the fluctuations in the output voltage detection and to a large extent the form is close to an actric. Fluctuations with low frequency and a small amplitude are observed. From FFT, the analysis shows that the value of the harmonic with the frequency of management is very small compared to the previous case. On the other hand, the maximum value is a harmonic with a frequency of about 1 kHz, that is to say, the output voltage can be considered as constant with very small pulsations and deviations when the working mode is established.
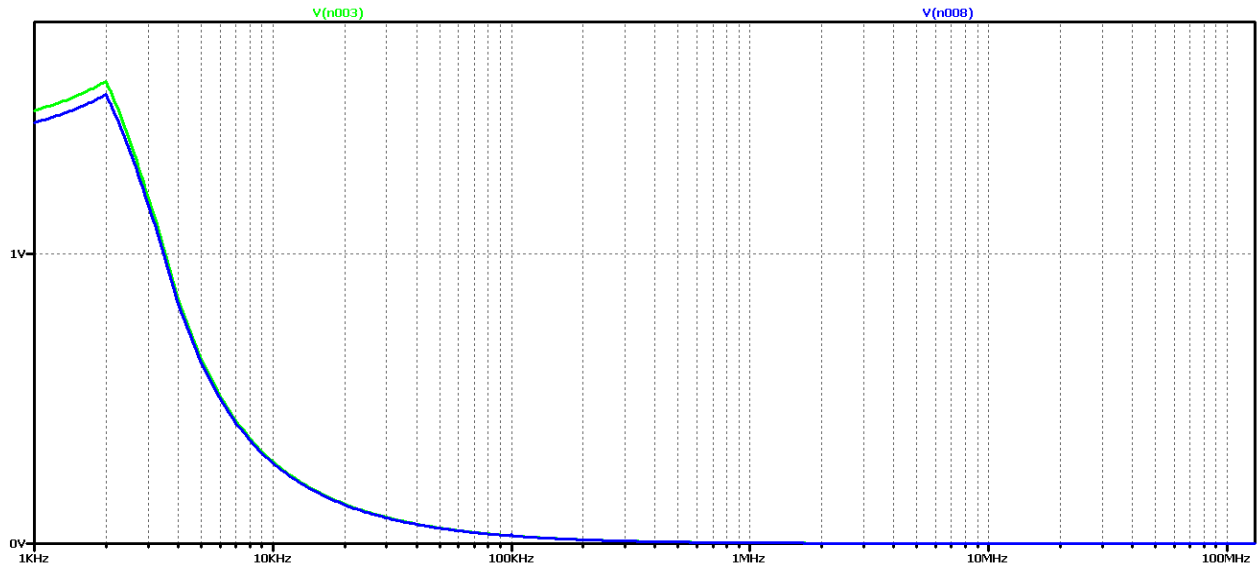
Figure. 2.11 FFT analysis of the output voltage of a Buck DC-DC converter at 10 times the value of the filter inductance.

For a more accurate examination of the results of the FFT analysis of the output voltage of Figure 2.12 is an increase for frequencies close to the operating frequency. This harmonic can be seen to have negligible value, and in some practical cases where we do not need high precision or there are limitations related to the value of the filter inductance, it can be assumed that we have in practice the required aperiodic transient.
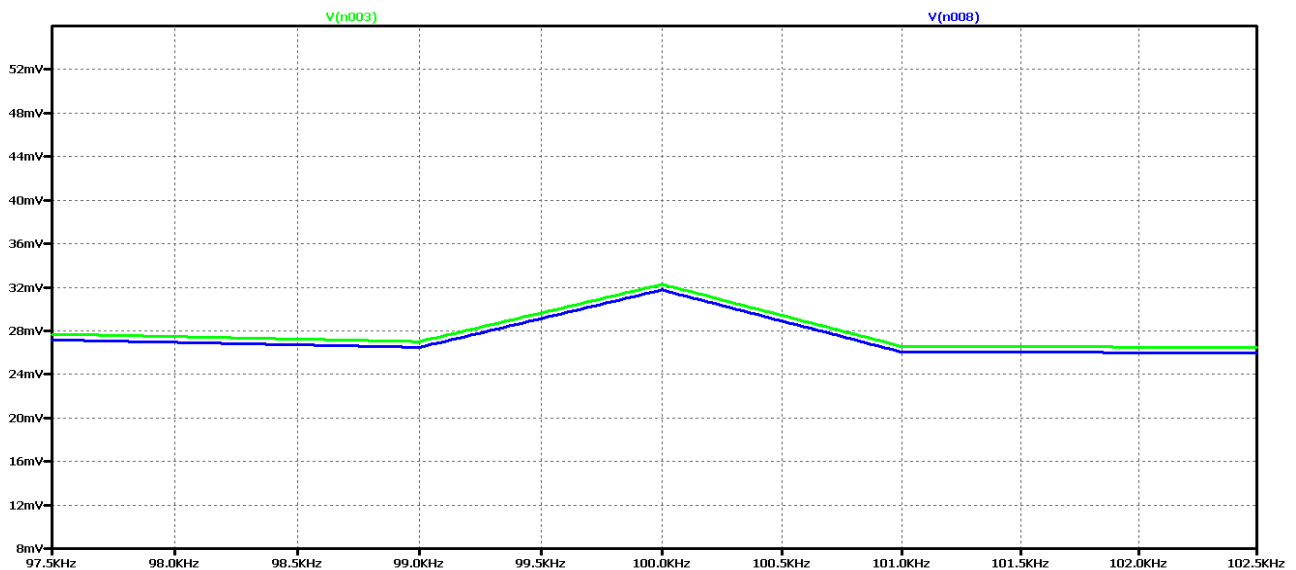
Figure. 2.12 FFT analysis of the output voltage of a Buck DC-DC converter at 10 times the value of the filter inductance for frequencies close to the control frequency.

21

The last experiment is to increase the value of the filter inductance 15 times. Figure 2.13 shows the output voltage form in this case. Obviously, we have achieved aperiodic mode with the best possible dynamic performance compared to the previous variants. In practice, in 0.6 ms we have the mode setup and transient startup completed. In Figure 2.14 shows the results of the FFT analysis of the output voltage in both cases - of a converter with ideal and real circuit elements.
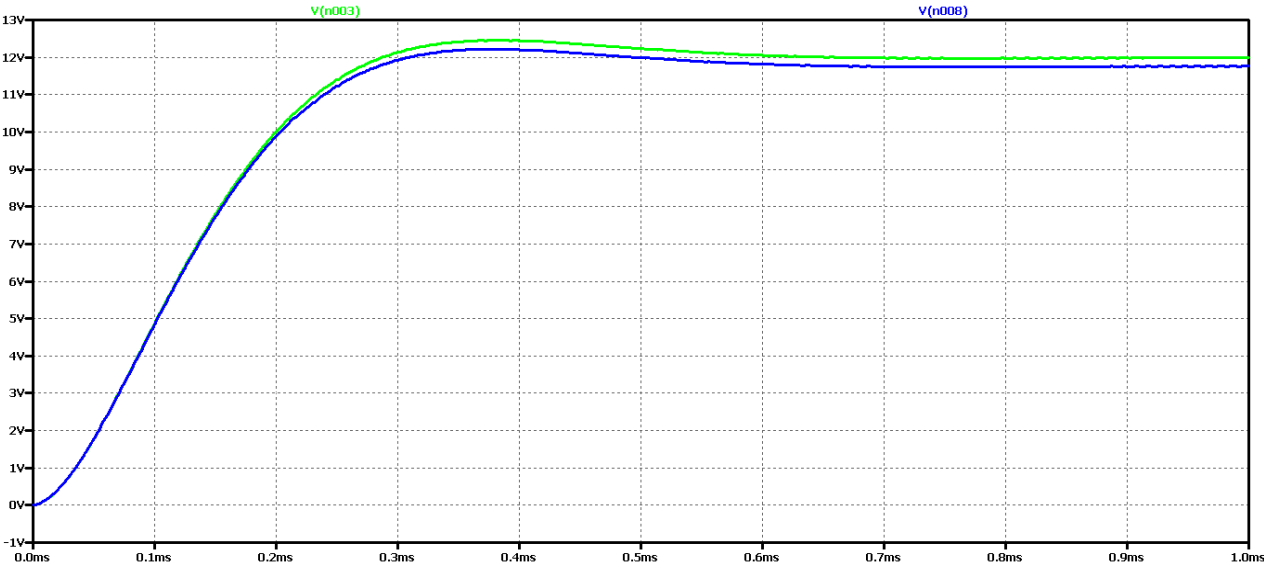
Figure 2.13 Simulation results of a Buck DC-DC converter at 15 times the value of the filter inductance

Here we can see that we have the largest constant component in comparison with the previous case. Furthermore, there is no deformation of the characteristic around the operating frequency, which was characteristic of previous cases.
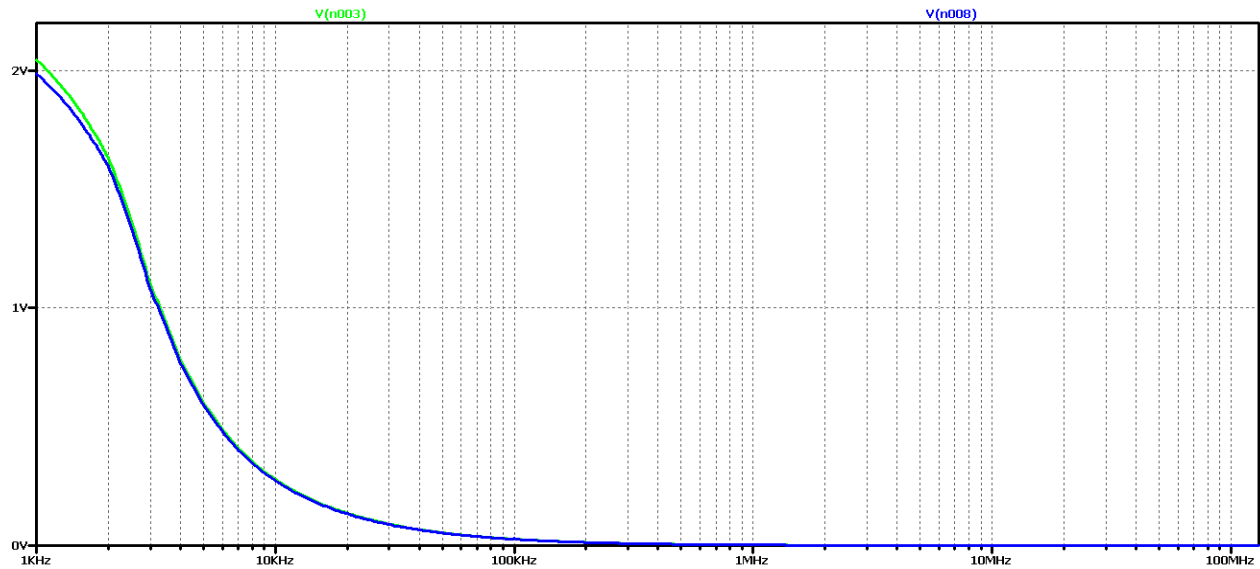
Figure 2.14 FFT analysis of the output voltage of a Buck DC-DC converter at 15 times the value of the filter inductance

Similar studies were made for two more cases of modulation coefficient values D - D = 0.3 and D = 0.7. The purpose is to check whether these dependencies are observed in these two additional options. D values are chosen in view of the fact that they are not practically larger or smaller than them, in view of a number of limitations.

Figure 2.15 shows the results for the output voltage form (V (n003 for a circuit with ideal elements, and V (n008 for a circuit with real elements);

It can be seen that at the value of the coefficient D = 0.3, the amplitude of the oscillations of the output voltage is significantly smaller than when D = 0.5. On the other hand, the duration of the transition process is at least twice less than the initial value of D.
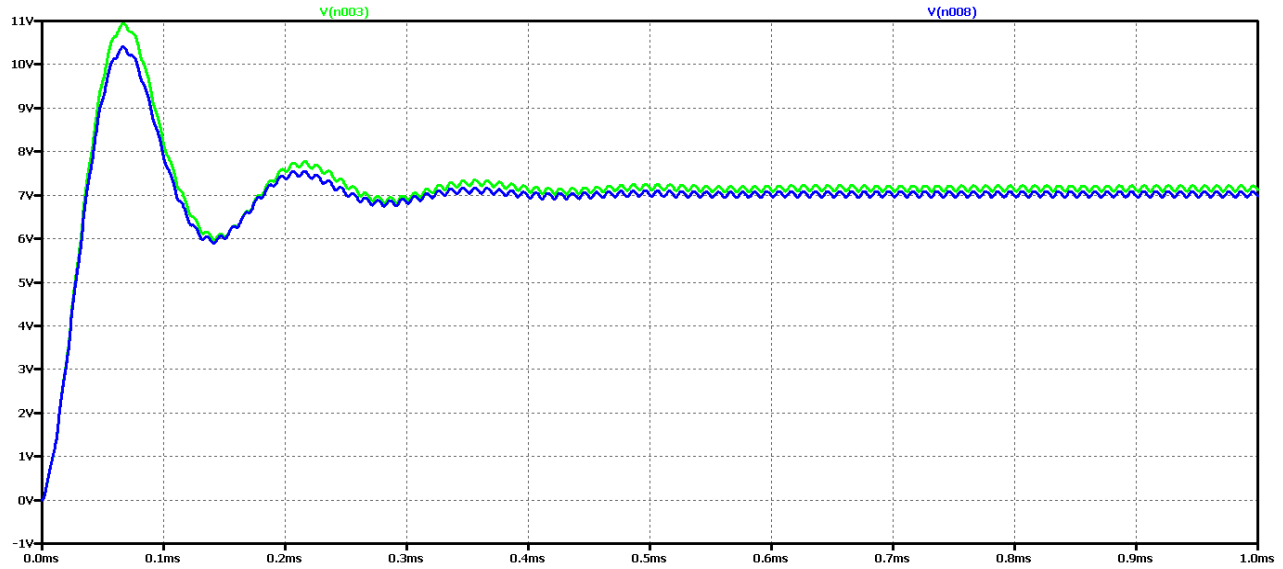
Figure 2.15 Simulation results of a Buck DC-DC converter

Again, the difference between the results with the real and the ideal elements is that with the ideal circuit the steady-state output voltage is higher and the oscillation amplitude is larger with less attenuation. In both cases it is an oscillatory type of transient process that is not desirable in practice due to the long transient process and poor dynamic properties of the scheme.

Figure 2.16 shows the results of Fourier transform (FFT analysis) of the output voltage.
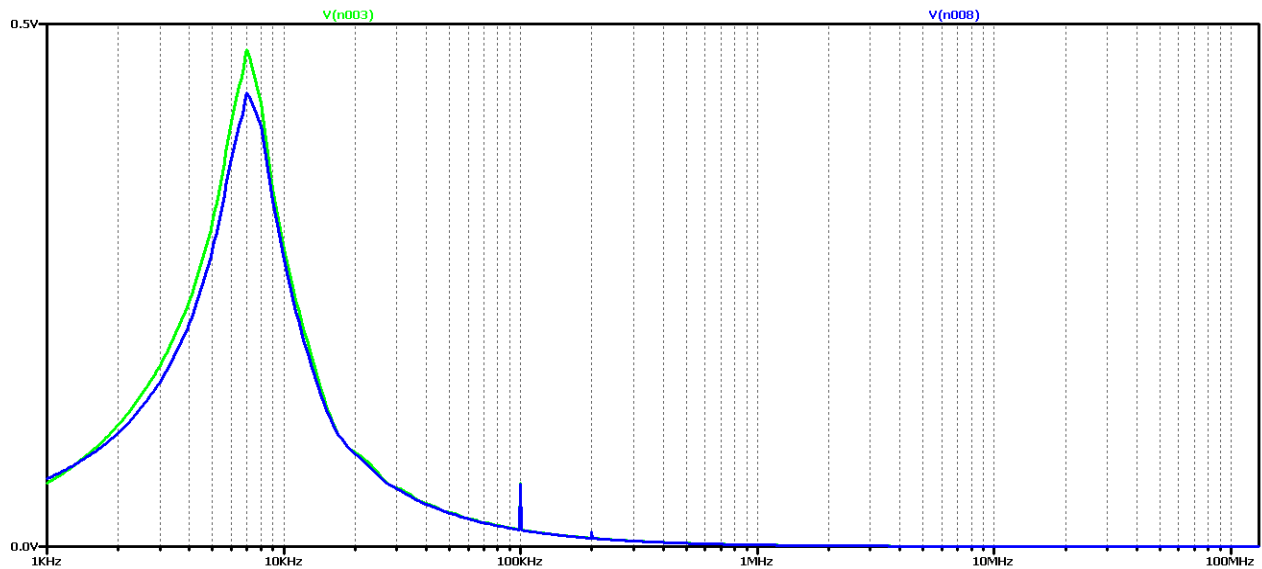
Figure 2.16 FFT analysis of the output voltage of a Buck DC-DC converter

It can be seen that the diagram again has a pronounced maximum at about 10kHz and a harmonic at 100kHz (operating frequency). Unlike the previous case, there is an additional harmonic at twice the frequency of the working one. Obviously, this diagram corresponds to the oscillatory type of the transition process.

Now let's try to achieve aperiodic transient by increasing the value of the filter inductance 5 times. The value of the filter capacitor will not change so as not to increase the ripple of the output voltage.
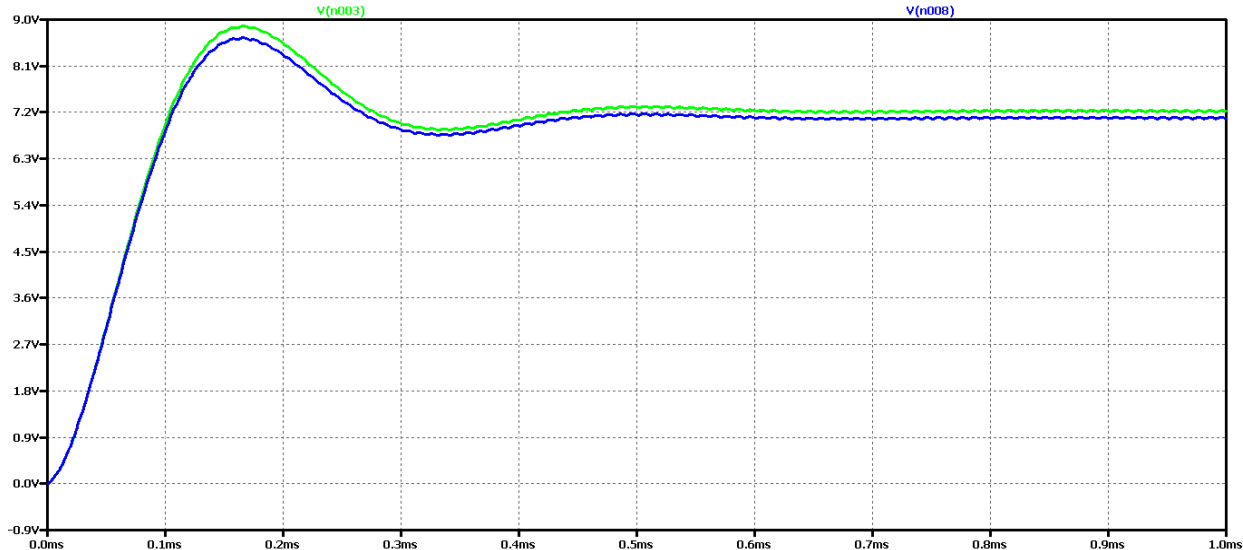
Figure 2.17 Simulation results of a Buck DC-DC converter with 5 times the value of the filter inductance
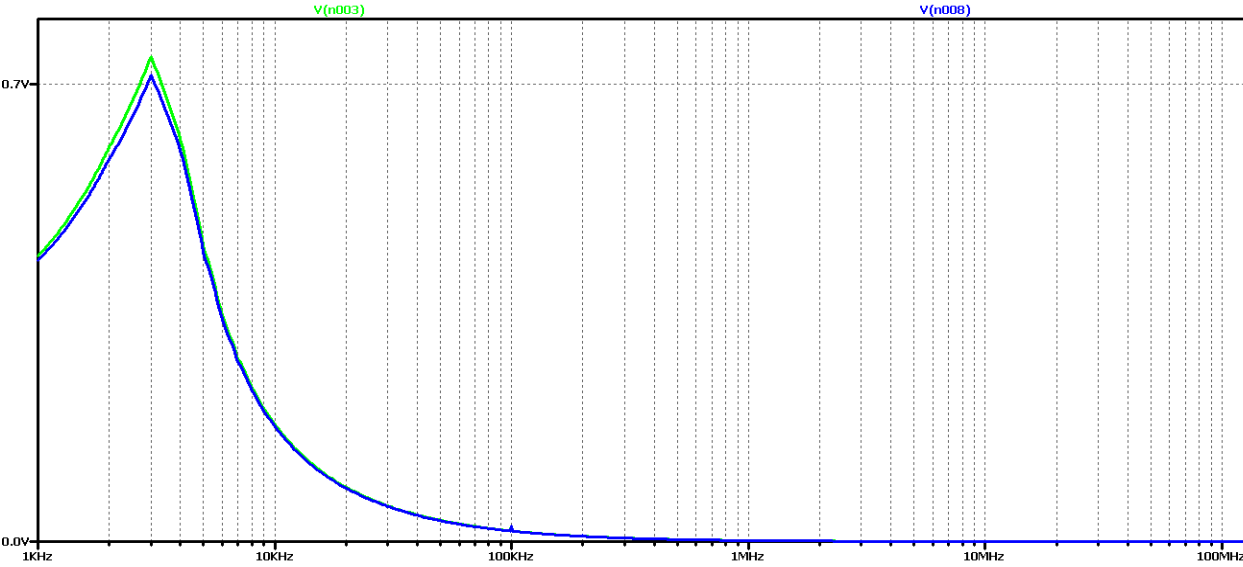
Figure 2.18 FFT analysis of the output voltage of a Buck DC-DC converter at 5 times the value of the filter inductance

25

It is seen that as the filter inductance increases, the oscillations in the output voltage are reduced. FFT analysis shows that the value of the harmonic with the control frequency decreases significantly compared to the previous case considered. On the other hand, there is a maximum harmonic frequency of about 2 kHz.

Now let's again increase the value of the filter inductance 10 times. In this way, we should achieve an aperiodic transition process or closer to it than the previous one.
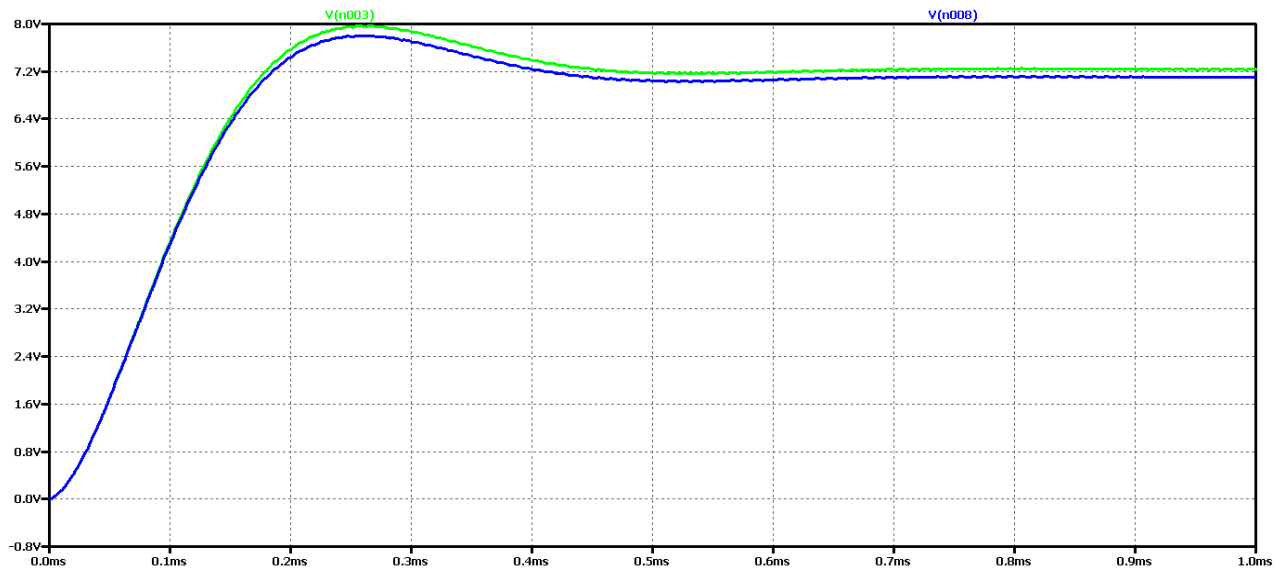
Figure 2.19 Simulation results of a Buck DC-DC converter at 10 times the value of the filter inductance

Increasing the filter inductance can be seen to significantly reduce the oscillations of the output voltage, and to a large extent the form is close to aperiodic. Low frequency and low amplitude oscillations are observed. FFT analysis shows that the value of the harmonic with the control frequency is very small compared to the previous case considered. On the other hand, the harmonic at a frequency of about 1 kHz has a maximum value, that is, the output voltage can largely be considered to be constant with very small pulsations and deviations when setting the

mode.
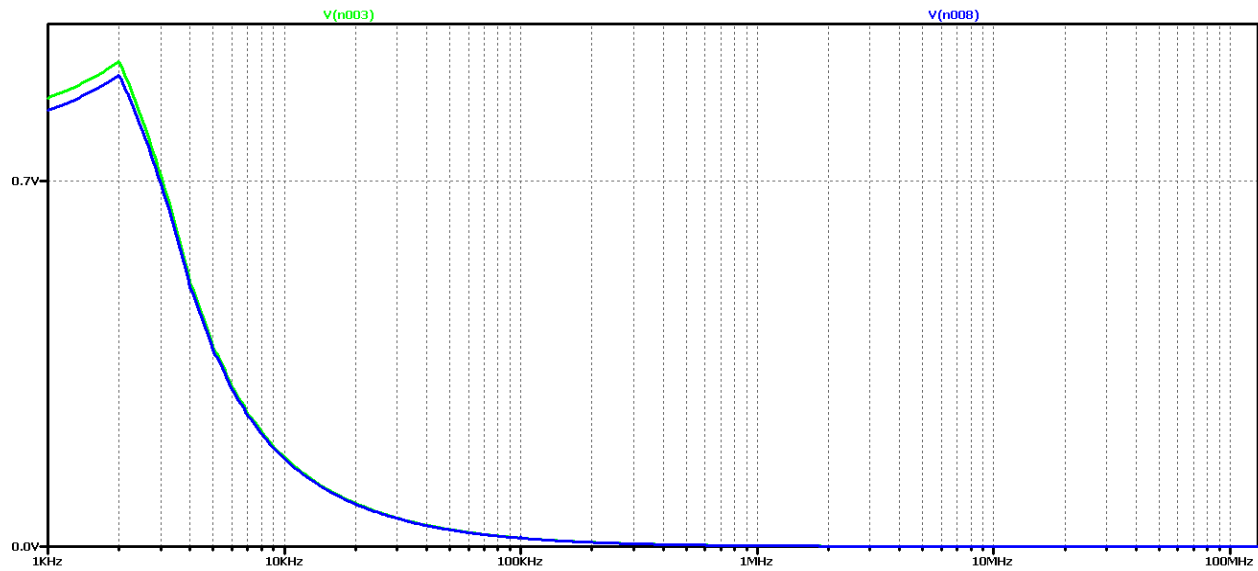
Figure 2.20 FFT analysis of the output voltage of a Buck DC-DC converter at 10 times the value of the filter inductance

For a more accurate examination of the results of the FFT analysis of the output voltage of Figure 2.21 is an increase for frequencies close to the operating frequency. This harmonic can be seen to have negligible value, and in some practical cases where we do not need high precision or there are limitations related to the value of the filter inductance, it can be assumed that we have in practice the required aperiodic transient.
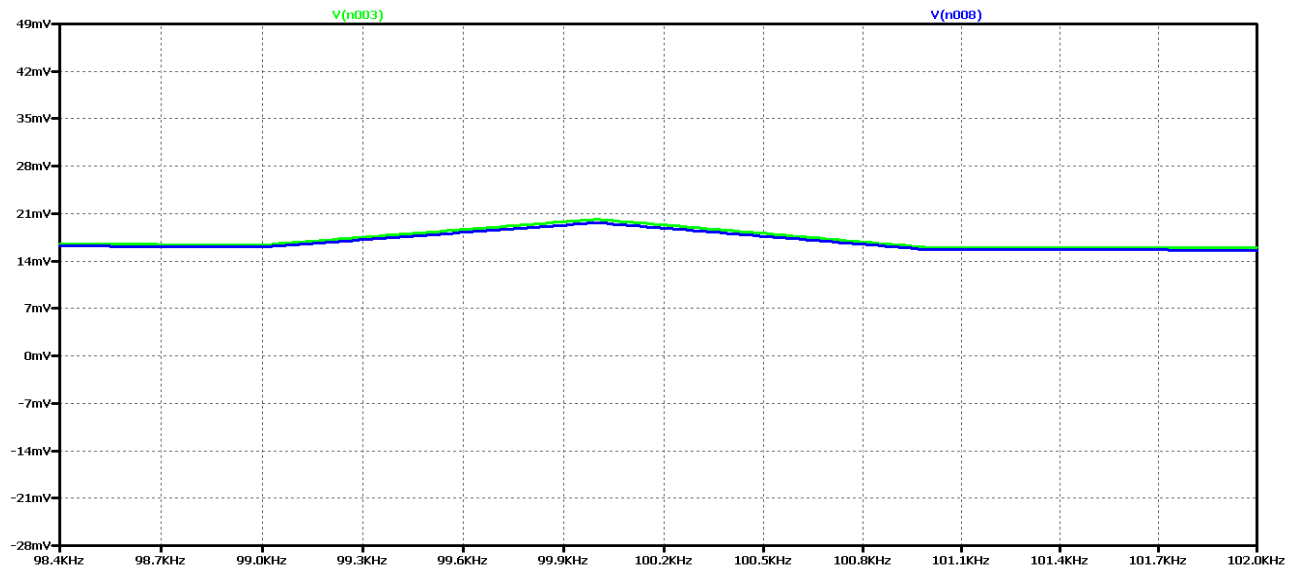
Figure 2.21 FFT analysis of the output voltage of a Buck DC-DC converter, at 10 times the value of the filter inductance for frequencies close to the control frequency

The last experiment is to increase the value of the filter inductance 15 times. Figure 2.22 shows the output voltage form in this case. Obviously, we have achieved aperiodic mode with the best possible dynamic performance compared to the previous variants. In practice, in 0.6 ms we have the mode setup and transient startup completed. In Figure 2.23 shows the results of the FFT analysis of the output voltage in both cases - of a converter with ideal and real circuit elements.
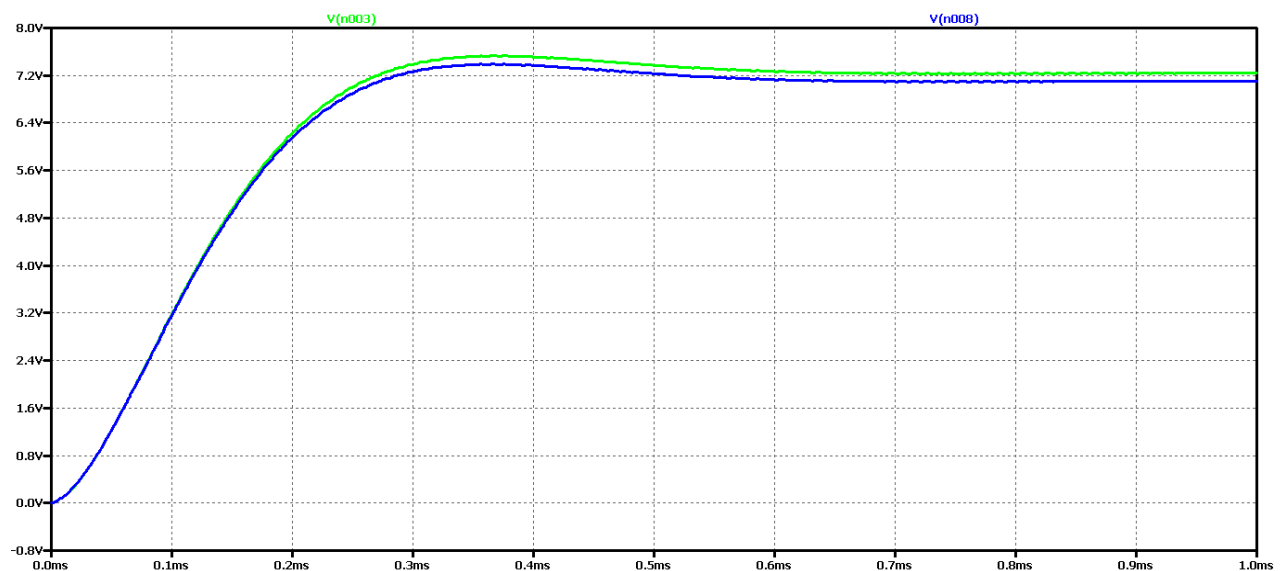
Figure 2.22 Simulation results of a Buck DC-DC converter at 15 times the value of the filter inductance

28

There is no deformation of the characteristic around the operating frequency, which was characteristic of previous cases. In addition, the value of the permanent ingredient again is higher than in previous cases, which is a sign of an aperiodic transient start-up process.
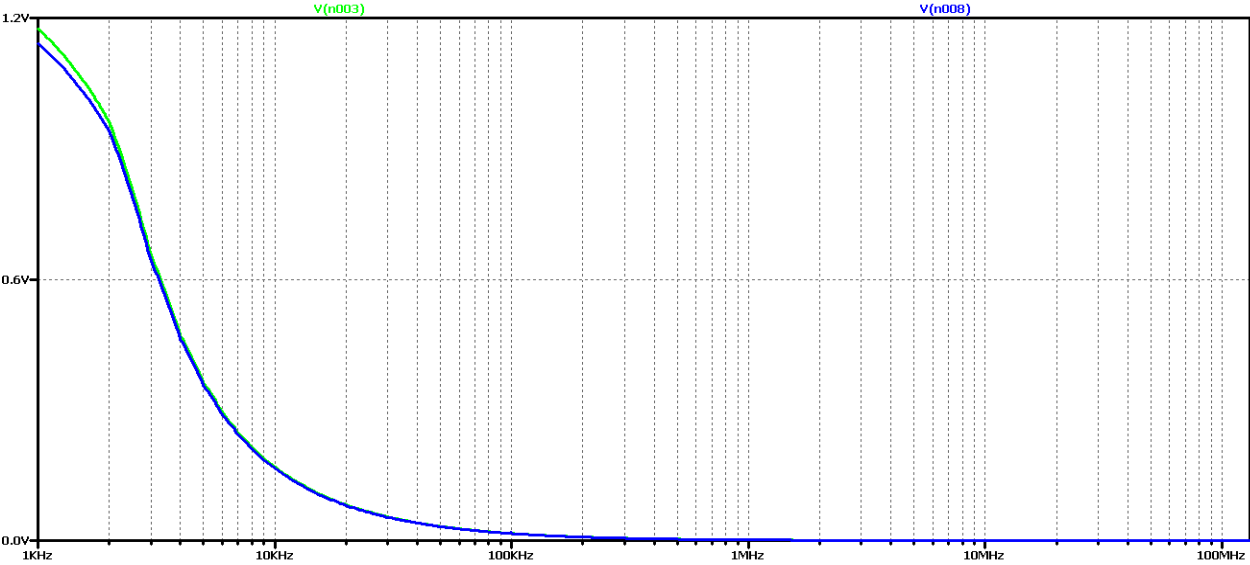
Figure 2.23 FFT analysis of the output voltage of a Buck DC-DC converter, at 15 times the value of the filter inductance

Similar studies have been made for another case of modulation coefficient values D –D = 0.7. The purpose is to verify that these dependencies are also observed in this additional variant.

It can be seen that at the value of the coefficient D = 0.7, the amplitude of the oscillations of the output voltage is greater than the case when D = 0.5. On the other hand, the duration of the transition process is commensurate with the initial value of D.
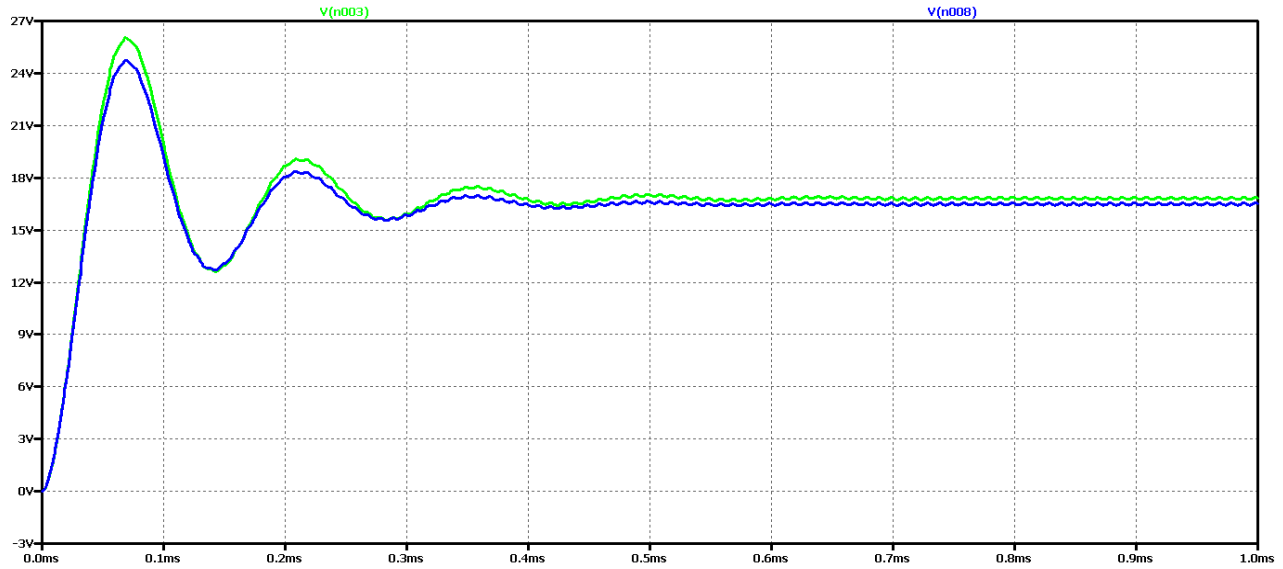
Figure 2.24 Simulation results of a Buck DC-DC converter

Again, the difference between the results with the real and the ideal elements is that with the ideal circuit the steady-state output voltage is higher and the oscillation amplitude is larger with less attenuation. In both cases it is an oscillatory type of transient process that is not desirable in practice due to the long transient process and poor dynamic properties of the scheme.

Figure 2.25 shows the results of the Fourier transform (FFT analysis) of the output voltage.
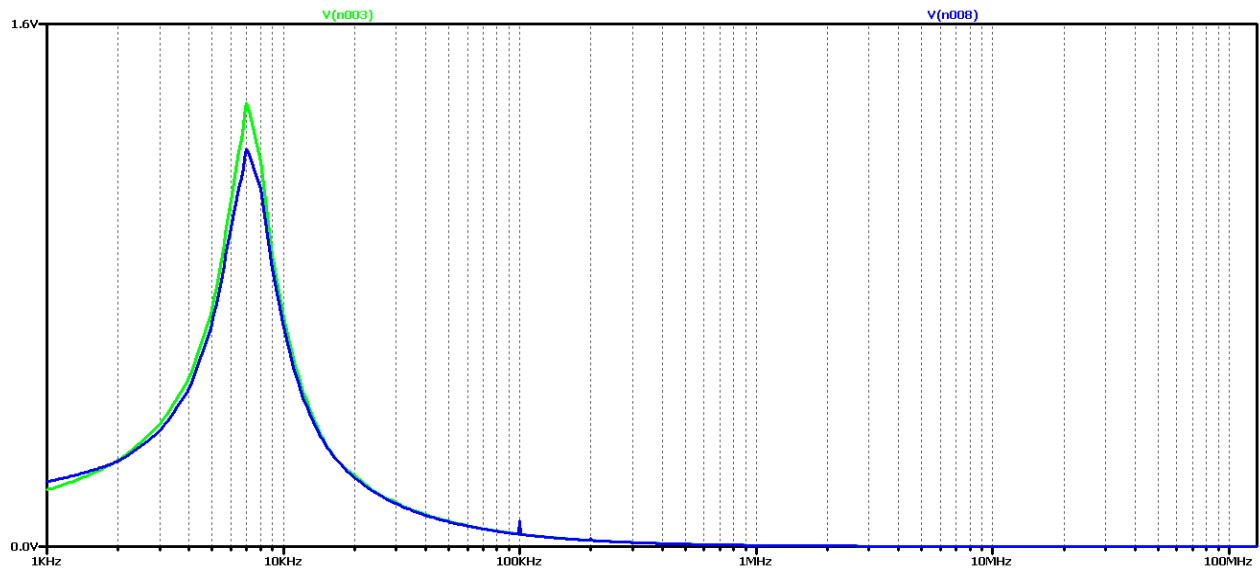
Figure 2.25 FFT analysis of the output voltage of a Buck DC-DC converter

It can be seen that the diagram again has a pronounced maximum at about 7kHz and a harmonic at 100kHz (operating frequency). Obviously, this diagram corresponds to the oscillatory type of the transition process.

Now let's try to achieve aperiodic transient by increasing the value of the filter inductance 5 times. The value of the filter capacitor will not change so as not to increase the ripple of the output voltage.
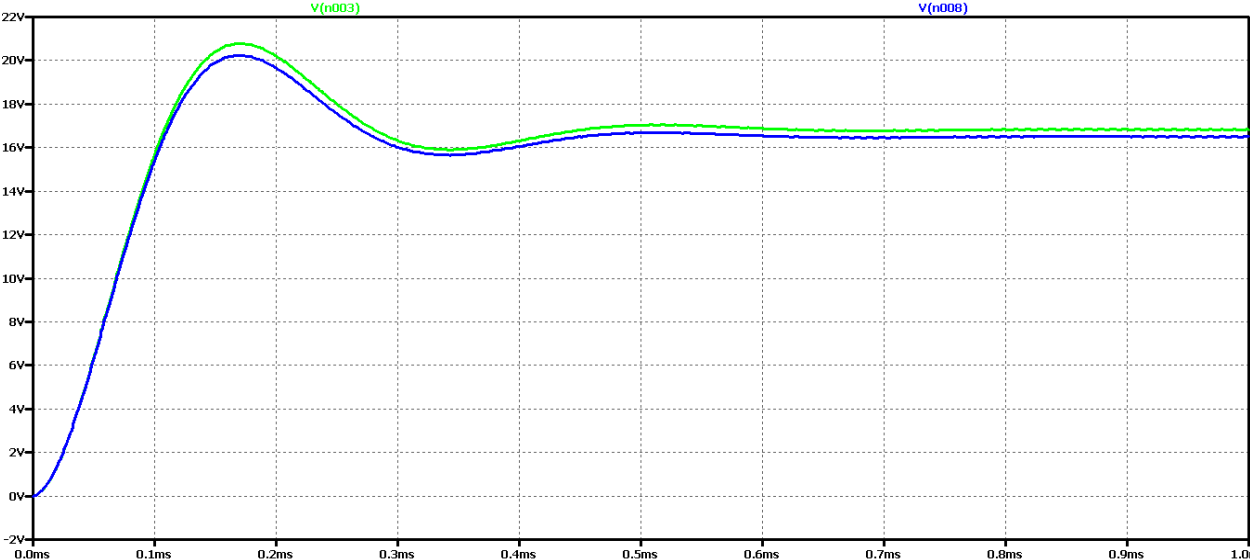
Figure 2.26 Simulation results of a Buck DC-DC converter with 5 times the value of the filter inductance
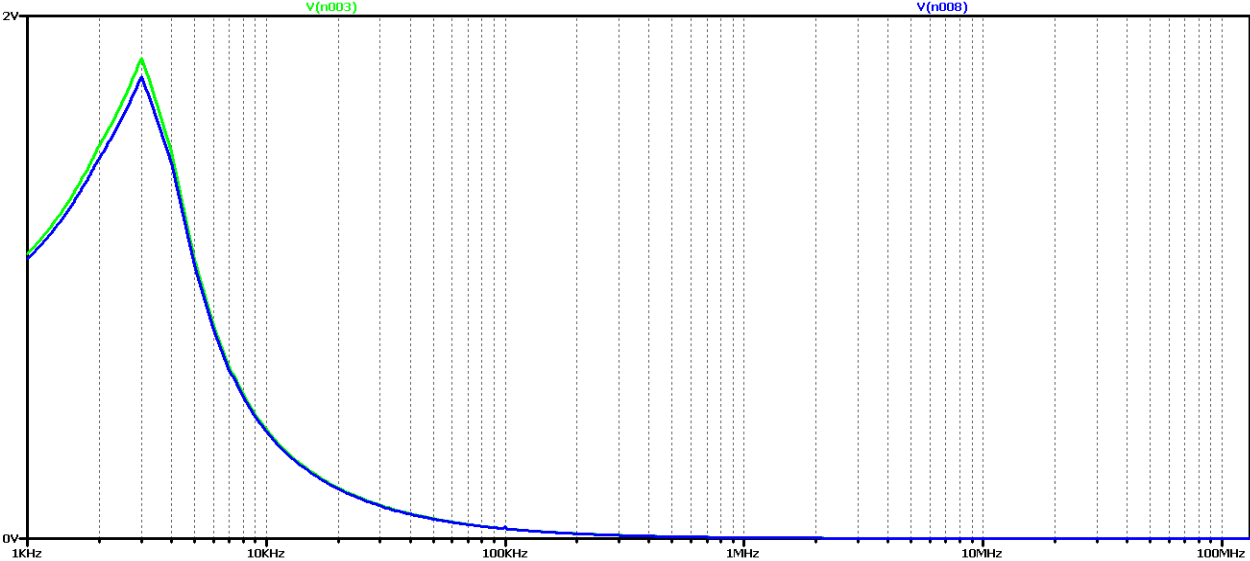
Figure 2.27 FFT analysis of the output voltage of a Buck DC-DC converter at 5 times the value of the filter inductance

31

It is seen that as the filter inductance increases, the oscillations in the output voltage are reduced. FFT analysis shows that the value of the harmonic with the control frequency decreases significantly compared to the previous case considered. On the other hand, there is a maximum harmonic frequency of about 2 kHz.

Now let's again increase the value of the filter inductance 10 times. In this way, we should achieve an aperiodic transition process or closer to it than the previous one.
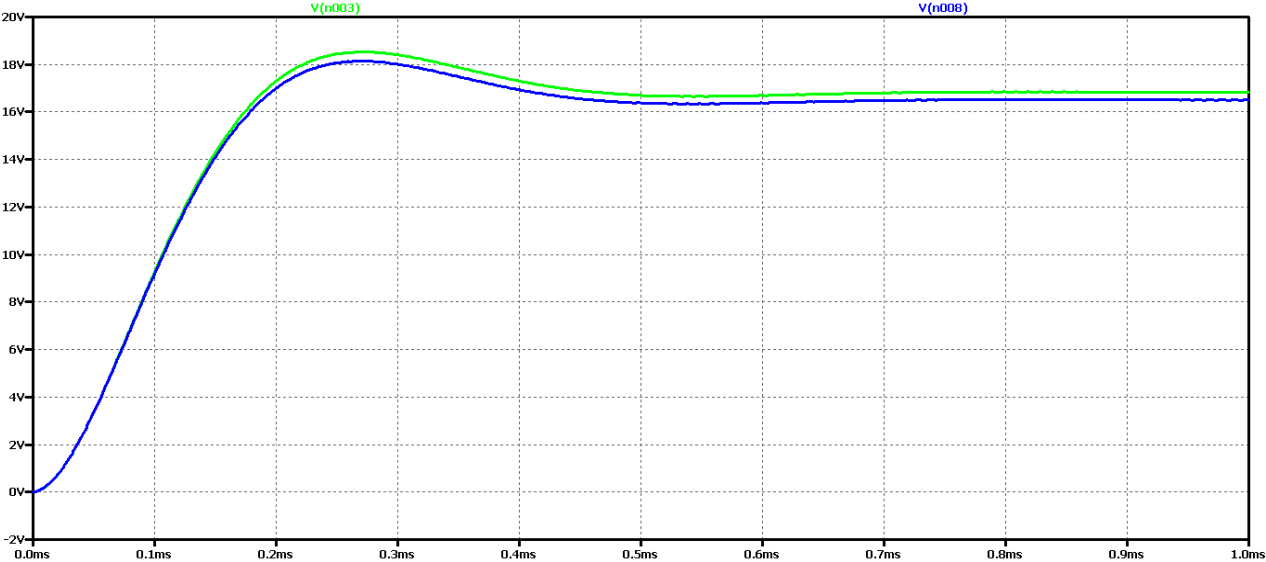
Figure 2.28 Simulation results of a Buck DC-DC converter at 10 times the value of the filter inductance

Increasing the filter inductance can be seen to significantly reduce the oscillations of the output voltage, and to a large extent the form is close to aperiodic. Low frequency and low amplitude oscillations are observed. FFT analysis shows that the value of the harmonic with the control frequency is very small compared to the previous case considered. On the other hand, the harmonic at a frequency of about 1 kHz has a maximum value, that is, the output voltage can largely be considered to be constant with very small pulsations and deviations when setting the mode.
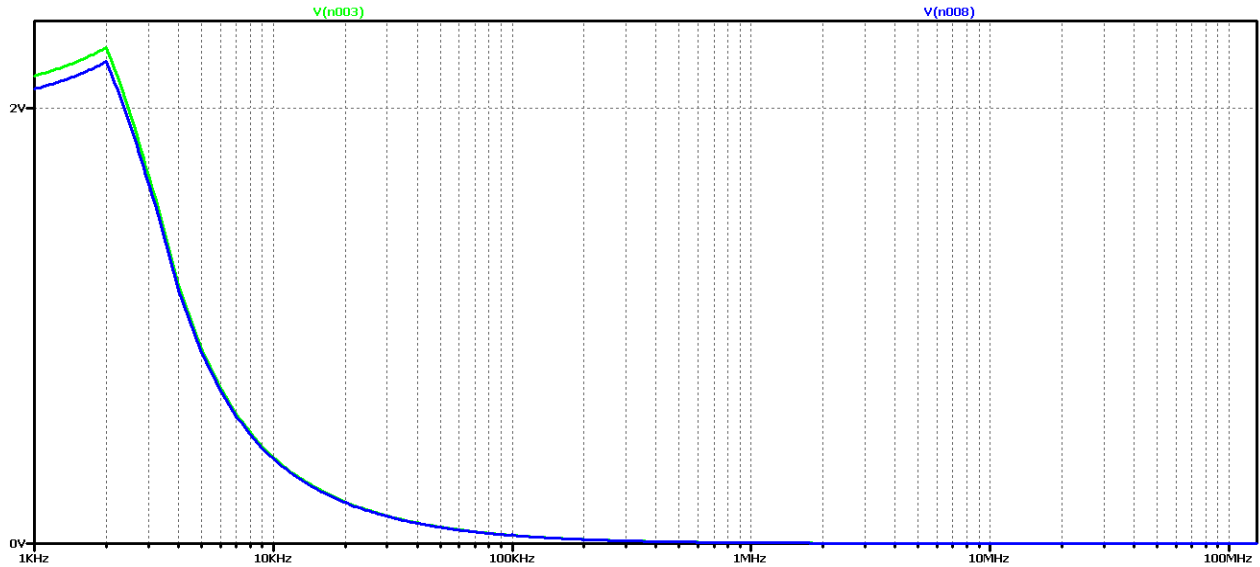
Figure 2.29 FFT analysis of the output voltage of a Buck DC-DC converter at 10 times the value of the filter inductance

For a more accurate examination of the results of the FFT analysis of the output voltage of Figure 2.30 is an increase for frequencies close to the operating frequency. This harmonic can be seen to have negligible value, and in some practical cases where we do not need high precision or there are limitations related to the value of the filter inductance, it can be assumed that we have in practice the required aperiodic transient.
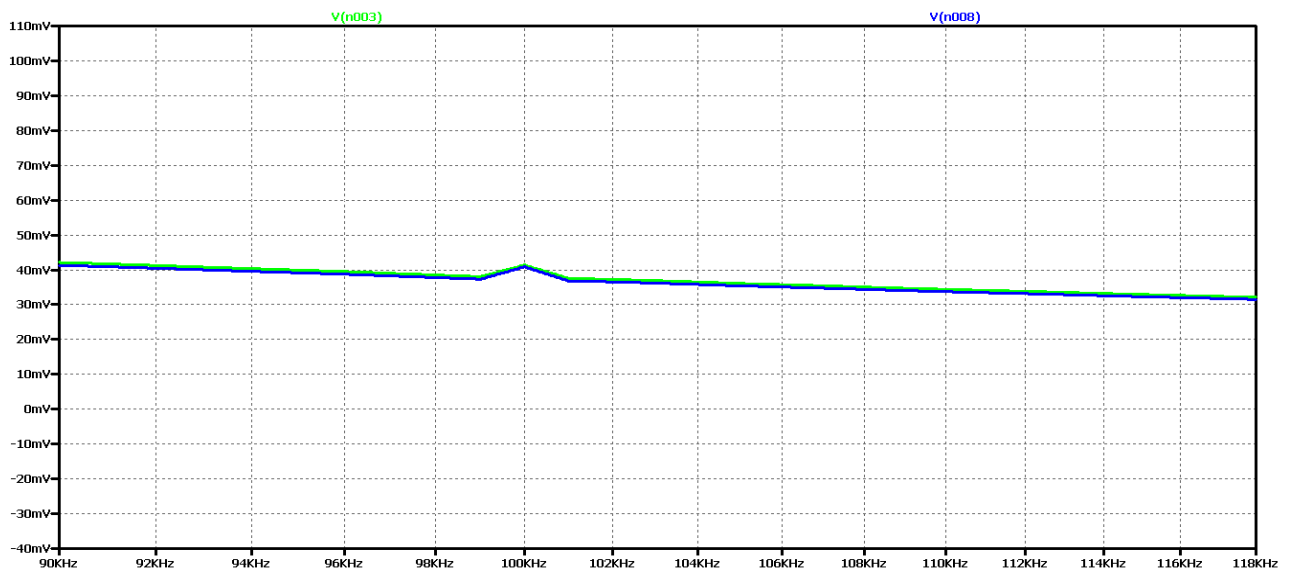
Figure 2.30 FFT analysis of the output voltage of the DC-DC converter at 10 times the value of the filter inductance for frequencies close to the control frequency

33

The last experiment is to increase the value of the filter inductance 15 times. Figure 2.31 shows the output voltage form in this case. Obviously, we have achieved aperiodic mode with the best possible dynamic performance compared to the previous variants. In practice, in 0.6 ms we have the mode setup and transient startup completed. In Figure 2.32 shows the results of the FFT analysis of the output voltage in both cases - of a converter with ideal and real circuit elements.
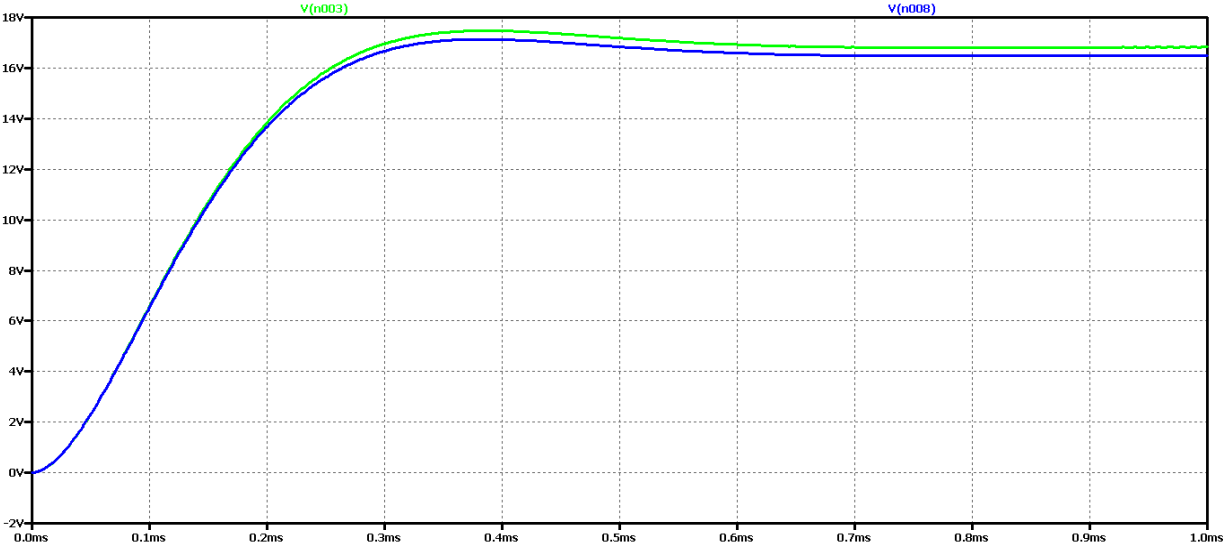
Figure 2.31 Simulation results of a DC-DC converter at 15 times the value of the filter inductance

There is no deformation of the characteristic around the operating frequency, which was characteristic of previous cases. In addition, the value of the permanent ingredient again is higher than in previous cases, which is a sign of an aperiodic transient start-up process.
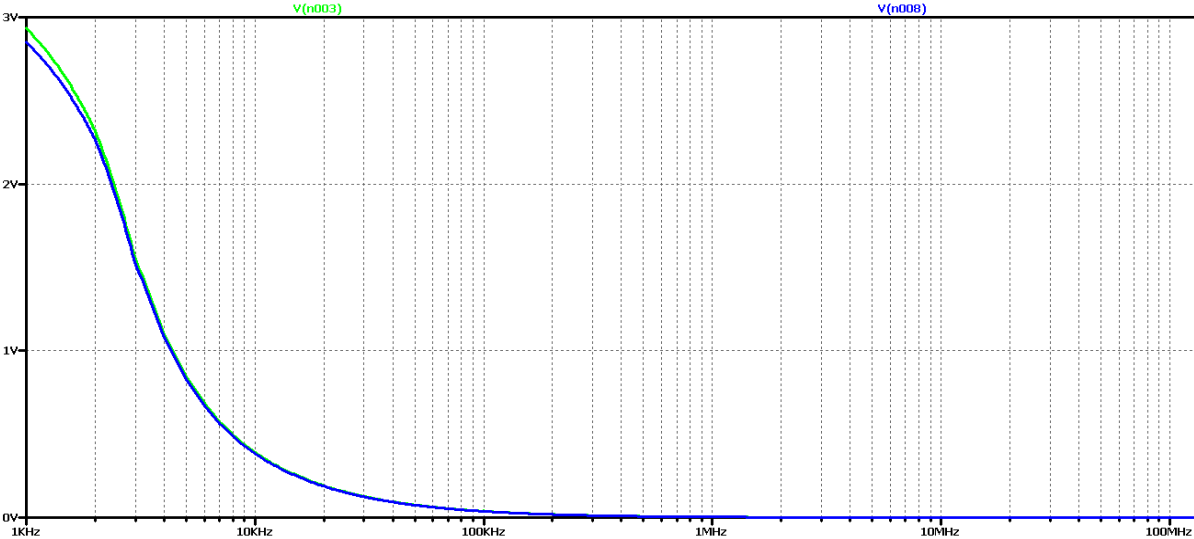
Figure 2.32 FFT analysis of the output voltage of a DC-DC converter at 15 times the value of the filter inductance

Let's compare the deviations from the established mode for the smallest value of the filter inductance in the three cases of modulation coefficient. In the first case - Figure 2.6 the maximum deviation in the worst case using ideal elements is from 18.5V to 12V or a ratio of 1.54; in the second case - Figure 2.15 the maximum deviation in the most severe case using ideal elements is from 11V to 7V or a ratio of 1.57; in the third case - Figure 2.24 the maximum deviation in the worst case using ideal elements is from 26V to 16.5V or a ratio of 1.575. In this way, a slight dependence of the maximum deviation of the output voltage on the modulation coefficient is also established, its smallest value at $D = 0.5$.

2.6. MODELING AND SIMULATION STUDIES OF BOOST CONVERTER

For the purpose of the study, a model of a Boost DC-DC boost converter in the LTspice medium was made. A standard methodology was used to determine the initial values of the circuit elements. The purpose of the study in this case is to find a connection between the actual form of the output voltage and the one obtained by using FFT analysis in order to achieve a periodic transient and the minimum possible duration of the transient. The studies were conducted in cases of continuous current mode, which is more commonly used in practice. Further studies are expected to summarize the results and the interruptible current regime. In Figure 2.33 shows a boost converter model. Examples of converter with ideal (schematic above) and real elements (diagram below) are considered. The purpose is to determine whether there is a significant difference in the nature and duration of the transients in the scheme.
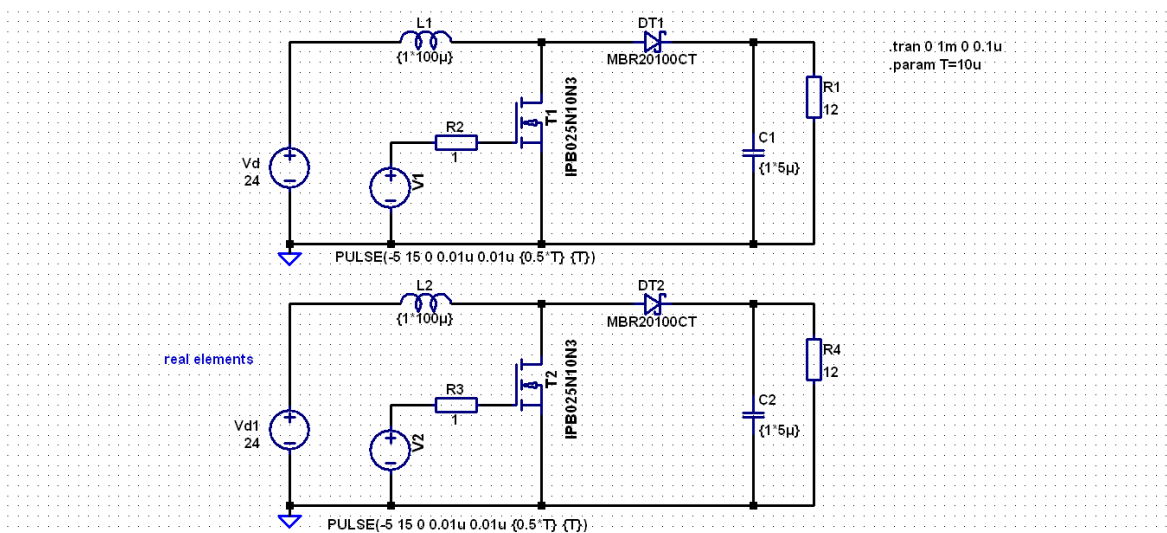
Figure 2.33 A simulation model of a Boost DC-DC converter

The following values of the circuit parameters are used: Input voltage Uin = 24V; Operating frequency f = 100kHz; filter inductor capacitor L = 100uH, load resistance 12 Ω. The purpose of the study is to change the value of the fill factor D (initial value 0.5) and due to the peculiarities of the operation of the filter capacitor circuit (initial value 5uF).

Figure 2.34 shows the results for the output voltage form (V (n003 for a circuit with ideal elements and V (n008 for a circuit with real elements);
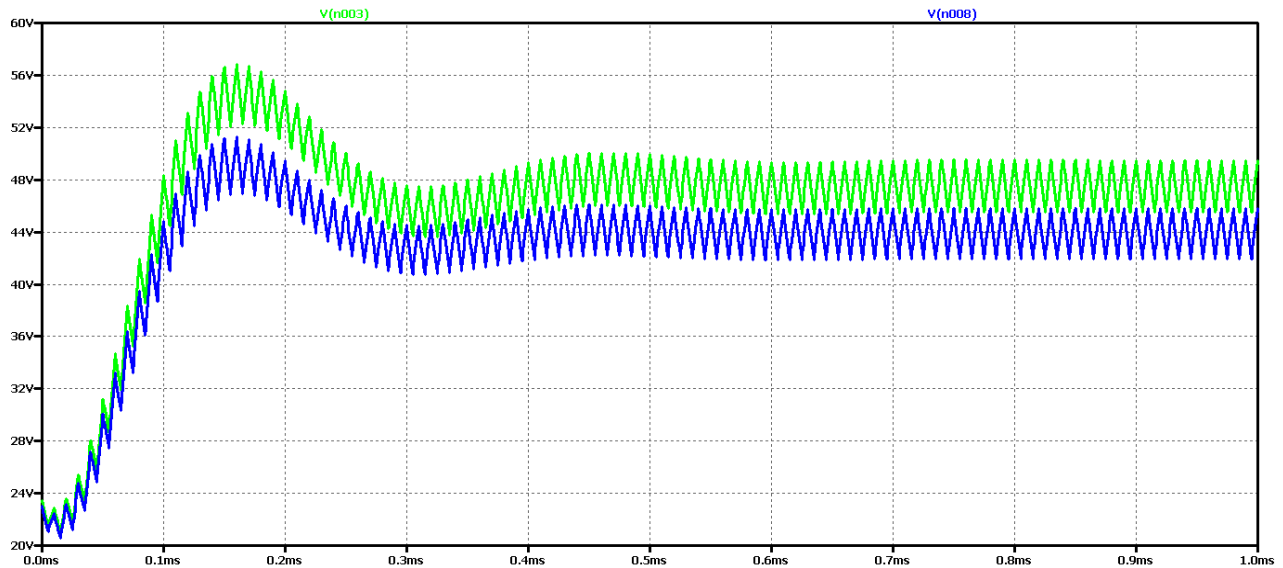
Figure 2.34 Simulation results of a Boost DC-DC converter

It can be seen that the difference between the results with the real and the ideal elements is that with the ideal circuit the output voltage in the steady state is higher and the amplitude of the oscillations is larger with less attenuation. On the other hand, the difference here is larger than at the output voltage of the lowering converter - that is, here the influence of the parasitic values of the elements as an absolute value is greater. In both cases it is an oscillatory type of transient process that is not desirable in practice due to the long transient process and poor dynamic properties of the scheme. This is eliminated with the presence of a soft start-up, but nevertheless this type of transient creates difficulties in the synthesis and setup of the controller. On the other hand, the parasitic elements in the real circuit reduce oscillations but impair the efficiency of the converters. Figure 2.35 shows the results of Fourier transform (FFT analysis) of the output voltage.
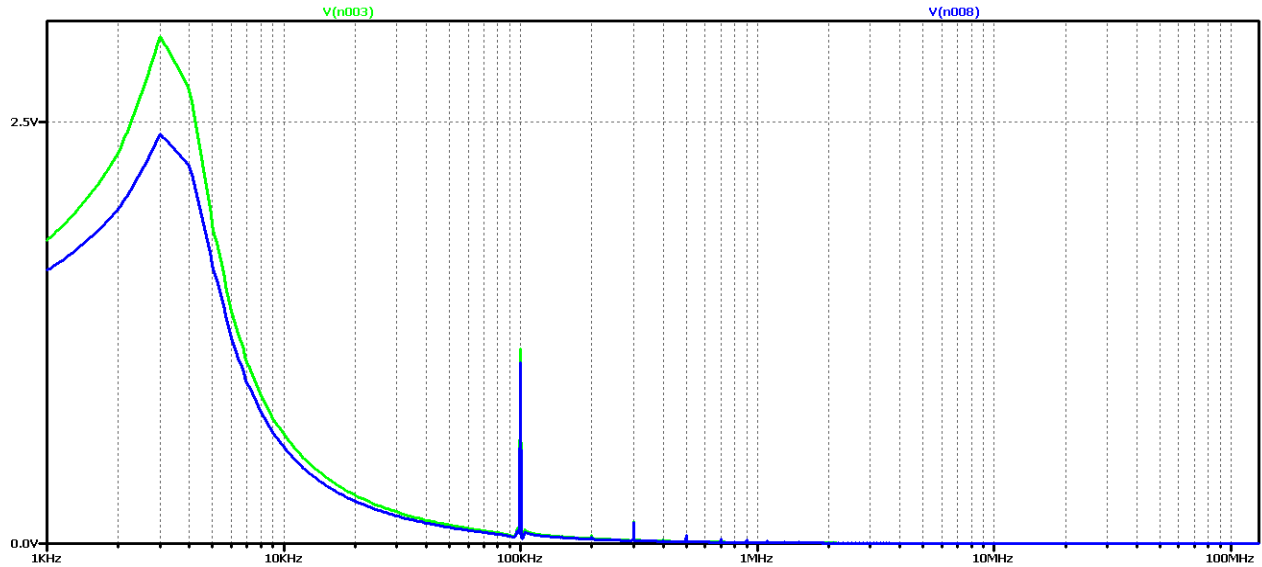
Figure 2.35 FFT analysis of the output voltage of a Boost DC-DC converter

It can be seen that the chart has a pronounced maximum at about 3kHz and the highest harmonic at 100kHz (operating frequency). Unlike the previous study, a number of harmonics with frequencies multiple of the controller are observed here. Obviously, this diagram corresponds to the oscillatory type of the transition process.

Now let's try to achieve a periodic transient by increasing the value of the filter capacitor 5 times. The value of the filter inductance will not change so as not to increase the output voltage drop-off at the beginning of the establishment process.
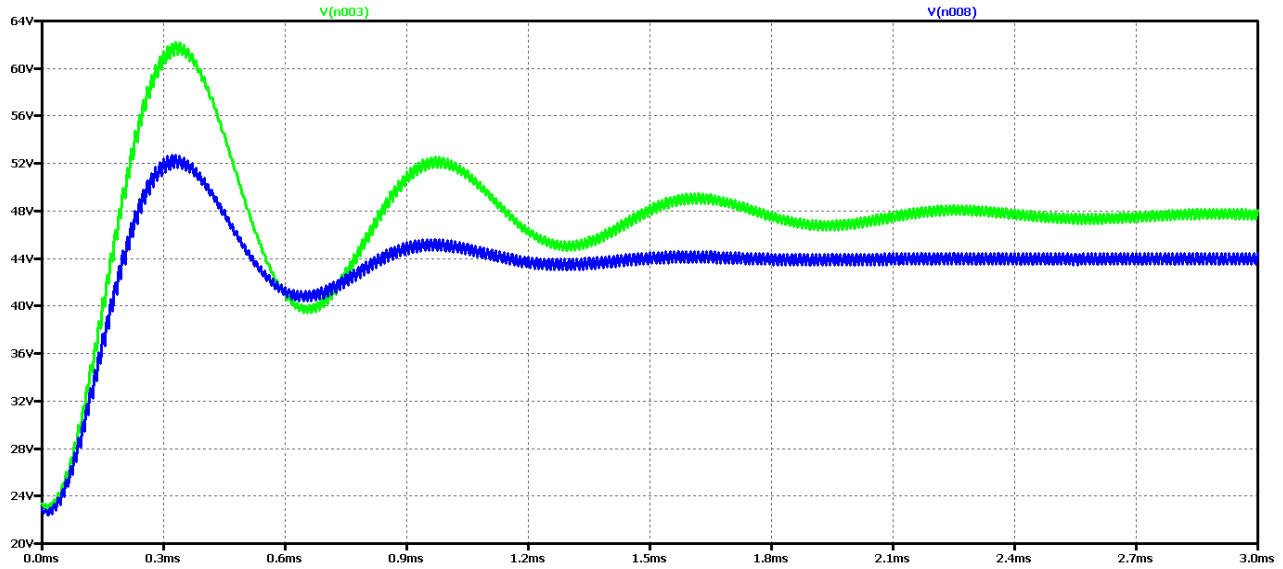
Figure 2.36 Simulation results of a Boost DC-DC converter at 5 times the filter capacity value

It is seen that as the filtering capacity increases, the oscillations in the output voltage setting, using real elements, decrease. On the other hand, with the ideal element scheme the process fluctuation even increases.
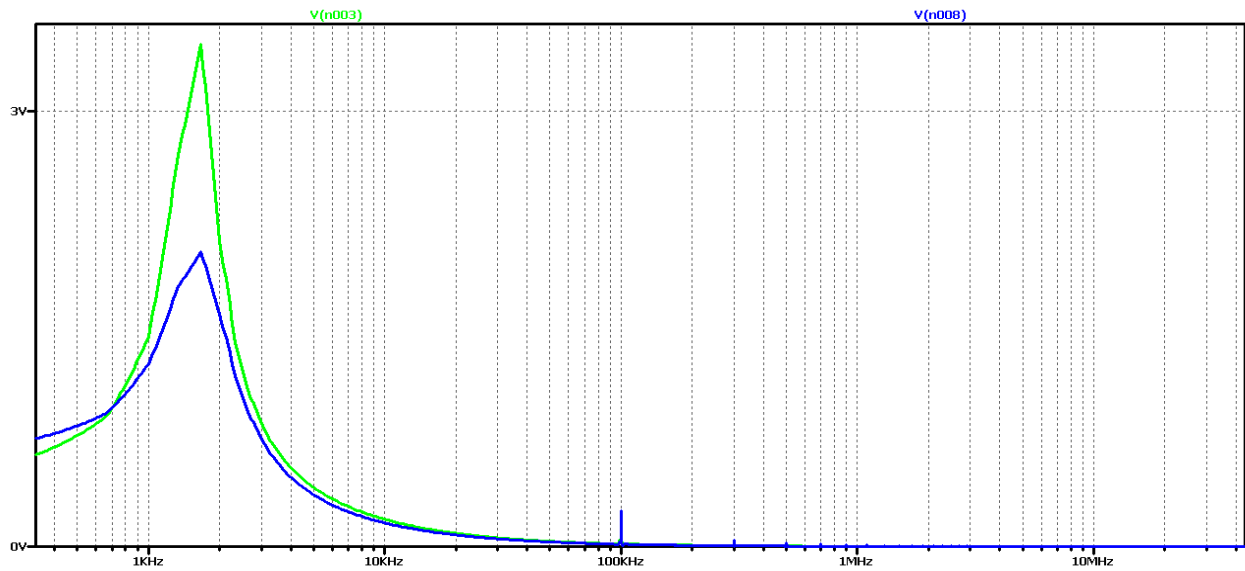
Figure 2.37 FFT analysis of the output voltage of a Boost DC-DC converter at 5 times the value of the filter capacitor

FFT analysis shows that the value of the harmonic with the control frequency decreases significantly compared to the previous case considered. The maximum value is harmonic at a

frequency of about 1.5 kHz and harmonics with a frequency multiple of the control frequency are still noticeable.

Now let's again increase the value of the filter capacity 10 times the initial value. In this way, we should achieve an aperiodic transition process or closer to it than the previous one.
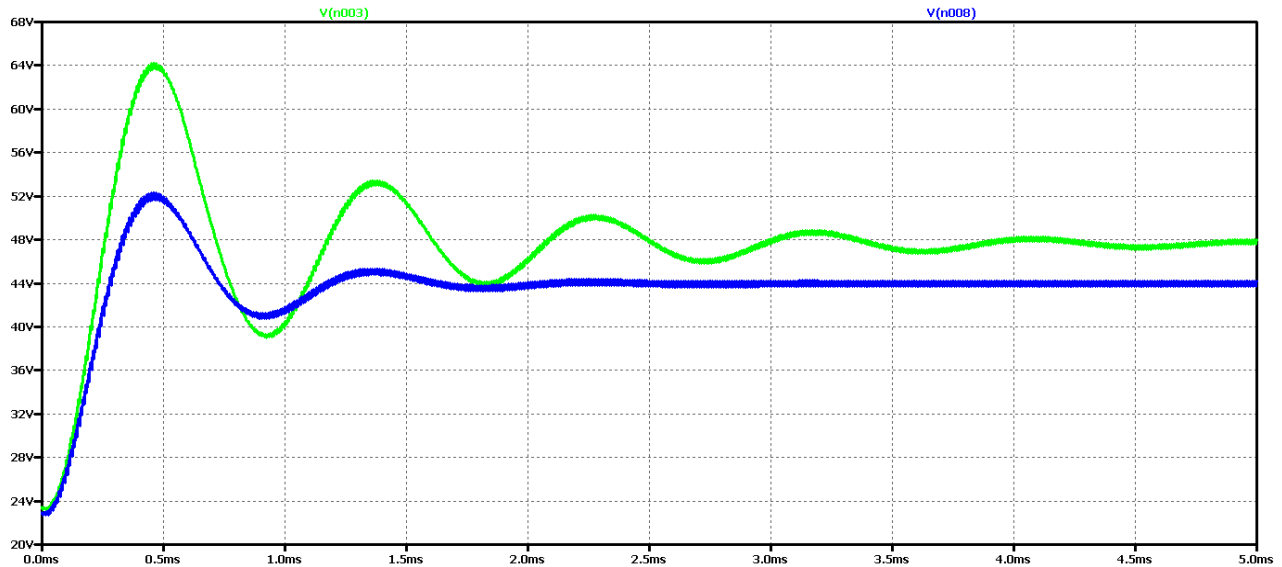
Figure 2.38 Simulation results of a Boost DC-DC converter at 10 times the value of the filter capacitor

Increasing the filter capacitor can be seen to significantly reduce oscillations in the output voltage, using real circuitry, and to a large extent the shape is close to aperiodic. Low frequency and low amplitude oscillations are observed. On the other hand, in the ideal element scheme, there is almost no change compared to the previous variant. FFT analysis shows that the value of the harmonic with the control frequency is very small compared to the previous case considered. On the other hand, there is a maximum value of a harmonic with a frequency of about 1 kHz, that is, the output voltage can largely be considered constant with very small pulsations and deviations when setting the mode.
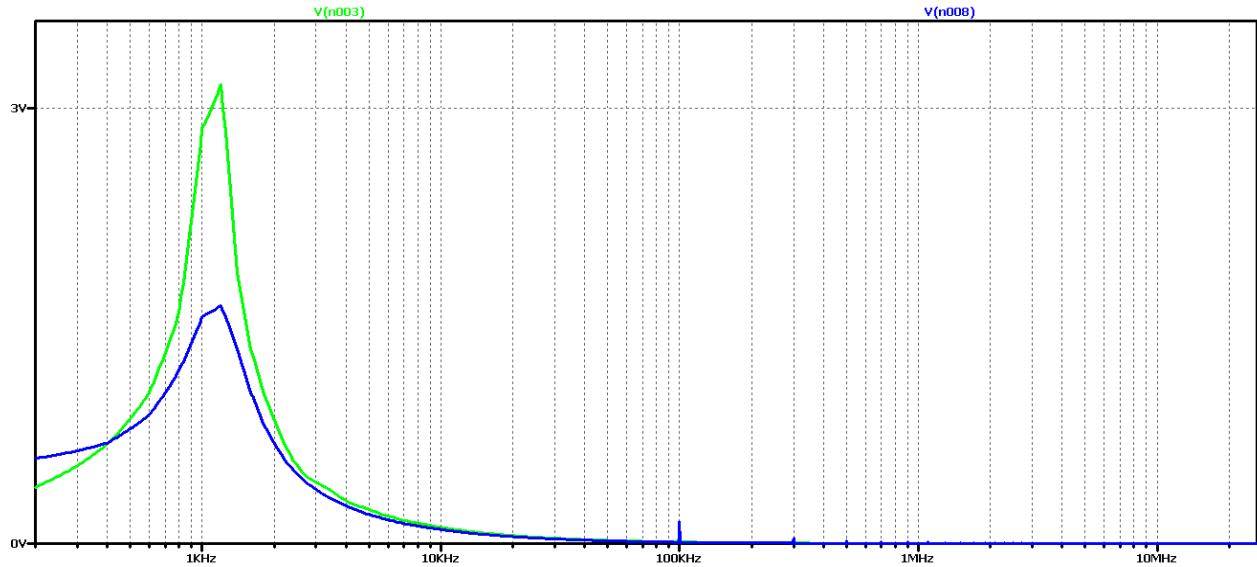
Figure 2.39 FFT analysis of the output voltage of a DC-DC converter at 10 times the value of the filter capacitor

For a more accurate examination of the results of the FFT analysis of the output voltage of Figure 2.40 is an increase for frequencies close to the operating frequency. This harmonic can be seen to have negligible value in real elements (curve in green) and in some practical cases where we do not need high precision or there are limitations related to the value of the filter capacitor, it can be assumed that in practice we have the required aperiodic transition.
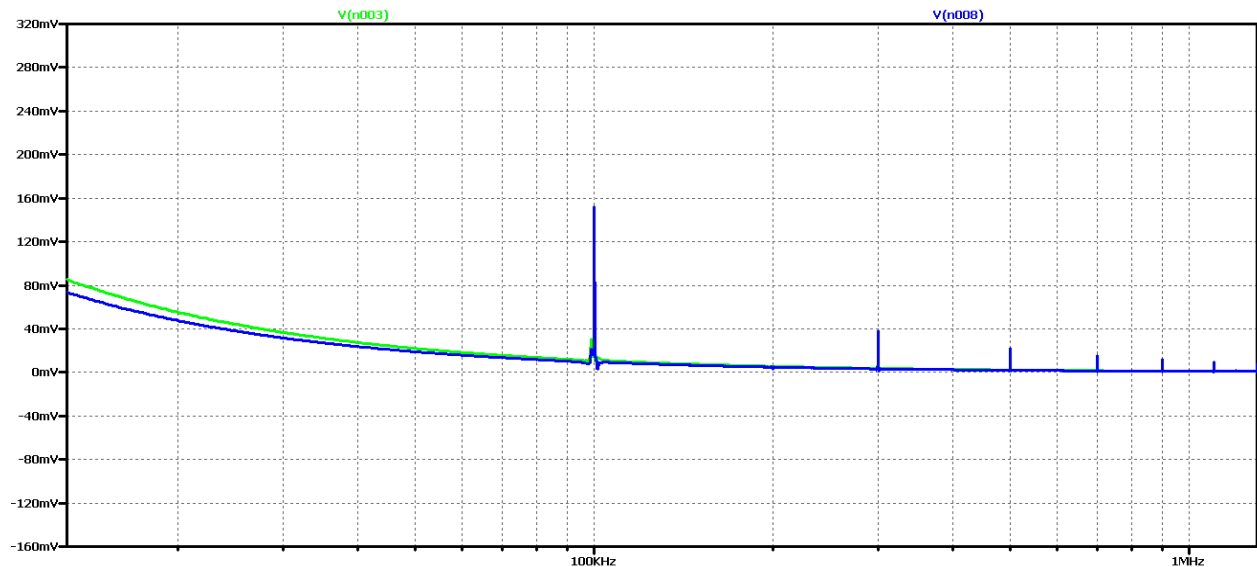
Figure 2.40 FFT analysis of the output voltage of a DC-DC converter at 10 times the value of the filter capacitor for frequencies close to the control frequency

However, for the case of real elements, the results of the analysis show a large number of harmonic ones.

Another experiment is to increase the value of the filter capacitor 15 times. Figure 2.41 shows the output voltage form in this case. Obviously, we have achieved a case close to the aperiodic regime with the best possible dynamic performance compared to the previous variants in the scheme with real elements. In practice, in 2 ms we have the mode setup and transient startup completed. Unfortunately, no change was seen in the ideal element scheme.
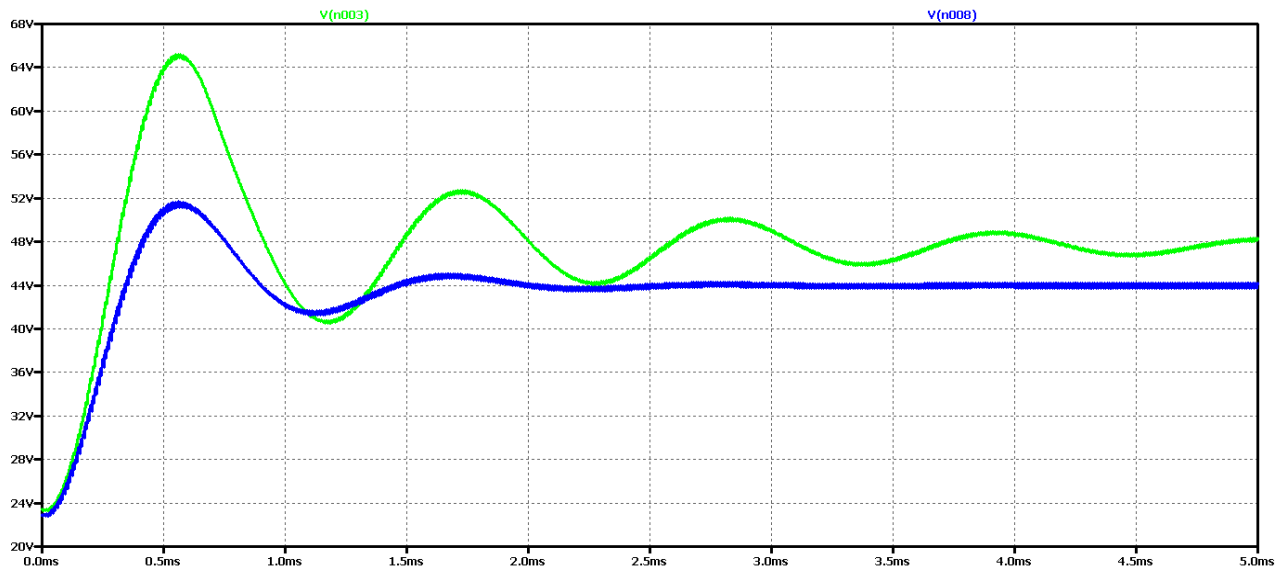
Figure 2.41 Simulation results of a Boost DC-DC converter at 15 times the value of the filter capacitor

In Figure 2.42 shows the results of the FFT analysis of the output voltage in both cases - of a converter with ideal and real circuit elements.

It can be seen here that we have the largest constant component compared to the previous cases, but there is still a deformation of the characteristic around the operating frequency, which was also characteristic of the previous cases.
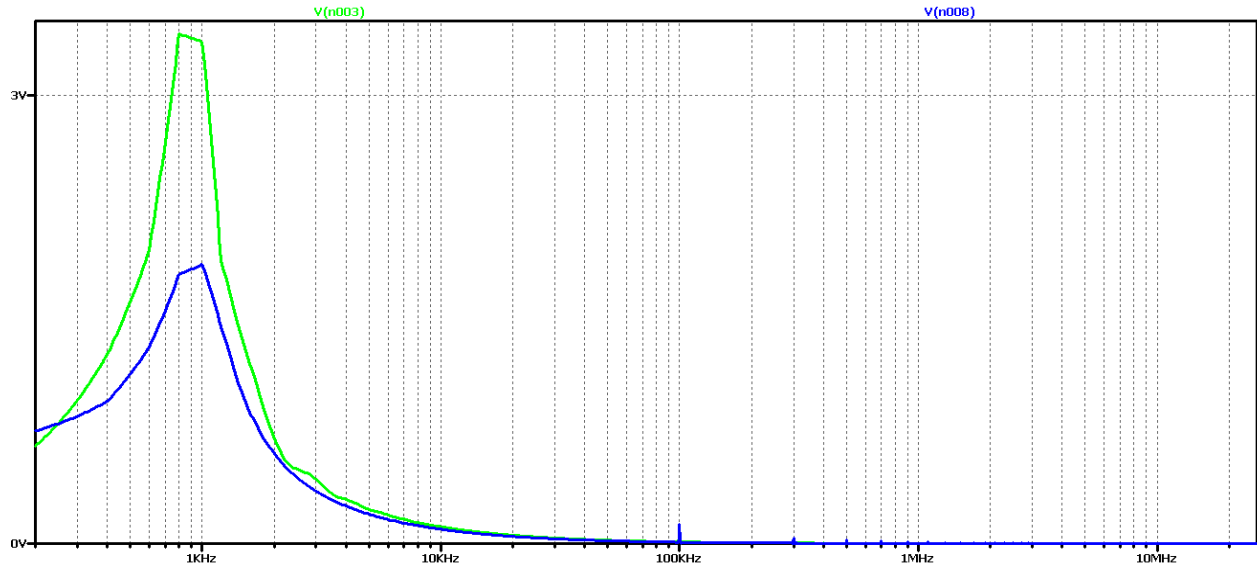
Figure 2.42 FFT analysis of the output voltage of a DC-DC converter at 15 times the value of the filter capacitor

Obviously with this value of filter inductance, regardless of the increase of the filter capacitor, no better transients will be obtained, the next experiment is to use model-based optimization to determine the values of the elements. The values of the filter inductance 500uH and the filter capacitor 2uF are obtained. To prevent the output voltage from falling off at the start of the process, a 5uF capacitor value is selected.

The results of the study are shown in Figure 2.43.
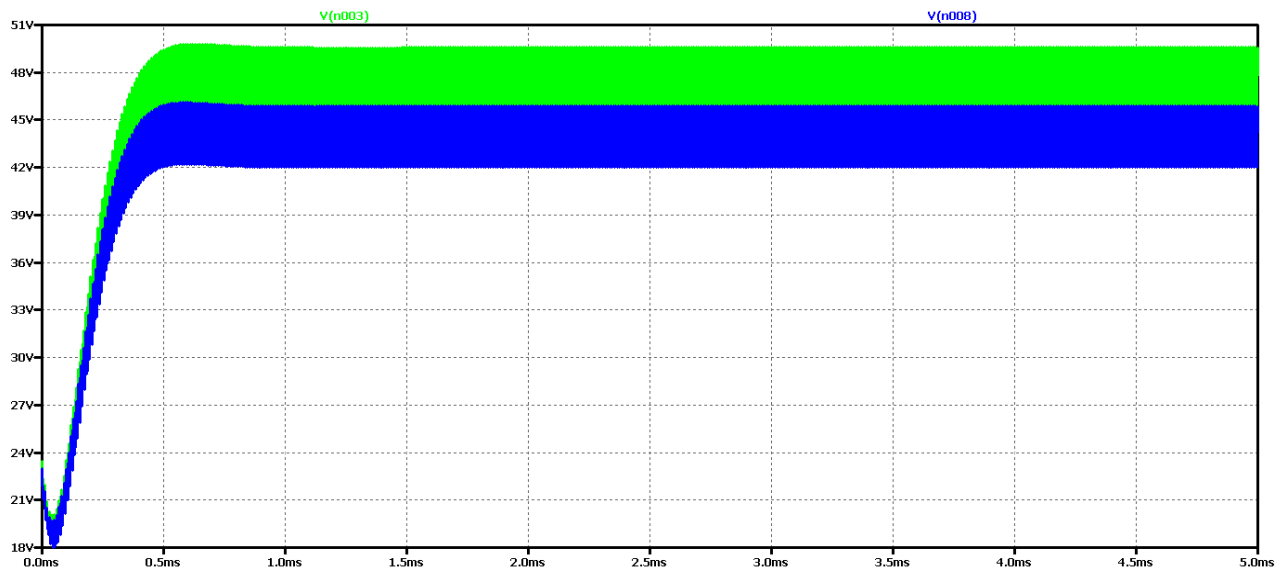
Figure 2.43 Output voltage of DC-DC converter at optimum values of filter elements

It is evident that the optimum values achieve the best dynamics - transient duration of 0.5 ms. On the other hand, due to the small value of the output capacitor, there is a slight drop in the output voltage.

In Figure 2.44 shows the results of Fourier transform (FFT analysis) of the output voltage. The presence of harmonic multiples of the control frequency can be seen due to the drop in output voltage. On the other hand, we have an aperiodic transition process, which is determined by the plateau at the beginning of the characteristic.
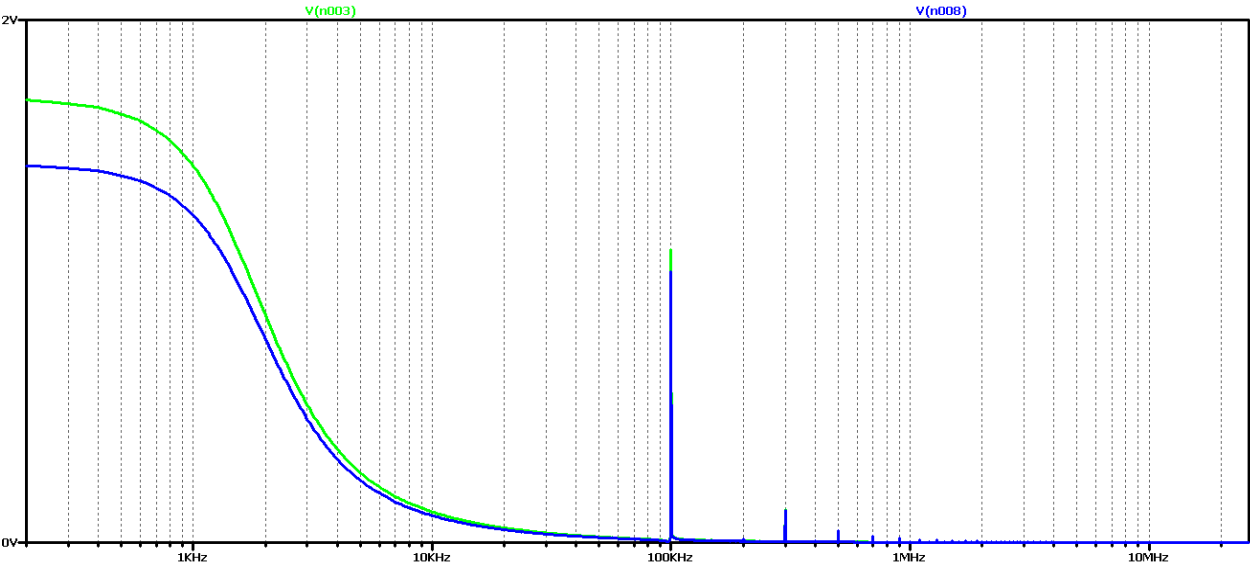
Figure 2.44 FFT analysis of the output voltage of a Boost DC-DC converter at optimum values of the filter elements

To test the hypothesis for the relationship between the output voltage form and the results of the FFT analysis, significantly higher values of the filter elements were taken: 55 times the value of the filter inductance and 3 times the filter capacitor.
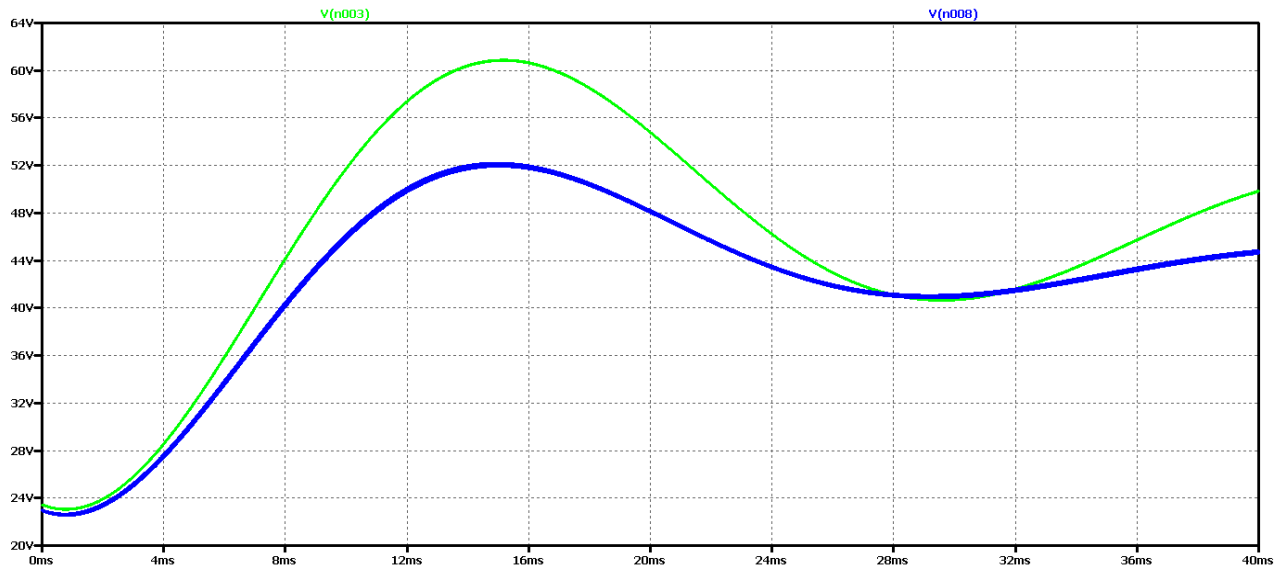
Figure 2.45 Output voltage form of Boost DC-DC converter, with maximum values of filter elements

It appears that there is a much worse dynamics than the previous case of optimal element values. And in the FFT analysis of Figure 2.46 - there are practically harmonic constituents only in the ideal element scheme, where the transient has not completed during the simulation time. From these results, it can be concluded that if we have an aperiodic ascertainment process, there are no harmonics multiple of the control frequency, and the plateau at the beginning of the characteristic is related to the output voltage drop.

In this way, due to the many experiments, a clear dependence and interrelation between the nature of the transients and the form and type of the characteristic from the FFT analysis of the output voltage begins to emerge.
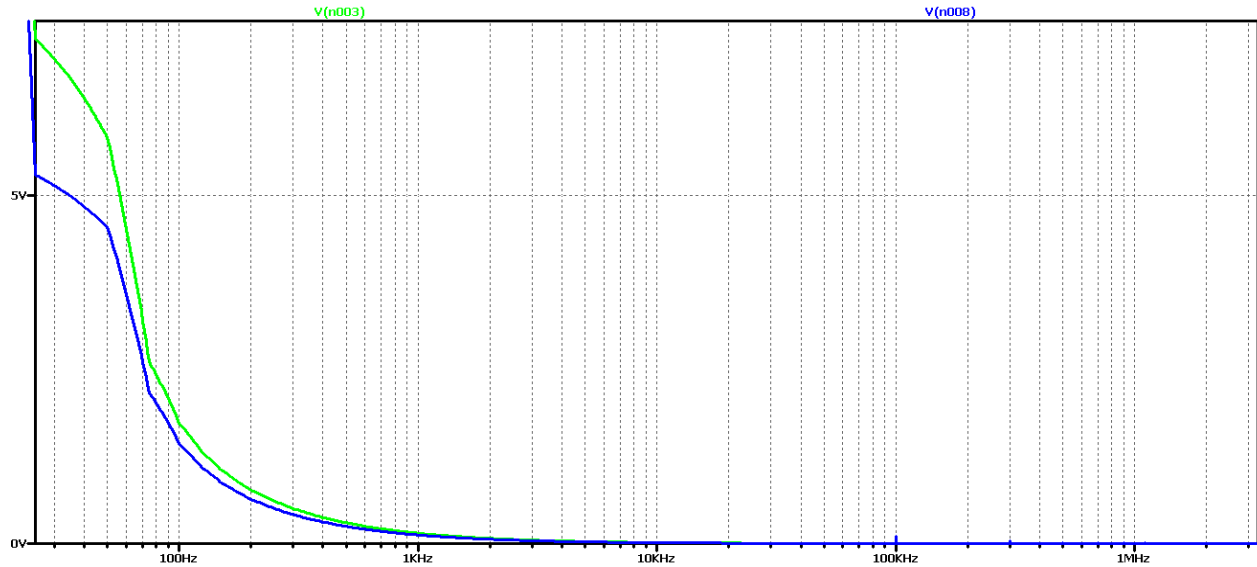
Figure 2.46 FFT analysis of the output voltage of a DC-DC converter, with maximum values of the filter elements

Similar studies were made for two more cases of modulation coefficient values D - D = 0.3 and D = 0.7. The purpose is to check whether these dependencies are observed in these two additional options. The values of D are chosen in view of the fact that they do not practically handle larger or smaller ones due to a number of constraints, such as maximum loads on the circuit elements.
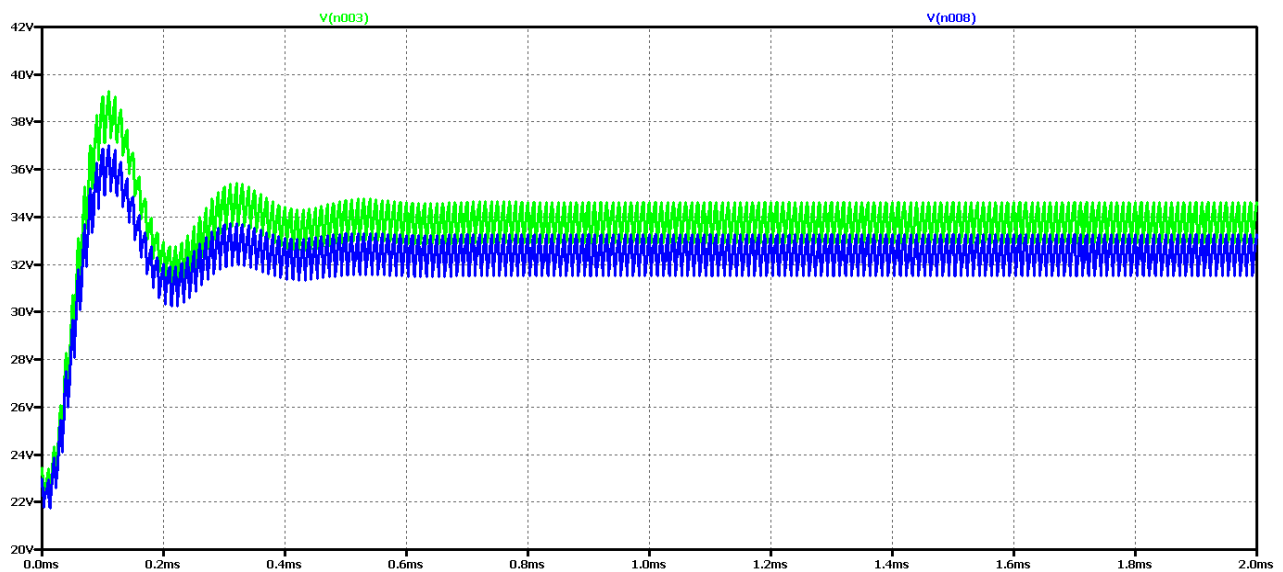
Figure 2.47 Simulation results of a Boost DC-DC converter

Figure 2.47 shows the results for the output voltage form (V (n003 for a circuit with ideal elements, and V (n008 for a circuit with real elements);

It can be seen that at the value of the coefficient D = 0.3, the amplitude of the oscillations of the output voltage is significantly smaller than when D = 0.5. On the other hand, the duration of the transition process is at least twice less than the initial value of D.
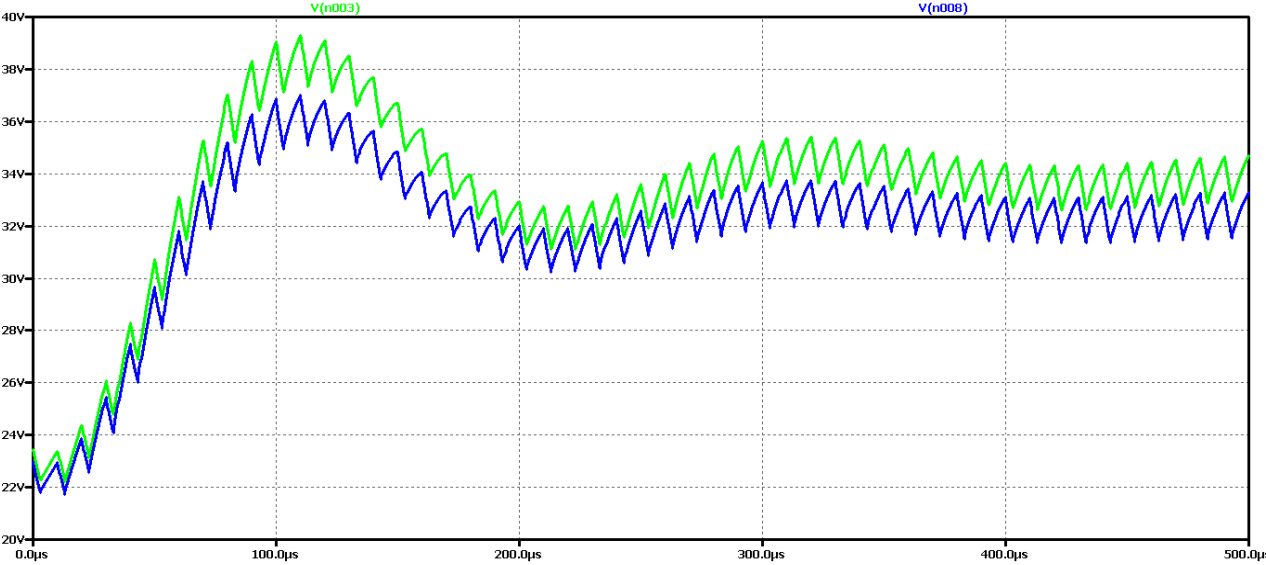
Figure 2.48 Detailed simulation results of a Boost DC-DC converter

Again, the difference between the results with the real and the ideal elements is that with the ideal circuit the steady-state output voltage is higher and the oscillation amplitude is larger with less attenuation. In both cases it is an oscillatory type of transient process that is not desirable in practice due to the long transient process and poor dynamic properties of the scheme.

Figure 2.49 shows the results of Fourier transform (FFT analysis) of the output voltage.

46
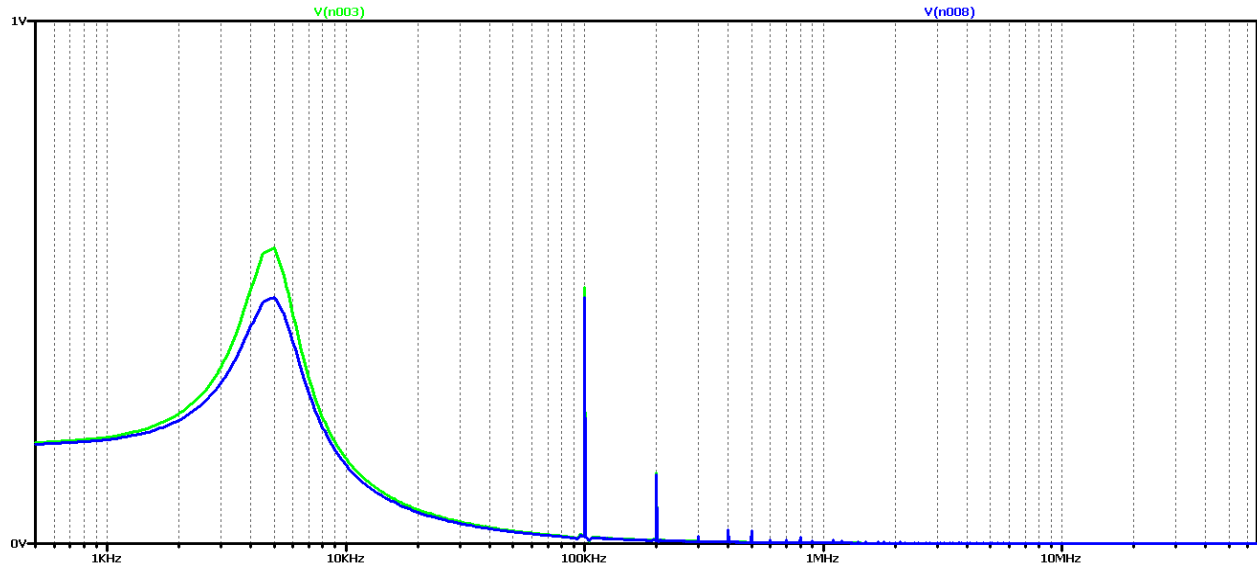
Figure 2.49 FFT analysis of the output voltage of a Boost DC-DC converter

It can be seen that the diagram again has a pronounced maximum at about 5kHz and a harmonic at 100kHz (operating frequency). Unlike the previous cases, there are additional harmonic multiples of the converter control frequency. Obviously, this diagram corresponds to the oscillatory type of the transition process.

From the comparison of the results at the value of the fill factor D = 0.5 (Figure33 and Figure34), full compliance can be seen.

Now let's try to achieve a periodic transient by increasing the value of the filter capacitor 5 times. The value of the filter inductance will not change so as not to increase the ripple current.
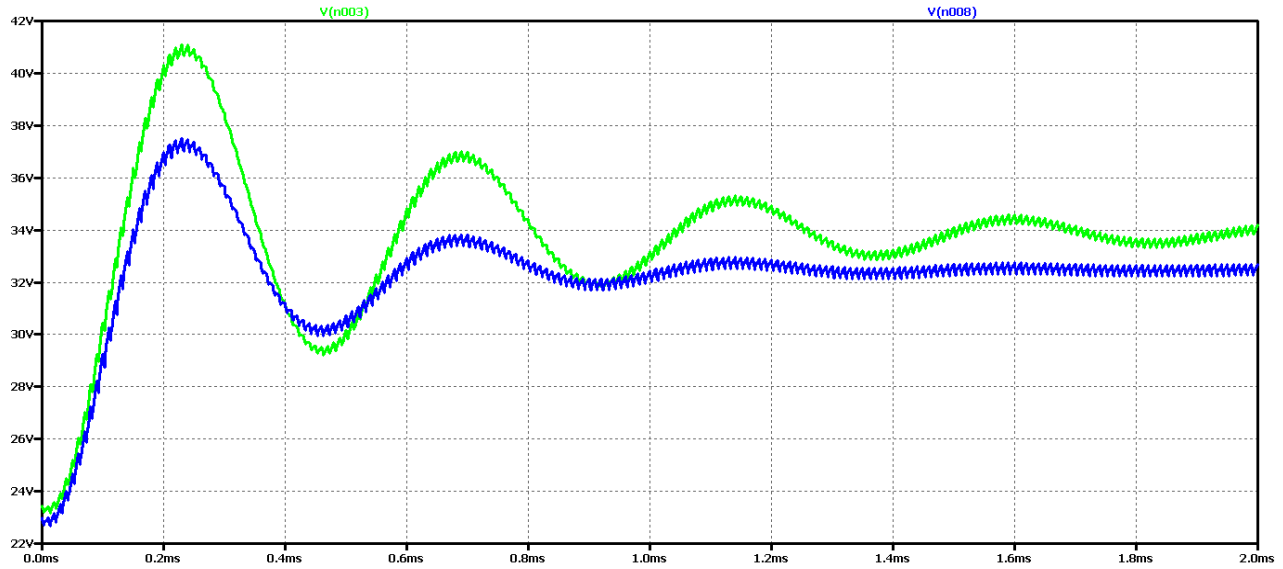
Figure 2.50 Simulation results of a Boost DC-DC converter at 5 times the filter capacity value
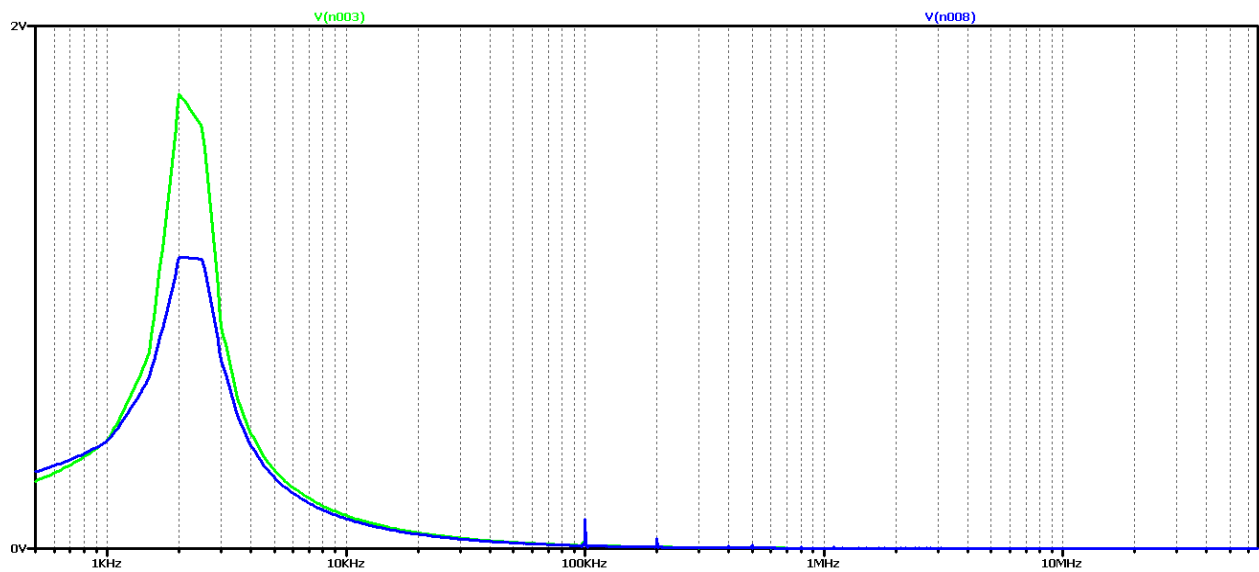
Figure 2.51 FFT analysis of the output voltage of a DC-DC converter at 5 times the value of the filter capacity

It is seen that as the filtering capacity increases, the oscillations in the output voltage setting, using real elements, decrease. On the other hand, with the ideal element scheme the process fluctuation even increases. This is reflected in the results of the FFT analysis with the addition of harmonic multiples of the converter control frequency. Since there is similarity in results, it makes no sense to literally repeat the one studied from the other value of the fill factor.

We will go straight to the final version by increasing the value of the filter capacitor 15 times. Figure 51 shows the output voltage form in this case. Obviously, we have achieved a case close to the aperiodic regime with the best possible dynamic performance compared to the previous variants in the scheme with real elements. In practice, in 2 ms we have the mode setup and transient startup completed. Unfortunately, no change has been observed with the ideal element scheme compared to the initial element values.
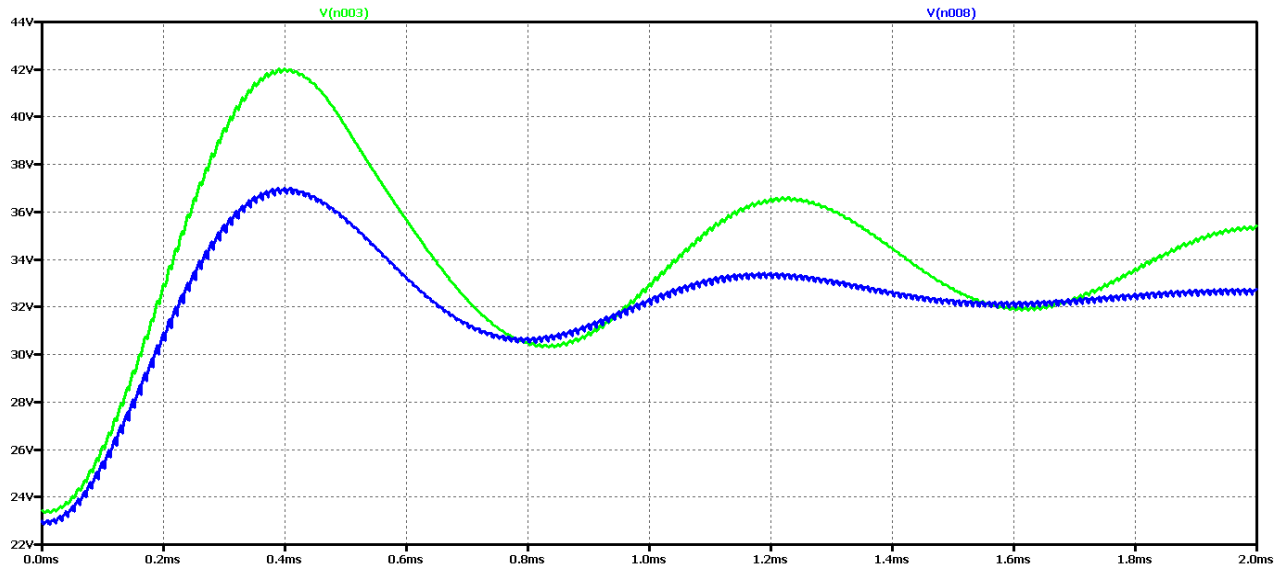
Figure 2.52 Simulation results of a Boost DC-DC converter at 15 times the value of the filter capacitor

Increasing the filter capacity appears to reduce to some extent the oscillations of the output voltage, and to a large extent the form is close to aperiodic. Low frequency and low amplitude oscillations are observed. The FFT analysis shows that the value of the harmonic with the control frequency is very small compared to the previous case considered (especially for real elements). On the other hand, there is a maximum value of the harmonic at a frequency of about 1.5 kHz, ie the output voltage can largely be considered constant with very small pulsations and deviations in the setting mode.
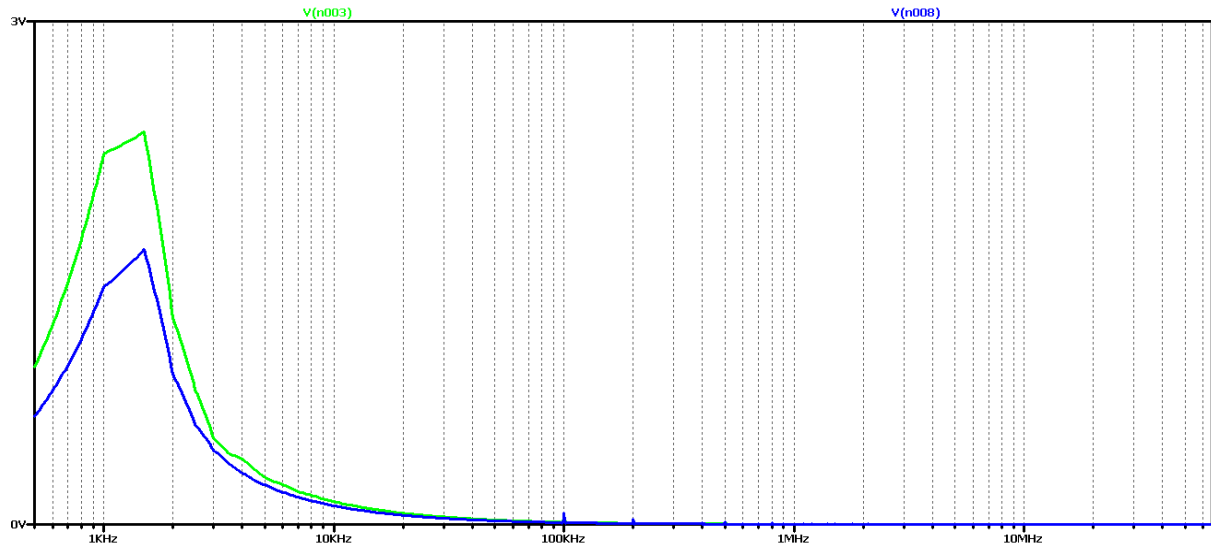
Figure 2.53 FFT analysis of the output voltage of a Boost DC-DC converter at 15 times the value of the filter capacitor

Obviously with this value of filter inductance, regardless of the increase of the filter capacitor, no better transients will be obtained, the next experiment is to use model-based optimization to determine the values of the elements. Here again, the values of the filter inductance 500uF and the filter capacitor 2uF were obtained. To prevent the output voltage from falling off at the start of the process, a 5uF capacitor value is selected.

The results of the study are shown in Figure 2.54.
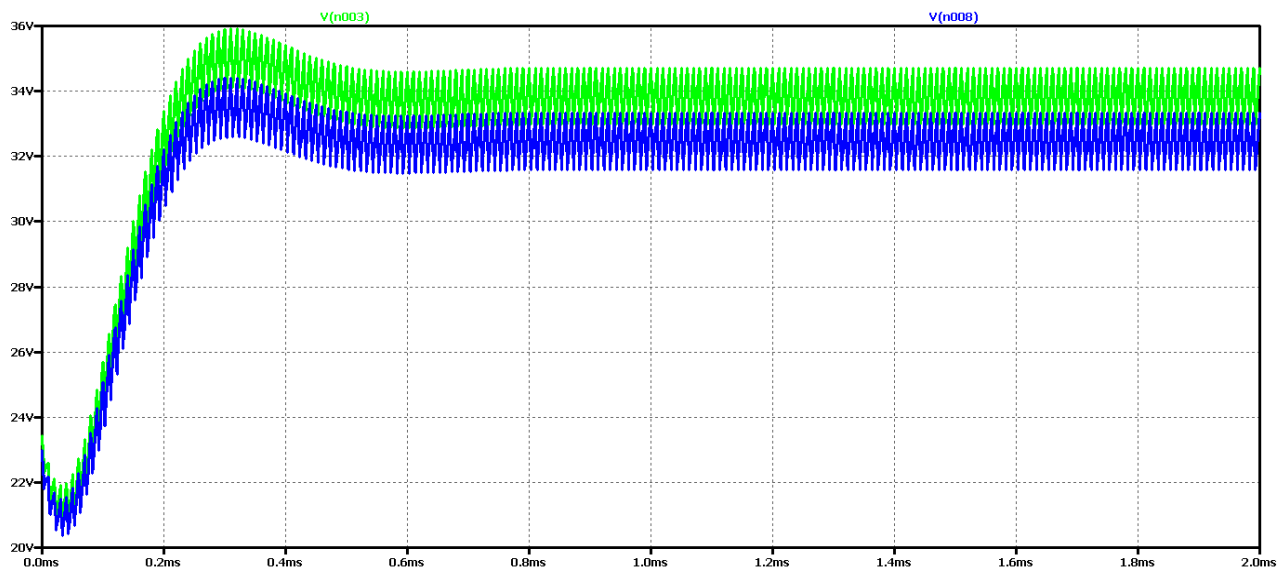
Figure 2.54 Shape of output voltage of Boost DC-DC converter at optimum values of filter elements

The optimum values can be seen to achieve the best dynamics - transient duration of about 0.5 ms. On the other hand, due to the small value of the output capacitor, there is a slight drop in the output voltage.

In Figure 2.55 shows the results of the Fourier transform (FFT analysis) of the output voltage. The presence of harmonic multiples of the control frequency can be seen due to the drop in output voltage (more pronounced in the circuit with ideal elements). On the other hand, we have an aperiodic transition process, which is determined by the plateau at the beginning of the feature.
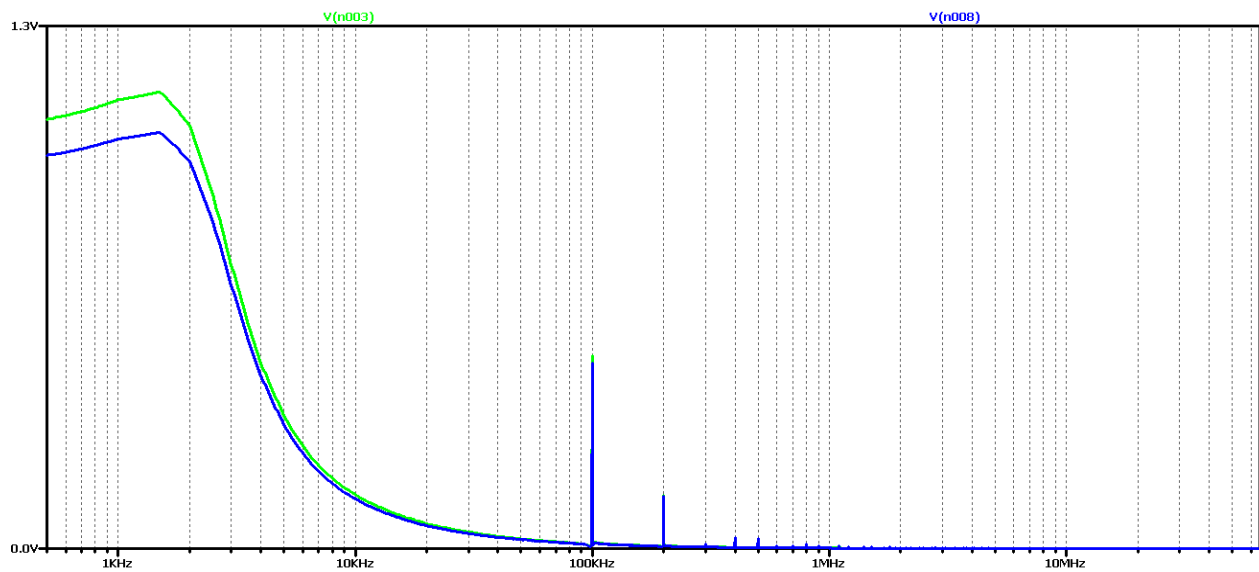
Figure 2.55 FFT analysis of the output voltage of a Boost DC-DC converter at optimal values of the filter elements

To test again the hypothesis for the relationship between the output voltage form and the results of the FFT analysis, significantly larger values of the filter elements were taken in subsequent studies: 100 times the value of the filter inductance and 15 times the filter capacitor.
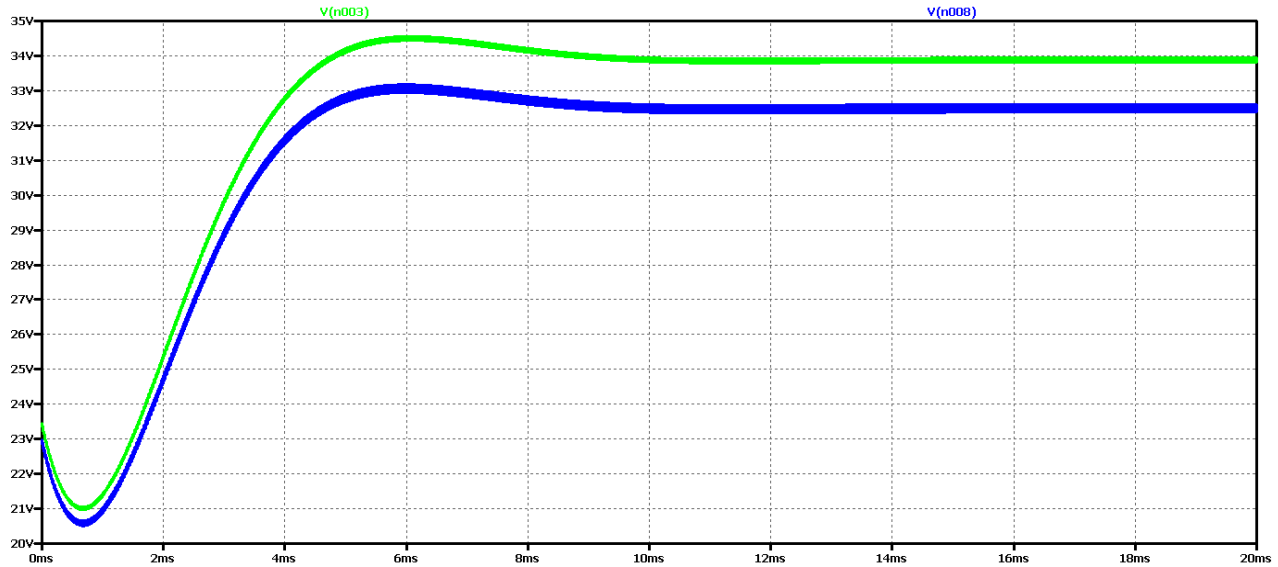
Figure 2.56 Output voltage form of DC-DC Boost converter, with maximum values of filter elements

It appears that there is a much worse dynamics than the previous case of optimal element values. And in the FFT analysis of Figure 2.57 - there are practically harmonic components only in the ideal element scheme, where the transient process has been completed for the simulation time. From these results, it can be concluded that if we have an aperiodic ascertainment process, there are no harmonics multiple of the control frequency, and the plateau at the beginning of the characteristic is related to the output voltage drop.

In this way, due to the many experiments, a clear dependence and interrelation between the nature of the transients and the form and type of the characteristic from the FFT analysis of the output voltage begins to emerge.
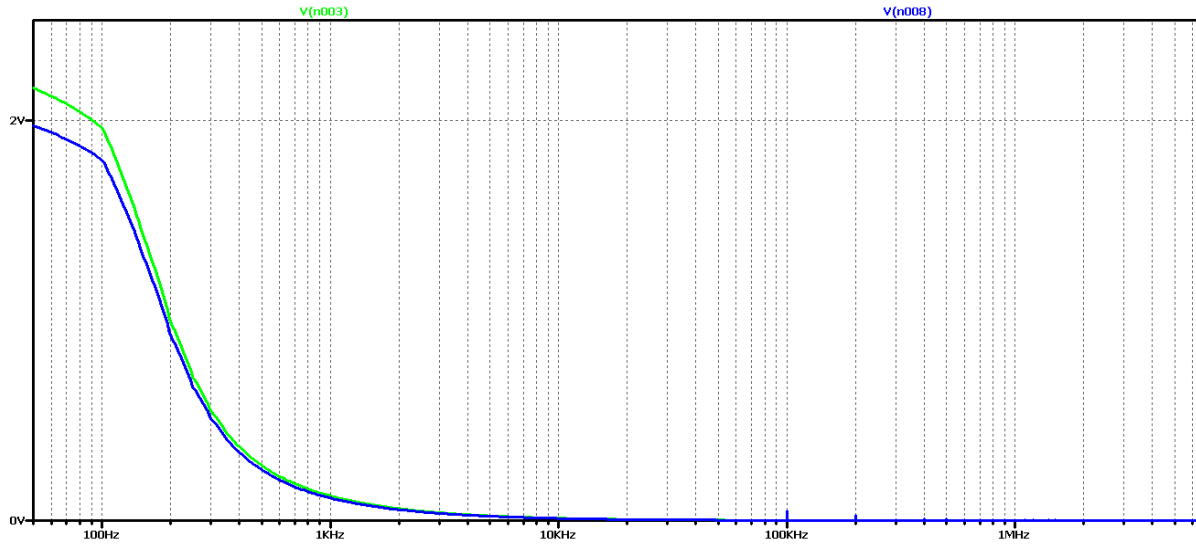
Figure 2.57 FFT analysis of the output voltage of a Boost DC-DC converter, with maximum values of the filter elements

Similar studies have been made for another case of modulation coefficient values D –D = 0.7. The purpose is to verify that these dependencies are also observed in this additional variant.

It can be seen that at the value of the coefficient D = 0.7, the amplitude of the oscillations of the output voltage is smaller than in the case when D = 0.5. On the other hand, the duration of the transient is shorter than the initial value of D. This is due to the peculiarities of the principle of operation of the converter.
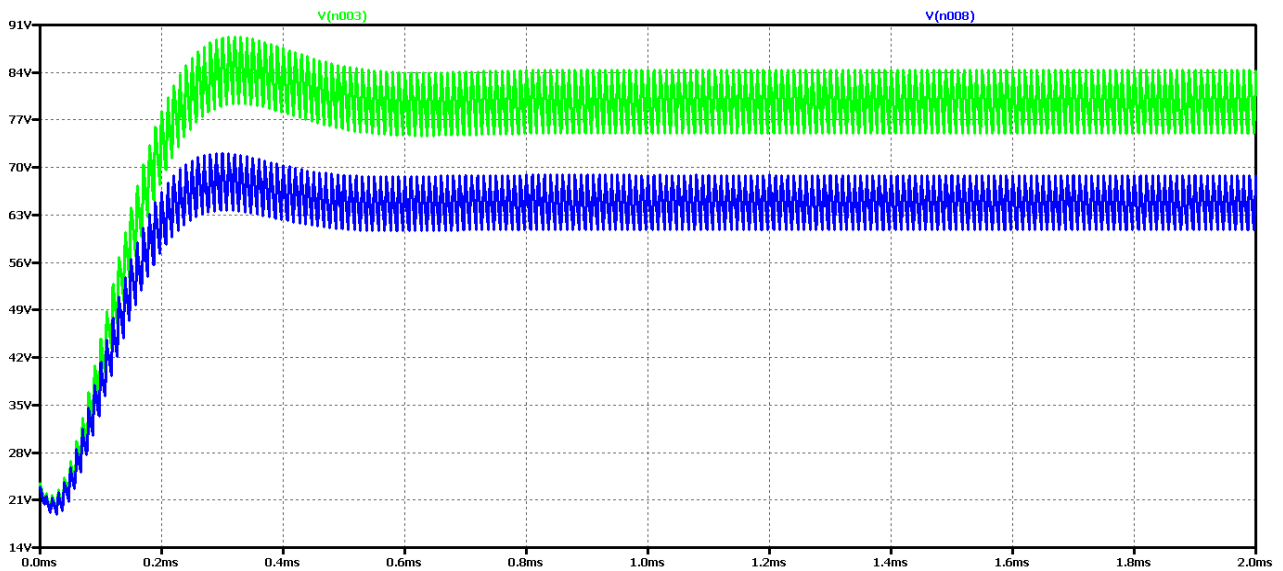
Figure 2.58 Simulation results of a Boost DC-DC converter

53

Again, the difference between the results with the real and the ideal elements is that with the ideal circuit the steady-state output voltage is higher and the oscillation amplitude is larger with less attenuation. In both cases, it is a close to aperiodic type of transient process.

Figure 2.59 shows the results of the Fourier transform (FFT analysis) of the output voltage.
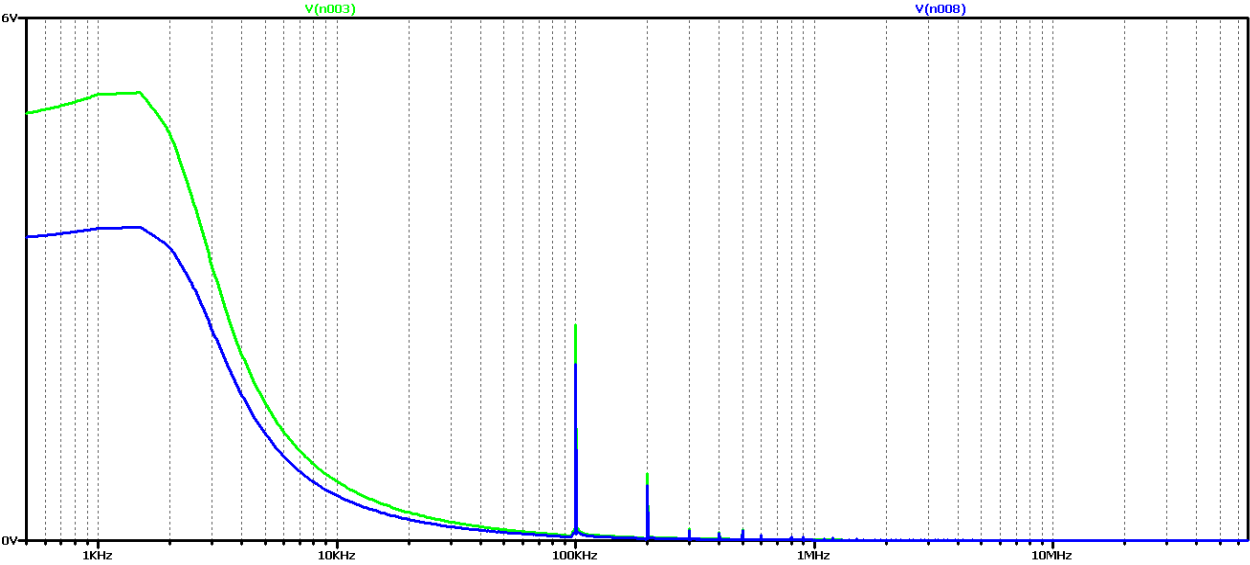
Figure 2.59 FFT analysis of the output voltage of a Boost DC-DC converter

It can be seen that in the diagram in this case there is no clearly expressed maximum and the content of harmonics multiples of 100kHz (operating frequency). Obviously, this diagram corresponds to an intermediate type of transition.

Now let's try to achieve a periodic transient by increasing the value of the filter capacitor 5 times. The value of the filter inductance will not change so as not to increase the ripple current.
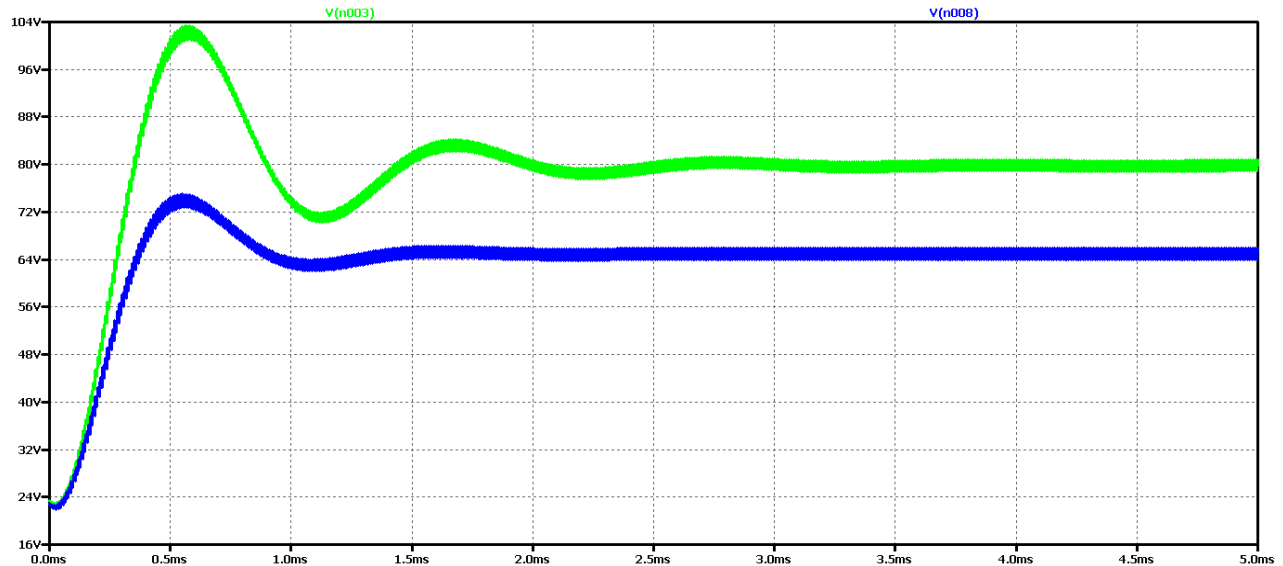
Figure 2.60 Simulation results of a Boost DC-DC converter at 5 times the filter capacity value
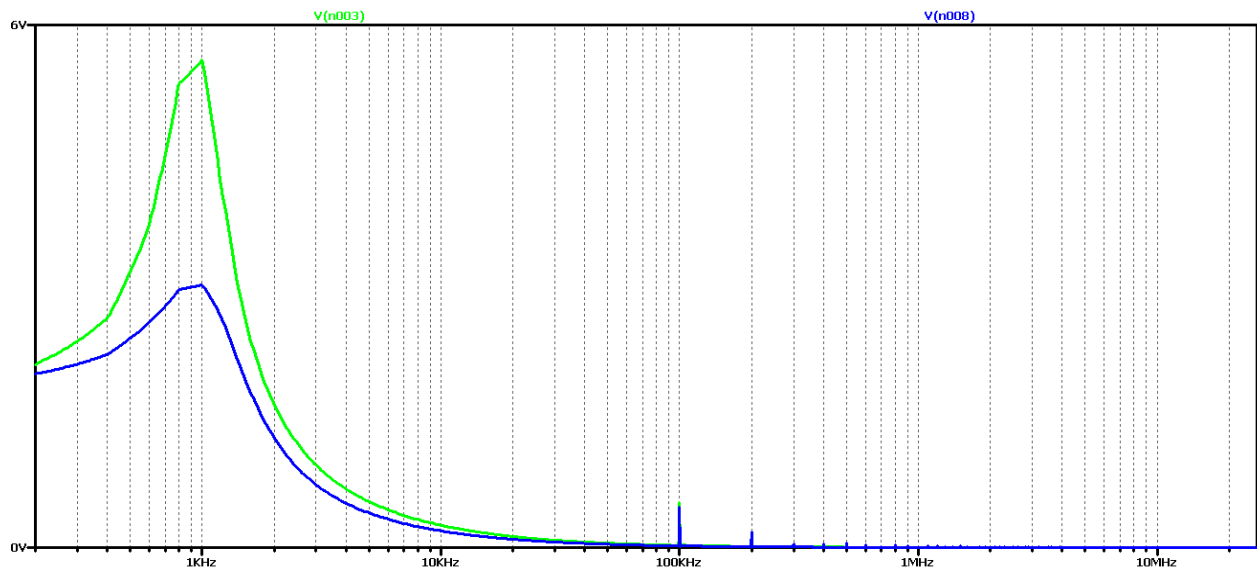
Figure 2.61 FFT analysis of the output voltage of a Boost DC-DC converter at 5 times the value of the filter capacity

It is seen that as the filtering capacity increases, the oscillations in the output voltage are reduced, especially when real elements are used. On the other hand, with the ideal element scheme the process fluctuation even increases. This is reflected in the results of the FFT analysis with the addition of harmonic multiples of the converter control frequency. Since there is a similarity in

the results of the previous values of the coefficient D, it does not make sense to repeat the ones literally investigated from the initial value of the fill factor.

We will go straight to the final version by increasing the value of the filter capacitor 15 times. Figure 2.62 shows the output voltage form in this case. Obviously, we have achieved a case close to the aperiodic regime with the best possible dynamic performance compared to the previous variants in the scheme with real elements. In practice, in 2 ms we have the mode setup and transient startup completed. Unfortunately, no change has been observed with the ideal element scheme compared to the initial element values.
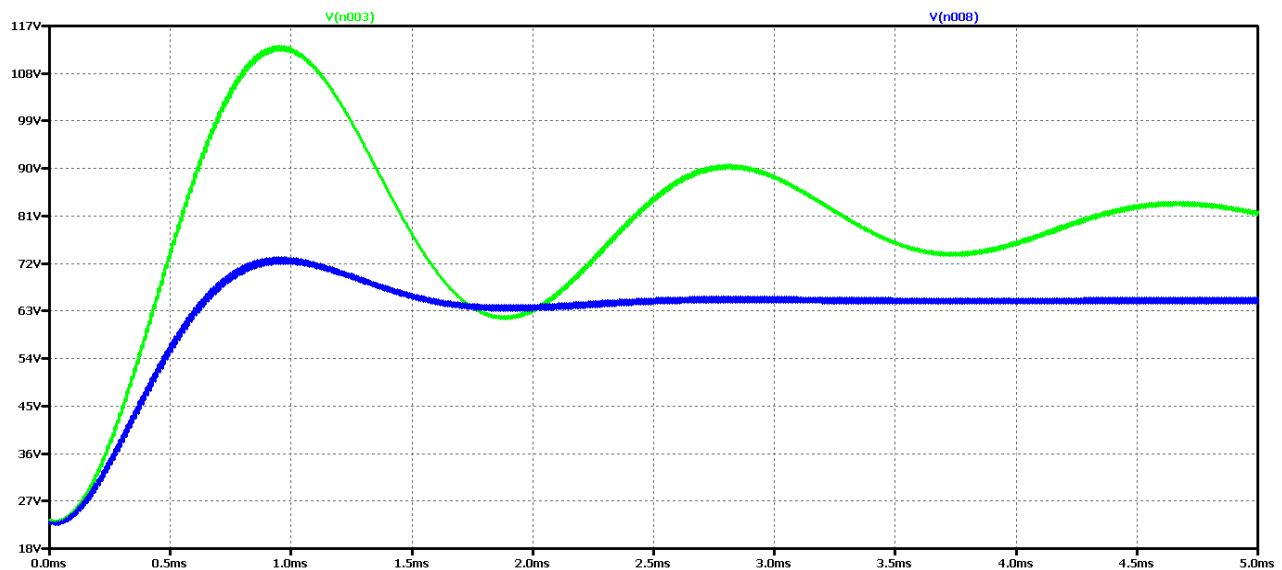
Figure 2.62 Simulation results of a Boost DC-DC converter at 15 times the value of the filter capacitor

Increasing the filter capacity appears to reduce to some extent the oscillations of the output voltage, and to a large extent the form is close to aperiodic. Low frequency and low amplitude oscillations are observed. From the FFT analysis it is found that the value of the harmonic with the control frequency is very small compared to the previous case considered (especially for real elements). On the other hand, there is a maximum value of the harmonic at a frequency of about 1.5 kHz, that is, the output voltage can to a large extent be considered to be constant with very small pulsations and deviations when setting the mode.
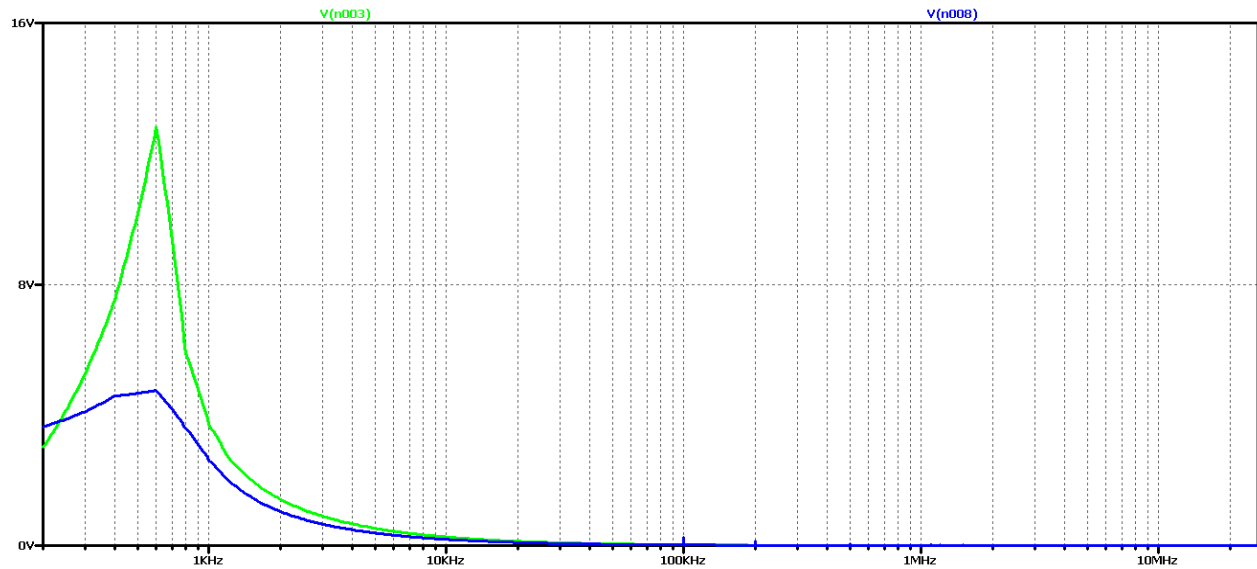
Figure 2.63 FFT analysis of the output voltage of a Boost DC-DC converter at 15 times the value of the filter capacitor

Obviously with this value of filter inductance, regardless of the increase of the filter capacitor, no better transients will be obtained, the next experiment is to use model-based optimization to determine the values of the elements. Here again, the values of the filter inductance 500uH and the filter capacitor 2uF were obtained. To prevent the output voltage from falling off, a capacitor value of 5uF is selected at the beginning of the process.
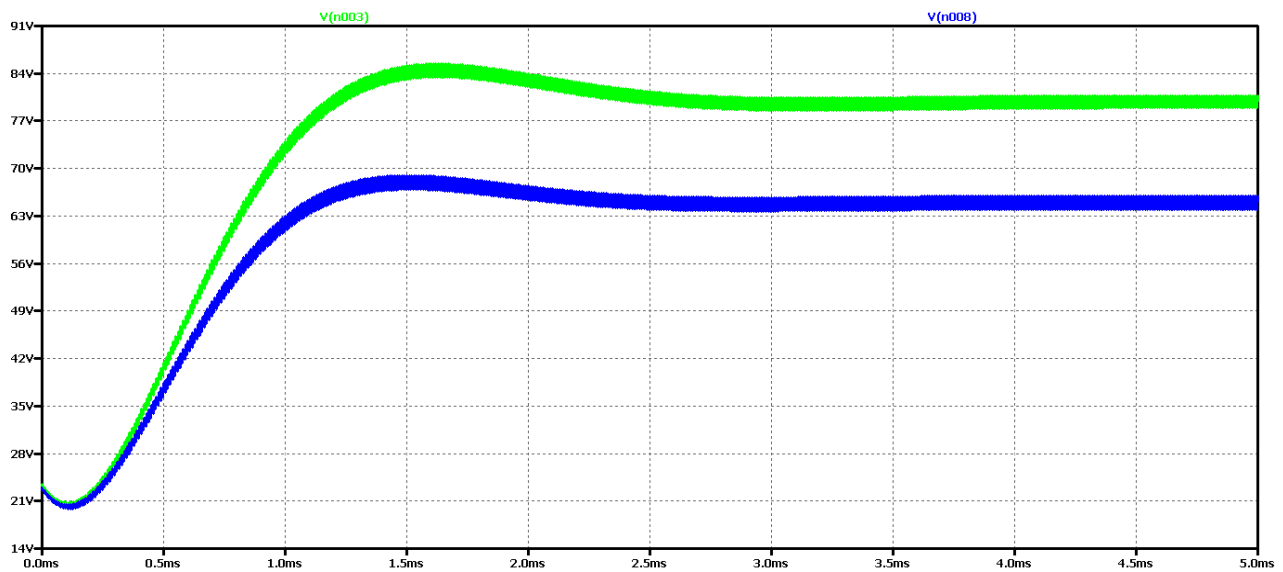
Figure 2.64 Output voltage form of Boost DC-DC converter at optimum values of filter elements

It is evident that the optimum values achieve the best dynamics - transient duration of about 0.5 ms., figure 2.64. On the other hand, due to the small value of the output capacitor, there is a slight drop in the output voltage.

In Figure 2.65 shows the results of the Fourier transform (FFT analysis) of the output voltage. The presence of harmonic multiples of the control frequency can be seen due to the drop in output voltage (more pronounced in the circuit with ideal elements). On the other hand, we have an aperiodic transition process, which is determined by the plateau at the beginning of the characteristic.
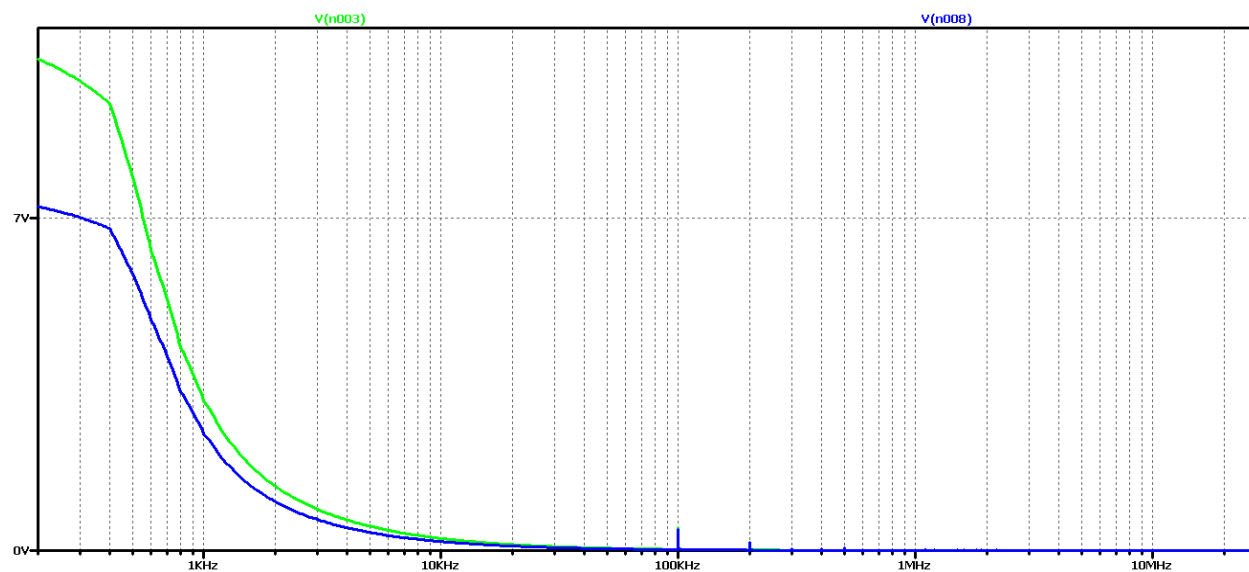
Figure 2.65 FFT analysis of the output voltage of an increasing DC-DC converter, at optimum values of the filter elements

To test again the hypothesis of the relationship between the output voltage form and the results of the FFT analysis, significantly larger values of the filter elements were taken in subsequent studies: 50 times the value of the filter inductance and 15 times the filter capacitor.
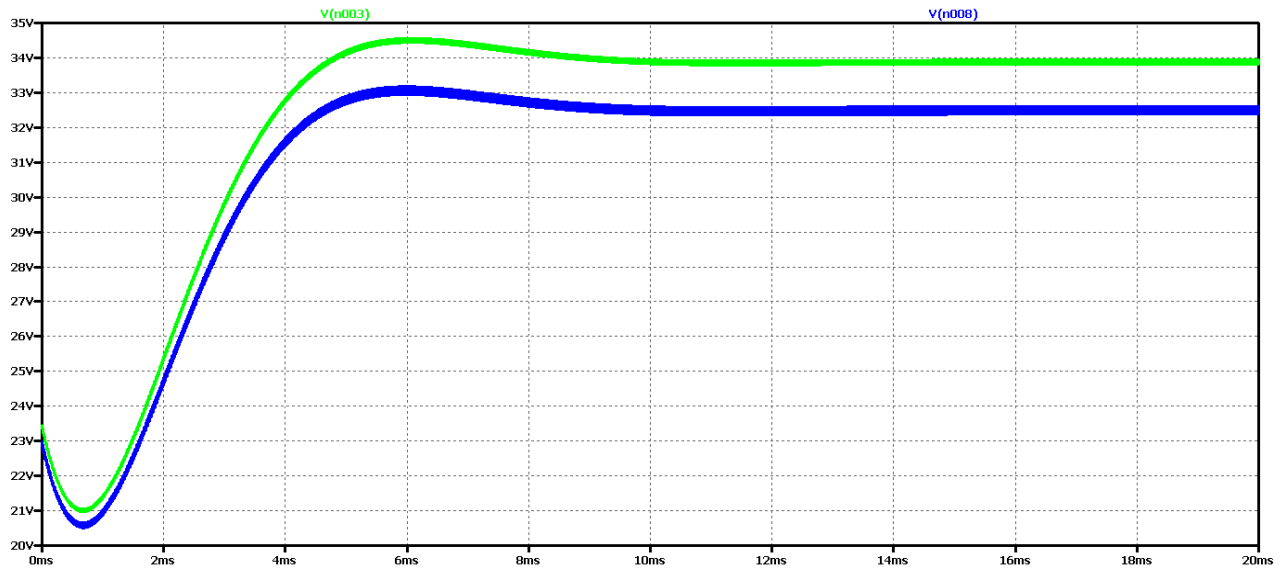
Figure 2.66 Output voltage form of Boost DC-DC converter, with maximum values of filter elements

It appears that there is a much worse dynamics than the previous case of optimal element values. And in the FFT analysis of Figure 2.67, there are practically harmonic components only in the ideal element scheme, where the transient process has been completed for the simulation time. From these results, it can be concluded that if we have an aperiodic ascertainment process, there are no harmonics multiple of the control frequency, and the plateau at the beginning of the characteristic is related to the output voltage drop.

In this way, due to the numerous experiments, a clear dependence and interrelation between the nature of the transients and the form and type of the characteristic from the FFT analysis of the output voltage begins to emerge.
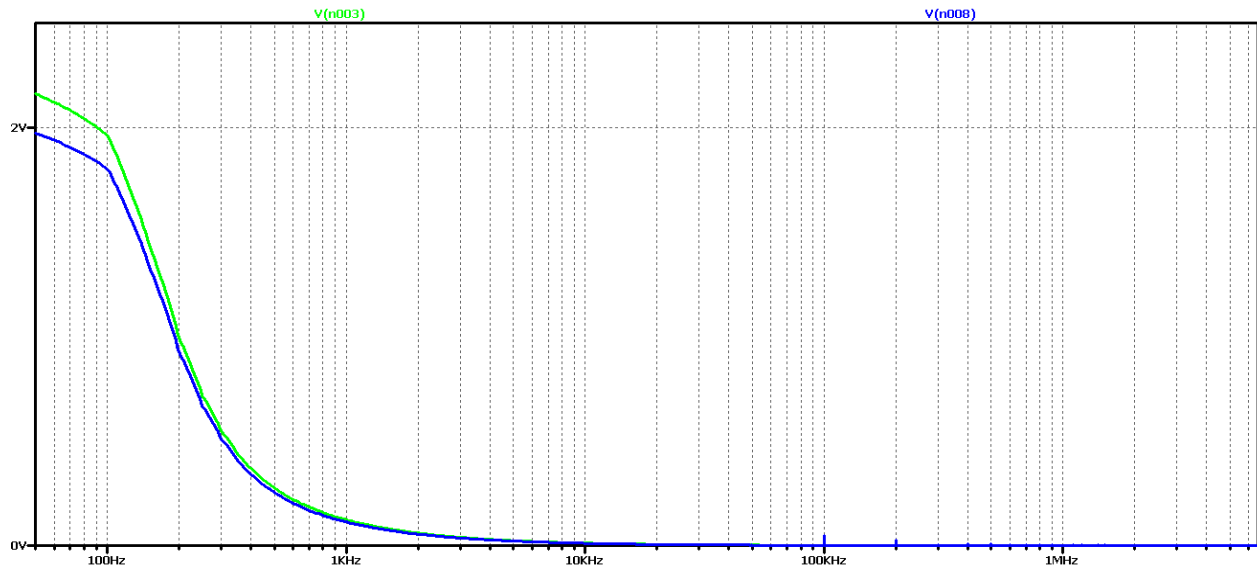
Figure 2.67 FFT analysis of the output voltage of a Boost DC-DC converter, at maximum values of the filter elements

Let's compare the deviations from the established mode for the lowest value of filter capacity in the three cases of modulation coefficient. In the first case - Figure 2.33 the maximum deviation in the most severe case using ideal elements is from 57V to 50V or a ratio of 1.14; in the second case - Figure46 the maximum deviation in the worst case using ideal elements is from 39V to 35V or a ratio of 1.114; in the third case - Figure 2.58 the maximum deviation in the worst case using ideal elements is from 90V to 84V or a ratio of 1.07. In this way, a slight dependence of the maximum deviation of the output voltage on the modulation coefficient is also established, its lowest value at D = 0.7.

2.7. MODELING AND SIMULATION STUDIES OF BUCK-BOOST CONVERTER

For the purpose of the study, a model of Buck-Boost DC-DC converter in the LTspice medium was made. A standard methodology was used to determine the initial values of the circuit elements. The purpose of the study in this case is to find a connection between the actual form of the output voltage and the one obtained by using FFT analysis in order to achieve a periodic transient and the minimum possible duration of the transient. The studies were conducted in cases of continuous current mode, which is more commonly used in practice. Further studies are expected to summarize the results and the interruptible current regime. In Figure 2.68 shows a model of a Buck-Boost converter. Examples of converter with ideal (schematic above) and real

elements (diagram below) are considered. The aim is to determine whether there is a significant difference in the nature and duration of the transients in the scheme.
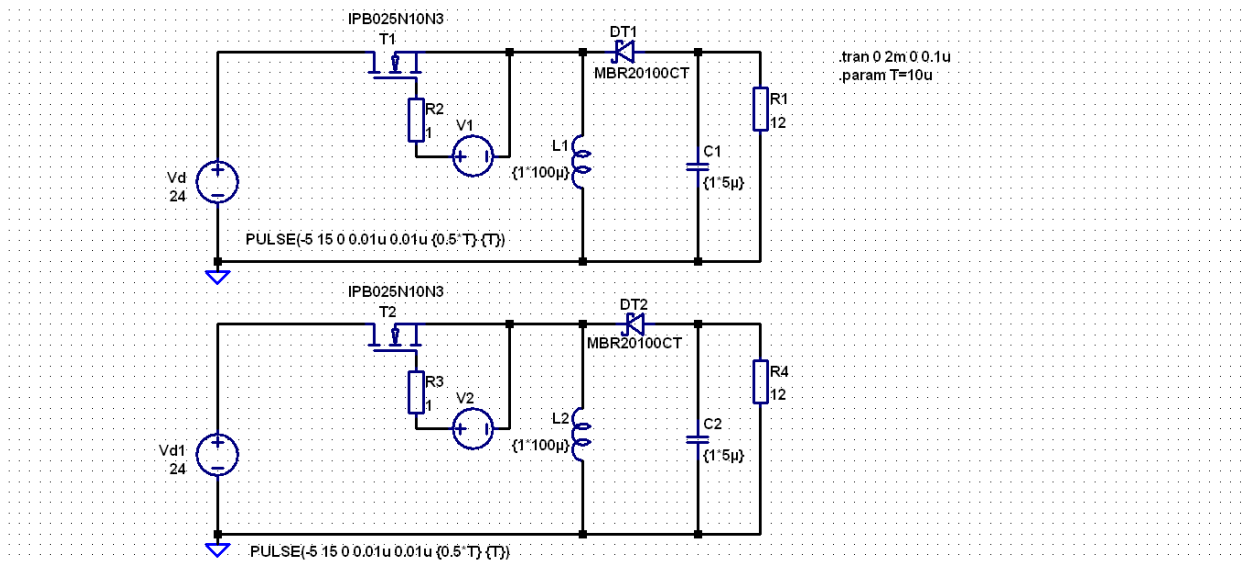
Figure 2.68 Simulation model of a Buck-Boost DC-DC converter

The following values of the circuit parameters are used: Input voltage Uin = 24V; Operating frequency f = 100kHz; filter capacitor C = 5uF, load resistance 12 Ω. The purpose of the study is to change the value of the fill factor D (initial value 0.5) and because of the peculiarities of the operation of the filter inductance scheme (initial value L = 100uH).

Figure 2.69 shows the results for the output voltage form (V (n003 for a circuit with ideal elements, and V (n008 for a circuit with real elements);

61
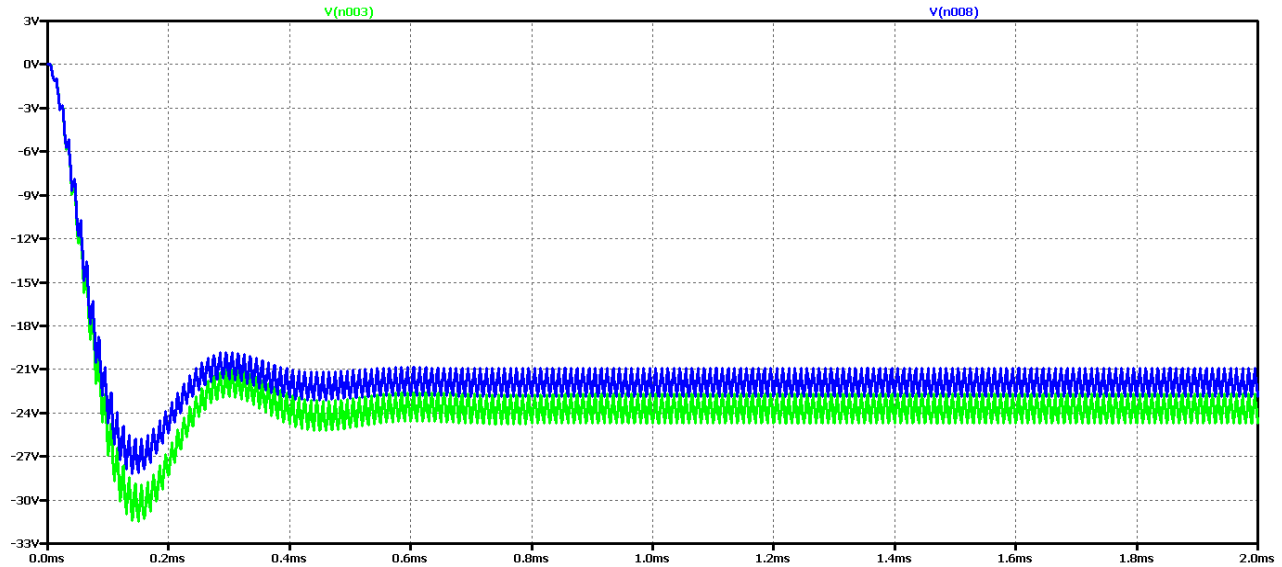
Figure 2.69 Simulation results of a Buck-Boost DC-DC converter

It can be seen that the difference between the results with the real and the ideal elements is that with the ideal circuit the output voltage in the steady state is higher and the amplitude of the oscillations is larger with less attenuation. On the other hand, because of the specificity of the circuit, we have an inverted output - that is, the output voltage is negative. In both cases, this is an oscillatory type of transient process that is not desirable in practice due to the presence of a long transient process, an increase in the voltage against the established regime and poor dynamic properties of the scheme. This is eliminated by having a soft start on startup, but nevertheless this type of transient creates difficulties in the synthesis and setup of the controller. On the other hand, the parasitic elements in the real circuit reduce oscillations but impair the efficiency of the converters. Figure 2.70 shows the results of Fourier transform (FFT analysis) of the output voltage.
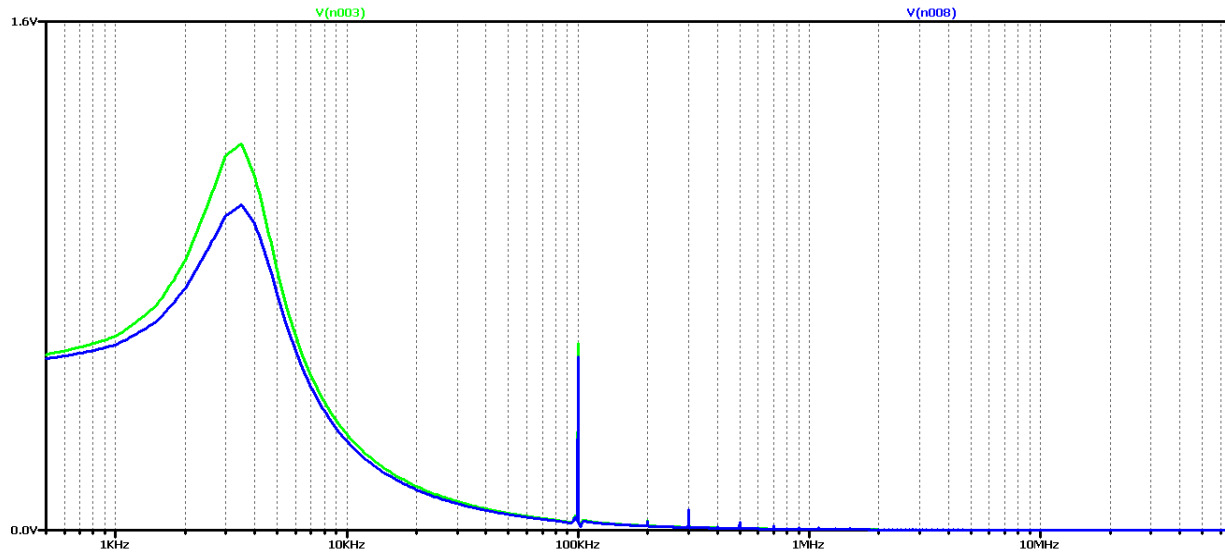
Figure 2.70 FFT analysis of the output voltage of the Buck – Boost DC-DC converter

It can be seen that the chart has a pronounced maximum at about 3.5kHz and the highest harmonic at 100kHz (operating frequency). As in the previous study, a number of harmonics with frequencies multiple of the controller are observed here. Obviously, this diagram corresponds to the oscillatory type of the transition process.

Now let's try to achieve aperiodic transient by increasing the value of the filter inductance 5 times. The value of the filter capacitor will not change so as not to alter the ripple of the output voltage.
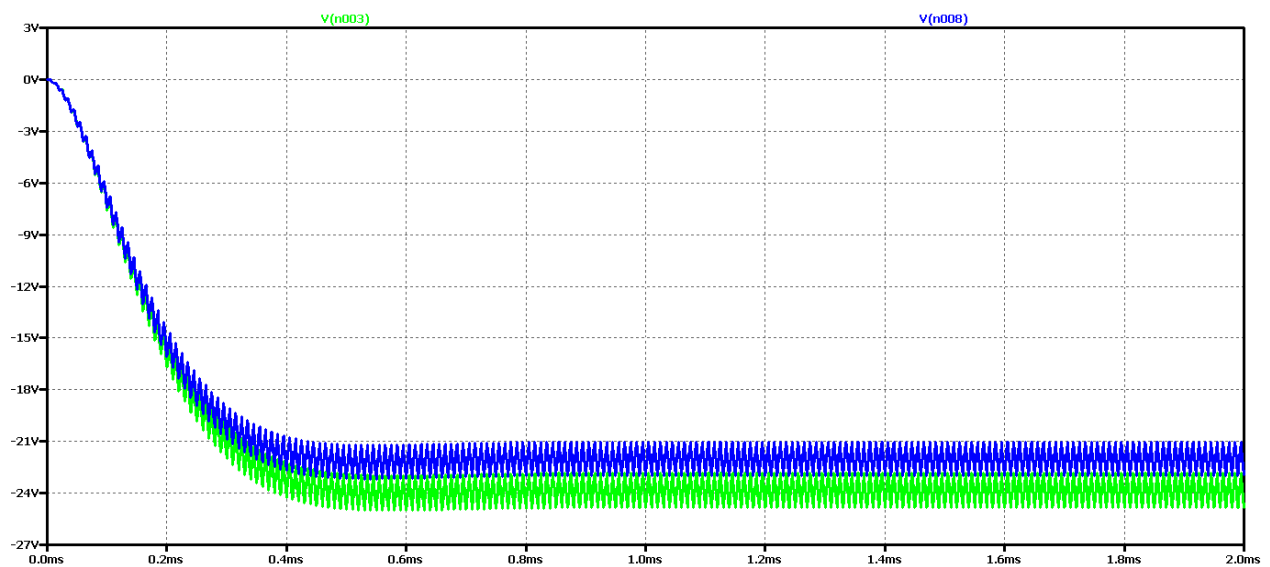
Figure 2.71 Simulation results of a Buck – Boost DC-DC converter with 5 times the value of the filter inductance

63

It can be seen that with increasing the value of the filter inductance, only 5 times the oscillations in determining the output voltage, using real elements, are significantly reduced. The same is observed with the ideal element scheme, the process fluctuation even increases.
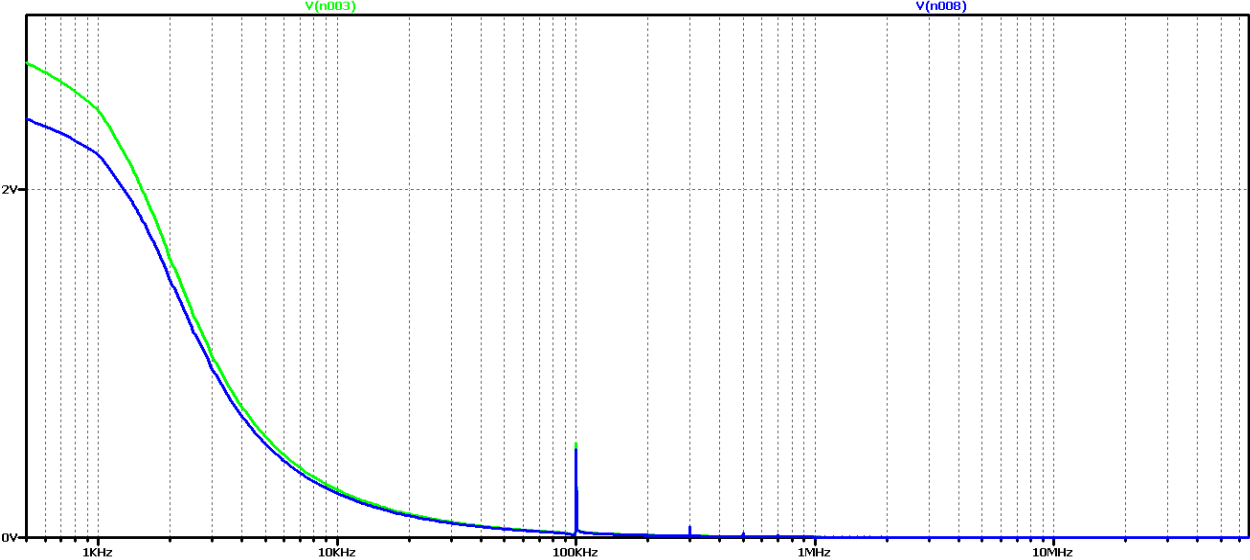
Figure 2.72 FFT analysis of the output voltage of the Buck – Boost DC-DC converter at 5 times the value of the filter inductance

From the FFT analysis it is found that the value of the harmonic with the control frequency is increasing compared to the previous case considered. A plateau begins to form at the beginning of the characteristics, which is a sign of a transition to a periodic transition. Still harmonic with a frequency multiple of the control frequency are still noticeable.

Now let's again increase the value of the filter inductance 10 times the initial value. In this way, we should achieve an aperiodic transition or closer to it than the previous variant.
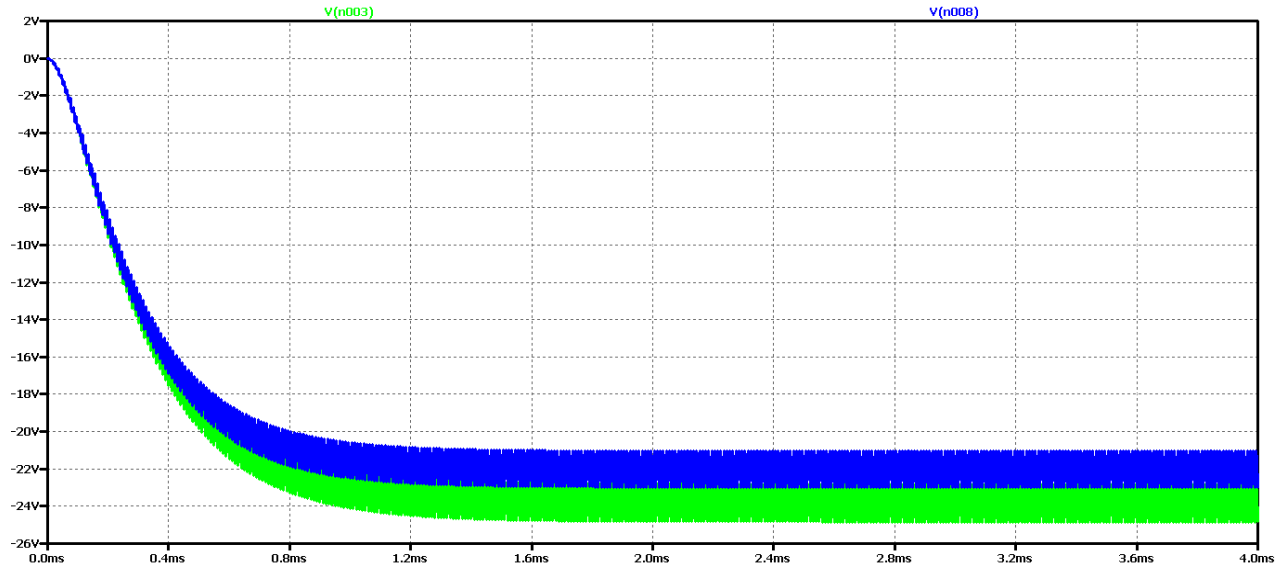
Figure 2.73 Simulation results of a Buck – Boost DC-DC converter, at 10 times the value of the filter inductance

Increasing the filter inductance can be seen to significantly reduce the oscillation of the output voltage and, to a large extent, the form is close to aperiodic. Low frequency and low amplitude oscillations are not observed. On the other hand, the output ripples are relatively large in the circuit and the output capacitor value should be increased. FFT analysis shows that the value of the harmonic with the control frequency is lower than the previous case considered, and the multiple harmonics are also of reduced amplitude compared to the previous case, that is, the output voltage can largely be considered constant with very small pulsations and variations in the working setup.
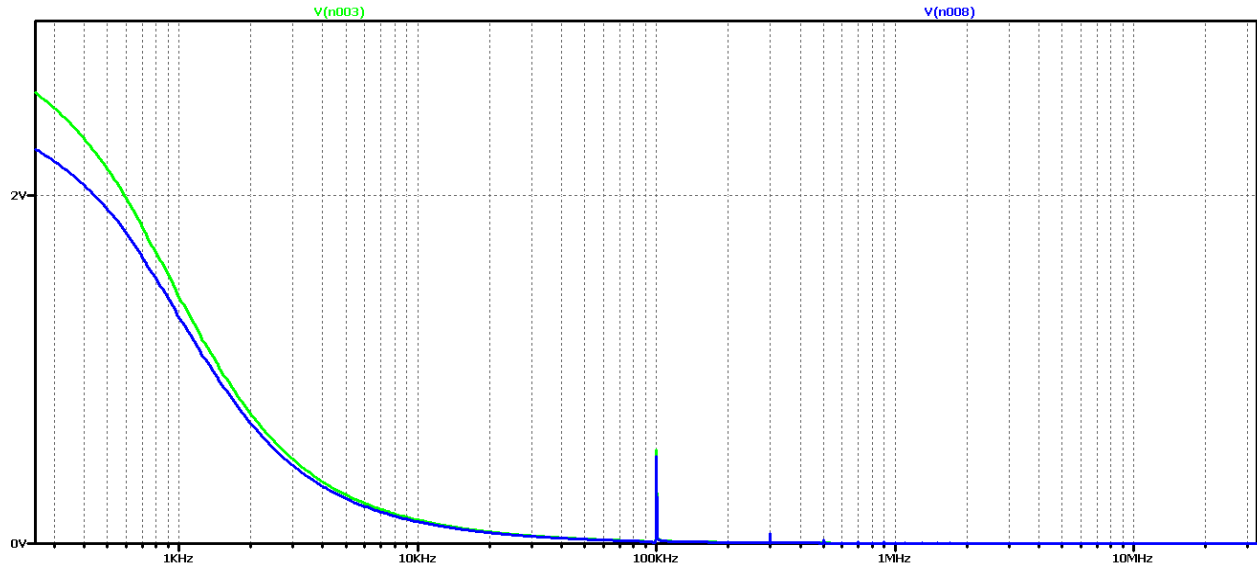
Figure 2.74 FFT analysis of the output voltage of the Buck – Boost DC-DC converter at 10 times the value of the filter inductance

For a more accurate examination of the results of the FFT analysis of the output voltage of Figure 2.75 is an increase for frequencies close to the operating frequency. This harmonic can be seen to have negligible value in real elements (curve in green) and in some practical cases where we do not need high precision or there are limitations related to the value of filter elements, it can be assumed that in practice we have the required aperiodic transition.
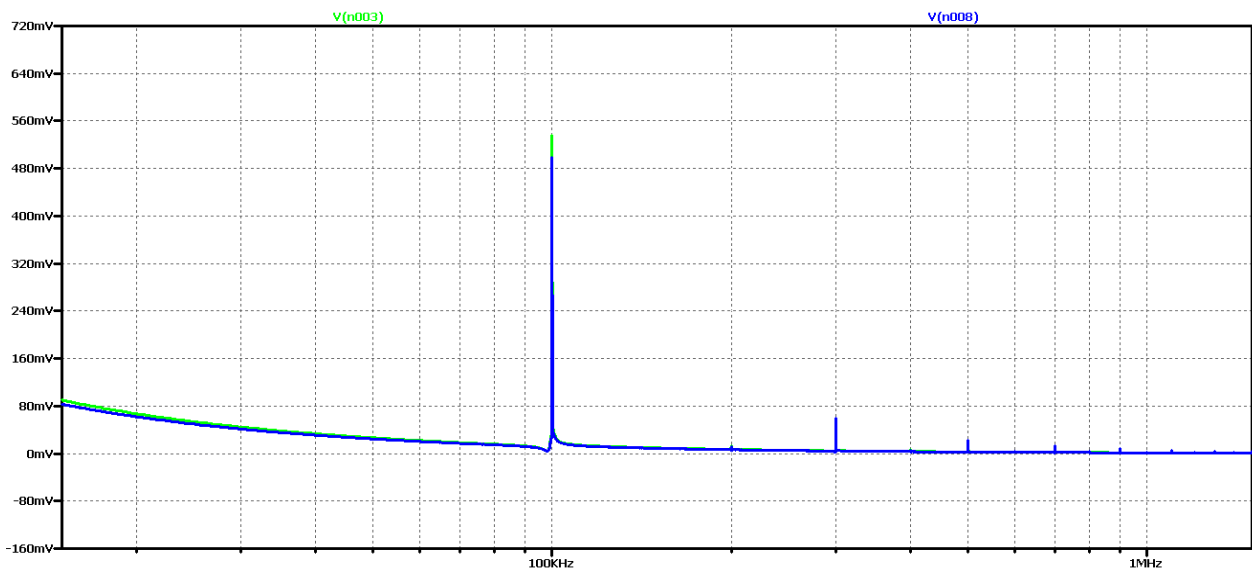
Figure 2.75 FFT analysis of the output voltage of the Buck – Boost DC-DC converter, at 10 times the value of the filter inductance, for frequencies close to the control frequency

66

Another experiment is to use the current scheme and increase the value of the filter capacitor 5 times. Figure 2.76 shows the form of the output voltage in this case. Obviously, we have achieved a case close to the aperiodic regime with the best possible dynamic performance compared to the previous variants in the scheme with real elements. In practice, in 2 ms we have the mode setup and transient startup completed. The results are similar for both variants of ideal element and real element schemes.
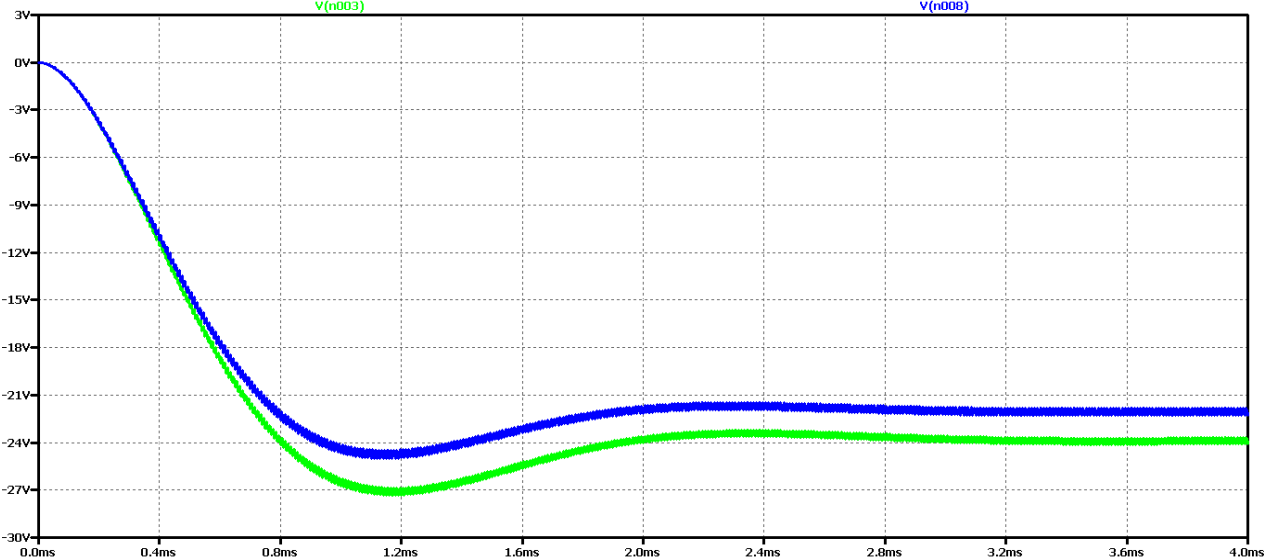
Figure 2.76 Simulation results of a Buck – Boost DC-DC converter, at 5 times the value of the filter capacitor and 10 times the filter inductance

In Figure 76 shows the results of the FFT analysis of the output voltage in both cases - of a converter with ideal and real circuit elements.

Here we can see that we have the largest constant component in comparison with the previous cases, but there is still a deformation of the characteristic at the beginning and the presence of harmonics multiples of the operating frequency, which was also characteristic of the previous cases.
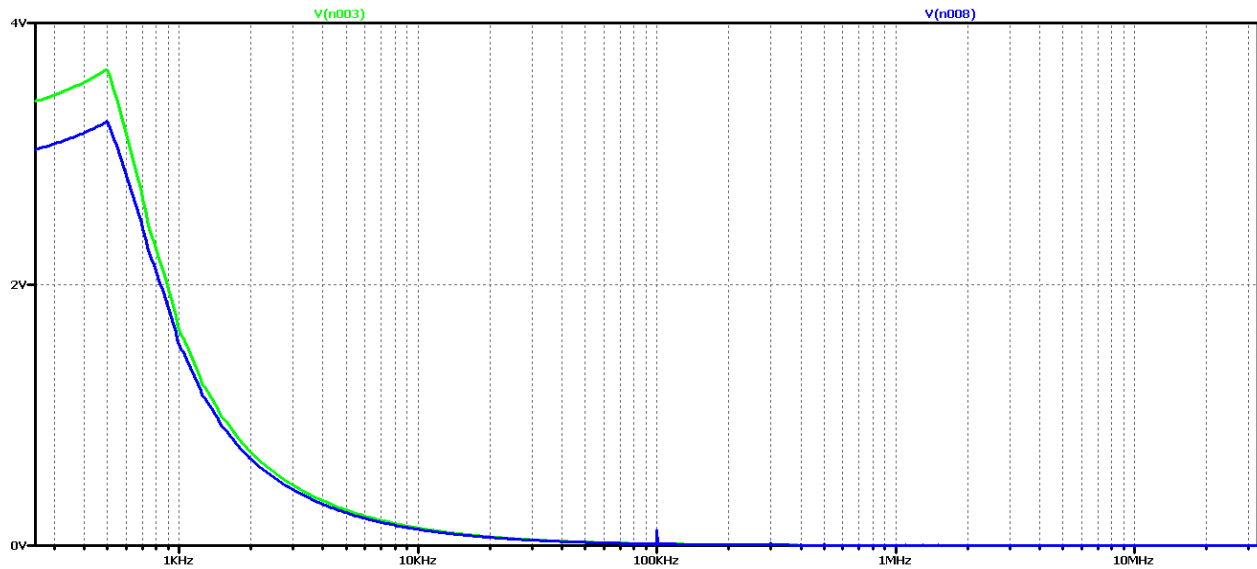
Figure 2.77 FFT analysis of the output voltage of the Buck – Boost DC-DC converter at 5 times the value of the filter capacitor and 10 times the filter inductance

Obviously with this value of filter inductance, regardless of the increase of the filter capacitor, no better transients will be obtained, the next experiment is to use model-based optimization to determine the values of the elements. The values of the filter inductance 500uH and the filter capacitor 2uF are obtained. To avoid excessive ripples of the output voltage, a 5uF capacitor value is selected.

The results of the study are shown in Figure 2.78.
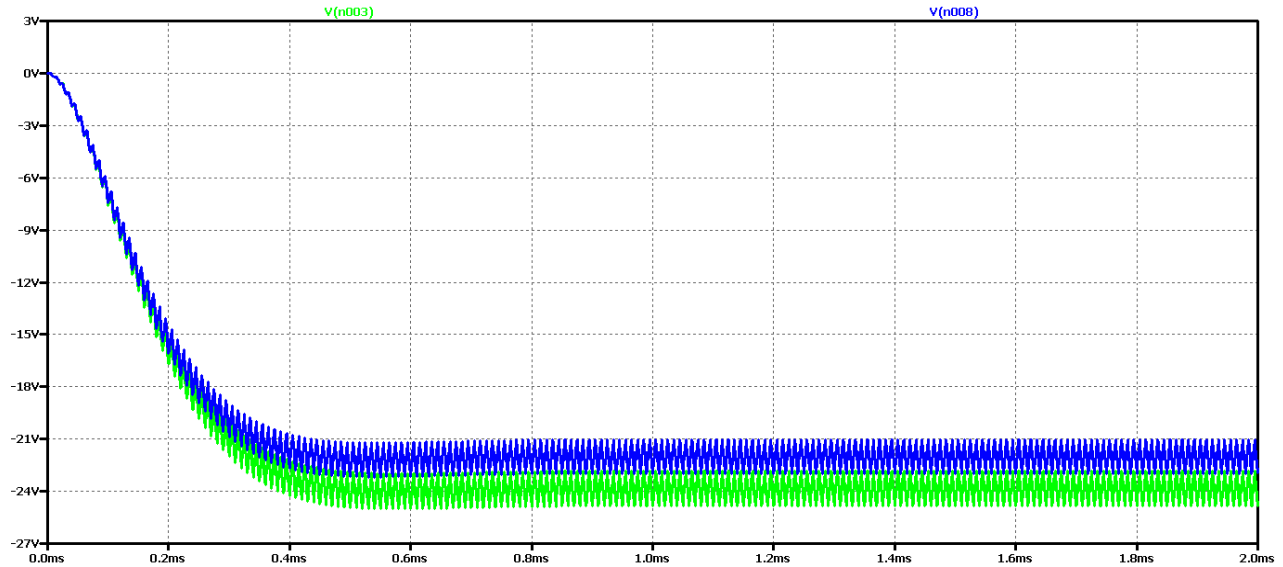
Figure 2.78 Output voltage of Buck – Boost DC-DC converter output at optimum values of filter elements

It is evident that the optimum values achieve the best dynamics - transient duration of 0.5 ms. On the other hand, due to the low value of the output capacitor, there is an increase in the output voltage ripples.

In Figure 2.79 shows the results of Fourier transform (FFT analysis) of the output voltage. The presence of harmonic multiples of the control frequency is visible due to the ripple of the output voltage. On the other hand, we have an aperiodic transition process, which is determined by the plateau at the beginning of the characteristic.
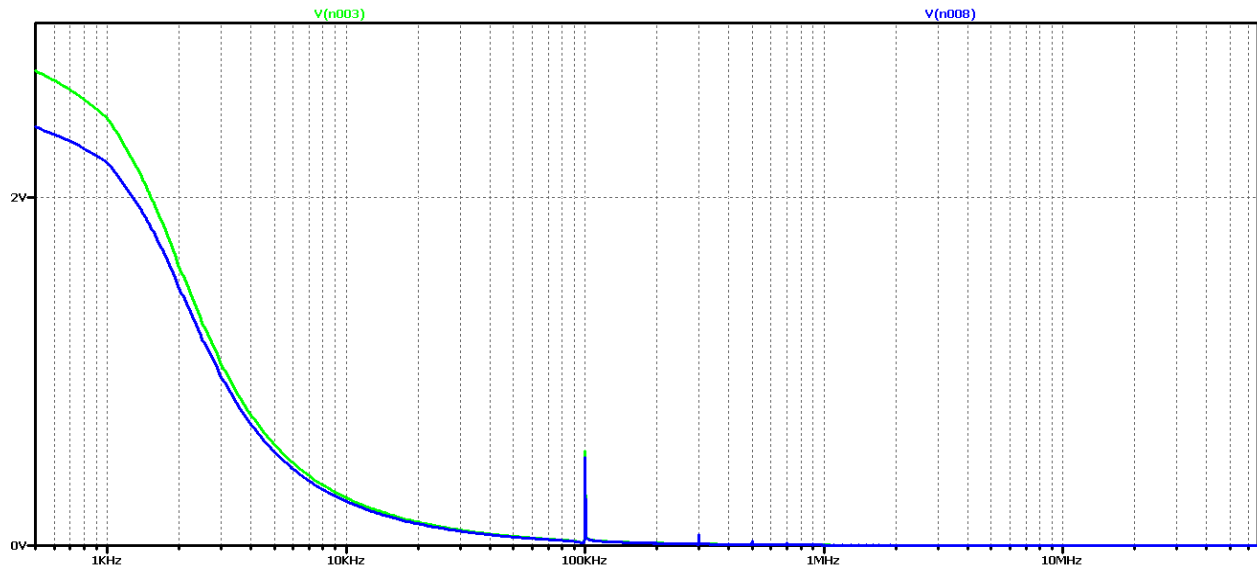
Figure 2.79 FFT analysis of the output voltage of the Buck – Boost DC-DC converter, at the optimum values of the filter elements

To test the hypothesis for the relationship between the output voltage form and the results of the FFT analysis, significantly higher values of the filter elements were taken: 50 times the value of the filter inductance and 3 times the filter capacitor.
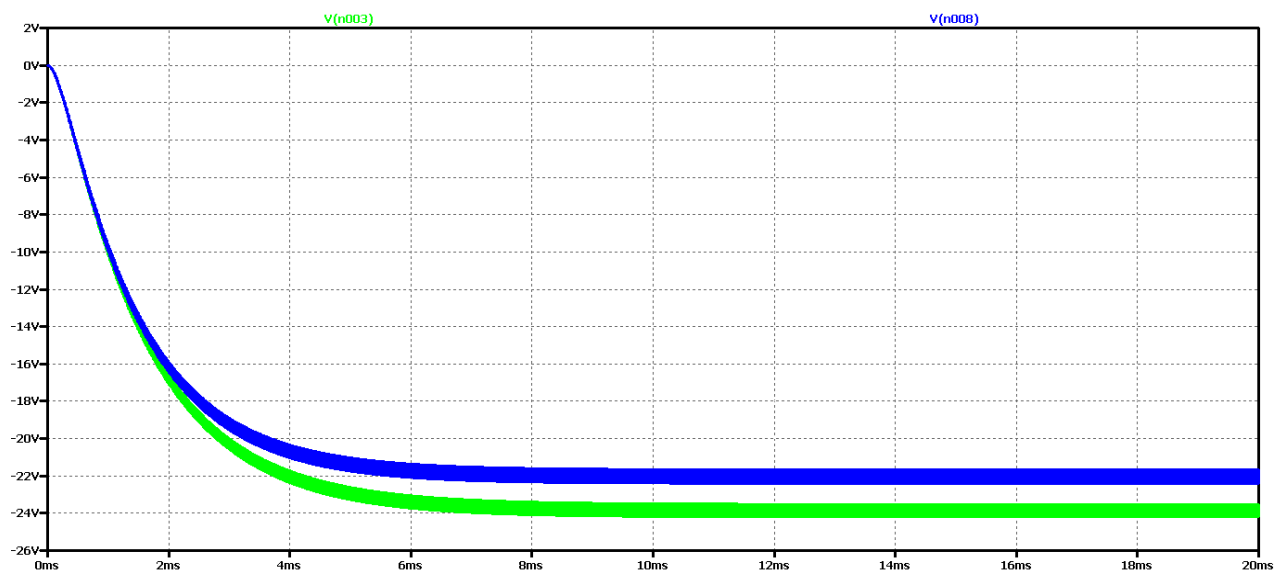
Figure 2.80 Shape of output voltage of Buck – Boost DC-DC converter, at maximum values of filter elements

It appears that there is a much worse dynamics than the previous case of optimal element values. And in the FFT analysis of Figure 2.81 - there are practically harmonic components only in the

70

ideal element scheme, where the transient process has been completed for the simulation time. From these results, it can be concluded that if we have an aperiodic ascertainment process, there are no harmonics multiple of the control frequency, and the plateau at the beginning of the characteristic is related to the output voltage drop.

In this way, due to the numerous experiments, a clear dependence and interrelation between the nature of the transients and the form and type of the characteristic from the FFT analysis of the output voltage.
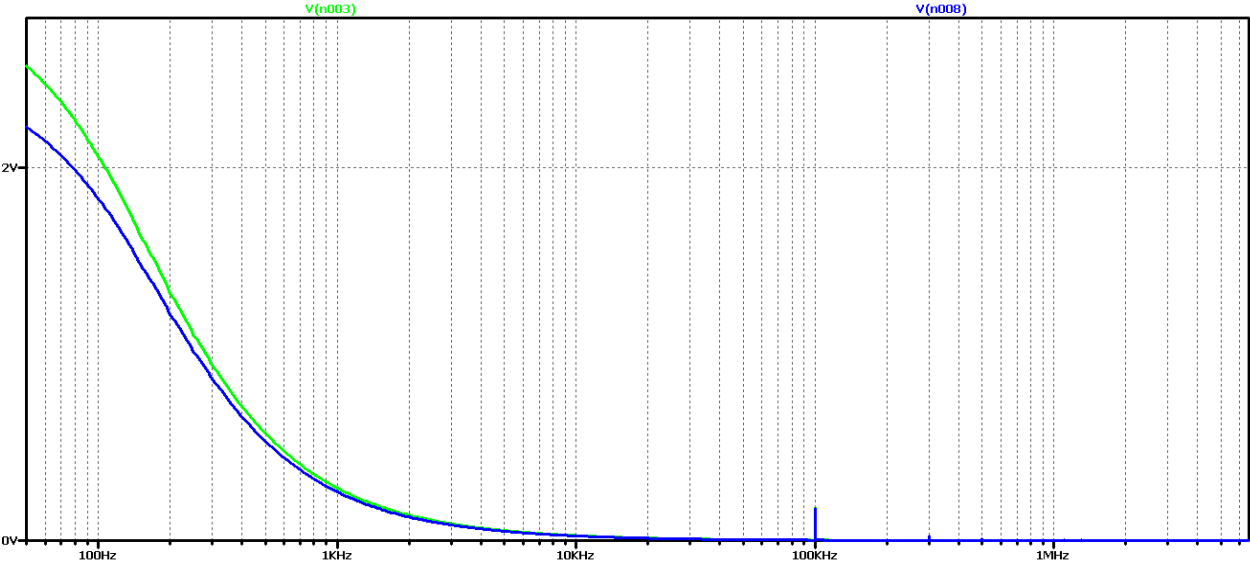
Figure 2.81 FFT analysis of the output voltage of the Buck – Boost DC-DC converter, at maximum values of the filter elements

Similar studies were made for two more cases of modulation coefficient values D - D = 0.3 and D = 0.7. The purpose is to check whether these dependencies are observed in these two additional options. The values of D are chosen in view of the fact that they do not practically handle larger or smaller ones due to a number of constraints, such as maximum loads on the circuit elements.

71
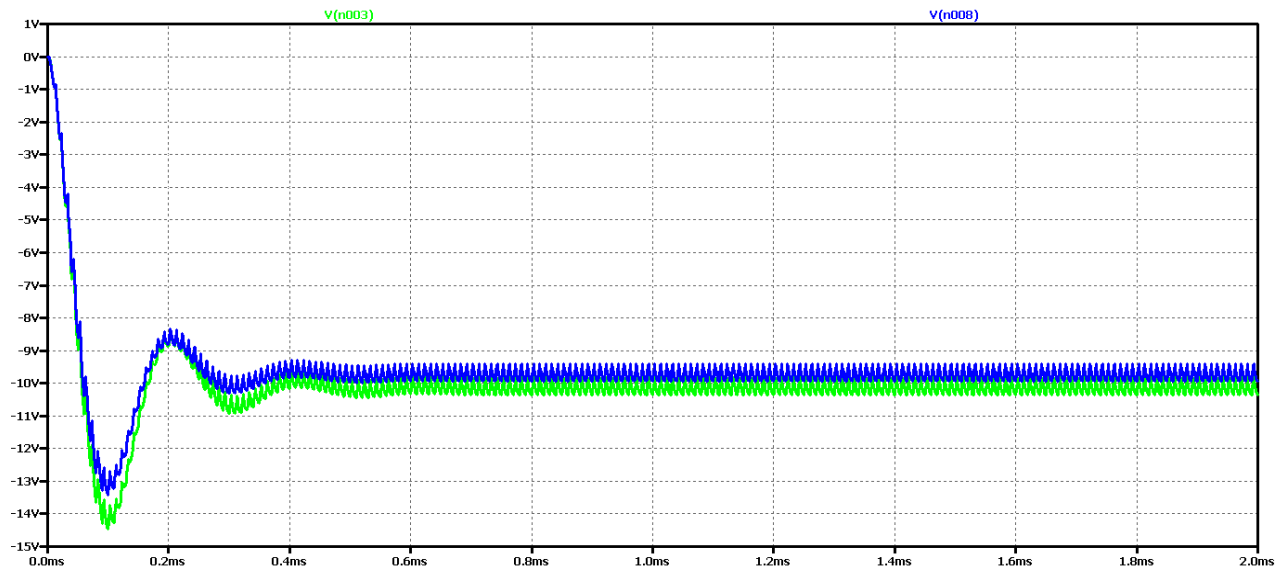
Figure 2.82 Simulation results of a Buck – Boost DC-DC converter

Figure 2.82 shows the results for the output voltage form (V (n003 for a circuit with ideal elements, and V (n008 for a circuit with real elements);

It can be seen that at the value of the coefficient D = 0.3, the amplitude of the oscillations of the output voltage is significantly smaller than when D = 0.5. On the other hand, the duration of the transition process is at least twice less than the initial value of D. A detailed view of the process is given in the following figure.
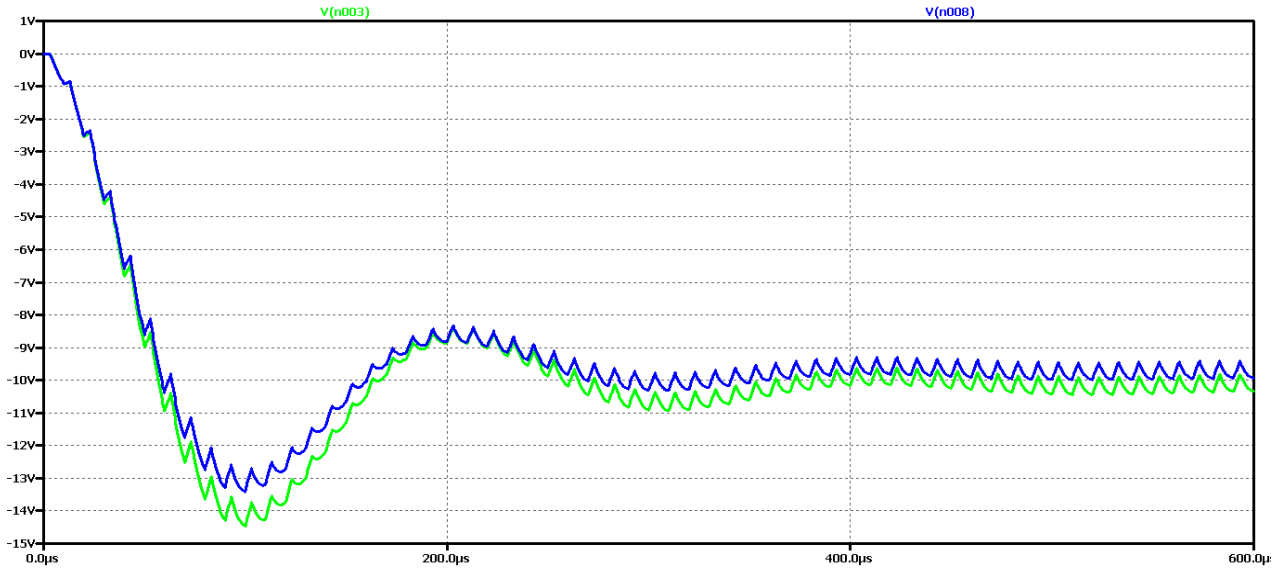
Figure 2.83 Detailed simulation results of a Buck – Boost DC-DC converter

Again, the difference between the results with the real and the ideal elements is that with the ideal circuit the steady-state output voltage is higher and the oscillation amplitude is larger with less attenuation. In both cases it is an oscillatory type of transient process that is not desirable in practice due to the long transient process and poor dynamic properties of the scheme.

Figure 2.84 shows the results of the Fourier transform (FFT analysis) of the output voltage.
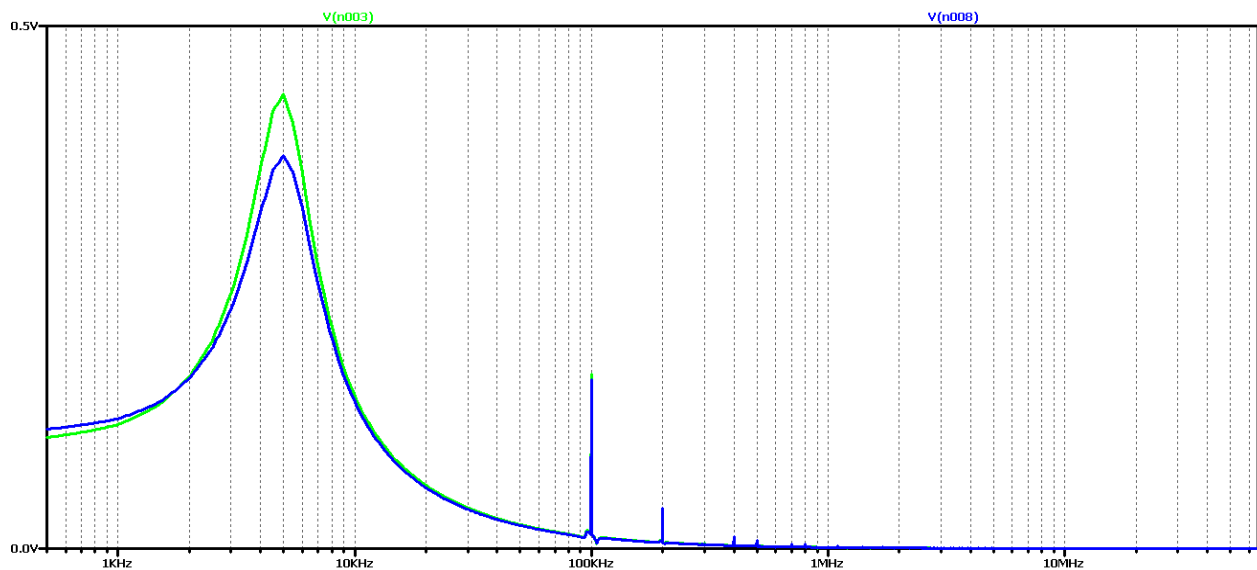
Figure 2.84 FFT analysis of the output voltage of a Buck – Boost DC-DC converter

It can be seen that the diagram again has a pronounced maximum at about 5kHz and a harmonic at 100kHz (operating frequency). As in the previous cases, there are additional harmonic multiples of the converter control frequency. Obviously, this diagram corresponds to the oscillatory type of the transition process.

From the comparison of the results at the value of the fill factor $D = 0.5$ (Figure 2.69 and Figure 2.70), full compliance can be seen.

Now let's try to achieve aperiodic transient by increasing the value of the filter inductance 5 times. The value of the filter capacitor will not change so as not to increase the ripple of the output voltage.
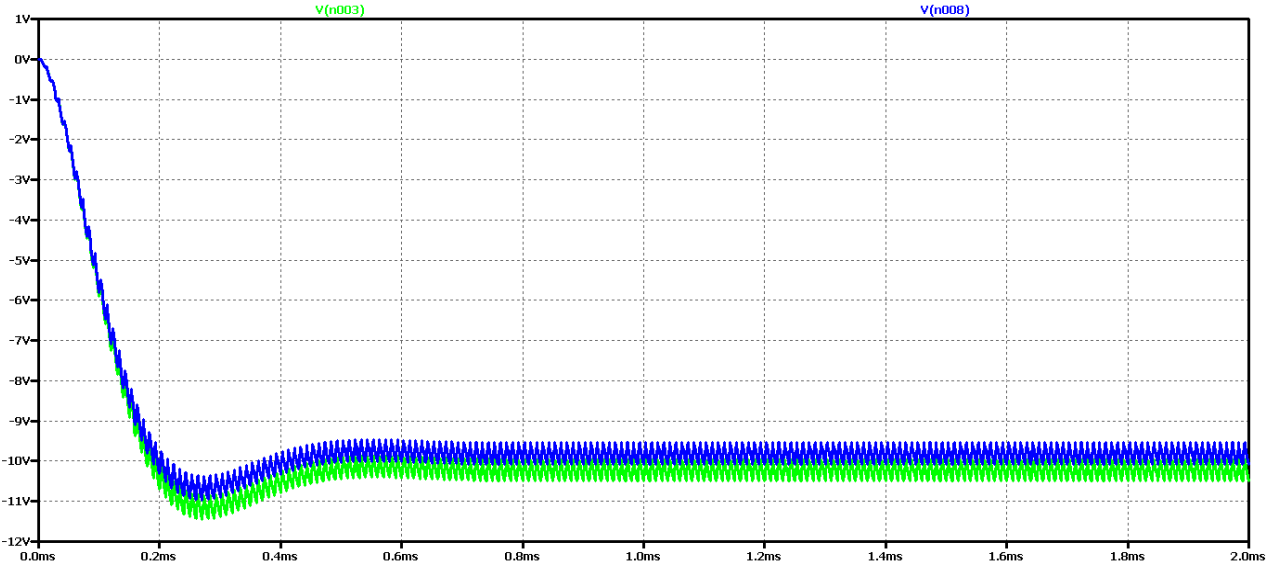
Figure 2.85 Simulation results of a Buck – Boost DC-DC converter, at 5 times the value of the filter inductance
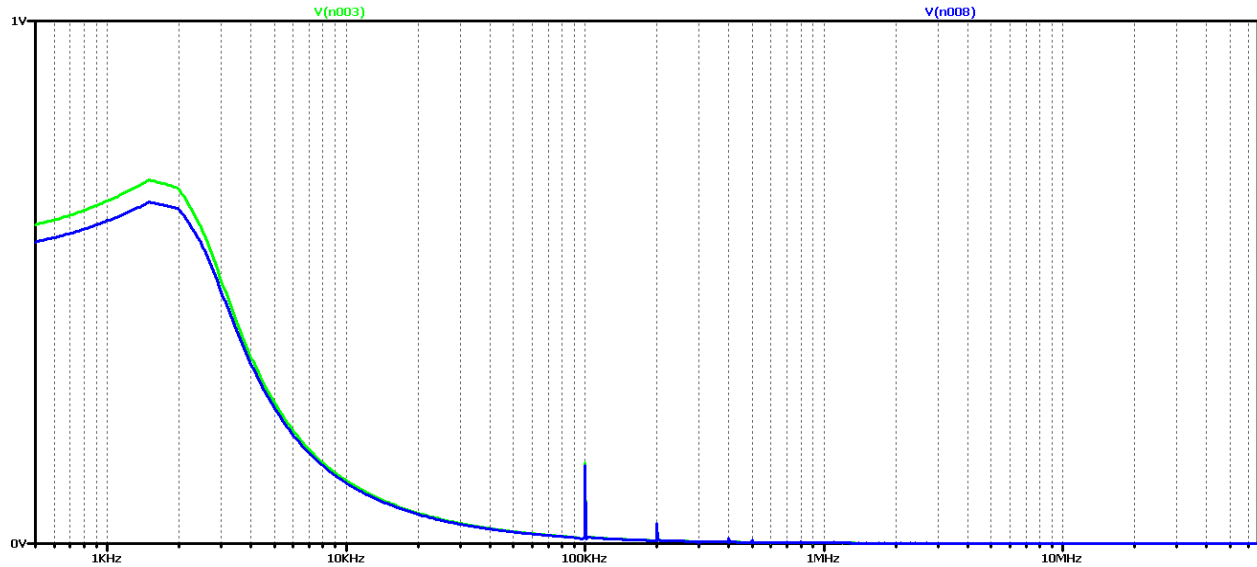
Figure 2.86 FFT analysis of the output voltage of the Buck - Boost DC-DC converter, at 5 times the value of the filter inductance

As the filter inductance increases, it can be seen that the oscillations of the output voltage are reduced, using both ideal and real elements. This is reflected in the results of the FFT analysis as the amplitude of harmonic multiples of the converter control frequency decreases. Because similarity is observed in the results, it makes no sense to literally repeat the studies from the other value of the fill factor.

We will go straight to the final version by increasing the value of the filter inductance 15 times. Figure 2.87 shows the output voltage form in this case. Obviously, we have achieved a case close to the aperiodic regime with the best possible dynamic performance compared to the previous variants in the scheme with real elements. In practice, in 2 ms we have the mode setup and transient startup completed. Unfortunately, no change from the initial element values was observed with the ideal element scheme.
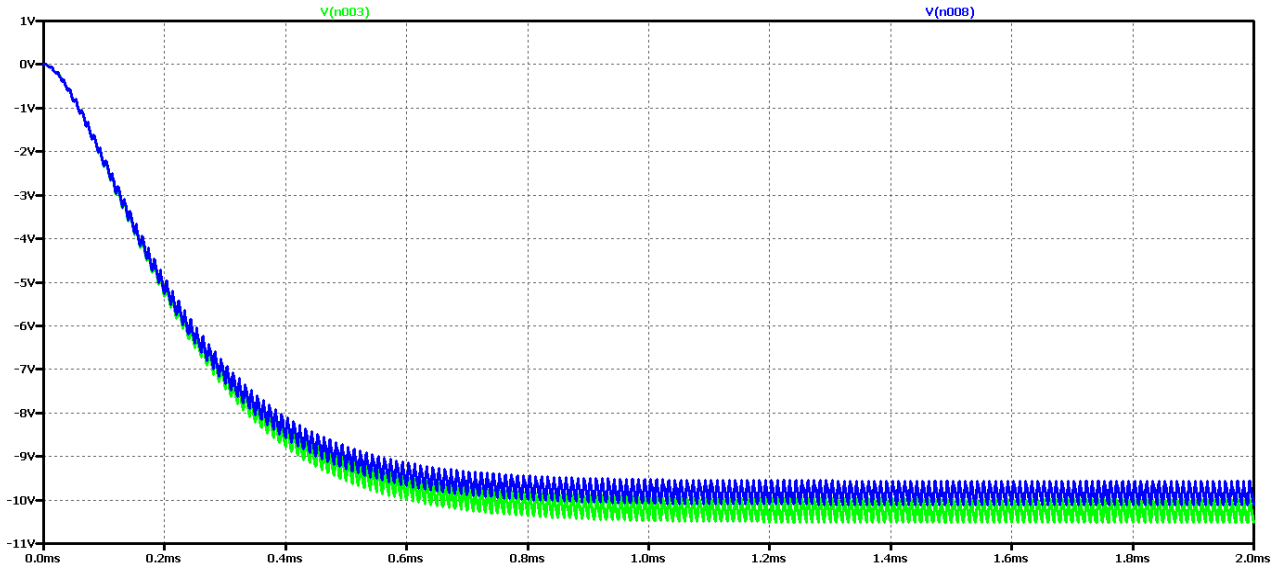
Figure 2.87 Simulation results of a Buck – Boost DC-DC converter at 15 times the value of the filter inductance

Increasing the filter capacity appears to reduce to some extent the oscillations of the output voltage, and to a large extent the form is close to aperiodic. Low frequency and low amplitude oscillations are observed. From the FFT analysis it is found that the value of the harmonic with the control frequency is very small compared to the previous case considered (especially for real elements). On the other hand, there is a maximum value of the harmonic at a frequency of about 1.5 kHz, ie the output voltage can largely be considered constant with very small pulsations and deviations in the setting mode.

Figure 2.88 FFT analysis of the output voltage of the Buck – Boost DC-DC converter at 15 times the value of the filter inductance

Obviously with this value of filter inductance, regardless of the increase in filter inductance, no better transients will be obtained, the next experiment is to use model-based optimization to determine the values of the elements. In this case, the values of the filter inductance 1000uH and the filter capacitor 2uF were obtained. To reduce the ripple of the output voltage, a capacitor value of 5u is selected.

The results of the study are shown in Figure 2.89.
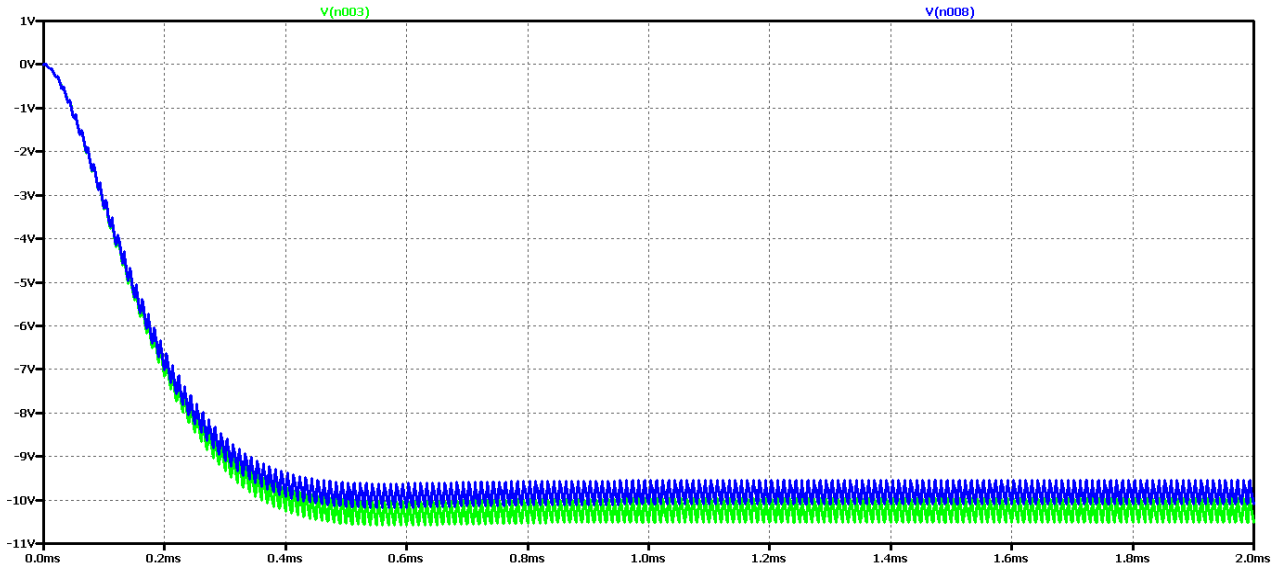
Figure 2.89 Output voltage of Buck – Boost DC-DC converter, at optimum values of filter elements

The optimum values can be seen to achieve the best dynamics - transient duration of about 0.5 ms. On the other hand, due to the low value of the output capacitor, increased ripples in the form of the output voltage.

In Figure 2.90 shows the results of the Fourier transform (FFT analysis) of the output voltage. The presence of harmonic, multiple frequency control, is more pronounced in the ideal element scheme. On the other hand, we have an aperiodic transient that is determined by the smooth descent at the beginning of the characteristic.
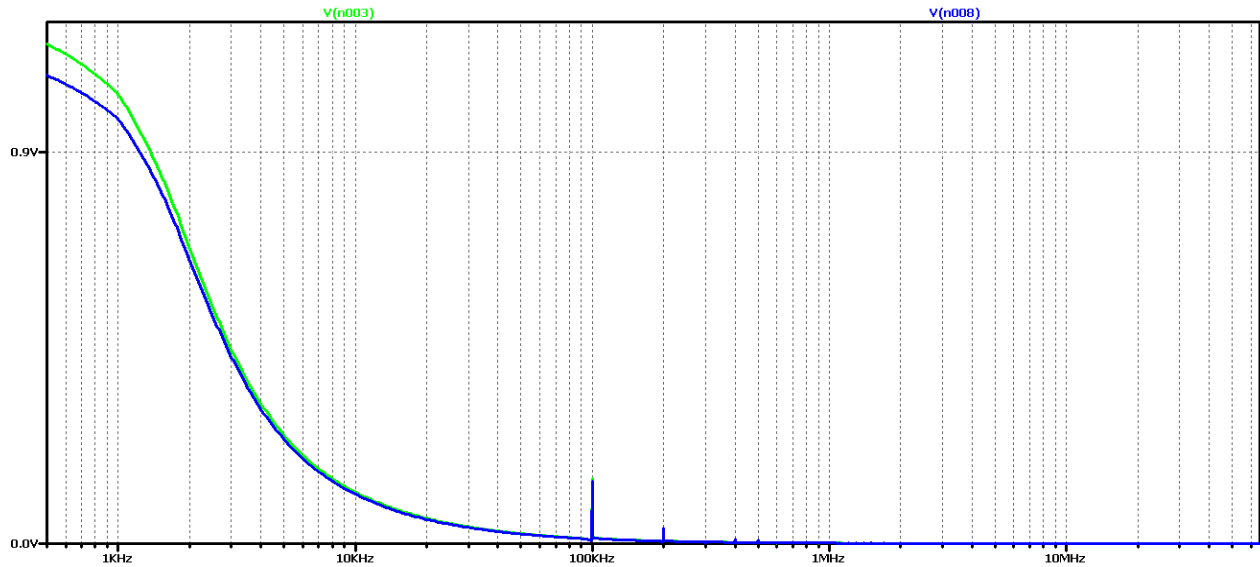
Figure 2.90 FFT analysis of the output voltage of the Buck – Boost DC-DC converter, at the optimum values of the filter elements

To test again the hypothesis of the relationship between the output voltage form and the results of the FFT analysis, significantly larger values of the filter elements were taken in subsequent studies: 100 times the value of the filter inductance and 3 times the filter capacitor.
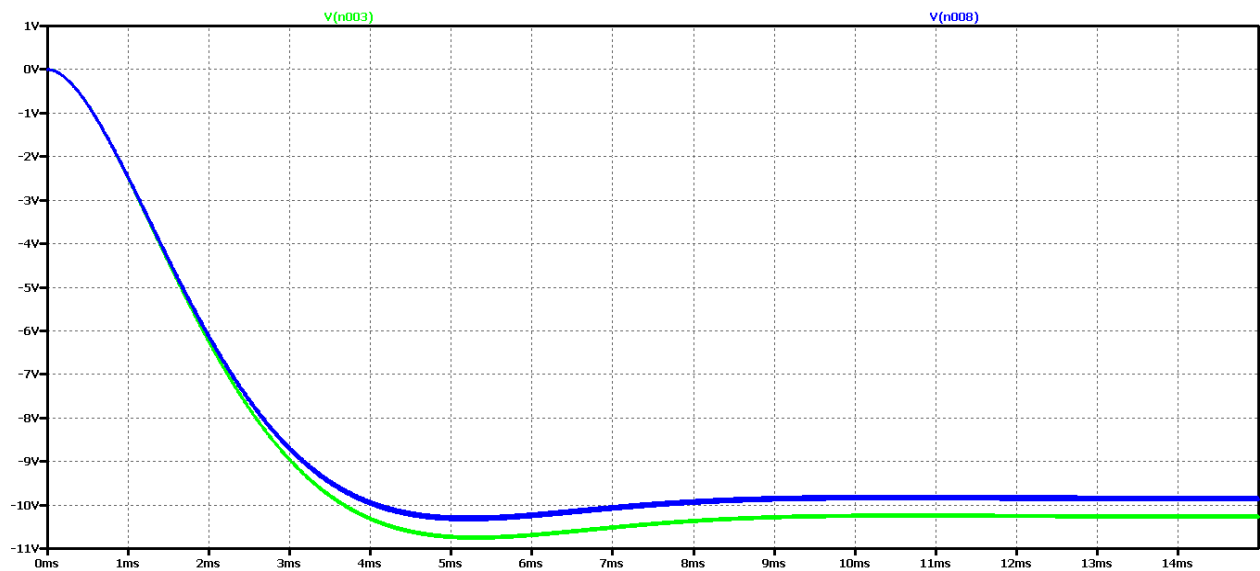
Figure 2.91 Output voltage of Buck – Boost DC-DC converter, at maximum values of filter elements

It appears that there is a much worse dynamics than the previous case of optimal element values. And in the FFT analysis of Figure 2.92 - there are practically harmonic constituents only in the

ideal element scheme, where the transient process has been completed for the simulation time. From these results, it can be concluded that if we have an aperiodic establishment process, there are no harmonics multiple of the control frequency, and a slow drop at the beginning of the characteristic is associated with an increase in the output voltage.

In this way, due to the numerous experiments, a clear dependence and interrelation between the nature of the transients and the form and type of the characteristic from the FFT analysis of the output voltage begins to emerge.
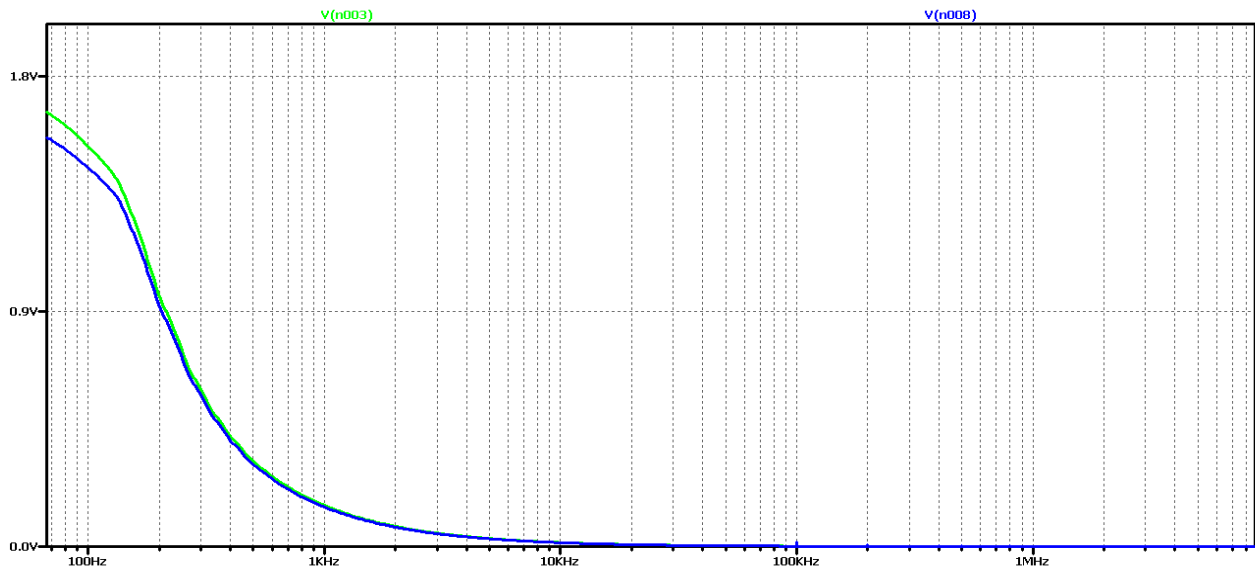
Figure 2.92 FFT analysis of the output voltage of the Buck – Boost DC-DC converter, at maximum values of the filter elements

Similar studies have been made for another case of modulation coefficient values D –D = 0.7. The purpose is to check whether these dependencies are observed in this additional variant.

It can be seen that at the value of the coefficient D = 0.7, the amplitude of the oscillations of the output voltage is smaller than in the case when D = 0.5. On the other hand, the duration of the transient is shorter than the initial value of D. This is due to the peculiarities of the principle of operation of the converter.
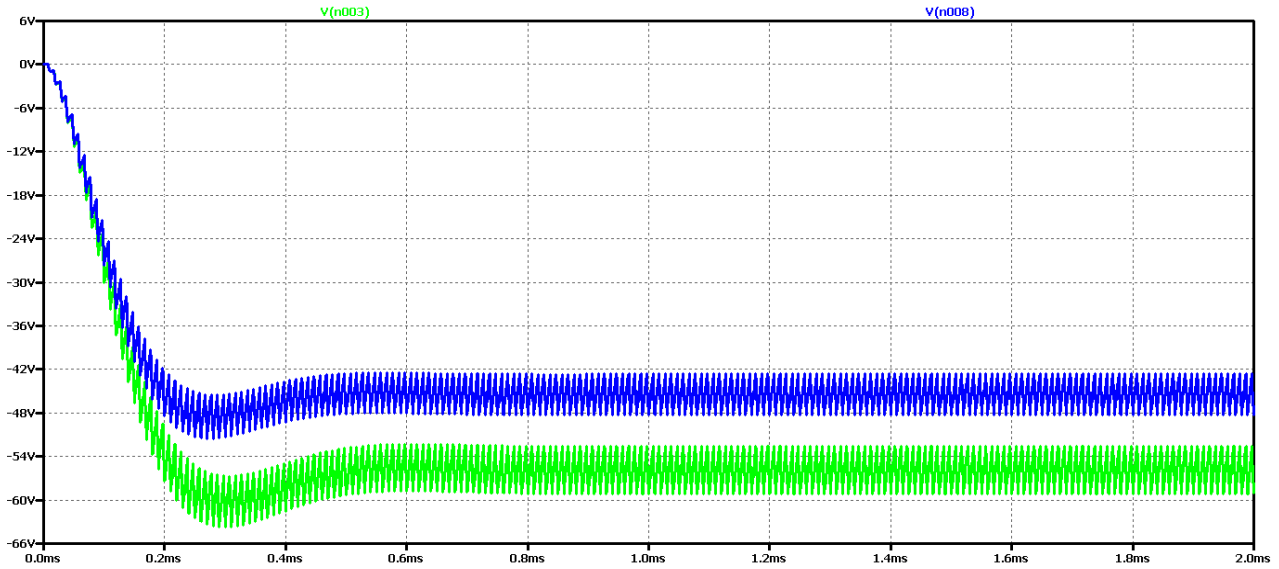
Figure 2.93 Simulation results of a Buck – Boost DC-DC converter

Again, the difference between the results with the real and the ideal elements is that with the ideal circuit the steady-state output voltage is higher and the oscillation amplitude is larger with less attenuation. In both cases, it is a close to aperiodic type of transient process.

Figure 2.94 shows the results of the Fourier transform (FFT analysis) of the output voltage.
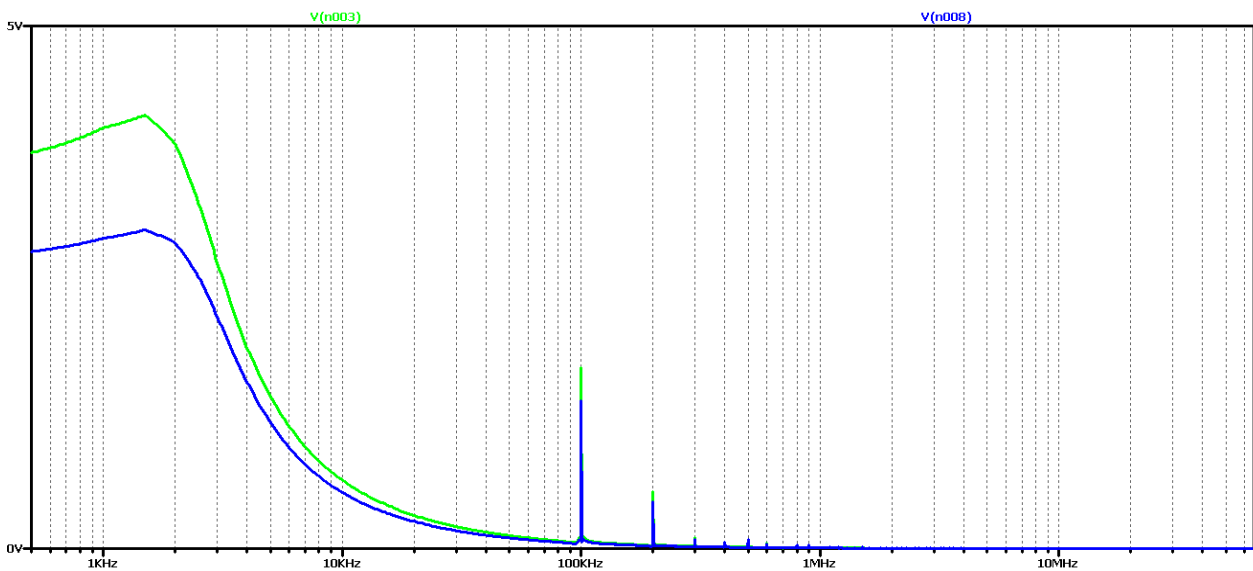
Figure 2.94 FFT analysis of the output voltage of the Buck – Boost DC-DC converter

It can be seen that in the diagram in this case there is no clear maximum and there is a high content of harmonics multiples of 100kHz (operating frequency). Obviously, this diagram corresponds to an intermediate type of transition.

Now let's try to achieve aperiodic transient by increasing the value of the filter inductance 5 times. The value of the filter capacity will not change so as not to increase the ripple of the output voltage.
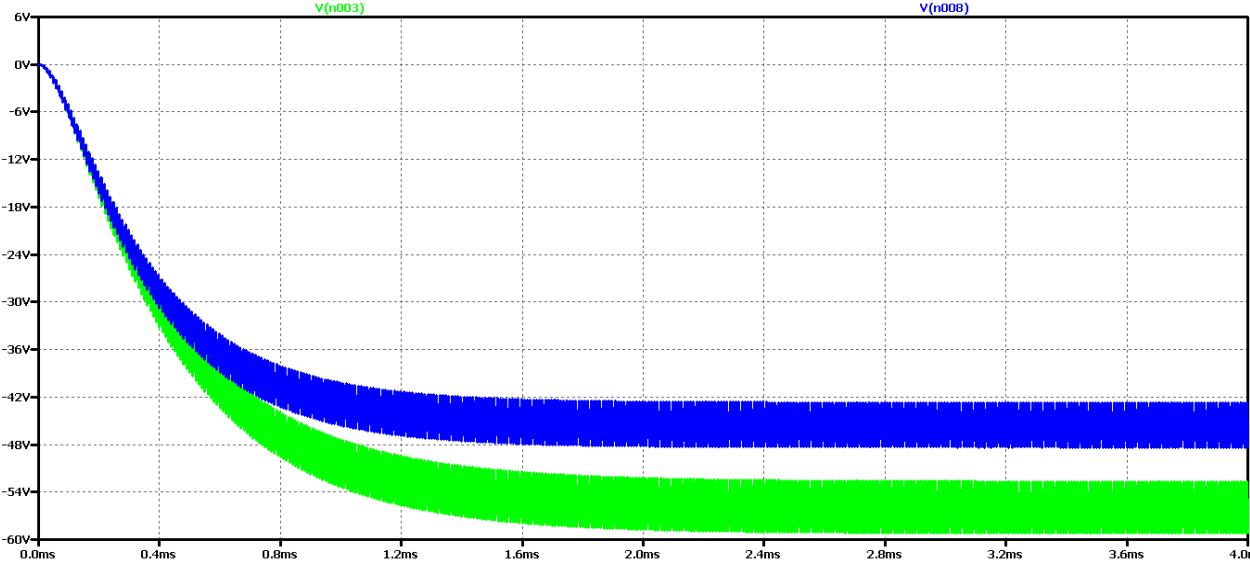
Figure 2.95 Simulation results of a Buck – Boost DC-DC converter, at 5 times the value of the filter inductance
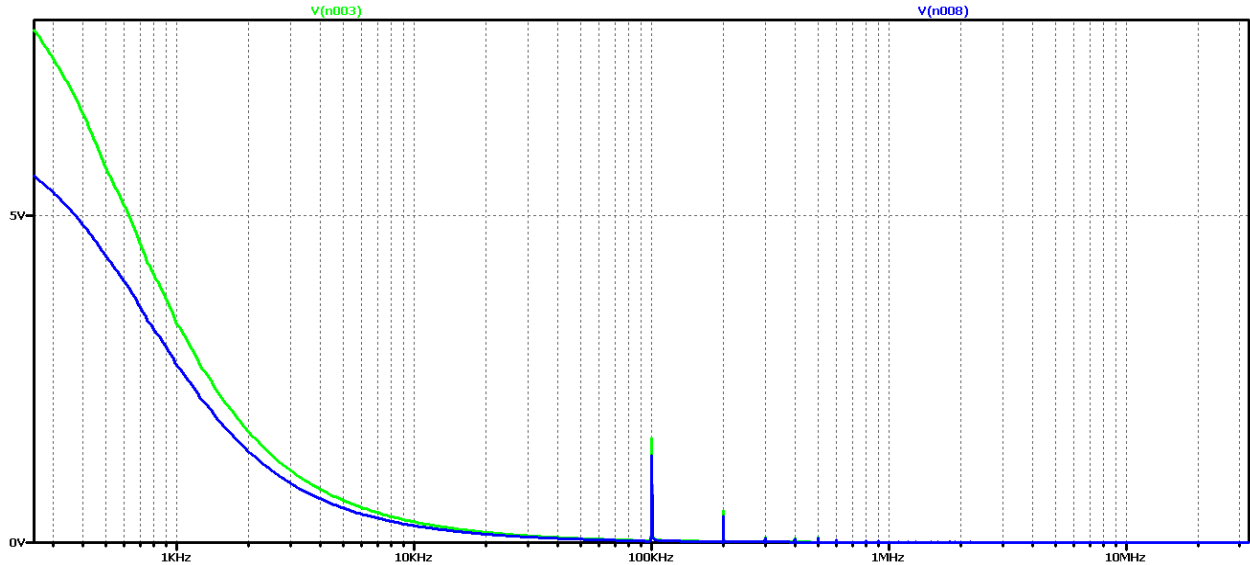
Figure 2.96 FFT analysis of the output voltage of the Buck – Boost DC-DC converter at 5 times the value of the filter inductance

82

As the filter inductance increases, it can be seen that the oscillations of the output voltage are reduced, especially when real elements are used. The results of the FFT analysis again show harmonic multiples of the converter control frequency. Since there is a similarity in the results of the previous values of the coefficient D, it does not make sense to repeat the literally studied from the initial value of the coefficient of filling.

To speed up the studies, as there is enough data collected, we will move to the final version by increasing the value of the filter inductance 15 times. Figure 2.97 shows the output voltage form in this case. Obviously, we have achieved a case close to the aperiodic regime with the best possible dynamic performance compared to the previous variants in the scheme with real elements. In practice, in 2 ms we have the mode setup and transient startup completed. Unfortunately, no change from the initial element values was observed with the ideal element scheme.
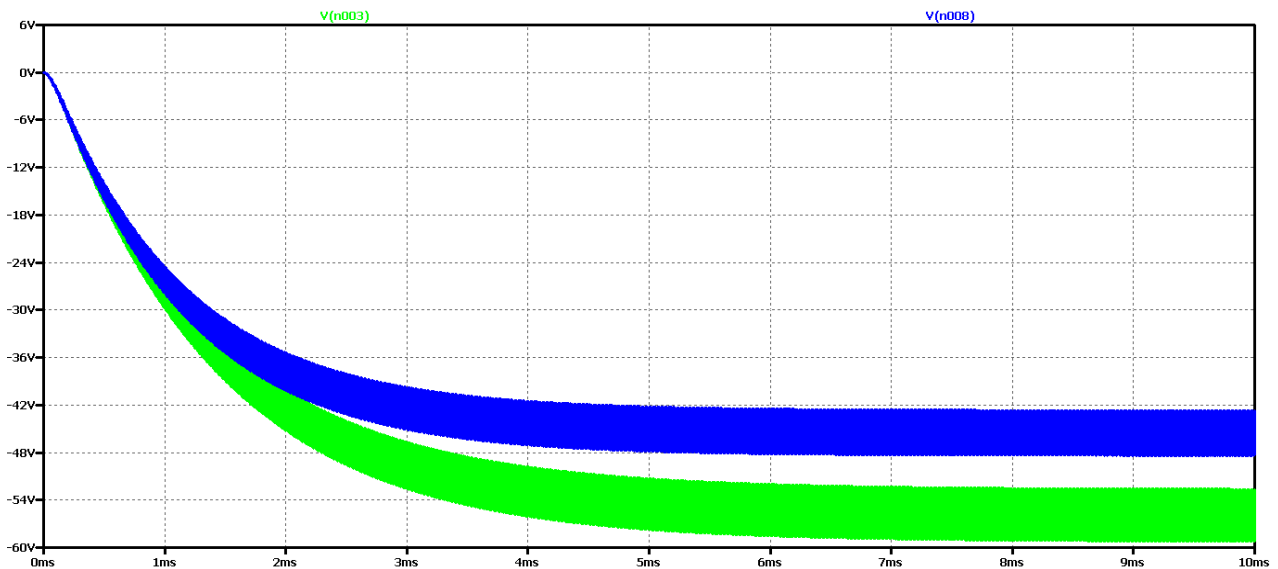
Figure 2.97 Simulation results of a Buck – Boost DC-DC converter, at 15 times the value of the filter inductance

Increasing the filter inductance appears to reduce to some extent the oscillations of the output voltage, and to a large extent the form is close to aperiodic. Low frequency oscillations in the form of the output voltage are not observed. From the FFT analysis it is found that the value of the harmonic with the control frequency is very small compared to the previous case considered (especially for real elements). On the other hand, there is a maximum value of the harmonic at a

frequency of about 1.5 kHz, ie the output voltage can largely be considered constant with very small pulsations and deviations in the setting mode.
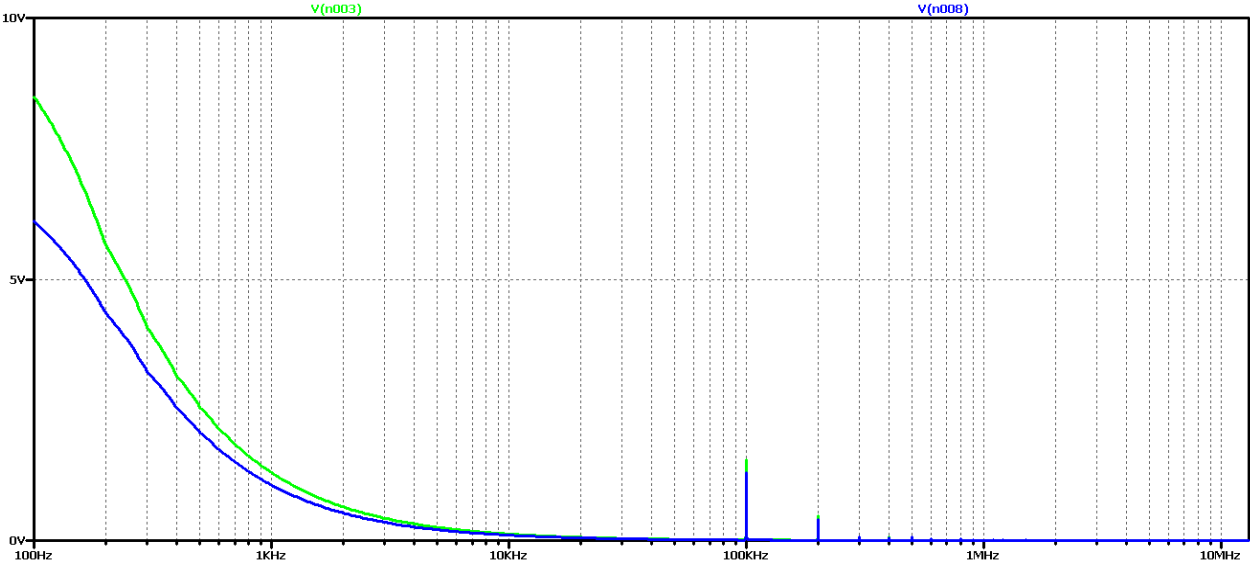
Figure 2.98 FFT analysis of the output voltage of the Buck – Boost DC-DC converter at 15 times the value of the filter inductance

Obviously with this value of filter inductance, no better transients will be obtained. The next experiment is using model-based optimization to determine the values of the elements. In this case, the values of the filter inductance 500uH and the filter capacitor 2uF are obtained. To prevent the output voltage from falling off at the start of the process, a 5uF capacitor value is selected.

The results of the study are shown in Figure 2.99.
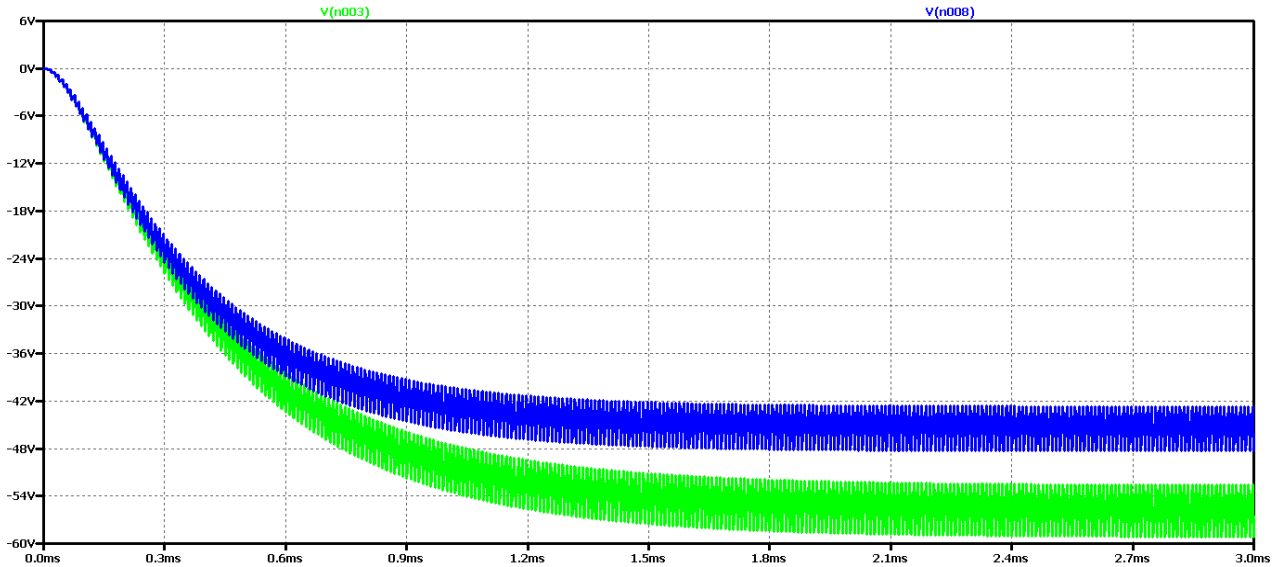
Figure 2.99 Output voltage of Buck – Boost DC-DC converter, at optimum values of filter elements

The optimum values can be seen to achieve the best dynamics - transient duration of about 0.5 ms. On the other hand, due to the small value of the output capacitor, there is a slight drop in the output voltage.

In Figure 2.100 shows the results of the Fourier transform (FFT analysis) of the output voltage. The presence of harmonic multiples of the control frequency can be seen due to the drop in output voltage (more pronounced in the circuit with ideal elements). On the other hand, we have an aperiodic transition process, which is determined by the plateau at the beginning of the characteristic.
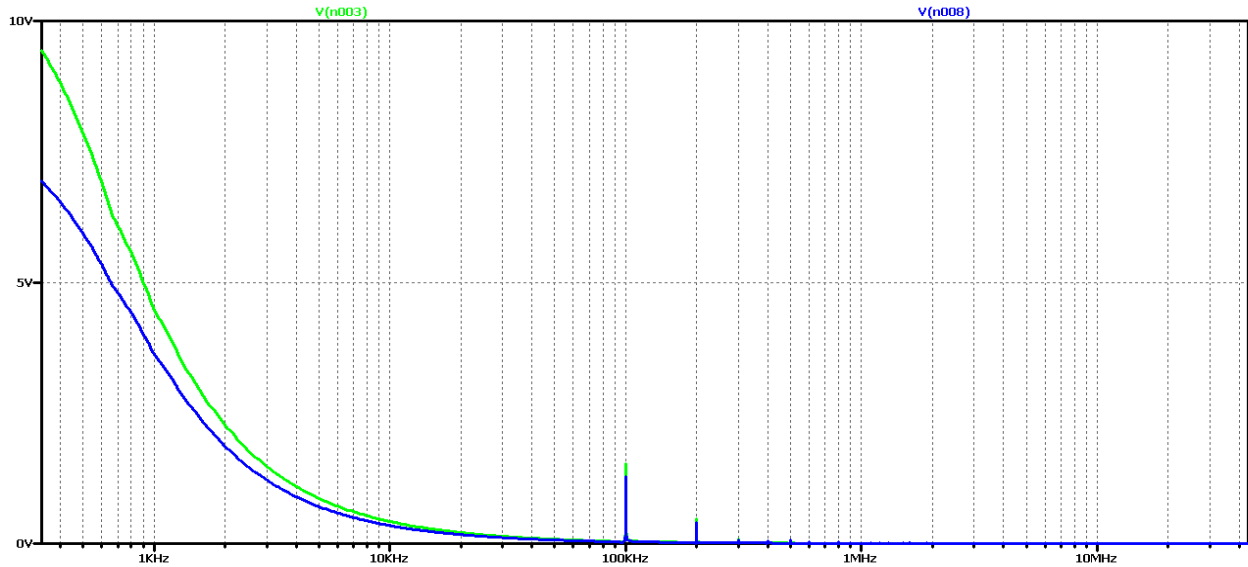
Figure 2.100 FFT analysis of the output voltage of the Buck – Boost DC-DC converter, at the optimum values of the filter elements

To test again the hypothesis of the relationship between the output voltage form and the results of the FFT analysis, significantly larger values of the filter elements were taken in subsequent studies: 50 times the value of the filter inductance and 3 times the filter capacitor.
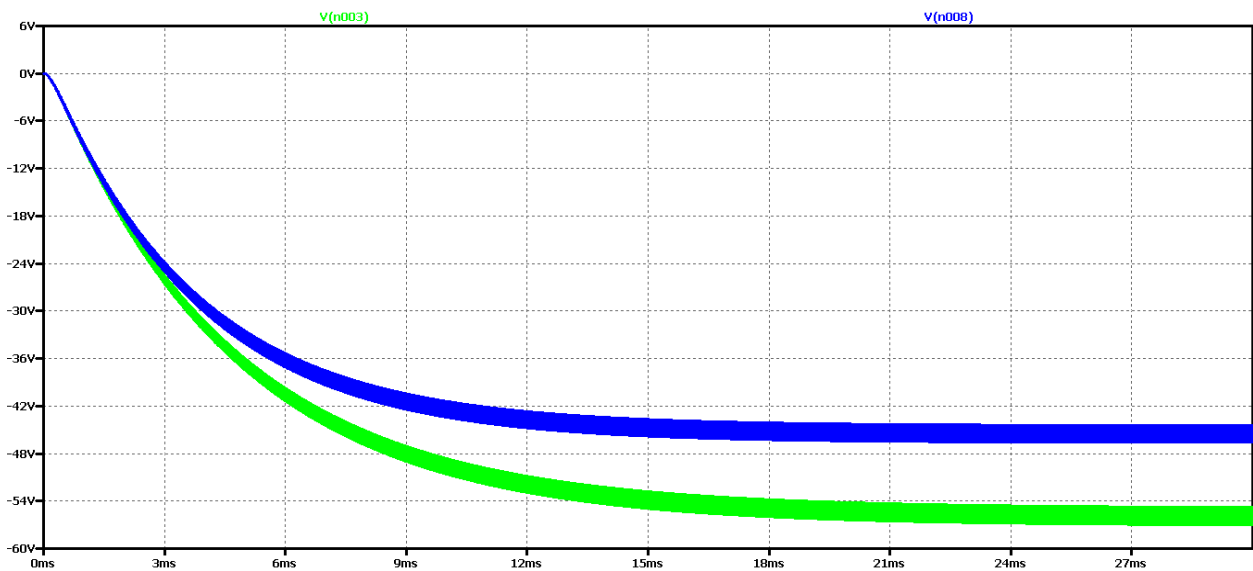
Figure 2.101 Buck – Boost DC-DC converter output voltage form, with maximum values of filter elements

It appears that there is a much worse dynamics than the previous case of optimal element values. And in the FFT analysis of Figure 2.102, there are practically harmonic components only in the

ideal element scheme, where the transient process has been completed for the simulation time. From these results, it can be concluded that if we have an aperiodic ascertainment process, there are no harmonics multiple of the control frequency, and the plateau at the beginning of the characteristic is related to the output voltage drop.

In this way, due to the numerous experiments, a clear dependence and interrelation between the nature of the transients and the form and type of the characteristic from the FFT analysis of the output voltage begins to emerge.
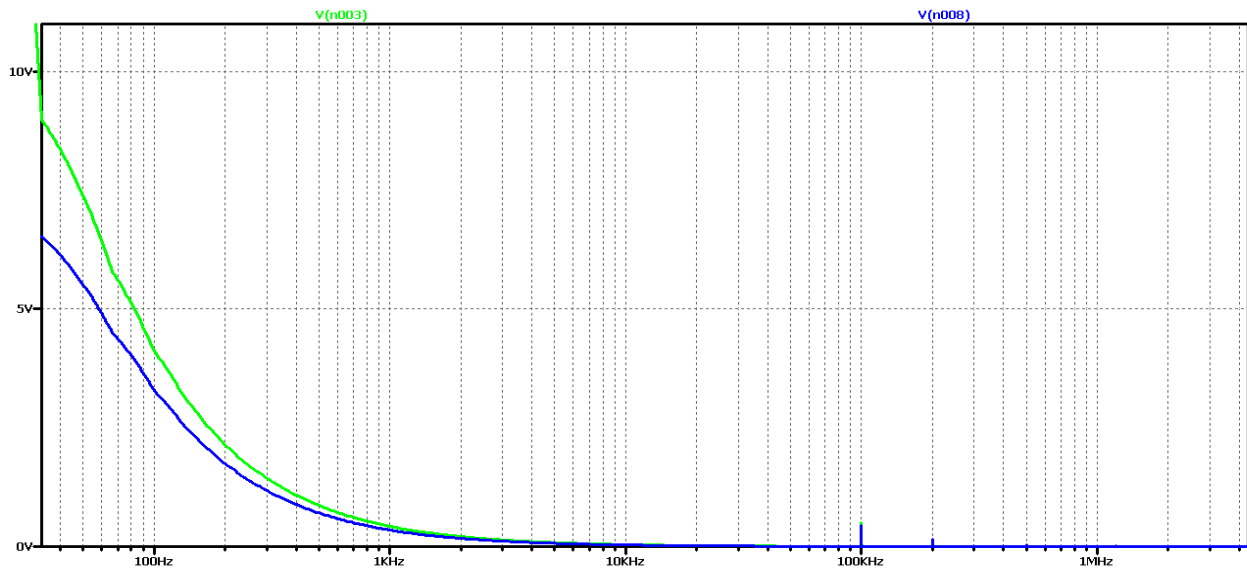
Figure 2.102 FFT analysis of the output voltage of the Buck – Boost DC-DC converter, with maximum values of the filter elements

Let's compare the deviations from the established mode for the lowest value of filter capacity in the three cases of modulation coefficient. In the first case - Figure 2.69 the maximum deviation in the worst case using ideal elements is from 31.5V to 25V or a ratio of 1.26; in the second case - Figure81 the maximum deviation in the worst case using ideal elements is from 14.5V to 10.5V or a ratio of 1.38; in the third case - Figure 2.93 the maximum deviation in the worst case using ideal elements is from 64V to 59V or a ratio of 1.084. In this way, a slight dependence of the maximum deviation of the output voltage on the modulation coefficient is also established, its smallest value again at D = 0.7.

2.8.   CONCLUSIONS:

- There is a clear relationship between the type of transient and the FFT analysis of the output voltage of the most commonly used DC-DC converter circuits: Buck, Boost and Buck - Boost. Generally speaking, the following relationship exists: the amplitude of the first harmonic gives information about the magnitude of the output voltage ripple, the larger the ripple, the greater its value. On the other hand, the presence of a plateau in the Fourier transform characteristic shows an aperiodic transient with the shortest duration.

- The use of optimization procedures greatly facilitates the design and synthesis of a controller;

- FFT analysis is a good enough tool for analyzing the output voltage form.

3. INTERACTIVE WEB BASED DESIGN OF POWER ELECTRONIC CONVERTERS

3.1. DC – DC CONVERTER DATA INTERCHANGE?

There are already a lot of different and new technologies for processing big data. Processing large sets of databases is not a novelty and has been done for many years in many ways and methods. The popularity of processing that data is getting bigger and bigger, and processing on large databases has been never simple as the price also like an important factor for mentioning (Xun Lu; Xia Zhang; Zhengyou Xia, 2015).

With current technologies, to perform any kind of analysis and processing or filtering of large databases, a scientist must possess expert knowledge in the fields of databases as well as mathematical functions and possibly any of the more serious software packages that serve that purpose. According to that, the using of the web applications makes these types of data processing a little easier and more user-friendly.

This dissertation provides an example of processing more data on the behavior of electronic components at variable voltage on already well-known and processed dc-dc converters. The scope of the chapter will be data processing and results gathered from the web application processing with algorithms for filtering from programing languages. Namely, the same data is displayed and processed with existing software packages such as LabView that is obtained in the next section.

This model of information system proposed for processing data is also flexible for working with a lot different type of data. The database is suitable for files that are arranged in strings for later processing. The information system can be uploaded to a server later and be reachable from any destination, uploading data files from distance and gathering one of the offered analysis in a very fast and reliable way. One feature that is also worth mentioning is that the user can upload data files that are of mass proportions like the data from the windmills, data from photovoltaic systems, data from air pollution or data from seismic excitation. Imagine working with that amount of data collected in 5 or 10 years with refresh rate of few seconds. That can be a real challenge even for the most professional and expensive software packages as well as experienced researchers in that field of investigation.

Another crucial feature that will be mentioned is the usability for the new researchers and students that are studying either big data processing or dc – dc converters. As known every start is not easy and the results can be very far. The young researchers sometimes lose this battle because they must pass a lot of techniques before previewing some results. This information model will provide faster result with aim to save the curiosity and the will of the new student to keep studying and tries to understand how the instruments or the phenomena that is investigating works.

Data that is uploaded for the needs of this dissertation for example is consisted in several files for each instrument and previewed in Microsoft Excel can be seen around 300 000 rows and 2 or more columns depends what element we are investigating. The information processing model provides differencing of the results to sections in order to better view of some point of the main harmonic. This is also important when investigation such amount of data.

The example proves that we can already take advantage of existing features from those software packages and integrate them into one application that is available everywhere, that is, uploaded to a server so that it can be used through cloud technology. This application may one day work with renewable energy sources located in and around the city of Sofia, or it may work with the generated energy of all windmills located around the town of Plovdiv (S. Sarabia; C. A. Figuero; F. A. Zelaya A.; A. Zamora; M.R.A. Paternina, 2018).

On the other hand, we can detect anomalies in air temperature, seas depending on the time period in order to quickly detect and alert the group of scientists dealing with these problems.
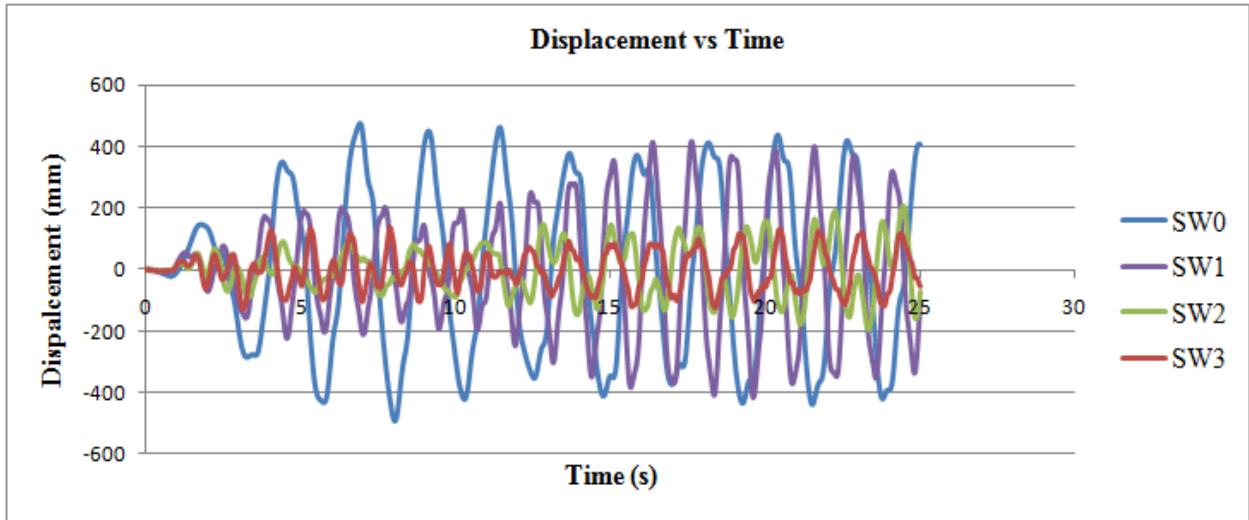
Figure 3.1 Example of measurements of displacements while ground seismic excitation

Figure 3.1 describes a measurement of displacements of four channels during a seismic excitation. From different layers can be seen different displacements when processed and presented on chart. From chart it is clearly visible how layers behave. With processing data every string and set of data is presented on graph or chart and the information can be easily seen.
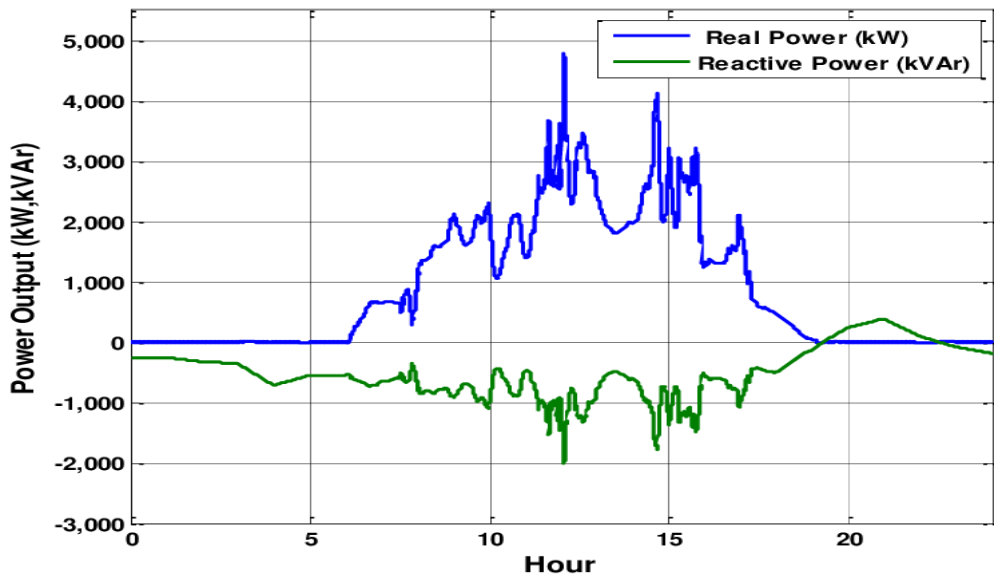
Figure 3.2 Photovoltaics system with output power regulation control

According to application usability, the latest technologies have been implemented, which are divided into several micro services to optimally solving the problem of big data analytics. UI / UX uses the latest version of the bootstrap CSS framework as the main tool for defining and designing the application to display the desired results.

The speed and functionality of the bootstrap package leads to a scalable solution in defining the front-end of the application with its immense popularity, great documentation and the ability to easily update existing code. In addition to typography, grid systems are used that allow easy and flexible modification of the layout of the web application and give structure and most importantly compatibility for use of multiple devices i.e. use at the same time of all smart phones, tablets, and all smart devices in today.

The in-app menu definitions also follow the bootstrap standards that give responsiveness when using different platforms and devices. The tables which are used allow for orderly and fast access to the most important part of the application, i.e. presenting the results of the database itself.

Another technology used in this thesis is JavaScript. Over time, this technology is gaining momentum in the creation of web applications and can be seen the creation of a huge number of packages developed in JavaScript. With JavaScript can be processed data itself, a visual representation in the form of an interactive diagram. With JavaScript also can be created a seamless experience of using the application by creating XHR records to the server which speeds up data download and enhances the UX of the user. This allows the application to function without the user having to reload the web application itself (Seth Y. Fiawoo ; Robert A. Sowah, 2012).

This JavaScript-driven XHR Request, which is naturally asynchronous, binds in the background to a server that then contacts the Phyton Mathematical Library. During this connection, the back-end system in PHP downloads the XHR record, finds the data in the database and sends it to the Phyton Mathematical Library, which then returns processed results in the form of FFT, InverseFFT digital content. To improve the retrieval of this data when establishing a connection from PHP to the MySQL database a request is made according to pre-indexed keys in the big

data center (Sheng Zhou; Xiaoxiao Zhang; Xianhui Li; Gang Zheng; Gaokun Zhang, 2017). This then creates a list of data sorted and selected according to the given PHP parameters.

All these functionalities are under the control of Laravel's built-in authentication system. The system has created a process for creating and logging in users. This process is enabled in the background with a special MySQL database which is optimized for quick entry of new users as well as filtering of the already existing login prompt. This system works with encrypted data that requires username / email and password input. As part of the record file in the database, information is kept for each individual user who, when, at what time he / she has registered with the system, logged in or made any changes to his / her existing user profile.

Entering this data is a lengthy process, especially when entering a big number of queues because the database itself in the big data center is optimized for easier reading and processing of ready data (Jiansheng Li; Beixing Deng; Yongfeng Huang; Xing Li, 2011).

In this type of investigation, this dissertation uses data imported from multiple electronic components that are creating a DC-DC converter. Several converters are included in the dissertation to detect the difference in data. In addition, the converters have a large amount of data or queues, to show how the application works in case of overload. Namely, if the number of rows is in the order of several hundred thousand, the data shown in the diagrams is done in such a way that it groups the rows to display several large works in order to have a better view.

If 500,000 rows need to be processed, it would be uncomfortable to see such a mass of data at once so it would be better to group it into several parts where the user with a button located just below the diagram will navigate between the rows (Vitalijs Komashilovs; Aleksejs Zacepins; Valerijs Bezrukovs; Dmitrijs Bezrukovs; Janis Hofmanis, 2014). The idea of using an enormous size example stems from the desire to show that if the future is to import huge amounts of data adapted over several years, the application can easily and amicably meet this challenge.

3.3. METOLOGY OF WEB BASED DATA PROCESSING

In this section it is discussed about the graph view, page and functionalities that our application provides. A simple and user-friendly design is developed because it will be mostly used by engineers, so the focus is more on the fast execution and correctness of the data analyzes.
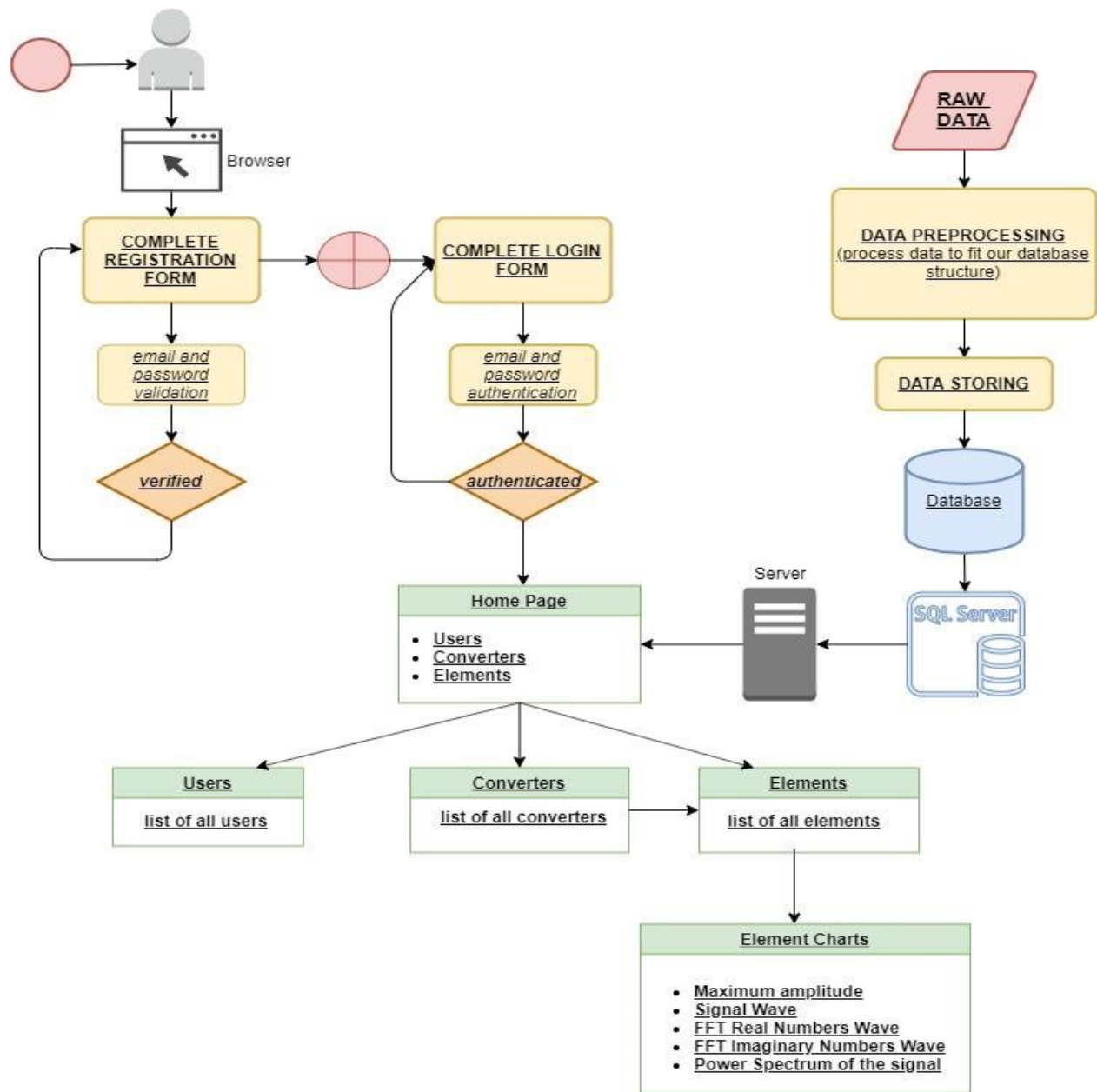
Figure 3.3 Dataflow diagram for web – based application

Figure 3.3 represent a dataflow of the web – base application, connections between components and complete path for using the application. The priority for choosing this type of approach in investigating strings from output voltage is the mobility and usability of this type of application. The tests can be performed on any machine that is connected to the internet. The whole project can be imported on cloud and used any time from anywhere, without installing on particular machine like other mentioned software solutions.
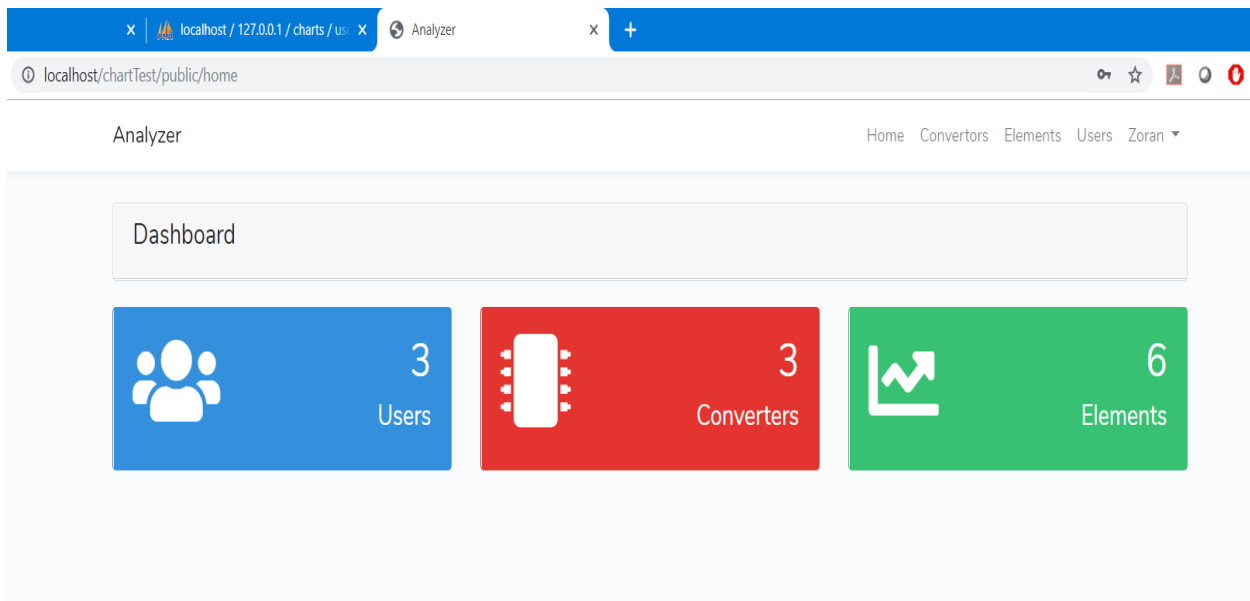
Figure 3.4 Home page of the web application

Figure 3.4 represent a view of users, converters and elements, where the user can navigate to the desired section. From the first page can be navigated to the Converters page where we can see a list from all converters that are stored in database. Right now, there are imported only the types of converters that are used in Chapter 2.
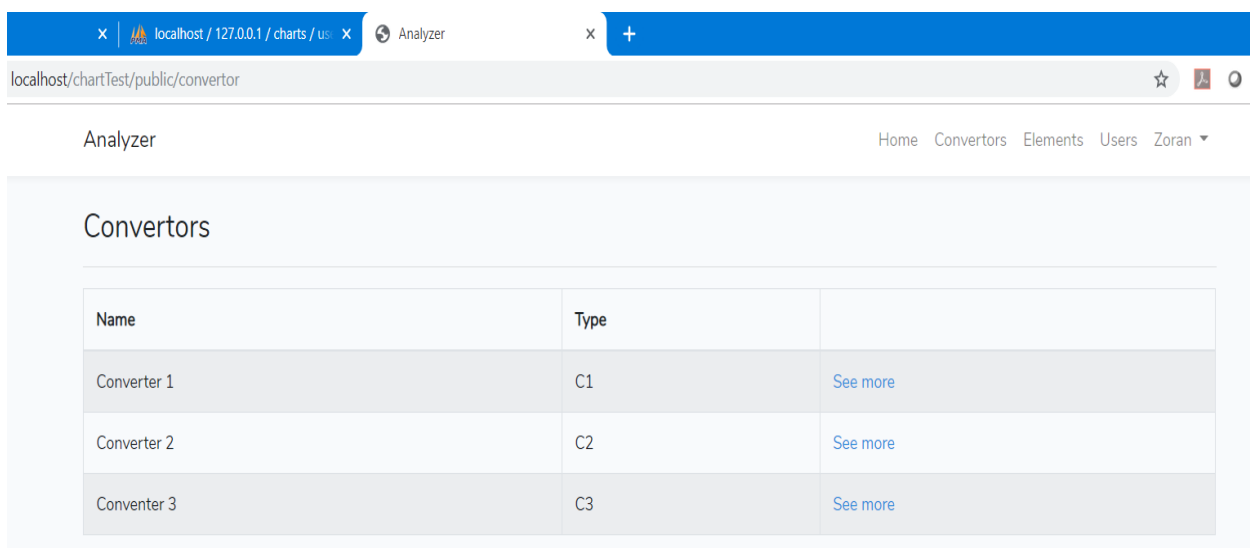
Figure 3.5 Converter's page

Figure 3.5 represent a window where users can choose what type of element they want to analyze and preview that is already imported. The graphic approach is simple and easy for use, that provides using it without certain advanced knowledge in the area of information technology or in electronic technology that is also important if the user is a for example first degree student.
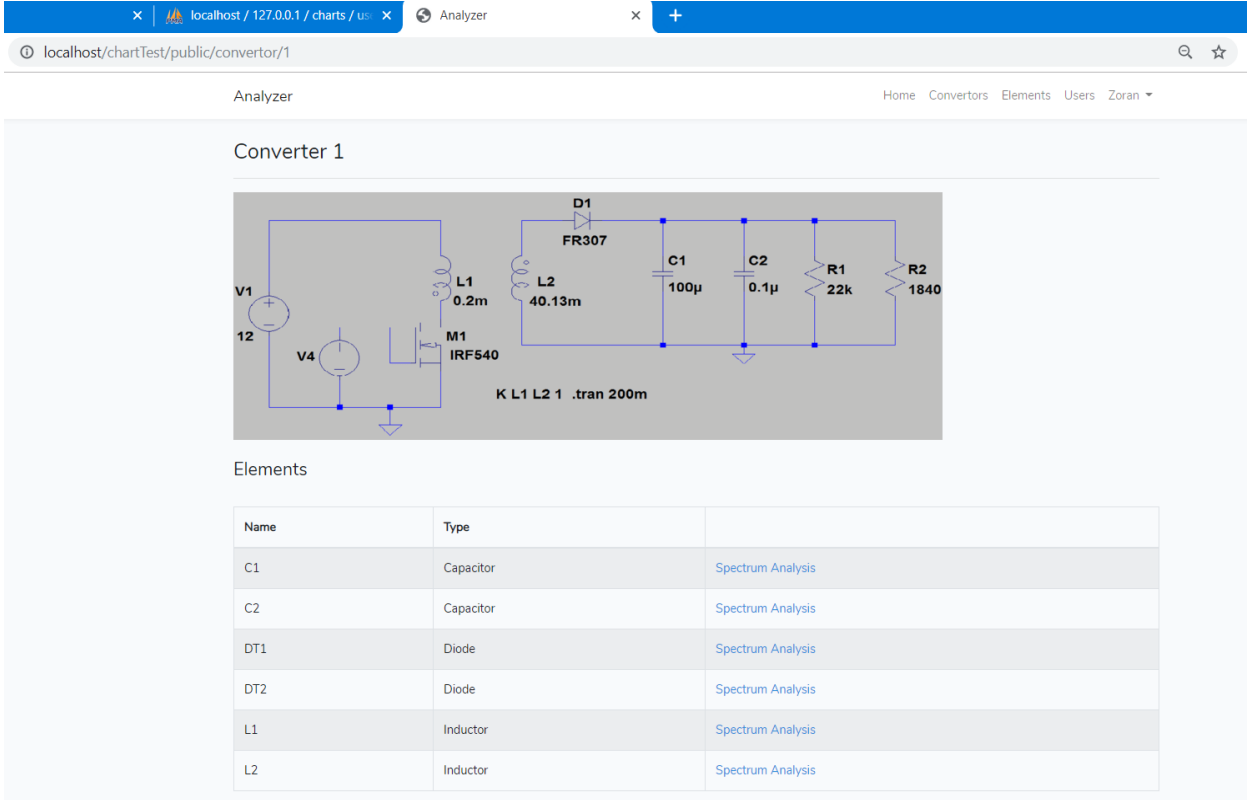
Figure 3.6 Page of one converter

Figure 3.6 represent a page where can be seen an image of the converter showing how its electrical network is designed and a table showing all converter's elements. Table has columns for element's name, type and link to see the data chart of the element. The scheme of the DC – DC converter additionally describes the main circuit that will be of importance for advanced users in the field of investigation.

With choosing Spectrum Analysis, a new page will be opened showing the data chart of the chosen element with every value of voltage by time, FFT analysis and inverse FFT. This chart is specially designed with library for drawing Charts in Laravel framework. After loading all data, the chart looks like on the picture bellow:
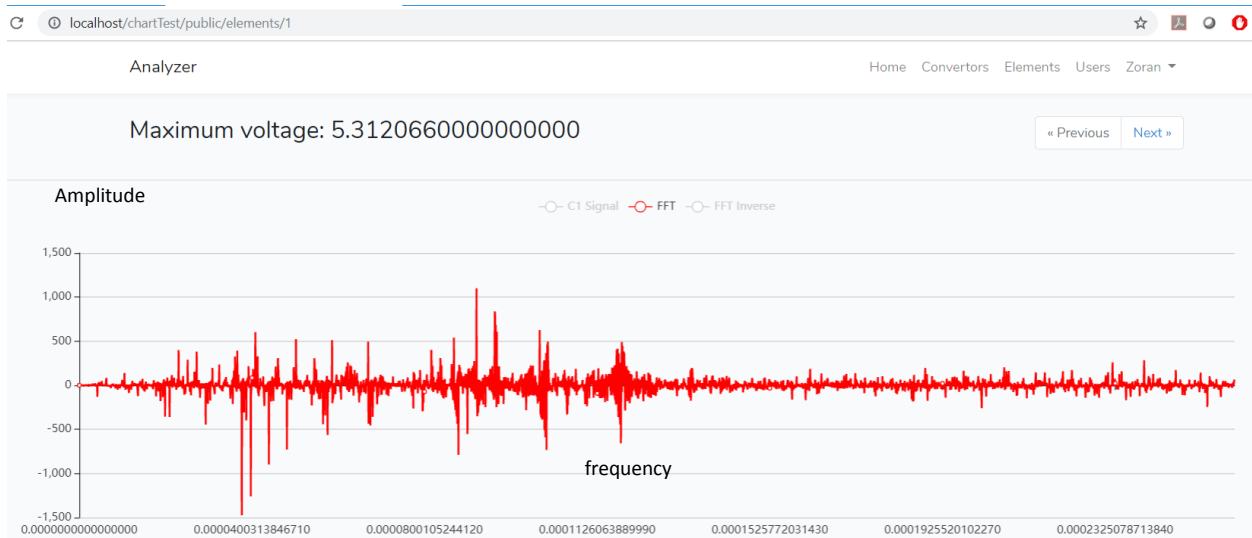
Figure. 3.7 Harmonic of FFT of output voltage signal

In Figure 3.7 can be seen that the element contains more than 140000 samples which are divided into 4096 samples per page. Maximum voltage is showing the highest voltage for this part of the signal. The button next will provide the next group of 4096 samples and with going previous or next can be analyzed the signal in detail.
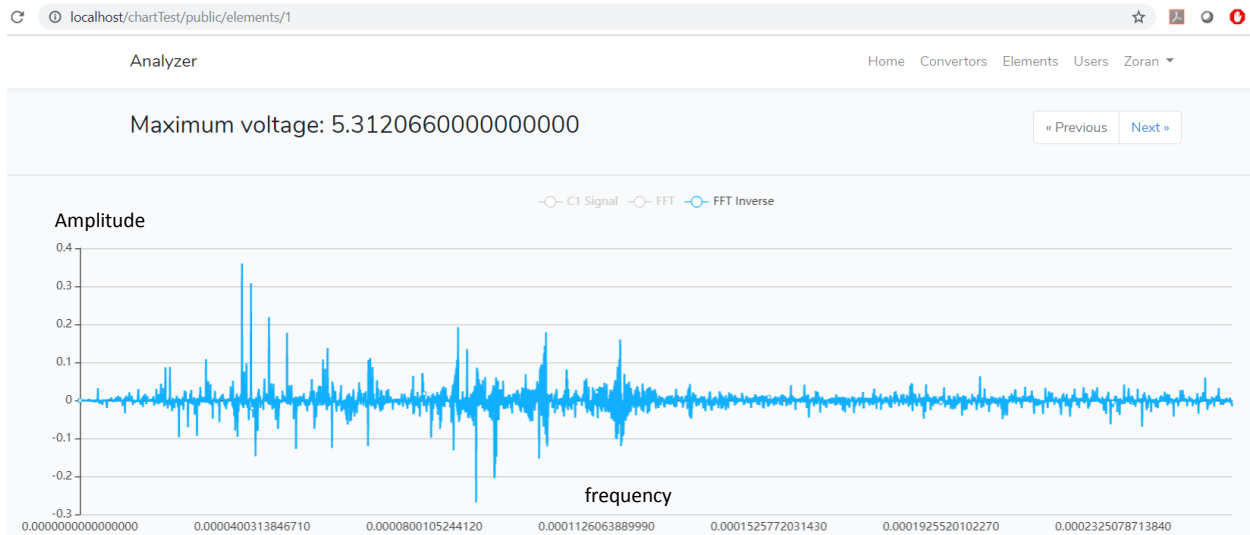
Figure. 3.8. Inverse Fast Fourier Transformation (IFFT) of the C1 signal

Figure 3.8. represents a harmonic of the inverse function of FFT. The signal shows how harmonic behave through time, or, the peaks and maximums are in the first half of the signal. Here it can be seen another color of representing harmonic for making a clearer approach of the result.
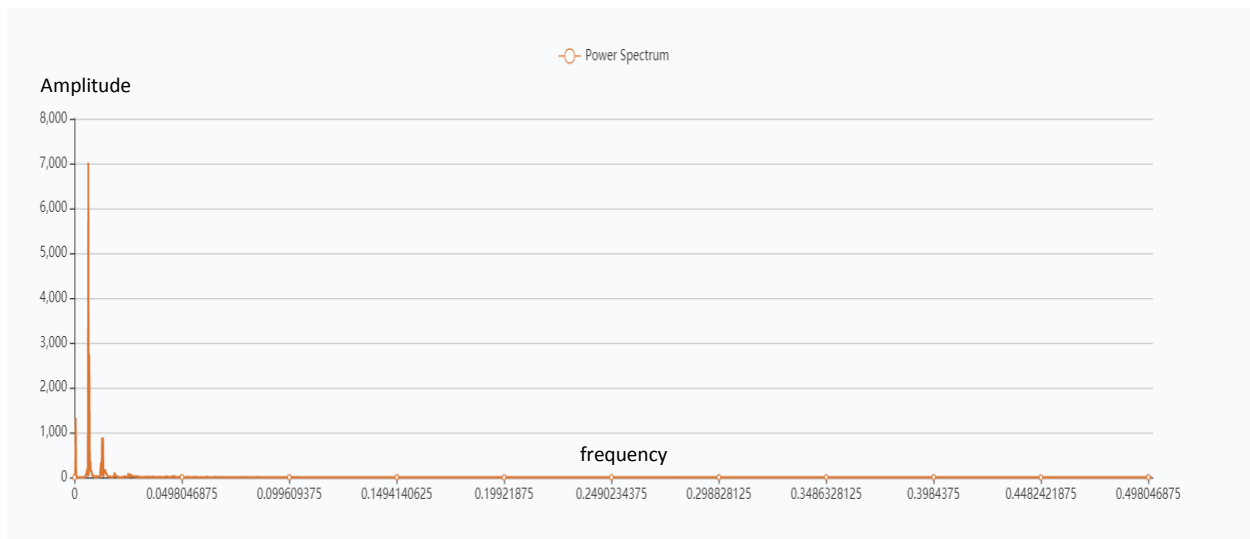
Figure 3.9. Power Spectrum of the C1 signal

On Figure 3.9 can be seen the power of the same harmonic in Figure 3.8. It is visible that the power is considered in the beginning of the signal as a one main maximum and fast decreasing to minor values to the end of the signal.

98

For calculating the power spectrum chart, it is used Python script which is better for calculating and measuring this kind of calculations. In the script it will be imported scipy.signal library for Python which is specially designed for handling complex math signal problems.

The technologies used in this application are assembled with the higher aim of easy upgrading, scaling and compatibility with any host or server. Well-known and well-developed technologies with complete documentation and support for longer periods have been used in project design. This makes it easy for this application to be upgraded and maintained in the future.

The idea of obtaining results that show how some instruments work ideally and how the same instruments work in a real case proves that there are deviations between the two cases. It has been several times mentioned in this dissertation that one of the most important aims is gathering real-world data and processed information from all the instruments in our daily lives. In addition to this dissertation, it is both simple and user-friendly - a web application that will provide a faster and simpler way of analyzing the basic features of any data type. In this particular case it is used the data that it is already analyzed through LTSpice in chapter 2 and LabView in chapter 4, and preview the same data with the same mathematical methods on different platforms.

3.5.   RESULTS FROM IDEAL AND REAL CONDITIONS OF INVESTIGATED DC – DC CONVERTERS

In this part are considered results that are gathered from two situations of investigating, real conditions and ideal conditions. Measurements are obtained through web application and are presented like figures bellow. The harmonics of the signal, the FFT and the power spectrum are shown.

Figure 3.10. View of Buck DC-DC converter in ideal operating conditions

Figure 3.11. View of Buck DC-DC converter in real-time operating conditions

The application clearly shows the difference in the maximum voltage between the two cases, ie, the figure 3.10 shows the result in ideal environment of 7,531V and in figure 3.11 are shown real conditions with a maximum of 7,391. These results are obtained from the full duration of this Buck converter output voltage signal.

Figure 3.12. View of Buck DC-DC converter in the first half of its life in ideal operating conditions

Figure 3.13. View of Buck DC-DC converter in the first half of its duration in real-time operating conditions

An overview of Figures 3.12. and 3.13. shows how the signal behaves in the first half of its duration in an ideal and real working conditions. It can be noticed that the difference is not easily noticeable in the first half of the signal itself, ie there is a very small difference which cannot be noticed by the curve itself.

101

Maximum voltage: 7.5318060000000000

« Previous   Next »

Amplitude

—O— V3 Signal

8
7
6
5
4
3
2
1
0

time

0.0004929900000000   0.0005700315227990   0.0006438720672650   0.0007214718480590   0.0007939353510280   0.0008730389333880   0.0009493453418430
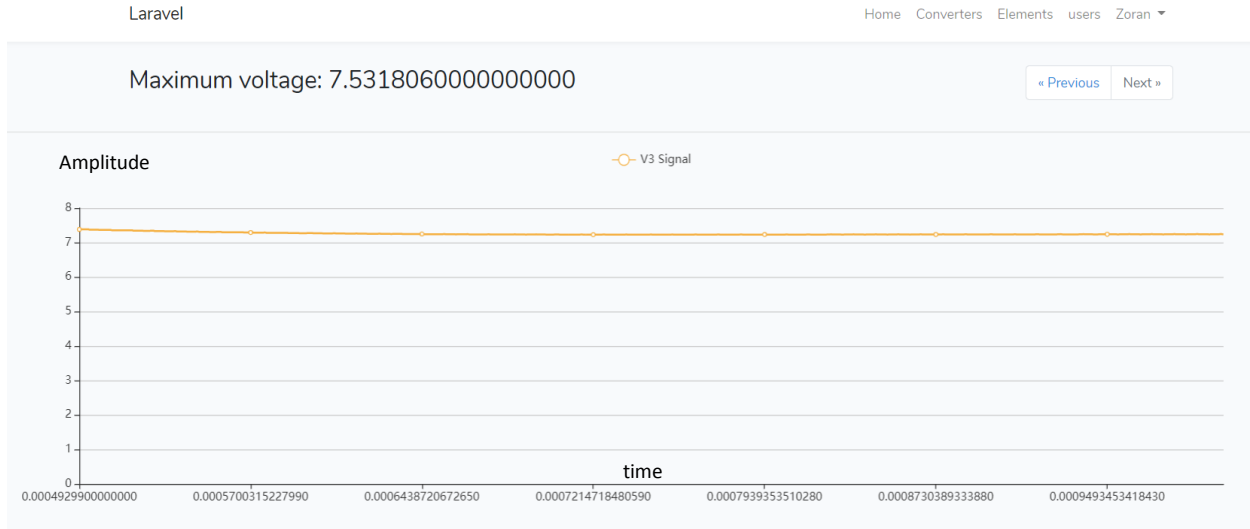
Figure 3.14. View of Buck DC-DC converter in the second half of its duration in ideal operating conditions.

Maximum voltage: 7.3915000000000000

« Previous   Next »

Amplitude

—O— V8 Signal

8
7
6
5
4
3
2
1
0

time

0.0004929900000000   0.0005700315227990   0.0006438720672650   0.0007214718480590   0.0007939353510280   0.0008730389333880   0.0009493453418430

Figure 3.15. View of Buck DC-DC converter in the second half of its duration in real-time operating conditions.

A detailed examination of the curves of Figures 3.14. and 3.15. shows how the signal behaves in the second half of its duration, both in ideal operating conditions and in real operating conditions. If it is looked closely it can be already seen that there is a slight difference between the two curves.
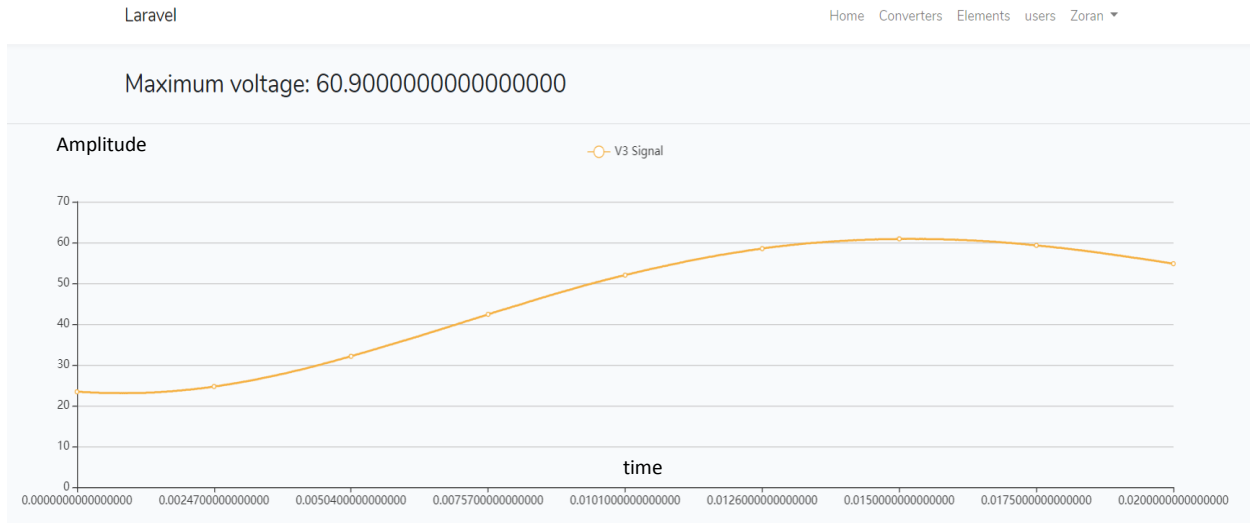
Figure 3.16. View of Boost DC-DC converter under ideal operating conditions
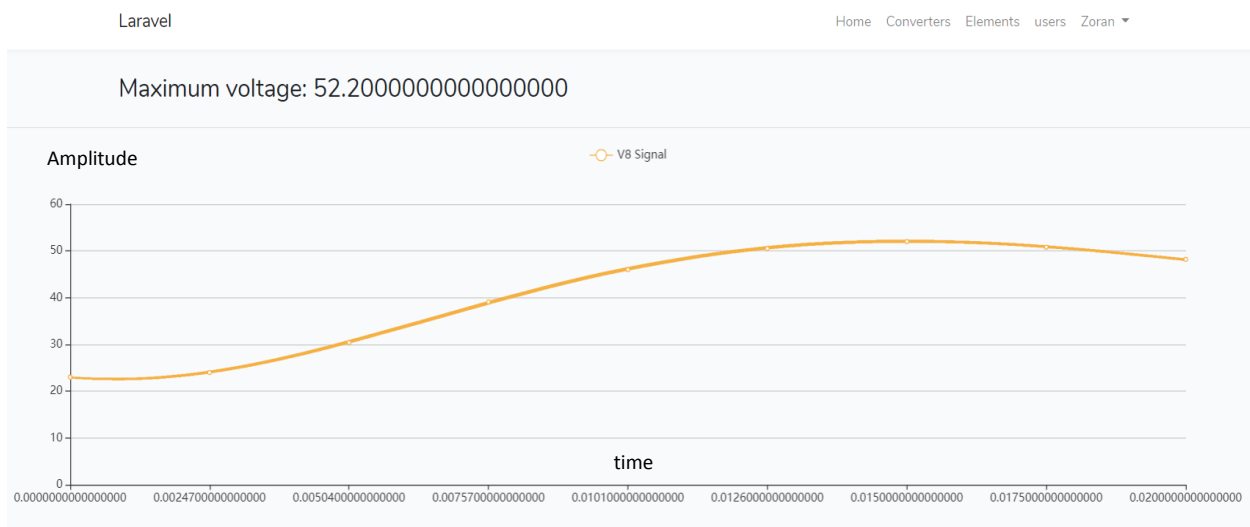
Figure 3.17. View of Boost DC-DC converter under real operating conditions

Figure 3.16 and Figure 3.17 represent a harmonic of a boost DC – DC converter. By looking at the overall behavior of the ideal and realistic operating conditions of the Boost Converter, can be seen a significant difference, ie, under ideal operating conditions we get a maximum value of 60,900V at Figure 3.16 and under real operating conditions there is value of 52,200V in Figure 3.17. This shows that using algorithms from programming languages like Php and Phyton we can get reliable results.
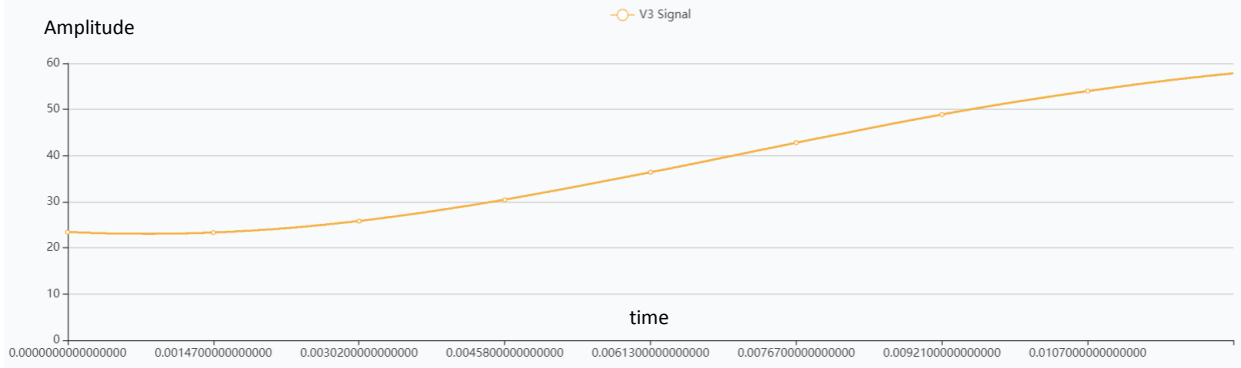
Figure 3.18. View of Boost DC-DC converter in the first half of its life under ideal operating conditions
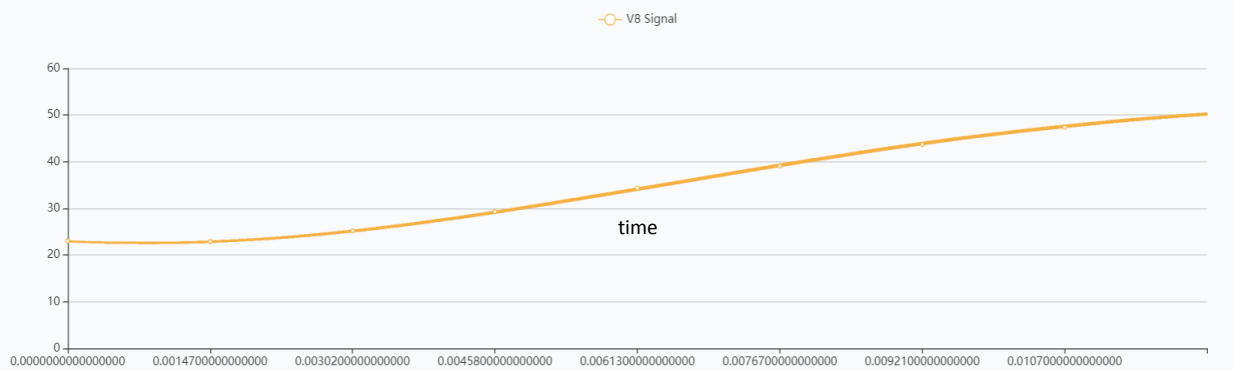
Figure 3.19. View of Boost DC-DC converter in the first half of its life in real-time operating conditions

Figures 3.18 and 3.19 show how the signal behave in ideal and real operating conditions, respectively. If closer look at the harmonic, it is noticable a slight difference at the end, that is, in the middle of the signal. In ideal working conditions the harmonic goes slightly higher than in real working conditions.
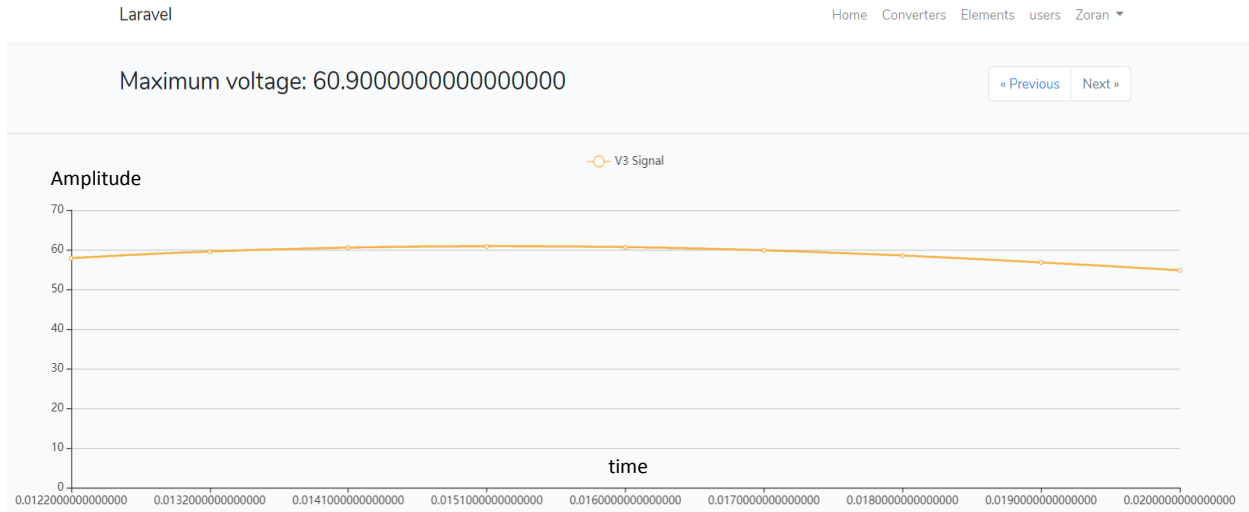
Figure 3.20. View of the Boost DC-DC converter in the second half of its duration in ideal operating conditions
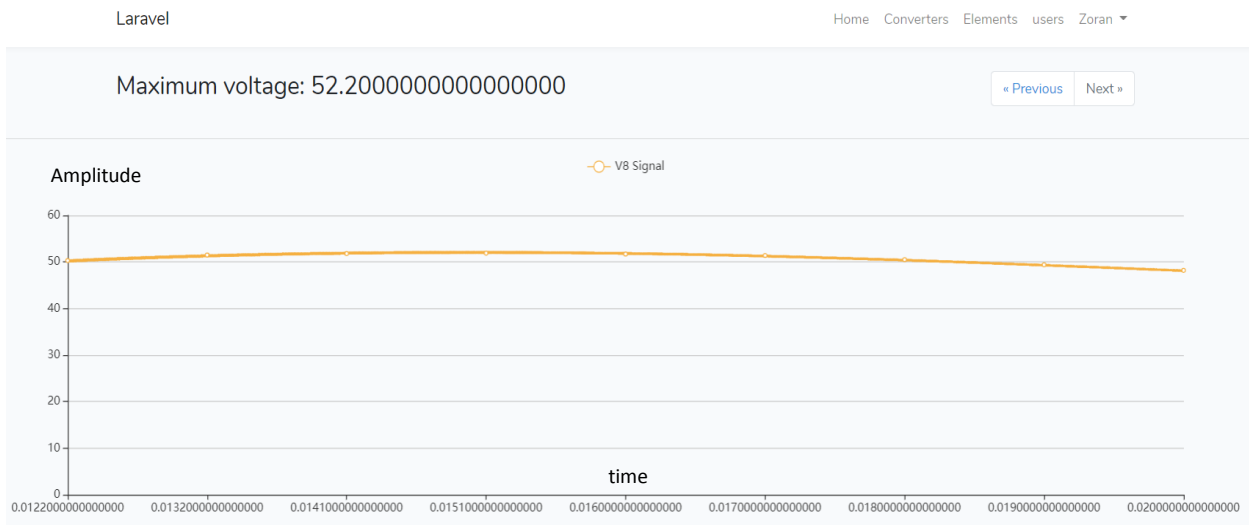
Figure 3.21. View of the Boost DC-DC converter in the second half of its duration in real-time operating conditions

Overview of the movement of the curve in the second half of the signal in both cases in Figures 3.20 and 3.21, it can be seen the difference between the ideal and the real case, that in the real case can be seen a significantly lower value.
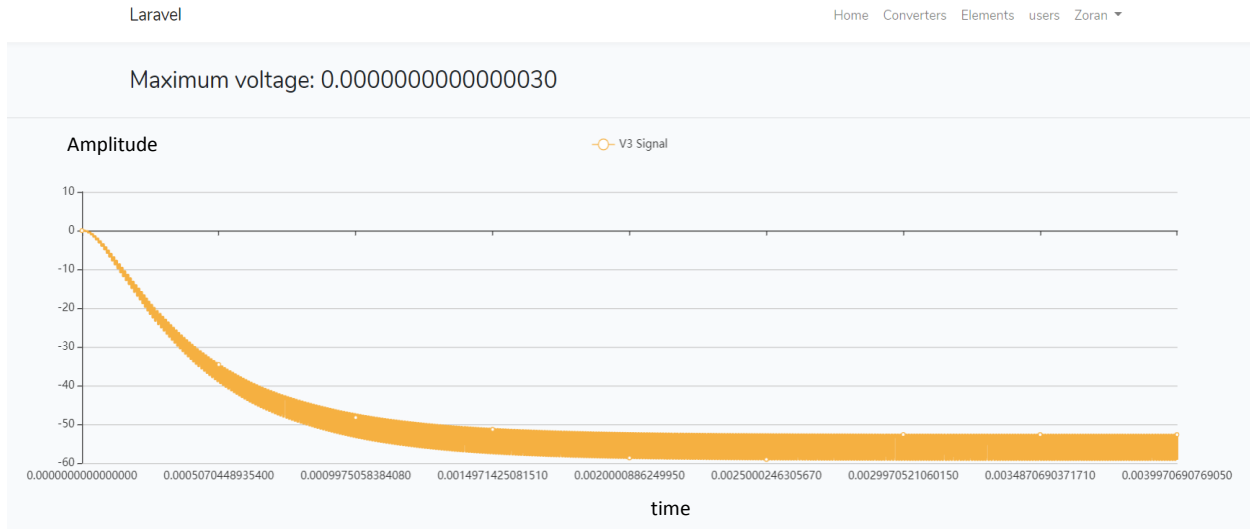
Figure 3.22. View of Buck-Boost DC-DC converter under ideal operating conditions
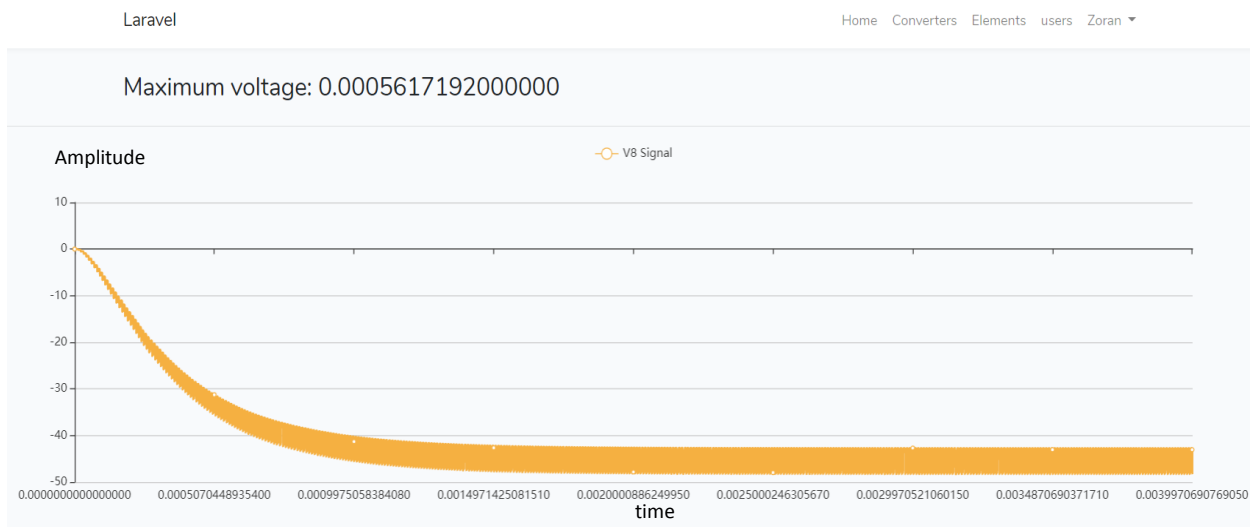
Figure 3.23 View of Buck-Boost DC-DC converter under real operating conditions

The third type of converters that are taken as an example to compare performance results in ideal and realistic conditions are Buck-Boost DC-DC converters. Here in figure 3.22 and figure 3.23 can be seen that under ideal working conditions we have a greater drop in the curve itself than in real working conditions..

106

Figure 3.24. View of Buck-Boost DC-DC converter in the first half of its duration in ideal operating conditions

Figure 3.25. View of Buck-Boost DC-DC converter in the first half of its duration in real-time operating conditions

Figure 3.24 and Figure 3.25 represent the difference in voltage at the first half of the signal. In the case of Buck-Boost converters, even when looking at the first half only of their duration, the same difference can be clearly seen when looking at the overall duration, ie, the significantly greater slope of the curve under ideal operating conditions that is shown in Figure 3.24.

107

Maximum voltage: 0.0000000000000030

Amplitude

─○─ V3 Signal
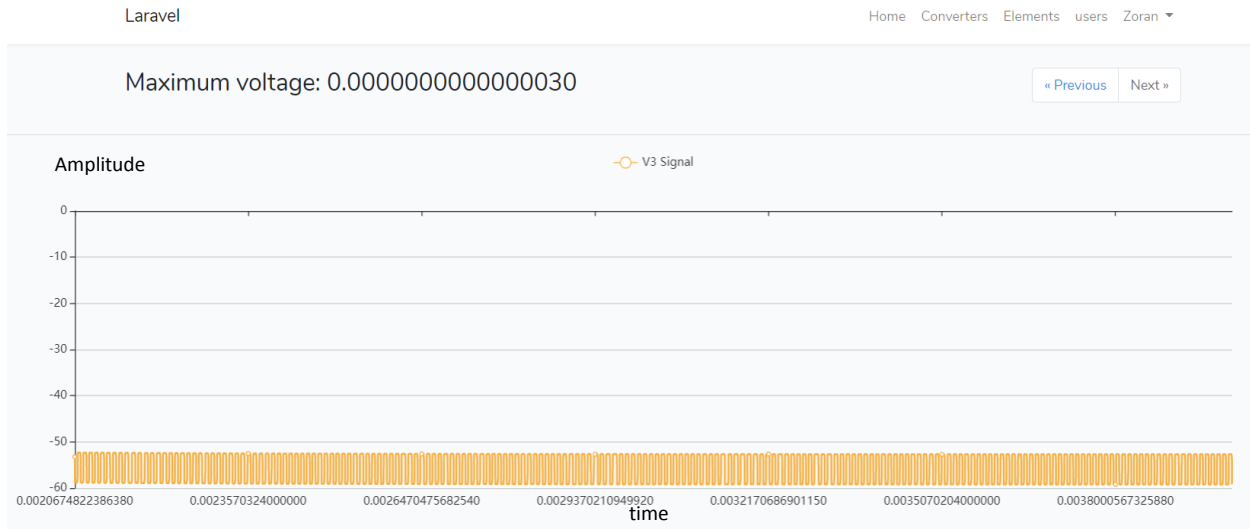
Figure 3.26. View of Buck-Boost DC-DC converter in the second half of its life under ideal operating conditions

Maximum voltage: 0.0005617192000000

Amplitude
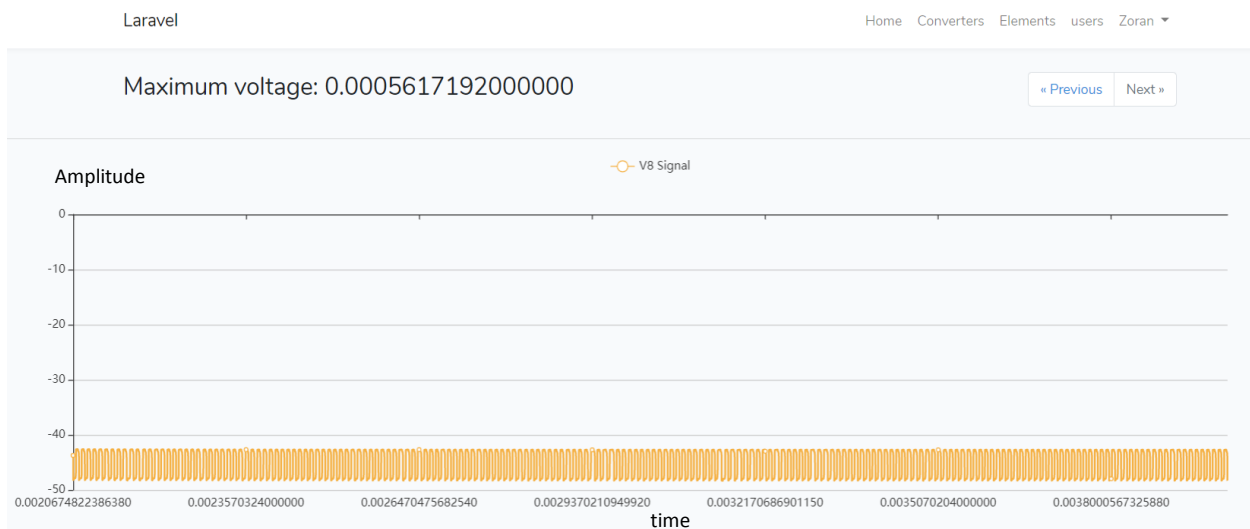
─○─ V8 Signal

Figure 3.27. View of Buck-Boost DC-DC converter in the second half of its duration in real-time operating conditions

Looking at the second half of the duration of this type of signals shown in Figures 3.26 and 3.27 shows a slight not visible difference between the signals. So, in this case of the second half of the signal the harmonics are not with a clear difference.

Figures showing only one half of the signal indicate that sometimes the scientist may need to look at only one time interval of a given signal because the nature of the signals will not always

be of the same nature and it may need strictly specific analysis interval from the entire data set that later can be presented as an algorithm to signal quickly any deviations, jumps, maximum values, and anomalies of any data type. This way of working with algorithms from certain programming languages also proves that if they did not currently have an LTSpice-like interface, the scientist who would like to do any analysis and comparison of a particular data set would be able to do it without a big difficulties, in a fast and efficient way with great accuracy through a web based application.

In addition to analyzing data ideally in the LTSpice desktop, this thesis shows what the results would look like if somebody need to analyze any type of data without considering the nature of the data in detail. The next few figures describe the energy of all three converters viewed from the application point of view and the programmatic algorithms for drawing this type of parameters.
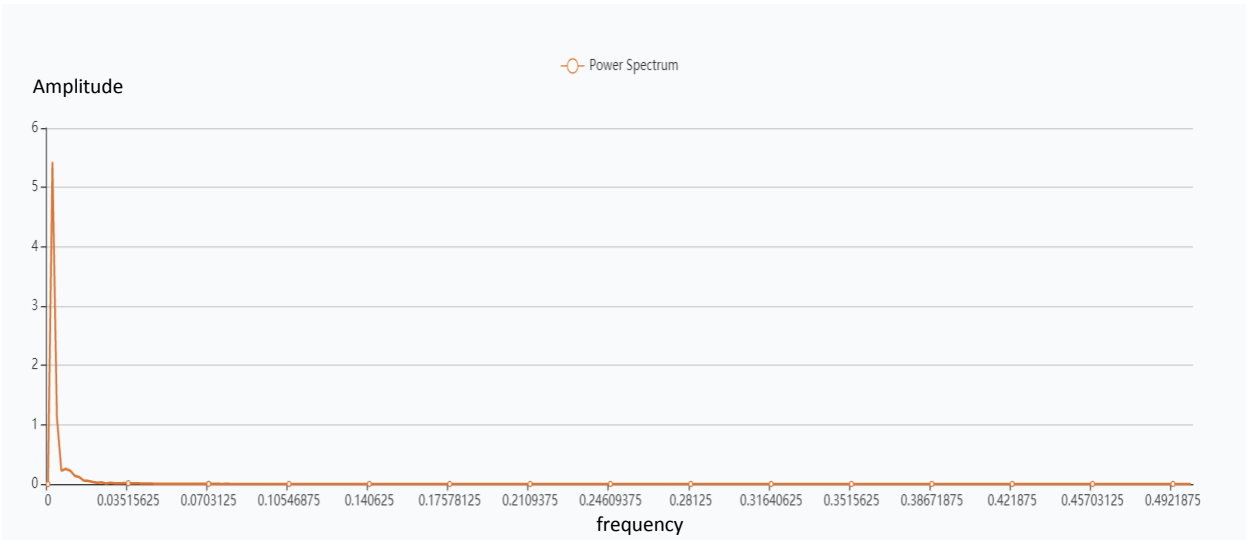
Figure 3.28. Power spectrum display in ideal Buck DC-DC converter operating conditions

Figure 3.28 shows the harmonic of the power spectrum at ideal work conditions at Buck DC – DC converter. It can be seen that the power has value around 5.5.
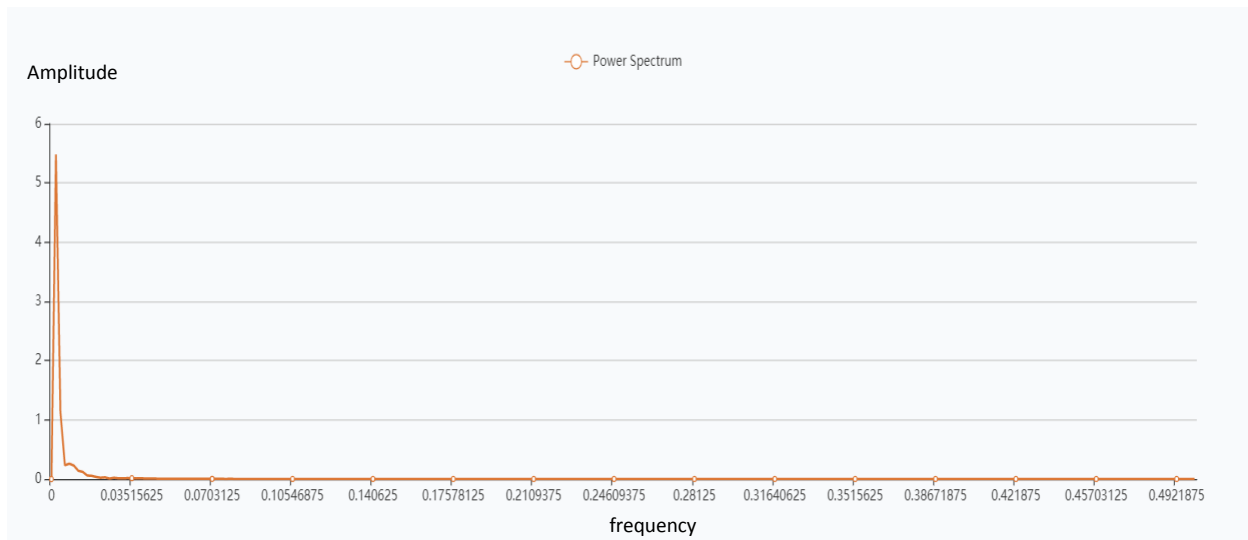
Figure 3.29. Display of power spectrum in real-time operating conditions of a Boost DC-DC converter

Figure 3.29 shows how the harmonic of the power behave at real-time operating conditions at Boost DC − DC converter, with the buck DC-DC converter the energy values are almost identical to that of Figure 3.28.
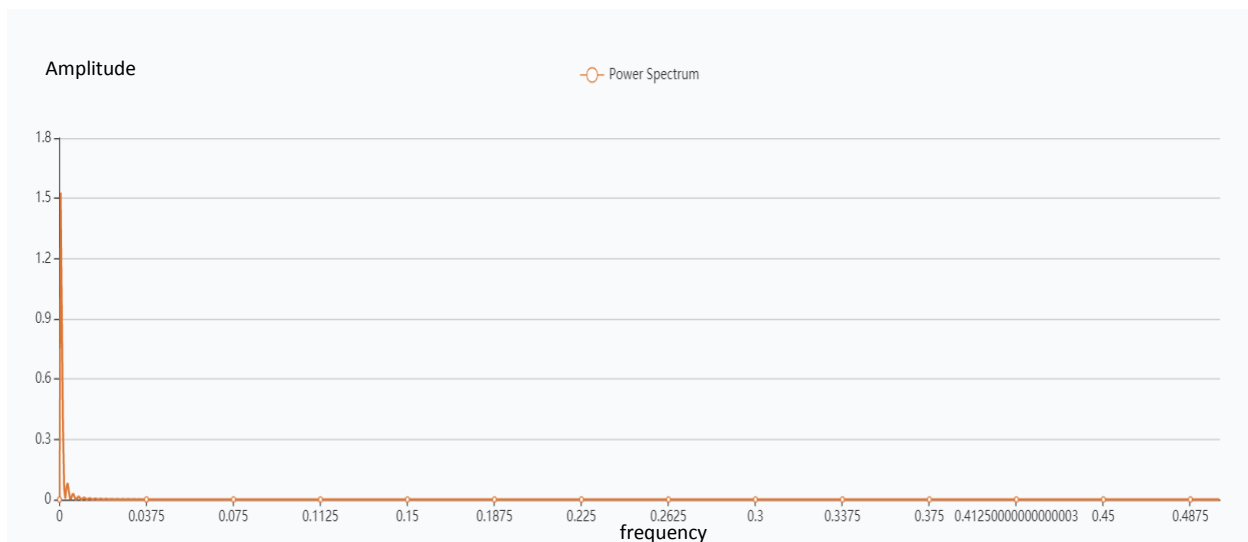
Figure 3.30. Power display at ideal operating conditions with Boost DC-DC converter

It can be seen from Figure 3.30 that the situation is not much different in character of the curve compared to Buck converter, ie, the energy gets a priority maximum at the beginning and later we have no major deviations.
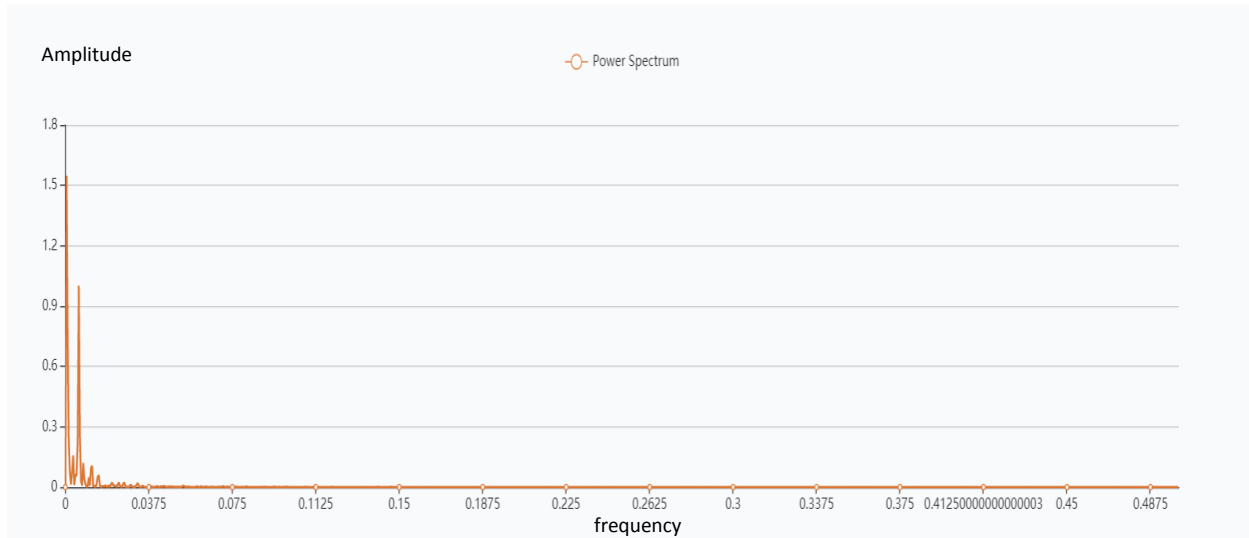
Figure 3.31. Display of real-time operating conditions of a Boost DC-DC converter

According to the movement of the curve, it can seen that in Figure 3.31 there is a very different situation to the figures in Figure 3.28, that is, under real operating conditions, with the Boost Converter, and also can be seen that there is a second higher jump in energy than the converter behavior under ideal operating conditions, which is easily noticed by the graph itself.
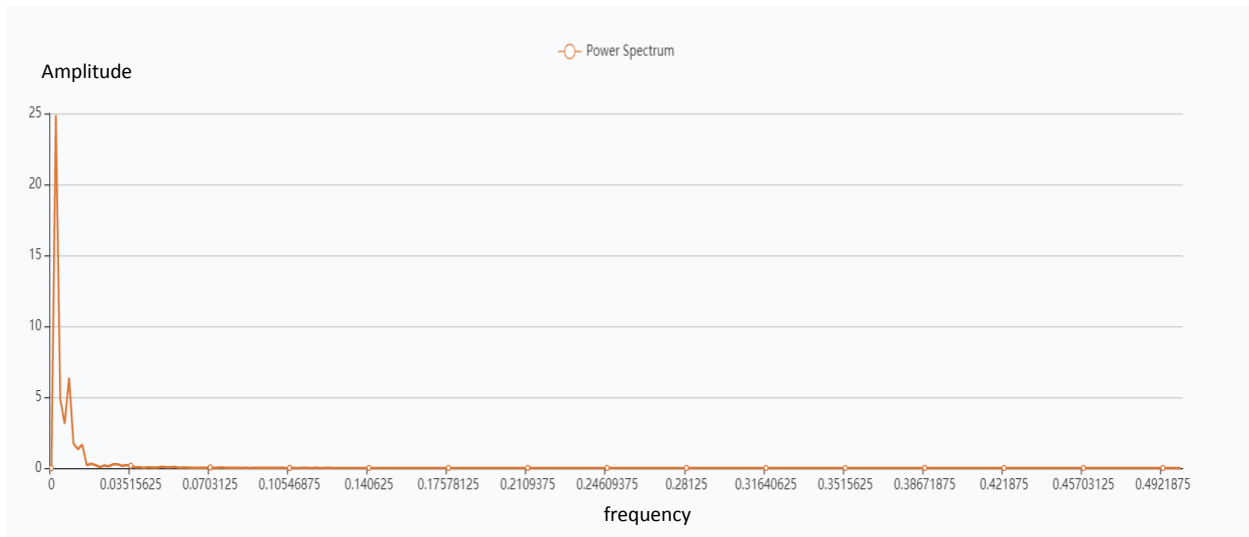
Figure 3.32. Power display at ideal operating conditions with Buck-Boost DC-DC Converter.

Figure 3.32 shows the energy behavior under ideal operating conditions of a Buck-Boost DC-DC converter. From the graph can be seen that the curve drops sharply with the exception of a small jump which has a very short duration and is at the very beginning immediately after the dip of the main peak.

111
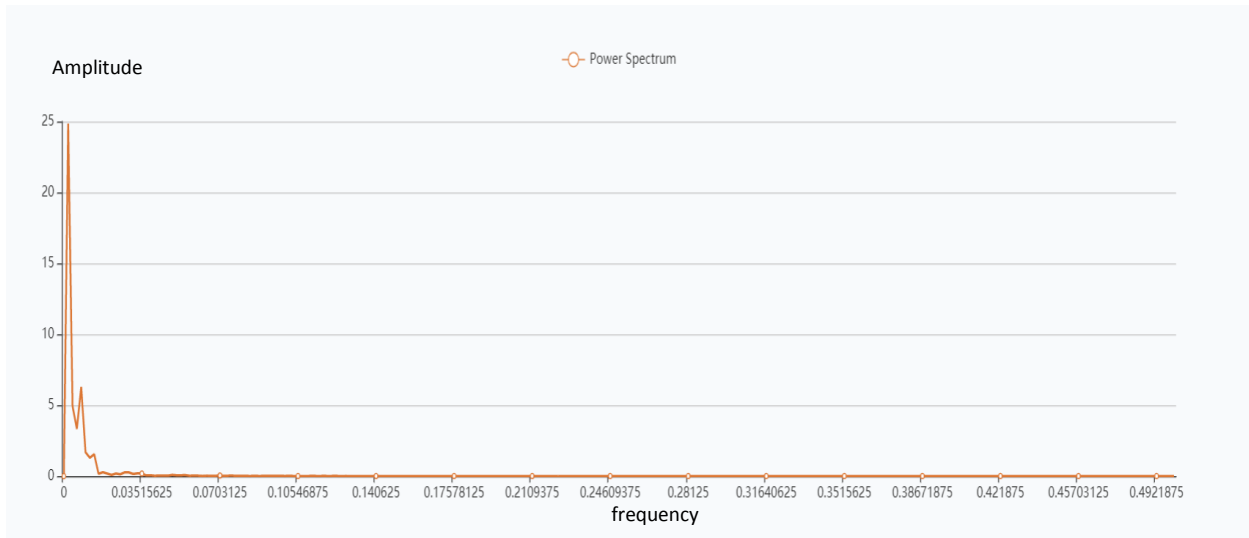
Figure 3.33. Real-time power spectrum display with Buck-Boost DC-DC converter

Figure 3.33 represents the energy behavior of a Buck-Boost DC-DC converter under real operating conditions. If closer look at Figures 3.32 and 3.33 it can be easily seen that the difference is not visible and drastic, that is, in the buck-boost converter the energy behaves the same way.
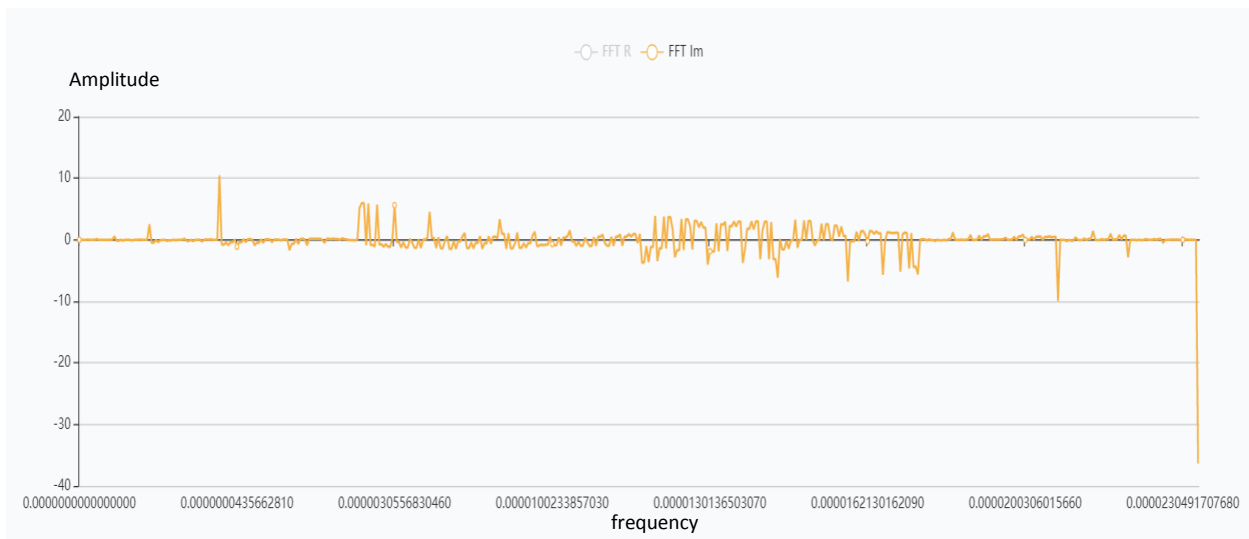
Figure 3.34. Display of imaginary part of FFT function of output voltage at Buck DC-DC converter under ideal operating conditions
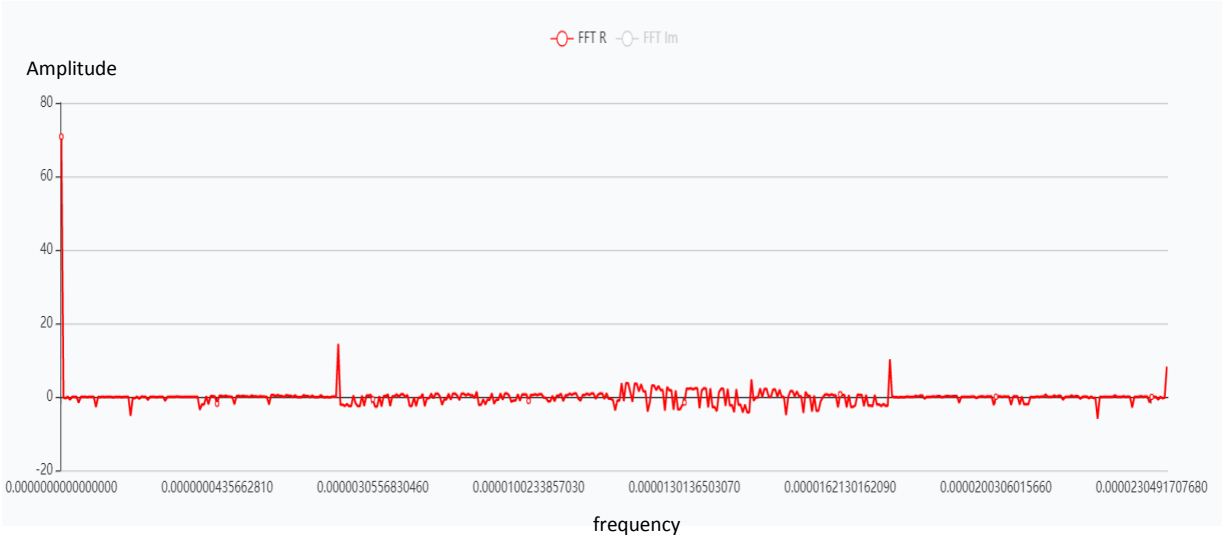
Figure 3.35. Display of the actual function of the FFT output voltage at the Buck DC-DC converter under ideal operating conditions

Figures 3.34 and 3.35 present the inverse and real part of the analysis with the FFT function of the data obtained from the output voltage of the Buck DC-DC converter under ideal operating conditions. It is important to note that this analysis serves to demonstrate the reliability of the FFT algorithm implemented through the Phyton programming language. The very nature of the results obtained is not the target of the analysis in this section. The main point is to make an analysis more accessible and easier to use if we already have data obtained from some measurement or analysis of any instrument such as DC-DC converters.
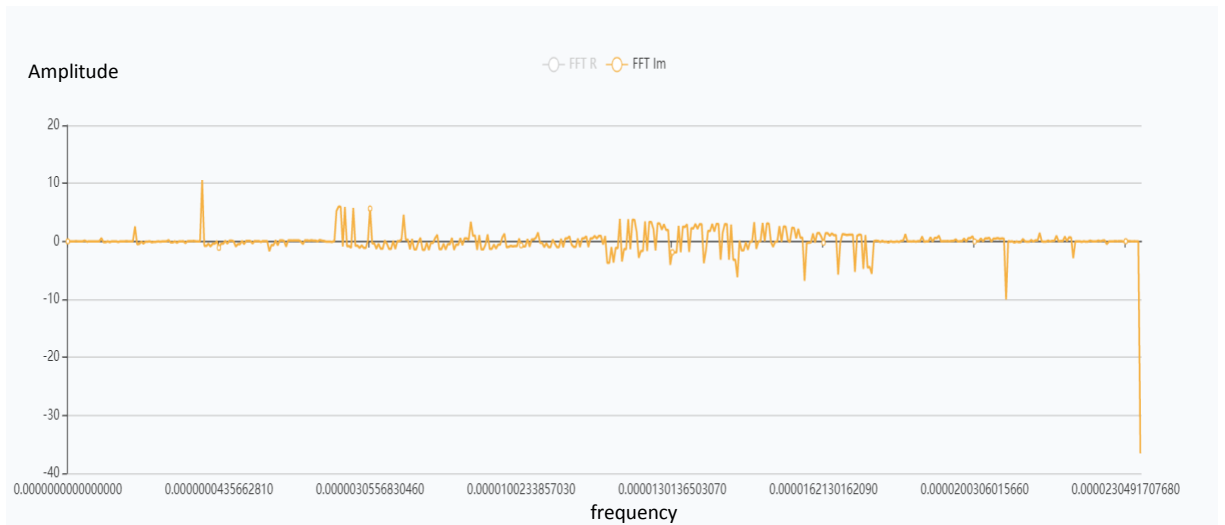
Figure 3.36. View of an imaginary part of the FFT from the output voltage of a Buck DC-DC converter in real-time operating conditions

113
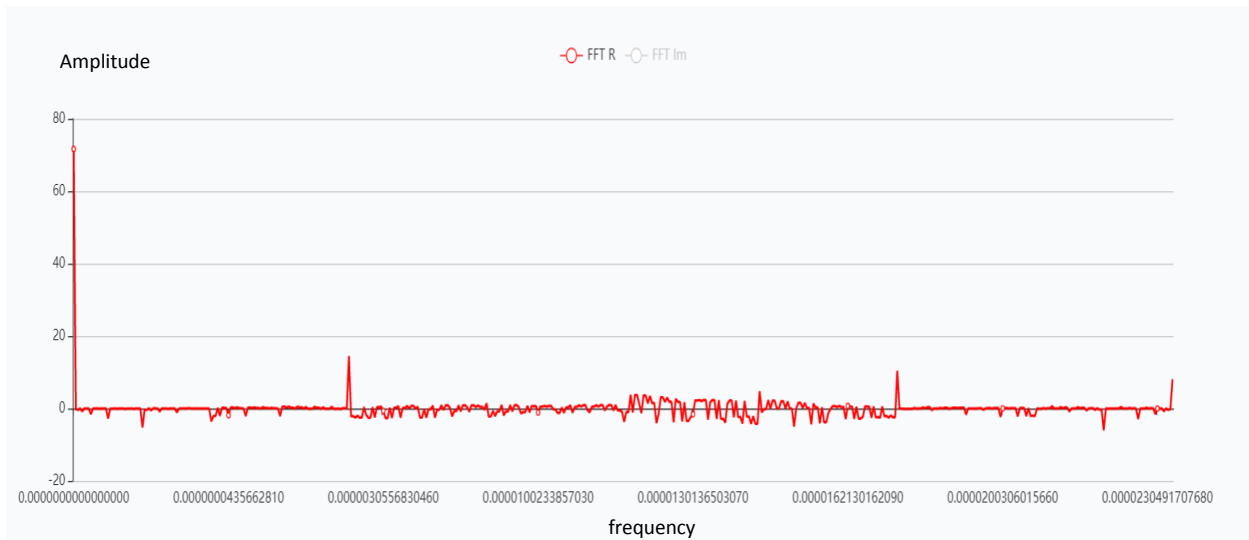
Figure 3.37. Display of the actual FFT portion of the output voltage at the Buck DC-DC converter in real-time operating conditions

Figures 3.36 and 3.37 show the inverse and real part of the FFT function under real operating conditions of the Buck DC-DC converter. It is clearly visible that several maximus and deviations in the signal that would allow us to better understand dependency if we ever needed it in another type of data analysis.
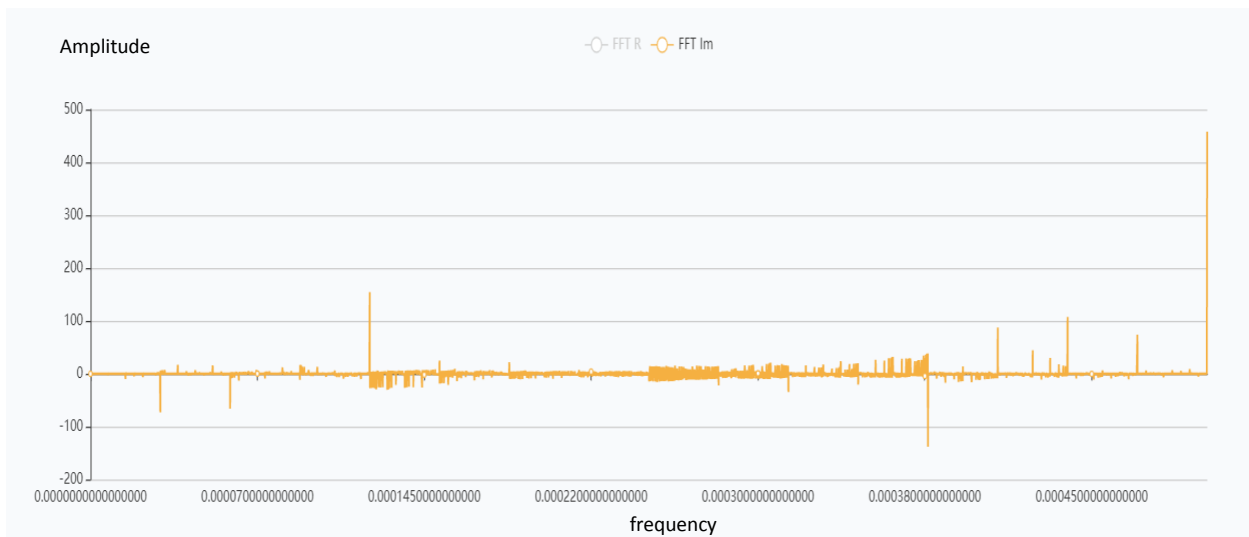
Figure 3.38. Illustration of an imaginary part of the output voltage of Boost DC-DC converter under ideal operating conditions
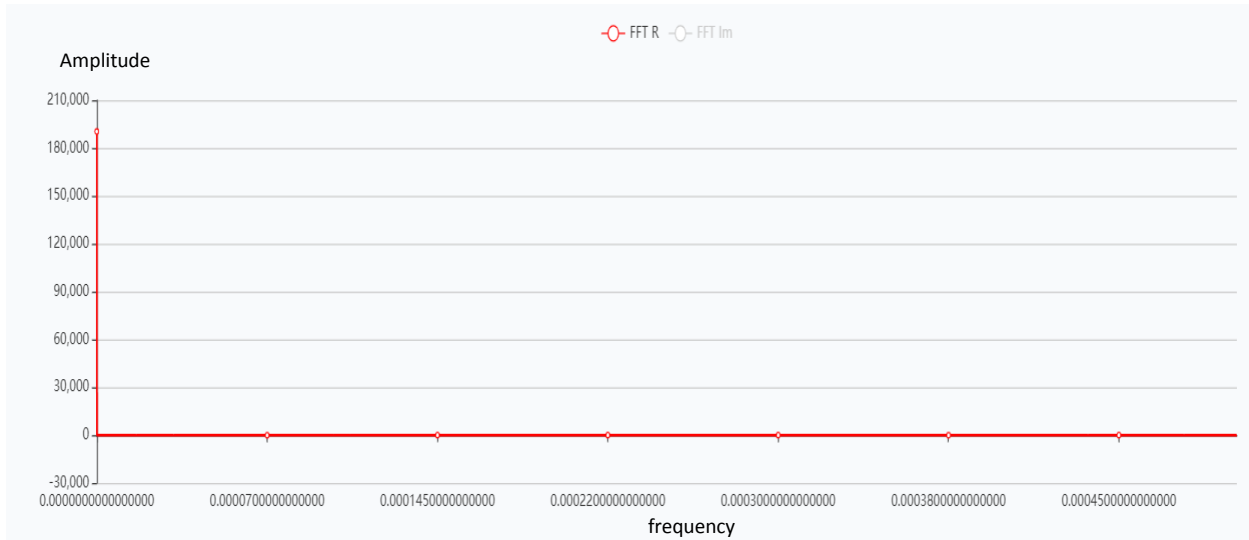
Figure 3.39. Display of realistic output voltage of Boost DC-DC converter under ideal operating conditions

Figures 3.38 and 3.39 refer to the Boost DC - DC converter, ie the imaginary and real part of the FFT function under ideal operating conditions.
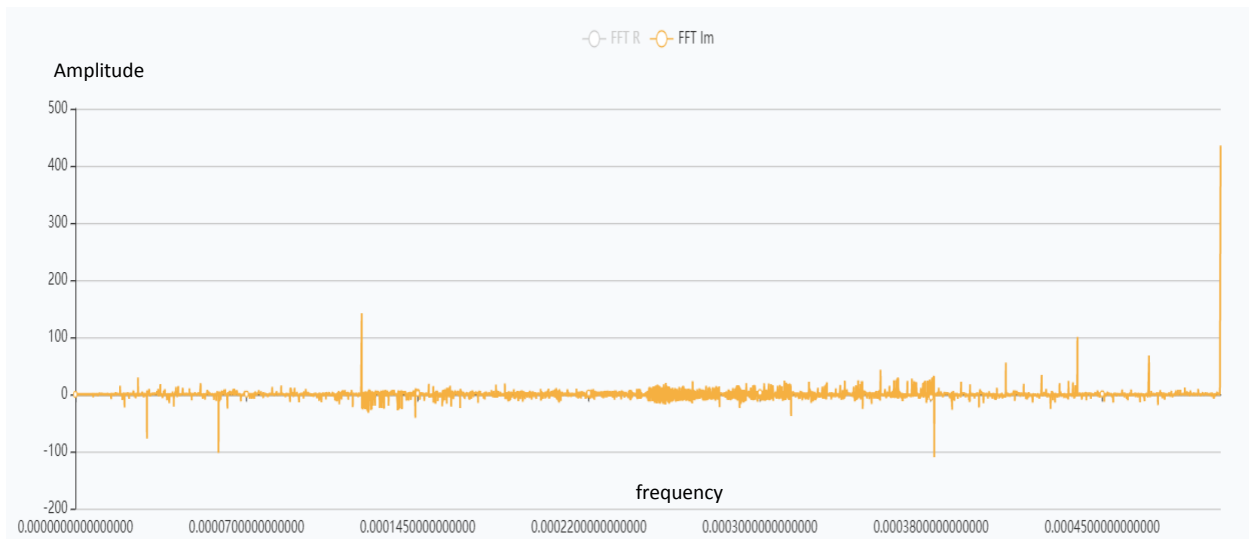
Figure 3.40. View of an imaginary part of the output voltage of a Boost DC-DC converter in real-time operating conditions

115
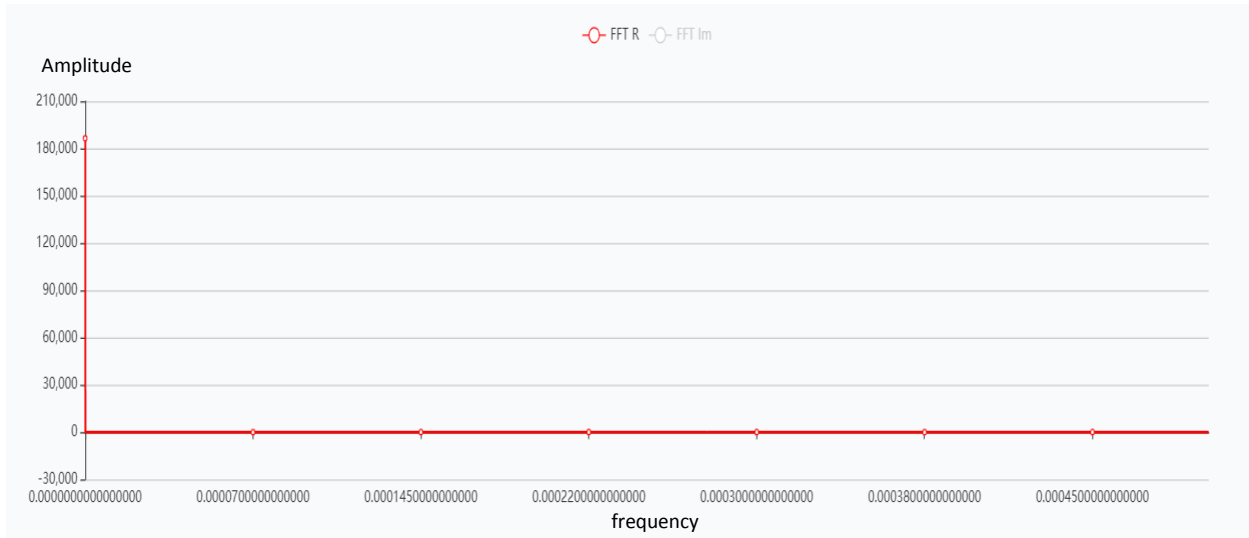
Figure 3.41. Display of real part of output voltage with Boost DC-DC converter under real operating conditions

Figure 3.40 and figure 3.41 point the same difference like in ideal conditions of the output voltage of the Boost DC – DC converter.
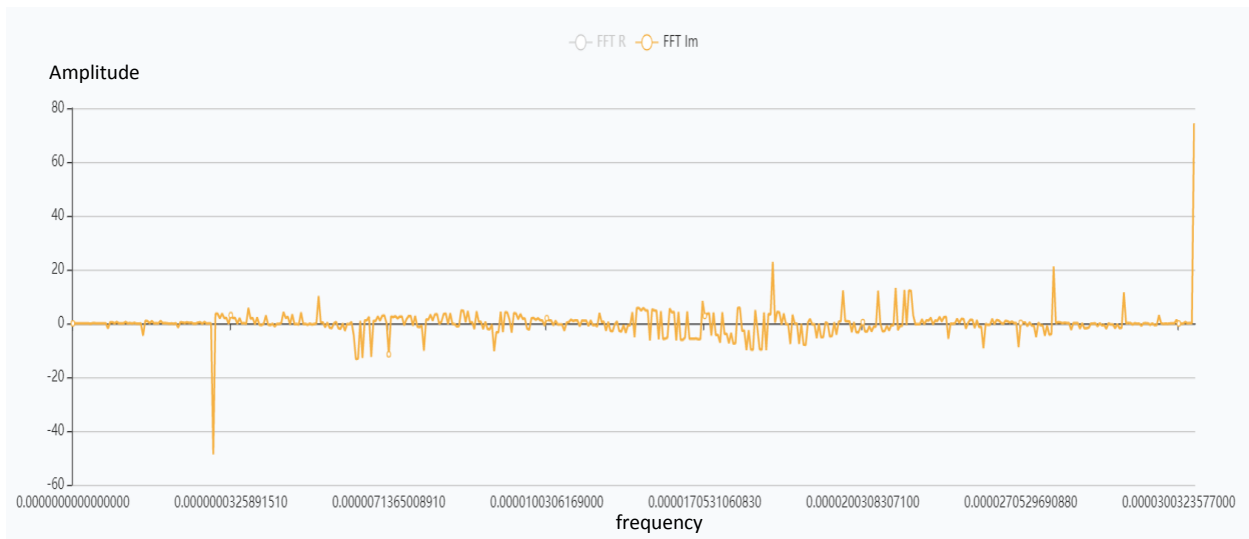
Figure 3.42. View of an imaginary part of the output voltage of a Buck-Boost DC-DC converter under ideal operating conditions
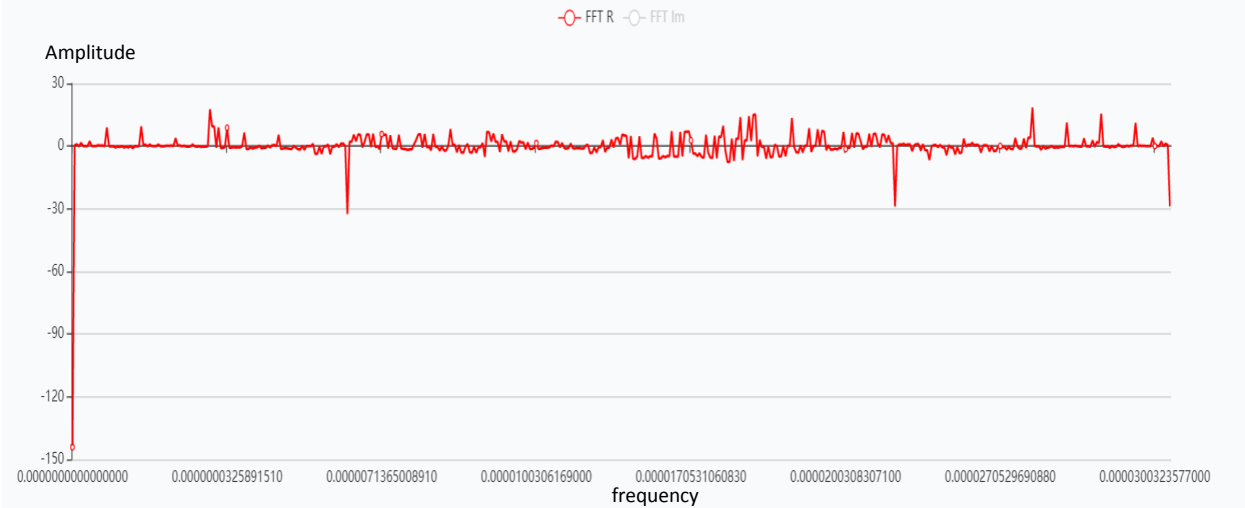
Figure 3.43. Real-time display of output voltage of Buck-Boost DC-DC converter under ideal operating conditions

Figure 3.42 and Figure 3.43 refer to real – time working conditions of the output voltage with the imaginary part (Figure 3.42) and real part (Figure 3.43). The harmonics are different and they are reversed.

Using these state-of-the-art technologies today gives the application space to work with hundreds of thousands of records as well as millions of records in the future. The software is built on the principle of wide compatibility and is not dependent on certain hardware limitations. This allows the application to be easily installed on any of the popular operating systems and platforms such as Linux, Windows, and many more. Software sharing enables it to work in simple server architecture from a single server as a host to a large cluster of larger server environments. This can make the application work as part of a microservice or as a whole system.

The future tests can be aimed to the produced energy of the alternative sources of energy such as the photovoltaic systems and the wind measurements in the territory of Republic of Bulgaria (Arar Hemza; Haouam Abdeslam; Rachid Chenni; Debili Narimene, 2016). The focus in this dissertation is generally focused on investigation of different approach of interactive design in processing signals from output voltage in electronic components for better results in future and developing of web application for more user – friendly approach in signal data investigation.

3.6. CONCLUSION

- As mentioned above, there are endlessly many examples of where it would be useful to work with large databases. Building this application enables it as a web service so that everyone will be able to access the web application at any time and sign in to continue using it. In addition to the current version which covers several dc - dc converters, the application can be upgraded not only in the field of electronics, but also in other sectors such as medicine, environmental protection, seismology and many other areas of great importance to all mankind.

- Due to the easy structure and the way of activating the application on any machine, the software can be further patented and offered to any sector that needs it. In the specific example presented in this dissertation, the functions that are most relevant to the given problem are selected, but it is important to note that in the future, according to the needs of the companies, the application can be upgraded with other analysis functions depending on the needs of the users themselves..

- Computers, mathematical methods, programming languages, and all the measuring instruments of our time should be rationally used to make the operation of the industry much easier and to prevent adverse events. So the main purpose here is to show the power and power of analyzing and processing large-scale, high-speed databases through a web-based application and using the latest technologies in the field of programming languages.

On the market can be found a lot of software packages for processing big mass data and all professional packages come with a license that have a certain price. One software solution is for example "LabVIEW" from National Instruments. Besides the price of the license, for working with such a type of software, there are needed certain knowledge in some areas like mathematics, electro technique, physics or object – oriented programing languages. On other hand, for the younger audience involved in similar type of processing any type of data, LabVIEW provides more user-friendly approach with graphic content that is more understandable and interesting working with.

LabVIEW is an interactive software for program developing and execution especially designed for engineers, scientists, and people who need to make a complex multifunctional system. What makes LabVIEW different is that it is not a traditional programming in which programmers use text written in program languages like C++ or Java, but instead, you can create programs using graphical language with functional nodes or graphical notation through which data will flow.

The graphical language in LabVIEW is called the "G" language and it's especially designed for visual programming. With this language programmers use icons instead of text to create an application and that makes programming faster and easier. Thanks to the adaptable graphic user interface LabVIEW is ideal for simulations, general programming and the most important functionality – making a virtual instrument called "VI's".

LabVIEW is compatible with Windows, Linux or Mac OS X. Programs made with LabVIEW can also run on these platforms and they can also work with embedded platforms as Digital Signal Processors (DSPs), microprocessors etc.

LabVIEW offers graphical programming approach that helps you visualize every aspect of your application, including hardware configuration, measurement data, and debugging. This visualization makes it simple to integrate measurement hardware from any vendor, represent complex logic on the diagram, develop data analysis algorithms, and design custom engineering user interfaces. It is best suited for developing code for automated test systems, systems used for validating designs (whether early stage R&D, design characterization or reliability) and systems

used to test products before they leave the factory (manufacturing test). LabVIEW was originally focused on taking measurements from various lab instruments, but it's expanded drastically from its inception.

LabVIEW can be used to perform a huge number of mathematical and logic functions, including basic arithmetic, if/then/else-if conditional statements, case statements, FFTs, filtering, PID control loops, etc. There are huge libraries of functions to pull from. You can also interface to code developed in other languages, through DLLs. .NET assemblies, and run-time interpreters like for example MATLAB.

Another unique capability that LabVIEW offers is real-time compilation and the ability to execute function blocks without requiring the process of a test case. Each LabVIEW function is designed with a user interface, so you can interact with your code immediately after you write it.

Analog signals are continuous signals that have time-variant quantities. Typical analog signals are voltage, temperature, sound, load and pressure. These signals have three primary characteristics which are signal shape, level and frequency.

Analog signals can have different values, so level is used to define vital information about the measured analog signal. Level of the signal is very important because it represents the physical feature like temperature in a room, intensity of light source, pressure etc. When measuring the level of a signal we must choose best accuracy system for DAQ because that is very important when working with analog signals. Shape can categorize signals in many groups like sine, sawtooth, triangle or square. Knowing the shape of a signal is also very important because with that we can analyze the signal, find peak values, DC values and slope. Shape usually changes with time, but system accuracy is still very important. Examples of analyzing shape is heartbeats. Vibration, video signals etc. Third characteristic is frequency and it cannot be measured directly. For measuring and analyzing the frequency, engineers use special algorithm known as the Fourier transform.

The last chapter is overview of the buck, boost and buck – boost dc – dc converters in LabVIEW. Signals for the inductor current and the output voltage has been generated and there is a view of the frequency for the 3 types of converters. Important to mention is that the frequency harmonic

is of different type and can't be compared strictly with the harmonic that have been obtained through LTSpice.
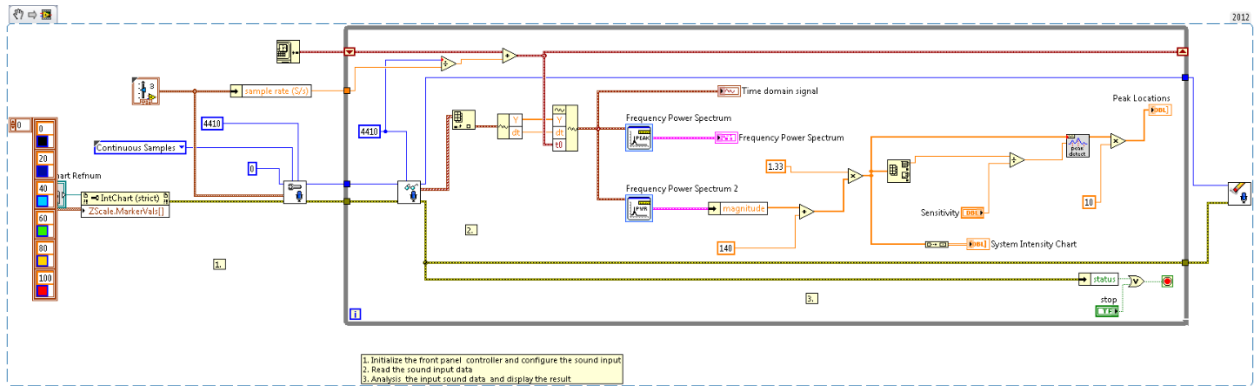
Figure 4.1. Example of FFT spectrogram in audio analysis

Figure 4.1 represent an example of block diagram scheme in LabVIEW for providing an FFT spectrogram in audio analysis. In this section is shown the difference between ideal vs. real condition of work of Buck, Boost and Buck – Boost DC – DC converters but, in very different light via LabView. The results of the output voltage from the analysis in LTSpice were exported like in a numeric string form and imported to several analysis virtual instruments in LabView. The difference between the ideal and real conditions of working are shown in the figures below.
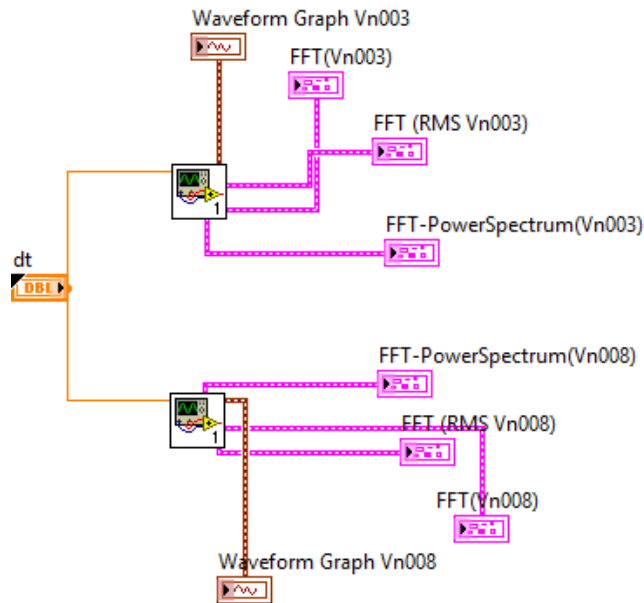
Figure 4.2. Block diagram for waveform diagrams

Figure 4.2 represent the block diagram of the waveform graphs in LabView. On the diagram can be seen several elements and connection and two separate virtual instruments. On the figure below is represented the virtual instrument that is included.
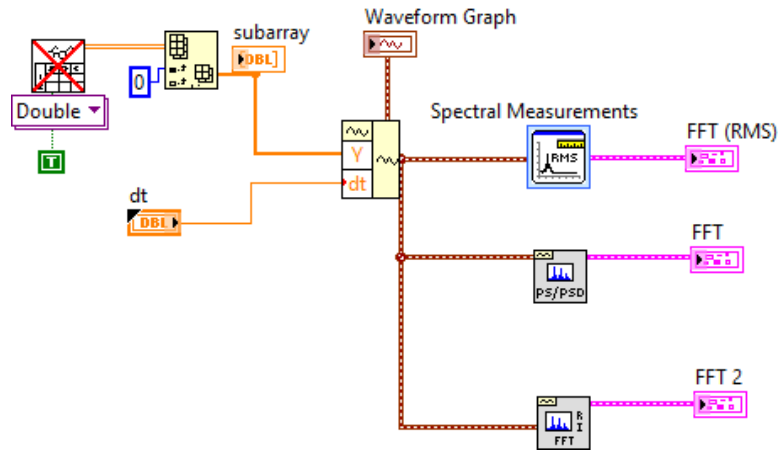
Figure 4.3. Block diagram for virtual instrument for browsing and analyzing files

Figure 4.3 represent a block diagram for VI of browsing and analyzing files. LabVIEW provides using od separate virtual instruments for different operations for further using independently in future analysis.

The section below shows several waveform graphs that referred to the output voltage and the FFT of the output voltage of the Buck DC – DC converters that are discussed in this dissertation. There are provided cases in ideal working conditions and in real working conditions.
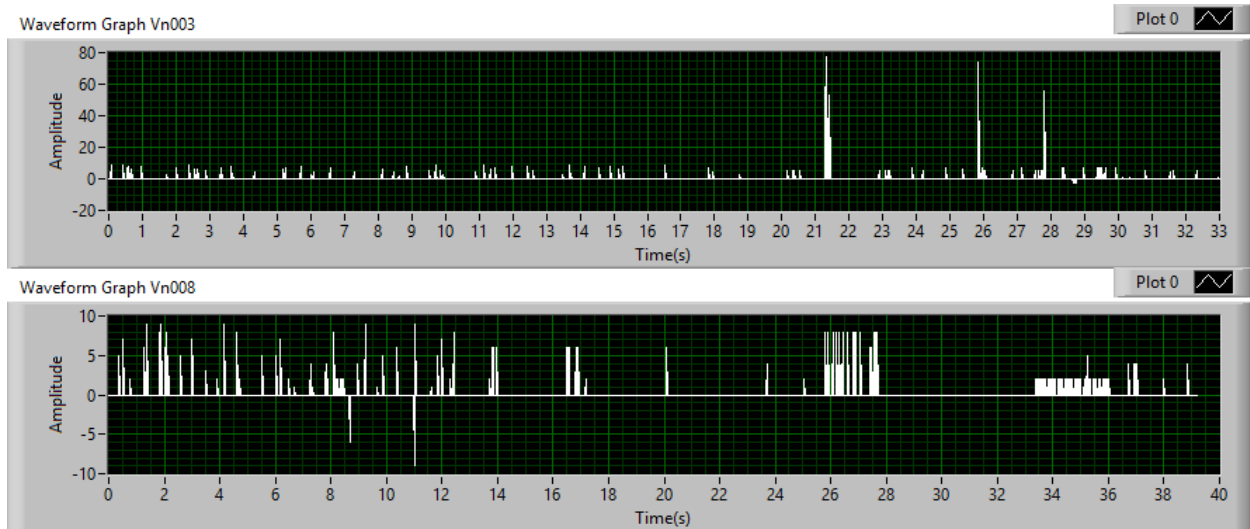
Figure 4.4. Waveform graph for Buck converter in ideal (Vn003) and real (Vn008) conditions of work

On the figure 4.4 are two different graphs with ideal (Vn003) and real (Vn008) harmonics. The results are different in the peaks and the maximum amplitude. At the graph Vn003 can be seen 3 main peaks at times near 21, 26 and 28. The maximum amplitude of the signal at Vn003 is around 80. At graph Vn008 there are not visible peaks that are dominant, and the maximum value is not going above 10 in the amplitude.
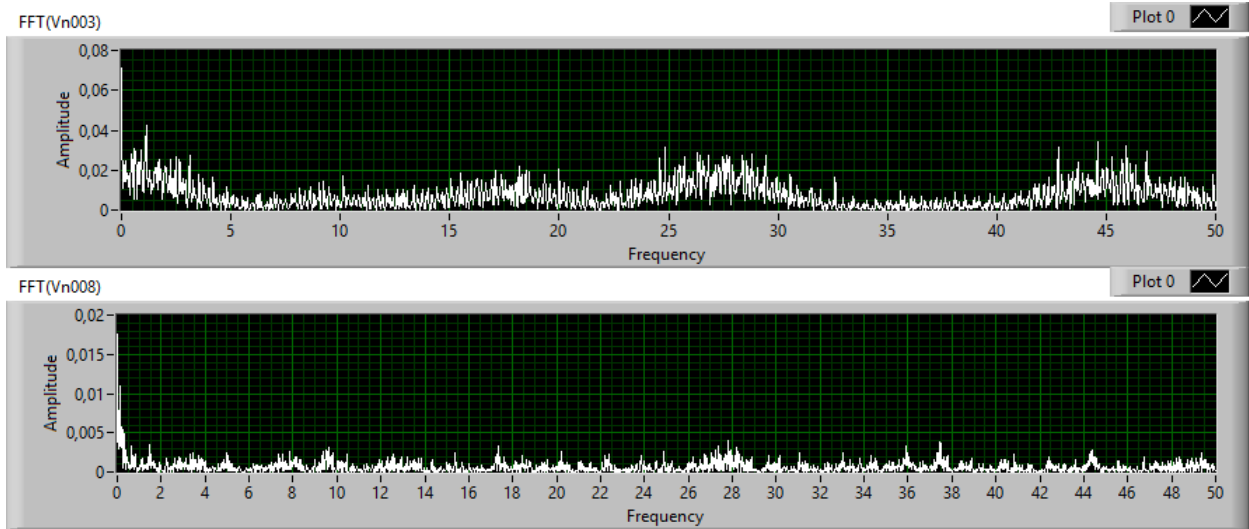
Figure 4.5. FFT of ideal (Vn003) and real (Vn008) conditions of work at buck dc – dc converter

Figure 4.5 represent that the type of the harmonic is with great similarity or we can say that at same points we have same curves of the harmonic. But if we take a look at the values, we will see that in ideal conditions of work (Vn003) we constantly have higher values through the whole harmonic versus real condition of work (Vn008).
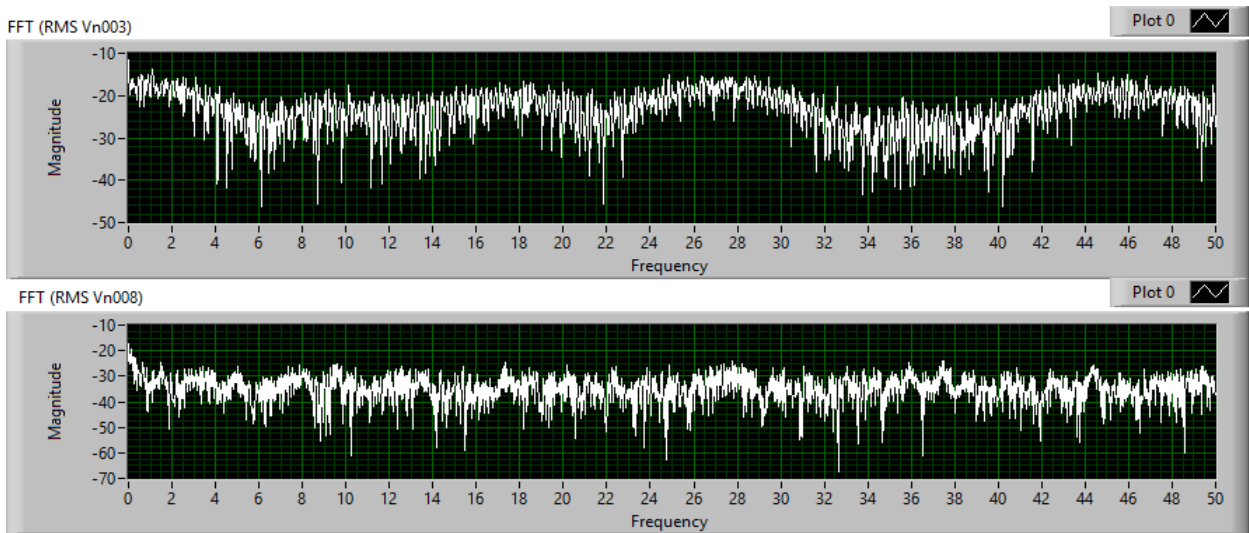
Figure 4.6. FFT (RMS) of ideal (Vn003) and real (Vn008) conditions of work at buck dc – dc converter

Figure 4.6 represent an additional view of the difference that is provided of the FFT (RMS) investigation of both cases, ideal vs. real conditions of work at buck dc – dc converters. RMS (root mean squared) will show the average (mean) power of the signal, that can be very

important in some cases. On the graph can be seen that like the analysis at only FFT there is big similarity in the harmonics between ideal and real conditions of work, but, the overall value of the amplitude is significant smaller at the real (Vn008) from the ideal conditions of work.
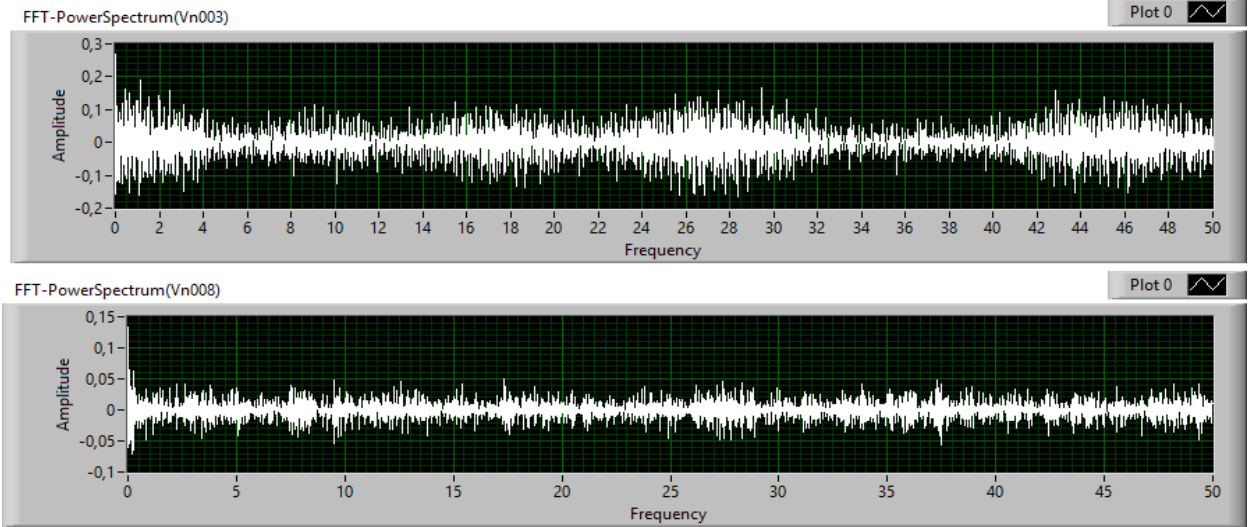
Figure 4.7. FFT (Power Spectrum) of ideal (Vn003) and real (Vn008) conditions of working at buck dc – dc converter

As last analysis that is obtained is the Spectral Density shown in Figure 4.7. It is always of great importance to estimate the energy of the signal using DFT. The signals shown at first look at ideal vs. real conditions of working are not extra different in aspect of the type of the curve. But, same as at FFT, the values in the amplitudes are different, the ideal Vn003 case has a much bigger values than the values obtained in Vn003 or real working conditions.

The section below shows several waveform graphs that referred to the output voltage and the FFT of the output voltage of the Boost DC – DC converters that are discussed in this dissertation. There are provided cases in ideal working conditions and in real working conditions.
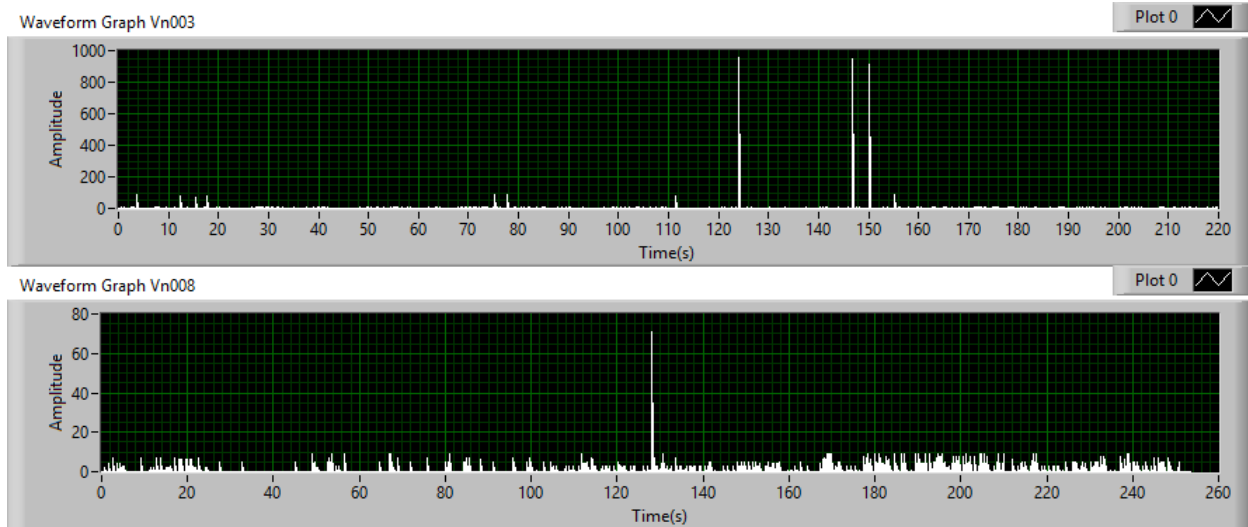
Figure 4.8. Waveform graph results of ideal (Vn003) and real (Vn008) conditions of work at Boost DC – DC converter

The figure 4.8 is showing the main difference in the signals in ideal and real conditions of working at Boost DC – DC converter. There are two types of differences visible from the graph. The first difference are the number and the maximum amplitude of the peaks in the two signals. It can be seen that in ideal conditions of working the peaks are 3 and with a very big amplitude from the rest of the signal. In the real conditions of working we have only one big peak that is different from the signal but not with that type of difference like in ideal conditions. The second type of difference between the signal is the overall working amplitude. If take a closer look, can be seen that in ideal conditions the amplitude is much higher than the real conditions of working.
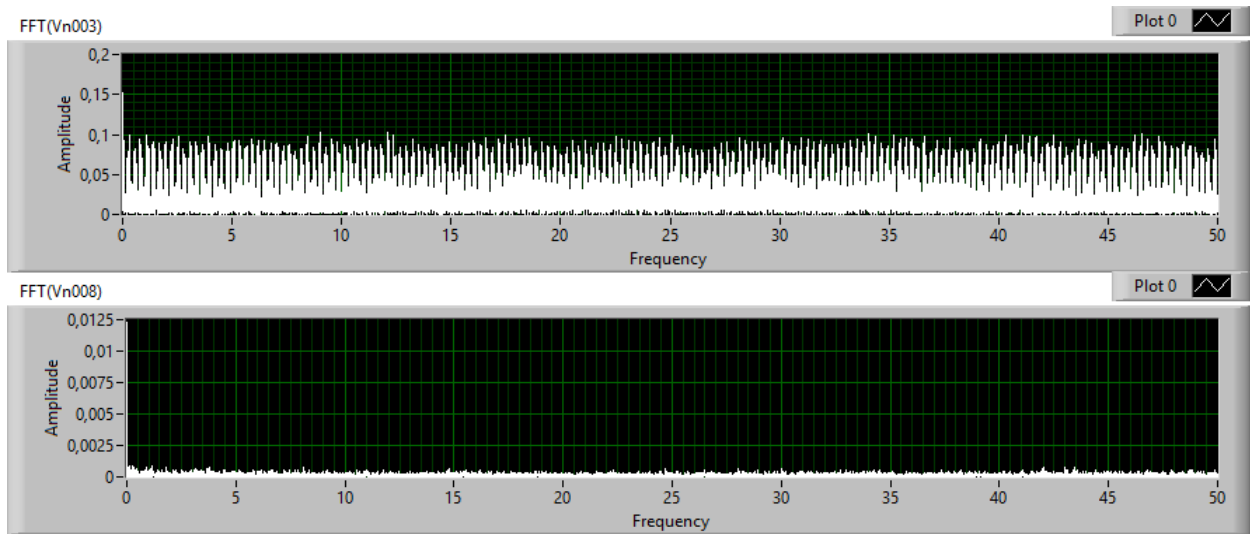
Figure 4.9. FFT of ideal (Vn003) and real (Vn008) conditions of working conditions at boost dc – dc converter

Summarizing the Figure 4.9 shows that in ideal (Vn003) over real (Vn008) conditions of working can be seen a much difference in the amplitude of the whole signal. In the real conditions of working the overall amplitude is much lower than the ideal conditions of working.
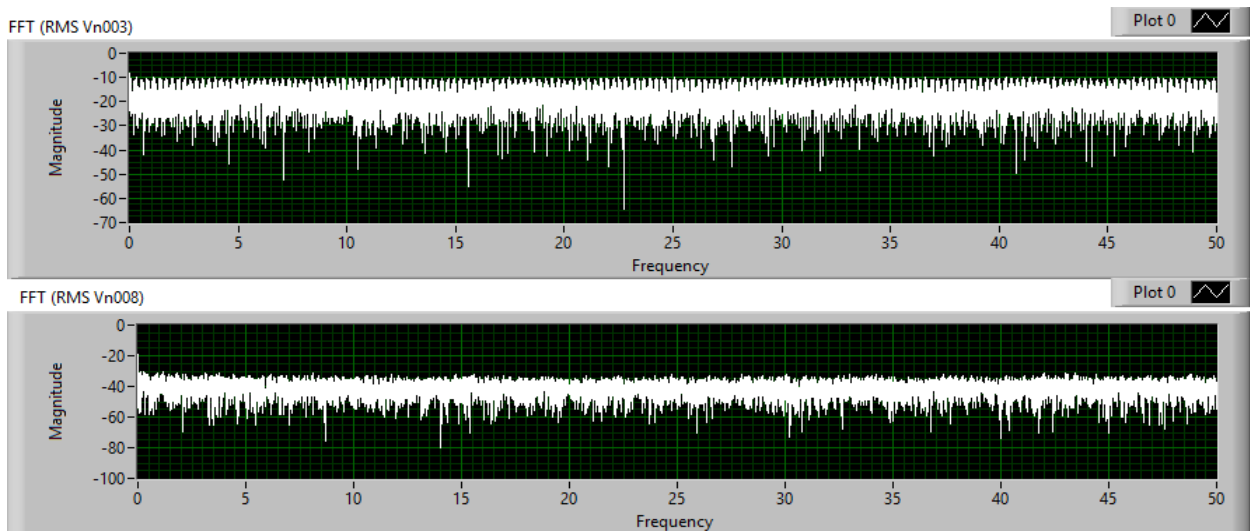
Figure 4.10. FFT(RMS) of ideal (Vn003) and real (Vn008) conditions of working at boost dc – dc converters.

Figure 4.10 is showing the main difference between ideal and real conditions of work of FFT (RMS) at Boost DC – DC converter. The ideal (Vn003) has a significantly higher overall signal values than the real (Vn008) conditions of working. The types of the signal peaks are not with a

127

very big difference, so, the signal is showing similar activity but with a smaller values at real conditions of work.
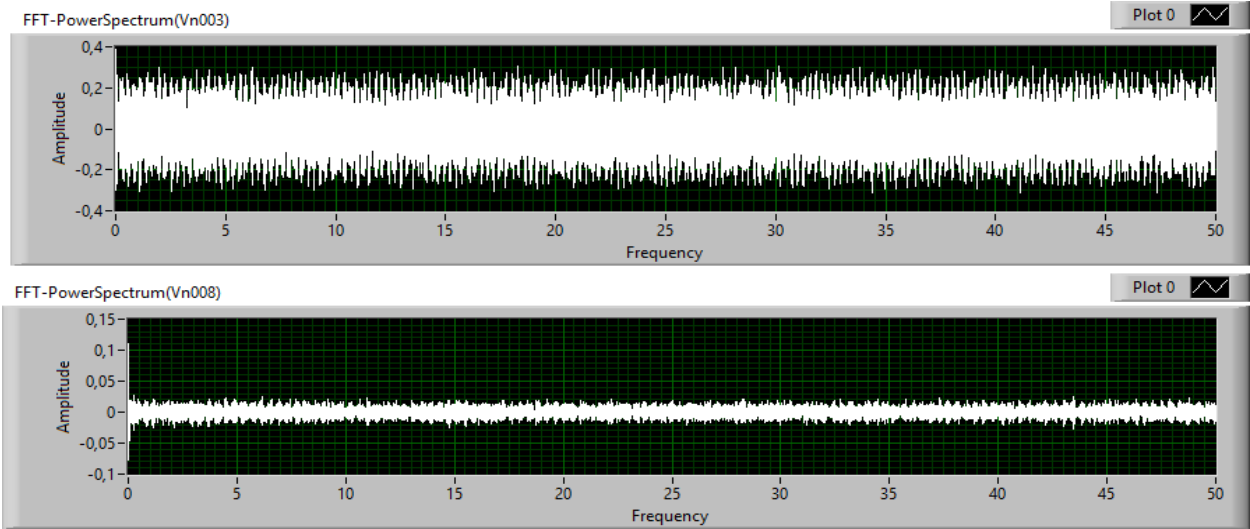
Figure 4.11. FFT (Power Spectrum) of ideal (Vn003) and real (Vn008) conditions of work at boost dc – dc converter

The power that is shown in Figure 4.11 in the ideal (Vn003) signal is with a higher overall value through the whole signal than the power that is shown in the signal (Vn008) that is at real condition of working. This proves that at Boost DC – DC converters, the real power in running conditions is much lower than the power shown in ideal conditions of working.

The section below shows several waveform graphs that referred to the output voltage and the FFT of the output voltage of the Buck - Boost DC – DC converters that are discussed in this dissertation. There are provided cases in ideal working conditions and in real working conditions.
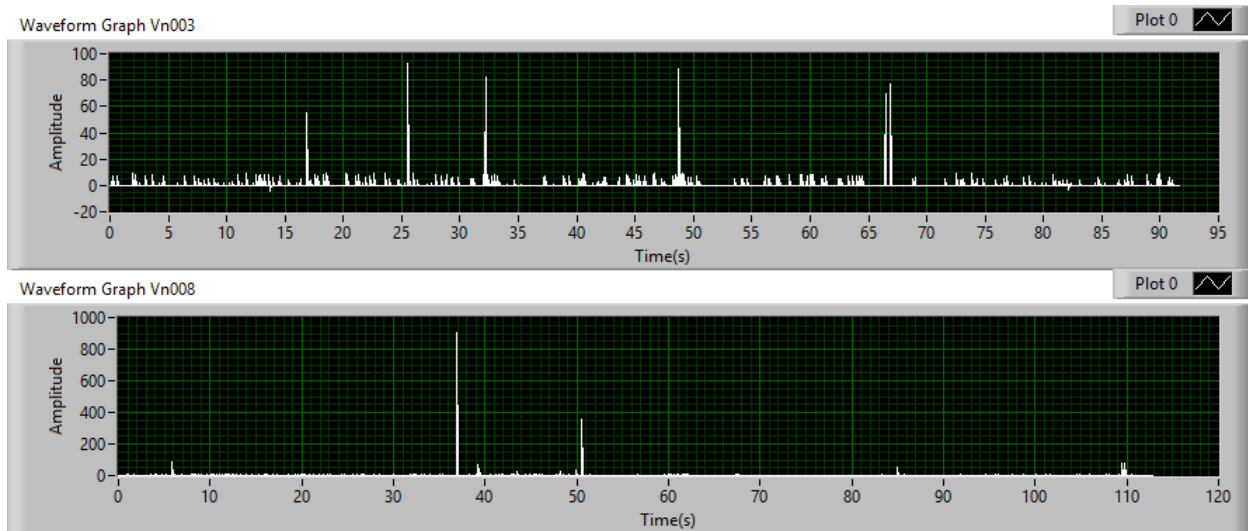
Figure 4.12. Waveform graphs of ideal (Vn003) and real (Vn008) conditions of working at buck – boost dc – dc converter

The last investigated converter is the Buck – Boost DC – DC converter. As a remind, here is analyzed only the output voltage of this type of converter. The main waveform in shown in the Figure 4.12. At first look the difference is visible at the two conditions, ideal vs. real, or, at the ideal conditions (Vn003) can be seen that there are few more peaks than the real (Vn008) conditions of work. Another difference is that the amplitude of the only two peaks at the real (Vn008) case is a lot bigger than the amplitude in the peaks at ideal conditions of work, that is a different case from buck, and Boost DC – DC converter.
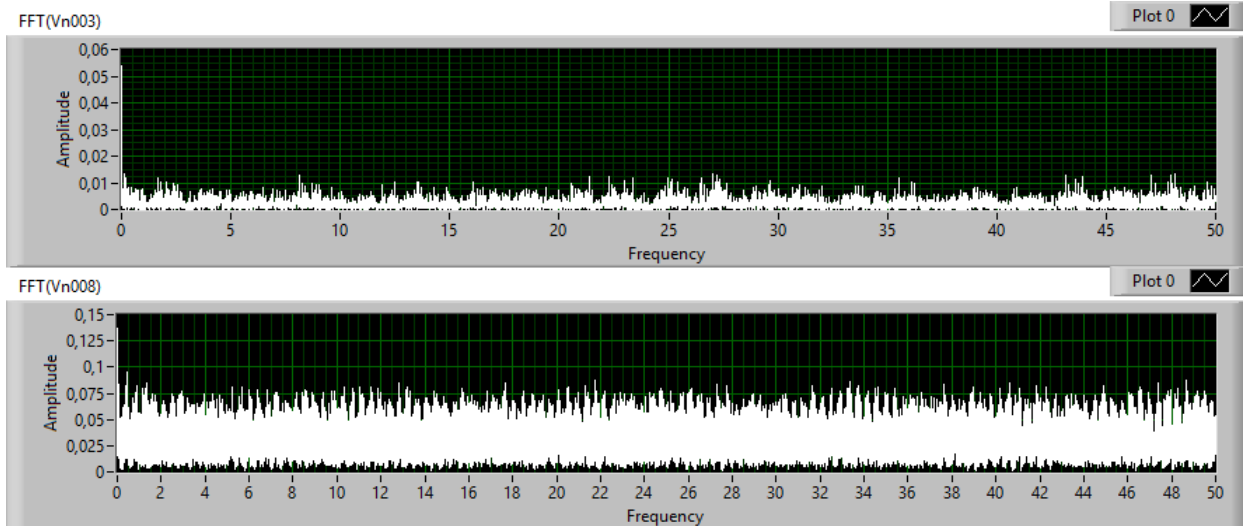
Figure 4.13. FFT of ideal (Vn003) and real (Vn008) conditions of work at Buck – Boost DC – DC converter

At Figure 4.13 is visible that the situation is different than the previous cases at Buck and Boost DC – DC converter, or, at the real conditions of work (Vn008) are bigger overall amplitude of the signal than the ideal (Vn003) conditions of work. The type of the signal if we exclude the amplitudes is not very different.
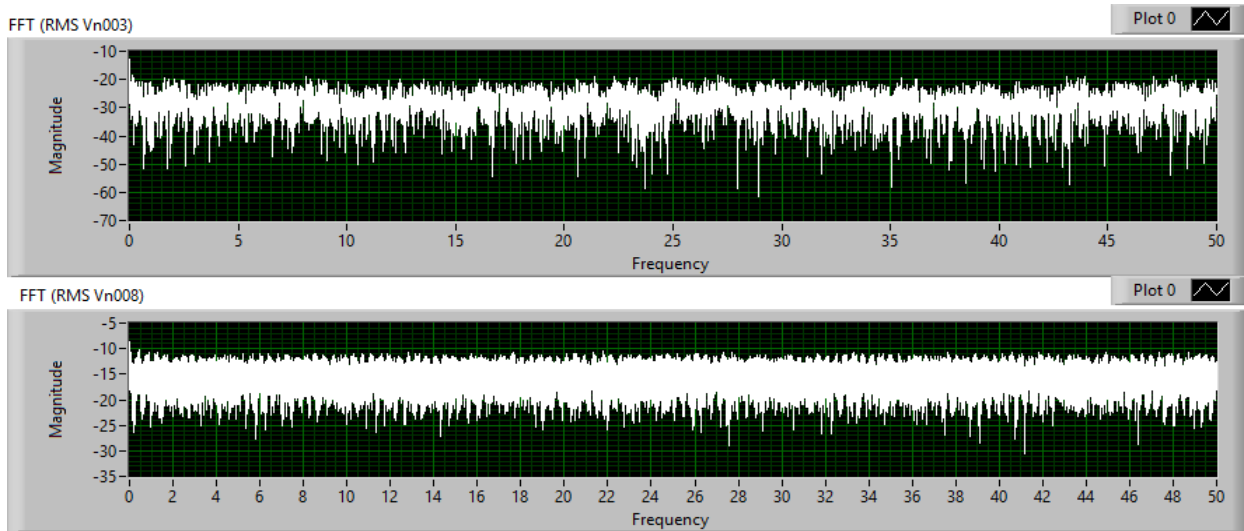
Figure 4.14. FFT (RMS) at ideal (Vn003) and real (Vn008) conditions of work at Buck – Boost DC – DC converter

The average power of the two cases that are obtained (ideal and real) is shown in the Figure 4.14 above. Once again can be seen that at ideal (Vn003) conditions of work there is bigger values in

130

the amplitude in the two sides of the frequency axis. The graph with the real conditions of work (Vn008) is with smaller amplitudes among the horizontal axis.
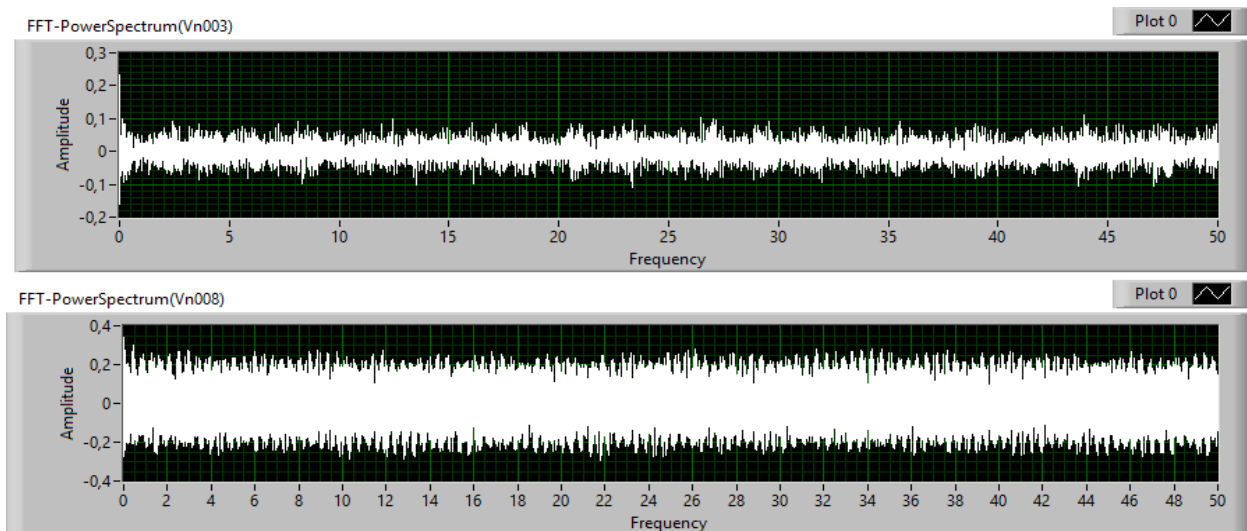
Figure 4.15. FFT (Power Spectrum) at ideal (Vn003) and real (Vn008) conditions of working at Buck – Boost DC – DC converter

The Figure 4.15 shows the energy among the signal at the two working conditions of the Buck – Boost DC – DC converter. It is visible that in real (Vn008) conditions of working there is much bigger amplitude of the overall length of the signal than in ideal (Vn003) conditions of working. This proves that Buck – Boost DC – DC converters are with different behavior than the other Buck and Boost DC – DC converter.

- The LabVIEW analysis shows the values and the processing of the same values in the three types of converters. As one of the most serious software solutions, LabVIEW confirm the obtained results that are gathered in previous models such as the web information model for processing of big data proposed in Chapter 3. LabVIEW offers combining object – oriented programing techniques with mathematic and physics laws integrating for making complex VI's that can be used for complex analysis of big data files. It has a large library of processing functions that are automatic generated with previous correct connection of all elements. Using this type of solution for estimating results is very important for new researchers because of the several different techniques implemented in one software.

- The graphic interface is more user friendly for the younger researcher that are affected of same type of problems. They can obtain results and operate with variables in real – time conditions of the instrument that they have created for investigation.

- LabVIEW can be used for different types of signals and the VI's can be included in some another future analysis. It does not matter what type of data one will investigate, the same VI can be used with small changes in the connections of the blocks. This type of software makes the studying of the electronic components more interesting and the young students can more easily see the functionality of the electronic component with the output results.

The following Scientific, Scientific and Applied and Applied contributions were obtained as a result of the dissertation works:

- **Scientific contributions:**
  - A unified information model for data integration, interactive modeling and analysis of electronic elements is proposed, which allows the integration, storage, processing and visualization of data and models of electronic devices created with different software systems.

- **Scientific and Applied Contributions:**
  - A research is conducted and the dynamics of the power electronic converters in different operating modes are evaluated using Fourier analysis and basic relations between output parameters of the device and results of the analysis are proved. The evaluation of the power electronic devices is used as a basis in the interactive design.

- **Applied Contributions:**
  - Based on the proposed single information model, a Web-based information system is developed that allows integration, storage, processing and visualization of data and models of electronic devices;
  - Experimental research has been conducted to integrate the developed web-based information system with other software applications for modeling and analysis of power devices (LabView, LTspice);
  - On the basis of the experimental studies conducted, the test results were verified to evaluate the dynamics of power electronic converters of DC-DC type in different operating modes.

The guidelines for future research are related mainly to the possibilities found in developing of interactive systems for automated design of power electronics products and their union. This is due in large part to the fact that the components / devices and their models that make up the power electronic systems are commercially available and there are enough models developed for them as separate elements, while the problems related to their interaction and collaboration to satisfy the new consumer needs and performance indicators are not well studied. In addition,

it is an important task to integrate developed and ready-made models in various program environments and software platforms into a common environment, thus allowing a significant acceleration in the design and prototyping of finished products and products, while improving their quality.

PUBLICATIONS ON THE TOPIC OF THE DISSERTATION

- Vacheva, G., Hinov, N., Zlatev, Z. Modelling of DC/DC Boost Converter in Visual Programing Environments, 41st International Spring Seminar on Electronics Technology, ISSE 2018; Zlatibor; Serbia; Volume 2018-May, Article number 8443701, **DOI:** 10.1109/ISSE.2018.8443701

- Hinov, N., Vacheva, G., Zlatev, Z. Modelling a charging process of a supercapacitor in MATLAB/Simulink for electric vehicles, 44th International Conference on Applications of Mathematics in Engineering and Economics, AMEE 2018; Sozopol; Bulgaria; Volume 2048, 10 December 2018, Article number 060023, DOI: 10.1063/1.5082138

- Zlatev, Z., Hinov, N. Web based application for analyzing, storing and filtering mass data, 44th International Conference on Applications of Mathematics in Engineering and Economics, AMEE 2018; Sozopol; Bulgaria; 8 June 2018, Volume 2048, 10 December 2018, Article number 060024, DOI: 10.1063/1.5082139

- Zlatev, Z., Hinov, N. Signal processing and analysing big mass data using labview, TEM Journal, Volume 8, Issue 2, 1 May 2019, Pages 617-622, DOI: 10.18421/TEM82-40

- Zlatev, Z., Hinov, N. Spectral Analysis of Output Voltage for Buck and Boost DC-DC Converter, 10th National Conference with International Participation, ELECTRONICA 2019 – Proceedings May 2019, Article number 8825596, DOI: 10.1109/ELECTRONICA.2019.8825596

- Zlatev, Z., Hinov, N. Web application for analyzing power electronic converter data, 45th International Conference on Application of Mathematics in Engineering and Economics, AMEE 2019; Sozopol; Bulgaria; Volume 2172, 13 November 2019, Article number 110013, https://doi.org/10.1063/1.5133616

Models

```php
<?php

namespace App;

use Illuminate\Foundation\Auth\User as Authenticatable;
use Illuminate\Notifications\Notifiable;

class User extends Authenticatable
{
    use Notifiable;

    protected $fillable = [
        'name', 'email', 'password',
    ];

    protected $hidden = [
        'password', 'remember_token',
    ];

    protected $casts = [
        'email_verified_at' => 'datetime',
    ];
}
```

Picture 1: User Model

```php
<?php


namespace App\Models;


use Illuminate\Database\Eloquent\Model;


class Convertor extends Model
{
    protected $fillable = [
        'name',
        'type',
        'photo'
    ];


    public function elements()
    {
        return $this->hasMany('App\Models\Element');
    }
}
```

Picture 3: Convertor Data Model

```php
<?php


namespace App\Models;


use Illuminate\Database\Eloquent\Model;


class OsciData extends Model
{
    protected $fillable = [
        'time',
        'value',
        'element_id'
    ];


    public function element()
    {
        return $this->belongsTo('App\Models\Element', 'element_id');
    }
}
```

Picture 3: Element Data Model

```php
<?php

namespace App\Models;

use Illuminate\Database\Eloquent\Model;

class Element extends Model
{
    protected $fillable = [
        'name',
        'type',
        'convertor_id'
    ];

    public function convertor()
    {
        return $this->belongsTo('App\Models\Convertor', 'convertor_id');
    }
}
```

Picture 4: Oscillation Data Mode

Controllers

```php
<?php
    namespace App\Http\Controllers\Auth;


    use App\User;
    use App\Http\Controllers\Controller;
    use Illuminate\Support\Facades\Hash;
    use Illuminate\Support\Facades\Validator;
    use Illuminate\Foundation\Auth\RegistersUsers;


    class RegisterController extends Controller
    {
        use RegistersUsers;
        protected $redirectTo = '/home';


        public function __construct()
        {
            $this->middleware('guest');
        }
        protected function validator(array $data)
        {
            return Validator::make($data, [
                'name' => ['required', 'string', 'max:255'],
                'email' => ['required', 'string', 'email', 'max:255',
    'unique:users'],
                'password' => ['required', 'string', 'min:8', 'confirmed'],]);
        }
        protected function create(array $data)
        {
            return User::create([
                'name' => $data['name'],
                'email' => $data['email'],
                'password' => Hash::make($data['password']),]);
        }
    }
```

Picture 5: Register Controller

```php
<?php

namespace App\Http\Controllers\Auth;

use App\Http\Controllers\Controller;
use Illuminate\Foundation\Auth\AuthenticatesUsers;

class LoginController extends Controller
{



    use AuthenticatesUsers;

    protected $redirectTo = '/home';

    public function __construct()
    {
        $this->middleware('guest')->except('logout');
    }
}
```

Picture 6: Login Controller

```php
<?php

namespace App\Http\Controllers;

use Illuminate\Http\Request;
use App\Models\Convertor;
use App\User;
use App\Models\Element;

class HomeController extends Controller
{
    /**
     * Create a new controller instance.
     *
     * @return void
     */
    public function __construct()
    {
        $this->middleware('auth');
    }


    /**
     * Show the application dashboard.
     *
     * @return \Illuminate\Contracts\Support\Renderable
     */
    public function index()
    {
        $users=User::count();
        $converters=Convertor::count();
        $elements=Element::count();
            return view('home')->with(['users'=>$users, 'converters'=>$converters,
            'elements'=>$elements]);
    }
}
```

Picture 7: Home Controller

```php
<?php

namespace App\Http\Controllers;

use App\Models\Convertor;
use Illuminate\Http\Request;

class ConvertorController extends Controller
{
    public function index()
    {
        $convertors=Convertor::paginate(10);
        return view('convertors', ['convertors'=>$convertors]);
    }


}
```

Picture 8: Convertor Controller

```php
<?php

namespace App\Http\Controllers;

use GuzzleHttp\Client;
use App\Models\Element;
use App\Charts\TestHigh;
use Illuminate\Http\Request;
use Webit\Math\Fft\Dimension;
use Illuminate\Support\Facades\DB;
use Webit\Math\Fft\FftCalculatorRadix2;
use Webit\Math\ComplexNumber\ComplexArray;

class ElementController extends Controller
{
    public function index()
    {

        return view('elements.index', ['elements'=>Element::paginate(20)]);
    }


    public function show(Element $element)
    {
        $chart = new TestHigh;


        $data = DB::table('osci_data')->where('element_id', $element->id)-
>orderBy('id','ASC')
                    ->simplePaginate(4096);
        $collection = collect($data->all());


        $time_data = $collection->pluck('time')->toArray();
        $v_data = $collection->pluck('value')->toArray();


        $maxvoltage= max($v_data);


        $chart->labels($time_data);
        $chart->dataset($element->name.' Signal', 'line', $v_data)->color('#F5B041');
```

```php
$chartFFT=new TestHigh;
$calculator = new FftCalculatorRadix2();
$signal = ComplexArray::create($v_data);


//ComplexArray
$freq = collect($calculator->calculateFft($signal, Dimension::create(count($v_data))));
$fury = $freq->map(function ($values) {return $values->getReal();})->all(); //real numbers
$furyI = $freq->map(function ($values) {return $values->getImaginary();})->all(); //imaginary
numbers

        $chartFFT->labels($time_data);
        $chartFFT->dataset('FFT R', 'line', $fury)->color('#FF0000');
        $chartFFT->dataset('FFT Im', 'line', $furyI)->color('#F5B041');
    $client = new Client([
            'timeout'         => 30,
            'allow_redirects' => true,
            'headers' => [ 'Content-Type' => 'application/json' ]]);
    $jsondata = json_encode($v_data);
    $response = $client->request('POST', 'http://localhost:9000/test', ['body' =>
    $jsondata]);


    $chartPSD = new TestHigh;
      if ($response->getStatusCode() == 200) {
          $body = json_decode($response->getBody(), true);
          $chartPSD->labels($body[0]);
          $chartPSD->dataset('Power Spectrum', 'line', $body[1])->color('#DC7633');
      }
    return view('elements.view',
    compact('data','chart','chartFFT','maxvoltage','chartFFTfinal','chartPSD'));
    }
}
```

Picture 9 and 10: Element Controller

FFT Calculator

```php
<?php

namespace Webit\Math\Fft;

use Webit\Math\ComplexNumber\Complex;
use Webit\Math\ComplexNumber\ComplexArray;

class FftCalculatorRadix2 implements FftCalculator
{

    public function calculateFft(ComplexArray $signal, Dimension $dimension)
    {
        $dimension = $dimension->toInt();
        $signal = $this->prepareFttSignal($signal, $dimension);

        list($even, $odd) = $this->extractEvenOdd($signal);
        $evenItems = $dimension == 2 ? $even : $this->calculateFft($even, new
        Dimension($dimension / 2));

        $oddItems = $dimension == 2 ? $odd : $this->calculateFft($odd, new Dimension($dimension /
        2));

        $y = array();
        for ($i = 0; $i < $dimension / 2; $i++) {
            $ith = -2 * $i * M_PI / $dimension;
            $wi = new Complex(cos($ith), sin($ith));

            $y[2*$i] = $evenItems[$i]->add($wi->mul($oddItems[$i]));
            $y[2*$i + 1] = $evenItems[$i]->sub($wi->mul($oddItems[$i]));
        }
        return new ComplexArray($y);
    }


        return $signal;
    }
```

```php
    private function prepareFttSignal(ComplexArray $signal, $dimension)
        {
            $max = min(count($signal), $dimension);
            if ($max < $dimension) {
                return  $signal->merge(ComplexArray::create(array_fill(0,  $dimension-
$max, 0)));
            }

            return $signal;
        }
    private function extractEvenOdd(ComplexArray $signal)
    {
    $even = array();
    $odd = array();
    for ($i = 0; $i < count($signal) / 2; $i++) {
    $even[$i] = $signal->getItem(2 * $i);
    $odd[$i] = $signal->getItem(2 * $i + 1);
    }


    return array(new ComplexArray($even), new ComplexArray($odd));
    }
}
```

Picture 11 and 12: FFT Calculator Class

```php
<?php

namespace Webit\Math\ComplexNumber;

class ComplexArray implements \IteratorAggregate, \Countable, \ArrayAccess
{

    public function __construct(array $items)
    {
        ksort($items);
        foreach ($items as &$element) {
            if (! ($element instanceof Complex)) {
                $element = new Complex($element, 0);
            }
        }

        $this->items = array_values($items);
    }

    public static function create(array $items)
    {
        return new self($items);
    }
    public function merge(ComplexArray $complexArray)
    {
        return new ComplexArray(array_merge($this->items, $complexArray->items));
    }
     public function getItem($i)
    {
        return isset($this->items[$i]) ? $this->items[$i] : null;
    }
```

```php
public function getIterator()
    {
        return new \ArrayIterator($this->items);
    }


    public function offsetExists($offset)
    {
        return array_key_exists($offset, $this->items);
    }


    public function offsetGet($offset)
    {
        return $this->getItem($offset);
    }


    public function offsetSet($offset, $value)
    {
      throw new \LogicException('Can not set new value as long as ComplexArray is immutable.');
    }


    public function offsetUnset($offset)
    {
        throw new \LogicException('Can not unset value as long as ComplexArray is immutable.');
    }


    public function count()
    {
        return count($this->items);
    }
}
```

Picture 13 and 14: Complex Array Class

```php
<?php
namespace Webit\Math\ComplexNumber;


class Complex
{

      private $real;
      private $imaginary;


      public function __construct($real, $imaginary) {
            $this->real = $real;
            $this->imaginary = $imaginary;
      }
      public function getReal() {
              return $this->real;
      }
      public function getImaginary() {
            return $this->imaginary;
      }
       public function add(Complex $complex) {
                  return new static(
                        $this->getReal() + $complex->getReal(),
                        $this->getImaginary() + $complex->getImaginary()
                  );
      }
       public function sub(Complex $complex) {
                  return new static(
                         $this->getReal() - $complex->getReal(),
                  $this->getImaginary() - $complex->getImaginary()
        );
    }
public function mul(Complex $complex)
    {
        $real = $this->getReal() * $complex->getReal() - $this->getImaginary()
            * $complex->getImaginary();

        $imaginary = $this->getImaginary() * $complex->getReal() + $this->getReal()
            * $complex->getImaginary();
        return new static($real, $imaginary);
    }
```

```php
public function div(Complex $complex)
    {
        $denominator = (pow($complex->getReal(), 2) + pow($complex->getImaginary(), 2));
            if ($denominator == 0) {
            throw new \InvalidArgumentException('Can not divide be 0.');
        }
      $real = ($this->getReal() * $complex->getReal() + $this->getImaginary()
            * $complex->getImaginary()) / $denominator;
      $imaginary = ($this->getImaginary() * $complex->getReal()
            - $this->getReal() * $complex->getImaginary()) / $denominator;

        return new Complex($real, $imaginary);
    }


public function sqrt()
    {
        if ($this->getImaginary() == 0) {
            return new Complex(sqrt($this->getReal()), 0);
        }
        $x = $this->getReal();
        $y = $this->getImaginary();


        $delta = pow($x, 2) + pow($y, 2);
        $sgn = $y >= 0 ? 1 : -1;


        $real = sqrt(($x + sqrt($delta)) / 2);
        $imaginary = $sgn * sqrt((sqrt($delta) - $x) / 2);


        return new Complex($real, $imaginary);
    }


        );
    }
```

```
public function abs()
    {
        $x = abs($this->getReal());
        $y = abs($this->getImaginary());

        if ($x == 0 || $y == 0) {
            return max($x, $y);
        }
        return sqrt(pow($x, 2) + pow($y, 2));
    }


    public function getConjugated()
    {
        return new Complex($this->getReal(),-$this->getImaginary();
    }


    public function mulScalar($scalar)
    {
        return new Complex(
            $this->getReal() * $scalar,
            $this->getImaginary() * $scalar
        );
    }


    public function __toString()
    {
      return sprintf('%s%s%si', $this->getReal(), ($this->getImaginary() >= 0 ? '+' : ''),
      $this->getImaginary());
    }
}
```

Picture 15, 16 and 17: Complex Number Class

```php
<?php

namespace Webit\Math\Fft;

final class Dimension
{

    private $dimension;

    public function __construct($dimension)
    {
        if (! $this->isPowerOfTwo($dimension)) {
            throw new \InvalidArgumentException('Dimension must be power of number 2.');
        }

        $this->dimension = (int) $dimension;
    }

    public static function create($dimension)
    {
        return new self($dimension);
    }

    public function toInt()
    {
        return $this->dimension;
    }

    public function __toString()
    {
        return (string) $this->dimension;
    }
```

```
private function isPowerOfTwo($dimension)
    {
        if ($dimension == 0) {
            return false;
        }
     return ($dimension & $dimension - 1) == 0;
     }
}
```

Picture 18 and 19: Dimension Class

Power Spectrum Script

```python
from scipy import signal
import matplotlib.pyplot as plt
import numpy as np
import time, json
from http.server import BaseHTTPRequestHandler, HTTPServer


HOST_NAME = 'localhost'
PORT_NUMBER = 9000


class MyHandler(BaseHTTPRequestHandler):
    def do_HEAD(self):
        self.send_response(200)
        self.send_header('Content-type', 'text/html')
        self.end_headers()


    def do_POST(self):
        paths = {
            '/test': {'status': 200}
        }
        if self.path in paths:
            content_length = int(self.headers['Content-Length'])
            post_data = self.rfile.read(content_length)
            self.respond(paths[self.path], post_data)
        else:
            self.send_response(404)
            self.send_header('Content-type', 'text/html')
            self.end_headers()

    def handle_http(self, status_code, post_data, path):
        self.send_response(status_code)
        self.send_header('Content-type', 'application/json')
        self.end_headers()
```

```
data = json.loads(post_data)

        f, Pxx_den = signal.periodogram([float(i) for i in data])

        json_string = json.dumps([f.tolist(), Pxx_den.tolist()])
        return json_string.encode(encoding='utf_8')

        # return bytes(f, 'UTF-8')

    def respond(self, opts, post_data):
        response = self.handle_http(opts['status'], post_data, self.path)
        self.wfile.write(response)

if __name__ == '__main__':
    server_class = HTTPServer
    httpd = server_class((HOST_NAME, PORT_NUMBER), MyHandler)
    print(time.asctime(), 'Server Starts - %s:%s' % (HOST_NAME, PORT_NUMBER))
    try:
        httpd.serve_forever()
    except KeyboardInterrupt:
        pass
    httpd.server_close()
    print(time.asctime(), 'Server Stops - %s:%s' % (HOST_NAME, PORT_NUMBER))
```

Picture 20 and 21: Python Script for Power Spectrum

Views (Blades)

```
<!DOCTYPE html>
<html lang="{{ str_replace('_', '-', app()->getLocale()) }}">
<head>
    <meta charset="utf-8">
    <meta name="viewport" content="width=device-width, initial-scale=1">

    <!-- CSRF Token -->
    <meta name="csrf-token" content="{{ csrf_token() }}">

    <title>{{ config('app.name', 'Laravel') }}</title>

    <!-- Scripts -->
    <script src="{{ asset('js/app.js') }}" defer></script>

    <!-- Fonts -->
    <link rel="dns-prefetch" href="//fonts.gstatic.com">
    <link href="https://fonts.googleapis.com/css?family=Nunito" rel="stylesheet" type="text/css">
    <!-- Styles -->
    <link href="{{ asset('css/app.css') }}" rel="stylesheet">
    <!-- Icons -->
    <link rel="stylesheet" href="https://use.fontawesome.com/releases/v5.8.2/css/all.css"
integrity="sha384-oS3vJWv+0UjzBfQzYUhtDYW+Pj2yciDJxpsK1OYPAYjqT085Qq/1cq5FLXAZQ7Ay"
crossorigin="anonymous">

    <script src="https://cdnjs.cloudflare.com/ajax/libs/echarts/4.0.2/echarts-en.min.js"
charset="utf-8"></script>
</head>
<body>
    <div id="app">
        <nav class="navbar navbar-expand-md navbar-light navbar-laravel">
            <div class="container">
                <a class="navbar-brand" href="{{ url('/') }}">
                    {{ config('app.name', 'Laravel') }}
                </a>
                <button class="navbar-toggler" type="button" data-toggle="collapse" data-
target="#navbarSupportedContent" aria-controls="navbarSupportedContent" aria-expanded="false"
aria-label="{{ __('Toggle navigation') }}">
                    <span class="navbar-toggler-icon"></span>
                </button>
```

```
<div class="collapse navbar-collapse" id="navbarSupportedContent">
                    <!-- Left Side Of Navbar -->
                    <ul class="navbar-nav mr-auto">

                    </ul>
<!-- Right Side Of Navbar -->
<ul class="navbar-nav ml-auto">
<!-- Authentication Links -->
     @guest
         <li class="nav-item">
            <a class="nav-link" href="{{ route('login') }}">{{ __('Login') }}</a>
         </li>
      @if (Route::has('register'))
         <li class="nav-item">
            <a class="nav-link" href="{{ route('register') }}">{{ __('Register') }}</a>
         </li>
      @endif
      @else
          <li class="nav-item">
           <a class="nav-link" href="{{ route('home') }}">{{ __('Home') }}</a>
          </li>
          <li class="nav-item">
           <a class="nav-link" href="{{ route('convertor') }}">{{ __('Convertors') }}</a>
          </li>
          <li class="nav-item">
           <a class="nav-link" href="{{ route('elements') }}">{{ __('Elements') }}</a>
          </li>
          <li class="nav-item">
           <a class="nav-link" href="{{ route('users') }}">{{ __('Users') }}</a>
           </li>
```

```
              <li class="nav-item dropdown">
                <a id="navbarDropdown" class="nav-link dropdown-toggle" href="#" role="button"
        data-toggle="dropdown" aria-haspopup="true" aria-expanded="false" v-pre>
                  {{ Auth::user()->name }} <span class="caret"></span></a>


                <div class="dropdown-menu dropdown-menu-right" aria-labelledby="navbarDropdown">
                <a class="dropdown-item" href="{{ route('logout') }}"
                 onclick="event.preventDefault();
                  document.getElementById('logout-form').submit();">
                 {{ __('Logout') }}
                </a>

                    <form id="logout-form" action="{{ route('logout') }}" method="POST"
                    style="display: none;">
                     @csrf
                     </form>
                                </div>
                        </li>
                    @endguest
                 </ul>
            </div>
          </div>
      </nav>


      <main class="py-4">
          @yield('content')
      </main>
    </div>
</body>
</html>
```

Picture 21, 22 and 23: App Blade (Layout for all views)

```
<!doctype html>
<html lang="{{ str_replace('_', '-', app()->getLocale()) }}">
    <head>
        <meta charset="utf-8">
        <meta name="viewport" content="width=device-width, initial-scale=1">

        <title>Welcome</title>

        <!-- Fonts -->
        <link href="https://fonts.googleapis.com/css?family=Nunito:200,600" rel="stylesheet">

        <!-- Styles -->
        <style>
            html, body {
                background-color: #fff;
                color: #636b6f;
                font-family: 'Nunito', sans-serif;
                font-weight: 200;
                height: 100vh;
                margin: 0;
            }

            .full-height {
                height: 100vh;
            }

            .flex-center {
                align-items: center;
                display: flex;
                justify-content: center;
            }

            .position-ref {
                position: relative;
            }

            .top-right {
                position: absolute;
                right: 10px;
                top: 18px;
            }
```

```
.title {
      font-size: 84px;
}
.links > a {
      color: #636b6f;
      padding: 0 25px;
      font-size: 13px;
      font-weight: 600;
      letter-spacing: .1rem;
      text-decoration: none;
      text-transform: uppercase;
}
.m-b-md {
      margin-bottom: 30px;
}
    </style>
  </head>
  <body>
    <div class="flex-center position-ref full-height">
        @if (Route::has('login'))
            <div class="top-right links">
                @auth
                    <a href="{{ url('/home') }}">Home</a>
                @else
                    <a href="{{ route('login') }}">Login</a>
                    @if (Route::has('register'))
                        <a href="{{ route('register') }}">Register</a>
                    @endif
                @endauth
            </div>
        @endif
        <div class="content">
            <div class="title m-b-md">
                Welcome
            </div>
        </div>
    </div>
  </body>
</html>
```

```
@extends('layouts.app')
@section('content')
<div class="container">
    <div class="row justify-content-center">
        <div class="col-md-12">
            <div class="card">
                <div class="card-header"><h4>Dashboard</h4></div>
            </div>
                <div class="row">
                    <div class="col-lg-4 col-md-6" style="margin-top: 20px">
                        <div class="card border-primary">
                            <a href="{{ route('users') }}">
                            <div class="card-body bg-primary text-white">
                                <div class="row">
                                    <div class="col-3">
                                        <i class="fa fa-users fa-5x"></i>
                                    </div>
                                    <div class="col-9 text-right">
                                        <h1>{{$users}}</h1>
                                        <h4>Users</h4>
                                    </div>
                                </div>
                            </div>
                            </a>
                        </div>
                    </div>
```

```
<div class="col-lg-4 col-md-6" style="margin-top: 20px">
                        <div class="card border-danger">
                             <a href="{{ route('convertor') }}">
                                 <div class="card-body bg-danger text-white">
                                     <div class="row">
                                         <div class="col-3">
                                             <i class="fa fa-microchip fa-5x"></i>
                                         </div>
                                         <div class="col-9 text-right">
                                             <h1>{{$converters}}</h1>
                                             <h4>Converters</h4>
                                         </div>
                                     </div>
                                 </div>
                             </a>
                        </div>
                    </div>
<div class="col-lg-4 col-md-6" style="margin-top: 20px">
                        <div class="card border-success">
                             <a href="{{ route('elements') }}">
                                 <div class="card-body bg-success text-white">
                                     <div class="row">
                                         <div class="col-3">
                                             <i class="fas fa-chart-line fa-5x"></i>
                                         </div>
                                         <div class="col-9 text-right">
                                             <h1>{{$elements}}</h1>
                                             <h4>Elements</h4>
                                         </div>
                                     </div>
                                 </div>
                             </a>
                        </div>
                    </div>
                </div>
        </div>
    </div>
</div>
```

Picture 26 and 27: Dashboard view

```
@extends('layouts.app')
@section('content')
    <div class="container">
        <h3>Convertors</h3>
        <hr>
        <div class="table-responsive">
            <table class="table table-bordered table-striped">
                <thead>
                    <tr>
                        <th>Name</th>
                        <th>Type</th>
                        <th></th>
                    </tr>
                </thead>
                @if(count($convertors)>0)
                    <tbody>

                        @foreach ($convertors as $convertor)
                        <tr>

                            <td>{{ $convertor->name}}</td>
                            <td>{{ $convertor->type }}</td>
                            <td><a href="convertor/{{$convertor->id}}">See more</a></td>
                        </tr>
                        @endforeach
                    </tbody>
                @else
                    <h5>There are no convertors to show</h5>
                @endif
            </table>
        </div>
    </div>
@endsection
```

Picture 28: Convertors view

163

```
@extends('layouts.app')
@section('content')
<style>
.responsive {
  max-width: 100%;
  height: auto;
}
</style>
<div class="container">
    <h3>{{$convertor->name}}</h3>
    <hr>
    <img src="{{ url('storage/'.$convertor->photo) }}" alt="" title="" class="responsive"/>
    <br><br>
    <h4>Elements</h4>
    <br>
    <div class="table-responsive">
        <table class="table table-bordered table-striped">
            <thead>
                <tr>
                    <th>Name</th>
                    <th>Type</th>
                    <th></th>
                </tr>
            </thead>
            <tbody>
                @foreach ($convertor->elements as $element)
                <tr>
                    <td>{{ $element->name}}</td>
                    <td>{{ $element->type }}</td>
                <td><a href="{{route('show-element', ['element'=>$element->id])}}">
                        Spectrum Analysis</a></td>
                </tr>
                @endforeach
            </tbody>
        </table>
    </div>
</div>
@endsection
```

Picture 29: One convertor view

```
@extends('layouts.app')


@section('content')
    <div class="container">
        <h3>Elements</h3>
        <hr>
        <div class="table-responsive">
            <table class="table table-bordered table-striped">
                <thead>
                    <tr>
                        <th>ID</th>
                        <th>Name</th>
                        <th>Type</th>
                        <th></th>
                    </tr>
                </thead>

                <tbody>
                @foreach($elements as $element)
                <tr>
                    <td>{{ $element->id }}</td>
                    <td>{{ $element->name}}</td>
                    <td>{{ $element->type }}</td>
                    <td><a href="{{route('show-element', ['element'=>$element->id])}}">
                        Spectrum Analysis</a></td>
                </tr>
                @endforeach
            </tbody>
        </table>
    </div>
    {{ $elements->links() }}
    </div>
@endsection
```

Picture 30: Elements view

```
@extends('layouts.app')


@section('content')
        <div class="container">
                <div class="row">
                        <div class="col-6"><h3>Maximum voltage: {{$maxvoltage}} </h3></div>
                        <div class="col-6"><div class="float-right">{{ $data->links()
}}</div></div>
                </div>
        </div>
        <hr>
        {!! $chart->container() !!}


        {!! $chart->script() !!}
        <br>


        {!! $chartFFT->container() !!}


        {!! $chartFFT->script() !!}
        <br>
        {!! $chartPSD->container() !!}


        {!! $chartPSD->script() !!}
@endsection
```

Picture 31: One element view with signal, FFT and power spectrum chart

Routes

Picture 32: Routes

```php
<?php


Route::get('/', function () {
    return view('welcome');
});


Auth::routes();


Route::middleware(['auth'])->group(function () {
    Route::get('home', 'HomeController@index')->name('home');
    Route::view('users', 'users.index', ['users'=>\App\User::paginate(20)])->name('users');
    Route::get('chart', 'ChartController@testHighChart')->name('chart');
    Route::get('convertor', 'ConvertorController@index')->name('convertor');
    Route::get('convertor/{convertor}', 'ConvertorController@show');


    Route::get('elements', 'ElementController@index')->name('elements');
    Route::get('elements/{element}', 'ElementController@show')->name('show-element');
});
```

BIBLIOGRAPHY

[1]. Earthquake epicenter location using time-frequency representations T.A. de Perez ; M. Juanatey ; M.C. Stefanelli ; M. Abondano ; A. Viloria Proceedings of the 1998 Second IEEE International Caracas Conference on Devices, Circuits and Systems. ICCDCS 98. On the 70th Anniversary of the MOSFET and 50th of the BJT. (Cat. No.98TH8350) Year: 1998

[2]. Zhao, J. (2011, June). Automating measurement bench of DC-DC converter in LabVIEW. In 2011 6th IEEE Conference on Industrial Electronics and Applications (pp. 897-900). IEEE.

[3]. A Global Leader in Automated Test and Automated Measurement Systems, National Instrumenst, Retrieved from: www.ni.com , [accessed: 05 January 2019].

[4]. Gicev, V., & Trifunac, M. D. (2007). Permanent deformations and strains in a shear building excited by a strong motion pulse. Soil Dynamics and Earthquake Engineering, 27(8), 774-792.

[5]. Kelly, K. R., Ward, R. W., Treitel, S., & Alford, R. M. (1976). Synthetic seismograms: A finite-difference approach. Geophysics, 41(1), 2-27.

[6]. Dai, N., Vafidis, A., & Kanasewich, E. (1994). Composite absorbing boundaries for the numerical simulation of seismic waves. Bulletin of the seismological society of America, 84(1), 185-191.

[7]. Harvey, A. F., & Cerna, M. (1993). The fundamentals of FFT-based signal analysis and measurement in LabVIEW and LabWindows. Application Note, 41.

[8]. Brown, S. (2007). Seismic analysis and shake table modeling: Using a shake tablefor building analysis (Doctoral dissertation, University of Southern California).

[9]. Vetterling, W. T., Teukolsky, S. A., Press, W. H., & Flannery, B. P. (1989). Numerical recipes. University Press.

[10]. Zhang, P., Yang, H., & Xu, Y. (2014). Power big data and its application scenarios in power grid. Proc. CSEE, 34, 85-92.

[11]. Doan, A., Naughton, J., Baid, A., Chai, X., Chen, F., Chen, T., ... & Huang, J. (2009). The case for a structured approach to managing unstructured data. arXiv preprint arXiv:0909.1783.

[12]. Shen, D. R., Yu, G., Wang, X. T., Nie, T. Z., & Kou, Y. (2013). Survey on NoSQL for management of big data. Journal of Software, 8, 1786-1803.

[13]. X. Y Wu, J. R Ming,.(2015). Research on the Big Data Management Model Based on Data Mining, Information Science, 33, 131-134.

[14]. A. F. Harvey and Michael Cerna, "The Fundamentals of FFT-Based Signal Analysis and Measurement in LabVIEW and LabWindows", (National Instruments, Application Note 041

[15]. A. V. Oppenheim and G. C. Verghese, "Introduction to Communication, Control, and Signal Processing" spring 2010

[16]. F.W.Isen, Synthesis Lectures on Signal Processing, 2008, ISBN:9781598298918 [1]H. Asadi and J. Hudgins, Computer Techniques for Dynamic Modeling of DC-DC Power Converters, 2018, ISBN:9781681734187.

[17]. J. Zhao, Automating Measurement Bench of DC-DC Converter in LabVIEW, Electric power and Automation engineering, Shanghai University of electric power 2103, Pingliang-Road, Yangpu, Shanghai, 200090, China

[18]. National Semiconductor Application Note 255, "Power Spectra Estimation", November, 1980

[19]. S. V. Vaseghi, "Advanced Digital Signal Processing and Noise Reduction, Second Edition", 2000.

[20]. www.ni.com.

[21]. M. P. Kazmierkowski, R. Krishnan, and F. Blaabjerg, Control in power electronics. Academic Press, 2002. 17. Zilin Li; K. W. E. Cheng; Jiefeng Hu, Modeling of basic DC-DC converters, Proceeding of 7th International Conference on Power Electronics Systems and Applications - Smart Mobility, Power Transfer & Security (PESA), 12-14 Dec. 2017

[21]. Modelling a charging process of a supercapacitor in MATLAB/Simulink for electric vehicles. Available from: https://www.researchgate.net/publication/329575184_Modelling_a_charging_process_of_a_supercapacitor_in_MATLABSimulink_for_electric_vehicles [accessed Dec 04 2019].

[22]. Polya Vassileva Gocheva, Nikolay Lyuboslavov Hinov and Valeri Petrov Gochev, Generalized net based estimations on switching topologies in electronic circuits, AIP Conference Proceedings 2048, 060025 (2018); https://doi.org/10.1063/1.5082140

[23]. Nikolay Lyuboslavov Hinov, Polya Vassileva Gocheva, Valeri Petrov Gochev and Bogdan Nikolov Gilev, Modeling and design of a boost converter with neural networks, AIP Conference Proceedings 2172, 110009 (2019); https://doi.org/10.1063/1.5133612

[24]. Gergana Vacheva, Nikolay Hinov and Dimitar Penev, Research procedure for buck-boost converter for small electric vehicles, AIP Conference Proceedings 1910, 060020 (2017); https://doi.org/10.1063/1.5014014

[25]. Michele de Gruttola, Salvatore Di Guida, Vincenzo Innocente and Antonio Pierro, Web application for detailed real-time database transaction monitoring for CMS condition data, AIP Conference Proceedings 1504, 966 (2012); https://doi.org/10.1063/1.4771858

[26]. Theodore C. Clarke and Paul C. Fisher, The Galileo Science Data System, AIP Conference Proceedings 283, 394 (1993); https://doi.org/10.1063/1.44406

[27]. SIMULATION OF A COMPLEX CLOSED- LOOP CONTROLLED POWER ELECTRONICS CIRCUIT IN SIMULINK, Hossein Mehrabani and Osman Kukrer, AIP Conference Proceedings 1052, 111 (2008); https://doi.org/10.1063/1.3008653

[28]. Robust stability of integral control of PWM DC–DC converters, Dariusz Czarkowski, L. Rai Pujara and Marian K. Kazimierczuk, AIP Conference Proceedings 271, 469 (1993); https://doi.org/10.1063/1.43248

[29]. State space analysis of boost DC/DC converter with voltage mode control, K. Latha Shenoy, C. Gurudas Nayak and Rajashekar P. Mandi, AIP Conference Proceedings 1859, 020062 (2017); https://doi.org/10.1063/1.4990215

[30]. Battery charging and discharging research based on the interactive technology of smart grid and electric vehicle, Mingyang Zhang, AIP Conference Proceedings 1971, 050004 (2018); https://doi.org/10.1063/1.5041195

[31]. Yudov D., V. Valchev, "Converters technic", Varna, Technical University –Varna, 2005 (in bulgarian).

[32]. www.infineon.com "Buck Converter Design" Design Note DN 2013-01V1.0 January 2013.

[33]. Barry Rowland, "Initial Evaluation of a DC/DC Switch Mode Power Supply", Application Note11. 2013 – 1TD04_0e, www.rohde-schwarz.com.

[34]. Liu Shulin, Li Yan; Liu Li, "Analysis of Output Voltage Ripple of Buck DC-DC converter and its design", 2nd International Conference on Power Electronics and Intelligent Transportation System (PEITS), 2009, pp. 112 –115.

[35]. David C. W. Ng, William Y. T. Wong, Ngai Wong, Karen W. H. Wan, David K. K. Kwong, "An Efficient Transfer-Function-Based Approach for the Fast Tuning and Design of DC-DC Converters", 2nd IEEE Conference on Industrial Electronics and Applications, 2007 pp. 682 –686

[36]. Tools in data science for better processing, Nur Syahela Hussien, Sarina Sulaiman and Siti Mariyam Shamsuddin, AIP Conference Proceedings 1750, 020017 (2016); https://doi.org/10.1063/1.4954530

[37]. Comparative characteristics and selection of optimal filtering algorithm signal using LabVIEW software package, A. A. Maslov and T. A. Lepikhin, AIP Conference Proceedings 1648, 450013 (2015); https://doi.org/10.1063/1.4912672

[38]. The use spectral and bispectral analysis for diagnosis of nonlinear dissipative medium, S. N. Gurbatov, I. Yu. Demin, N. V. Pronchatov- Rubtsov and A. V. Ryabov, AIP Conference Proceedings 1022, 50 (2008); https://doi.org/10.1063/1.2956270

[39]. Spectral Analysis of Suface Waves Combined to Laser Ultrasonics for the Non-Destructive Testing of High Performance Materials and Composites, E. Lafond and X. Zhang, AIP Conference Proceedings 894, 201 (2007); https://doi.org/10.1063/1.2717974

[40]. Mathematical model for studying the variation of the electrical parameters in functioning of nonlinear loads, Raluca Rob and Cezara Rat, AIP Conference Proceedings 1558, 1345 (2013); https://doi.org/10.1063/1.4825761

[41]. Conceptual model of a logical system processor of selection to electrical filters for correction of harmonics in low voltage lines, Arlys Lastre, Ives Torriente, Erik F. Méndez and Alexis Cordovés, AIP Conference Proceedings 1836, 020005 (2017); https://doi.org/10.1063/1.4981945

[42]. The efficiency and performance detection algorithm and system development for photovoltaic system through use of thermal image processing technology, Jwujenq Chen, Chialiang Lin and Chenglian Liu, AIP Conference Proceedings 1978, 470088 (2018); https://doi.org/10.1063/1.5044158

[43]. Mathematical models in simulation process in rehabilitation of persons with disabilities, Nina Gorie, Valer Dolga and Alina Mondoc, AIP Conference Proceedings 1493, 424 (2012); https://doi.org/10.1063/1.4765523

[44]. Designing Intelligent Instruments, Kevin H. Knuth, Philip M. Erner and Scott Frasso, AIP Conference Proceedings 954, 203 (2007); https://doi.org/10.1063/1.2821263

[45]. Measurement of temperature coefficient of photovoltaic modules in field and comparison with laboratory measurements

[46]. Rajiv Dubey ; Pranjal Batra ; Shashwata Chattopadhyay ; Anil Kottantharayil ; Brij M. Arora ; K. L. Narasimhan ; Juzer Vasi, 2015 IEEE 42nd Photovoltaic Specialist Conference (PVSC)

[47]. Integrated Design of Measurement and Control System for Photovoltaic Generation, Xu Xiaoli ; Zuo Yunbo, 2010 International Conference on Electrical and Control Engineering, Year: 2010

[48]. Data sampling speed versus energetic measurement errors in photovoltaic system monitoring, K. Kurokawa, Proceedings of 1994 IEEE 1st World Conference on hotovoltaic Energy Conversion - WCPEC (A Joint Conference of PVSC, PVSEC and PSEC), Year: 1994 | Volume: 1

[49]. Design techniques of distributed photovoltaic/energy storage system, Zilong Yang ; Zhuo Chen ; Lidong Guo ; Yuanyuan Chen ; Xinke Huang ; Yibo Wang, 2017 20th International Conference on Electrical Machines and Systems (ICEMS)

[50]. An Intelligent Power Online Monitoring and Measurement System of FGC Wind Photovoltaic Storage Integrated Power Station, Huang Shihui ; Yang Zhongliang ; Zhou Yu, 2018 IEEE International Telecommunications Energy Conference (INTELEC)

[51]. Wireless monitor system of the focusing and tracking photovoltaic generation system based on LabVIEW, Cao Yinxiang ; Gu Juping ; Mao Jingfeng ; Luo Laiwu ; Chen Kaian ; Miao Yangyang ; Liu Xuan, Proceedings of the 31st Chinese Control Conference, Year: 2012

[52]. A multifunctional data acquisition system for photovoltaic plants, Li Bian ; Xinjing Zou ; Yonghui Zhai ; Haitao Liu, 2012 International Conference on Systems and Informatics (ICSAI2012), Year: 2012

[53]. Photovoltaic system output simulation under various environmental conditions, Arar Hemza ; Haouam Abdeslam ; Rachid Chenni ; Debili Narimene, 2016 International Renewable and Sustainable Energy Conference (IRSEC), Year: 2016

[54]. Performance Monitoring and Test System for Grid-Connected Photovoltaic Systems, Xinjing Zou ; Bian Li ; Yonghui Zhai ; Haitao Liu, 2012 Asia-Pacific Power and Energy Engineering Conference

[55]. Lab VIEW modelling and simulation of a hydrogen based photovoltaic/wind energy system

[56]. M.L. Doumbia ; K. Agbossou ; C.-L. Proulx, 2009 8th International Symposium on Advanced Electromechanical Motion Systems & Electric Drives Joint Symposium

[57]. Wireless and Real-Time Photovoltaic Power Monitoring System, S. Sarabia ; C. A. Figueroa ; F. A. Zelaya A. ; A. Zamora ; M.R.A. Paternina, 2018 North American Power Symposium (NAPS)

[58]. Simulation and performance comparison of Silicon and Silicon carbide based DC-DC Buck Boost converter using LTSpice, Vidya Viswan ; A. M. Vipin ; T. P. Vishnu, 2015 International Conference on Power, Instrumentation, Control and Computing (PICC)

[59]. New technique for voltage tracking control of a boost converter based on the PSO algorithm and LTspice, Peyman Farhang ; Alin Marian Drimus ; Stefan Mátéfi-Tempfli, 2015 56th International Scientific Conference on Power and Electrical Engineering of Riga Technical University (RTUCON)

[60]. Effective Design Analysis of a DC-DC Boost Converter with Experimental Validation, Siddhant Kumar ; Adil Usmam, 2018 International Conference on Computation of Power, Energy, Information and Communication (ICCPEIC)

[61]. Modeling of power supplies for power modulators with LTspice, Michael Giesselmann ; Vishwajit Roy, IEEE Transactions on Dielectrics and Electrical Insulation, Year: 2019 | Volume: 26, Issue: 2 | Journal Article

[62]. High voltage gain DC-DC converter for DC microgrid, Anu Anto ; Anu Sunny, 2017 International Conference on Intelligent Computing, Instrumentation and Control Technologies (ICICICT)

[63]. Vibration energy gathering power management system based on DC/DC boost converter circuit, Zhang Qingxin ; Yu Li ; Gao Yunhong, 2016 Chinese Control and Decision Conference (CCDC)

[64]. Development of High Power LED driver using LTspice software, Muhammad Ikram Mohd Rashid ; Suliana Ab Ghani ; Mohamad Fakhrudin Sulaiman Mustahim, 2013 IEEE 7th International Power Engineering and Optimization Conference (PEOCO)

[65]. Design and development of an Android application to process and display summarised corporate data, Seth Y. Fiawoo ; Robert A. Sowah, 2012 IEEE 4th International Conference on Adaptive Science & Technology (ICAST)

[66]. A Study on Tourism Mobile Web Application based on Big Data Analysis Platform for the South of Thailand, Mallika Subongkod ; Sarun Duangsuwan ; Punyawi Jamjareegulgarn, 2018 22nd International Computer Science and Engineering Conference (ICSEC)

[67]. High Performance Database Processing, David Taniar, 2012 IEEE 26th International Conference on Advanced Information Networking and Applications, Year: 2012

[68]. The impact of web data processing on computer property: A study based on Hadoop, Xun Lu ; Xia Zhang ; Zhengyou Xia, 2015 International Conference on Smart and Sustainable City and Big Data (ICSSC)

[69]. Implementation of data generator for process mining applications, Mecit Yüzkat ; Buğra Şen ; Hasan Kaan Caymaz ; Fethullah Karabiber, 2015 23nd Signal Processing and Communications Applications Conference (SIU)

[70]. A real time data warehouse approach for data processing, Murat Obalı ; Bünyamin Dursun ; Zeki Erdem ; Abdül Kadir Görür, 2013 21st Signal Processing and Communications Applications Conference (SIU)

[71]. Service-Oriented Business Intelligence (SoBI) for Academic and Financial Data Integration in University, Ramos Somya ; Danny Manongga ; Magdalena. A. Ineke Pakereng, 2018 International Seminar on Application for Technology of Information and Communication

[72]. Modeling and application of data correlations among heterogeneous data sources, Licheng Cui ; Weishi Zhang ; Huawei Zhai ; Xiuguo Zhang ; Xiong Xie, 2010 2nd International Conference on Signal Processing Systems

[73]. Data analysis as a web service: A case study using IoT sensor data, Alireza Ahrabian ; Sefki Kolozali ; Shirin Enshaeifar ; Clive Cheong-Took ; Payam Barnaghi, 2017 IEEE International Conference on Acoustics, Speech and Signal Processing (ICASSP)

[74]. Lessons Learned and Cost Analysis of Hosting a Full Stack Open Data Cube (ODC), Application on the Amazon Web Services (AWS), Syed R Rizvi ; Brian Killough ; Andrew Cherry ; Sanjay Gowda, IGARSS 2018 - 2018 IEEE International Geoscience and Remote Sensing Symposium

[75]. A Web-based Enterprise Application Integration solution, Xiaogang Ji, 2009 2nd IEEE International Conference on Computer Science and Information Technology

[76]. Design and Implementation of Data Mining and Analysis Platform Based on Web Service Techniques, Sheng Zhou ; Xiaoxiao Zhang ; Xianhui Li ; Gang Zheng ; Gaokun Zhang, 2017 International Conference on Computer Technology, Electronics and Communication (ICCTEC)

[77]. Data management support of Web applications, D. Fishman, Proceedings 17th International Conference on Data Engineering

[78]. On data integration and data mining for developing business intelligence, Ping-Tsai Chung ; Sarah H. Chung, 2013 IEEE Long Island Systems, Applications and Technology Conference (LISAT)

[79]. Proposal for a Web Processing Services (WPS) Application Profile for 3D Processing Analysis, Sandra Lanig ; Alexander Zipf, 2010 Second International Conference on Advanced Geographic Information Systems, Applications, and Services

[80]. BDViewer — A Web-Based Big Data Processing and Visualization Tool, Yan Li ; Junming Ma ; Bo An ; Donggang Cao, 2018 IEEE 42nd Annual Computer Software and Applications Conference (COMPSAC)

[81]. The Application of Web Data Mining Technique in Competitive Intelligence System of Enterprise Based on XML, Chen Ting ; Niu Xiao ; Yang Weiping, 2009 Third International Symposium on Intelligent Information Technology Application

[82]. Enable Web-Based Interactive Applications of High-Resolution 3D Medical Image Data, Danzhou Liu ; Kien A. Hua ; Ning Yu, 2007 IEEE International Conference on Multimedia and Expo

[83]. VDT: A data integration model for web applications, Jiansheng Li ; Beixing Deng ; Yongfeng Huang ; Xing Li, 2011 Second International Conference on Mechanic Automation and Control Engineering

[84]. Improving Data Transmission in Web Applications via the Translation between XML and JSON, Guanhua Wang, 2011 Third International Conference on Communications and Mobile Computing

[85]. Research on the data mining based web searching, Zhi-Qin Zha ; Bo Gao ; Xiong Yang, 2010 International Conference on Computer Application and System Modeling (ICCASM 2010)

[86]. Web application for processing and analysis of the raw wind measurement data, Vitalijs Komashilovs ; Aleksejs Zacepins ; Valerijs Bezrukovs ; Dmitrijs Bezrukovs ; Janis Hofmanis, 2014 IEEE 15th International Symposium on Computational Intelligence and Informatics (CINTI)

[87]. Data analytics and web insights in area of data mining and analytics, Abzetdin Adamov, 2017 International Conference on Innovations in Electrical Engineering and Computational Technologies (ICIEECT)

[88]. Comparison between Non-stationary Signals Fast Fourier Transform and Wavelet Analysis, Shumin Zhou ; Bin Tang ; Rui Chen, 2009 International Asia Symposium on Intelligent Interaction and Affective Computing

[89]. Application of adaptive network-based fuzzy inference system with fast Fourier transform for waveform analysis and classification, Adisorn Kamlungpetch ; Prajuab Inrawong ; Wutthichai Sa-nga-ngam, 2017 International Electrical Engineering Congress (iEECON)

[90]. Based on short-time fourier transform impulse frequency response analysis in the application of the transformer winding deformation, Yaning Li ; Wenbang Peng ; Xiaoyan Zhu ; Genyuan Wei ; Hong Yu ; Guochao Qian, 2016 IEEE International Conference on Mechatronics and Automation

[91]. Identification of voltage quality problems under different types of Sag/Swell faults with Fast Fourier Transform analysis, G. Devadasu ; M. Sushama, 2016 2nd International Conference

on Advances in Electrical, Electronics, Information, Communication and Bio-Informatics (AEEICB)

[92]. Determination of heart rate from photoplethysmogram using Fast Fourier Transform, N. H. Mohd Sani ; W. Mansor ; Khuan Y. Lee ; N. Ahmad Zainudin ; S. A. Mahrim, 2015 International Conference on BioSignal Analysis, Processing and Systems (ICBAPS)

[93]. Real Time Series DC Arc Fault Detection Based on Fast Fourier Transform, Muhammad Hafid Riza Alvy Syafi'i ; Eka Prasetyono ; Muhammad Khanif Khafidli ; Dimas Okky Anggriawan ; Anang Tjahjono, 2018 International Electronics Symposium on Engineering Technology and Applications (IES-ETA)

[94]. Enhanced accuracy in fast-Fourier-based methods for full-vector modal analysis of dielectric waveguides, A. Ortega-Monux ; J.G. Wanguemert-Perez ; I. Molina-Fernandez ; E. Silvestre ; P. Andres, IEEE Photonics Technology Letters, Year: 2006 | Volume: 18, Issue: 10

[95]. Improved fast fourier transform processing on fast acquisition algorithms for GPS signals, Lin Zhao ; Shuaihe Gao ; Yong Hao, 2009 9th International Conference on Electronic Measurement & Instruments

[96]. A general mapping technique for Fourier transform computation in nonlinear circuit analysis, P.J.C. Rodrigues, IEEE Microwave and Guided Wave Letters, Year: 1997 | Volume: 7, Issue: 11

[97]. Efficient spectral analysis of Fourier transform mass spectrometry (FTMS) data, D. Imanuel ; S.S. Abeysekera ; J.C. Rajapakse ; K. Duan, IEEE International Workshop on Biomedical Circuits and Systems, 2004.

[98]. Frequency response analysis for DC-DC converters without small-signal linearization J.H. Ly ; K. Siri, Eighteenth Annual IEEE Applied Power Electronics Conference and Exposition, 2003. APEC '03.

[99]. Performance improvement of DC-DC boost converter using steering circuit, Saswati Swapna Dash ; Subrat Kumar ; Byamakesh Nayak, 2015 Annual IEEE India Conference (INDICON)

[101]. Monitoring and Diagnosis for the DC–DC Converter Using the Magnetic Near Field Waveform, Yu Chen ; Xuejun Pei ; Songsong Nie ; Yong Kang, IEEE Transactions on Industrial Electronics, Year: 2011 | Volume: 58, Issue: 5

[102]. Spread spectrum in DC-DC full bridge voltage converter by a dual randomized PWM scheme, N. Boudjerda ; M. Melit ; B. Nekhoul ; K. El khamlichi Drissi ; K. Kerroum, 2008 International Symposium on Electromagnetic Compatibility - EMC Europe

[103]. Method for online battery AC impedance spectrum measurement using dc-dc power converter duty-cycle control, Zhiyong Xia ; Jaber A. Abu Qahouq, 2017 IEEE Applied Power Electronics Conference and Exposition (APEC)